Evoluzione spettrale delle Galassie

Materiale didattico per gli studenti

A.A. 2017/18 - Laurea Magistrale in Astrofisica e Cosmologia

Prof. Alberto Buzzoni

MORPHOLOGY

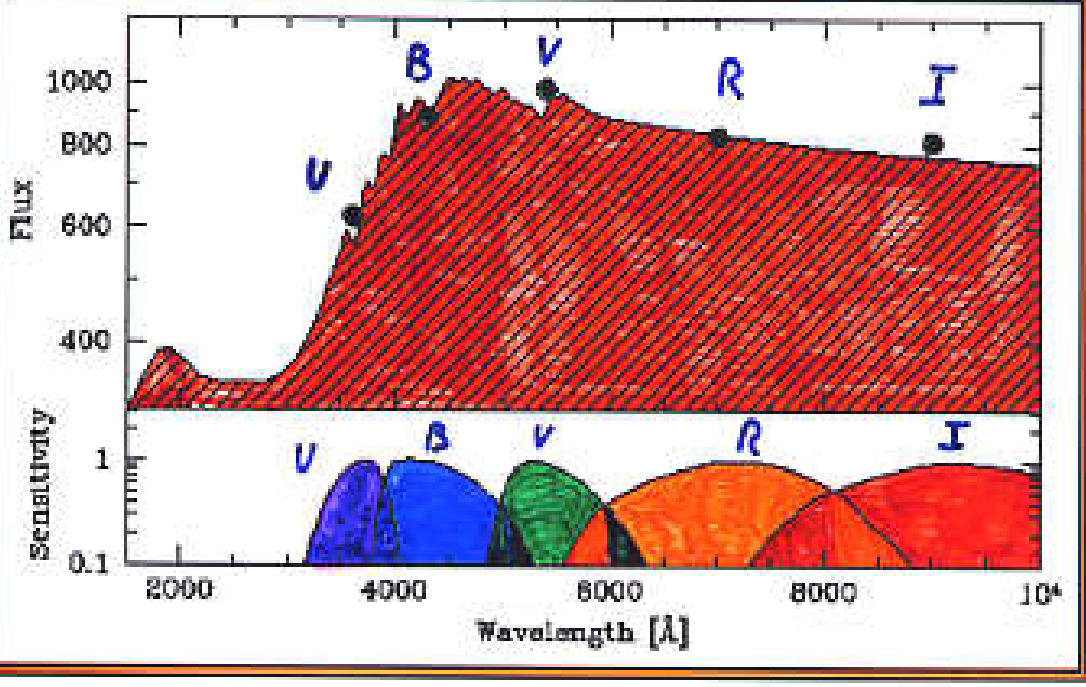

PHOTOMETRY

SPECTROSCOPY

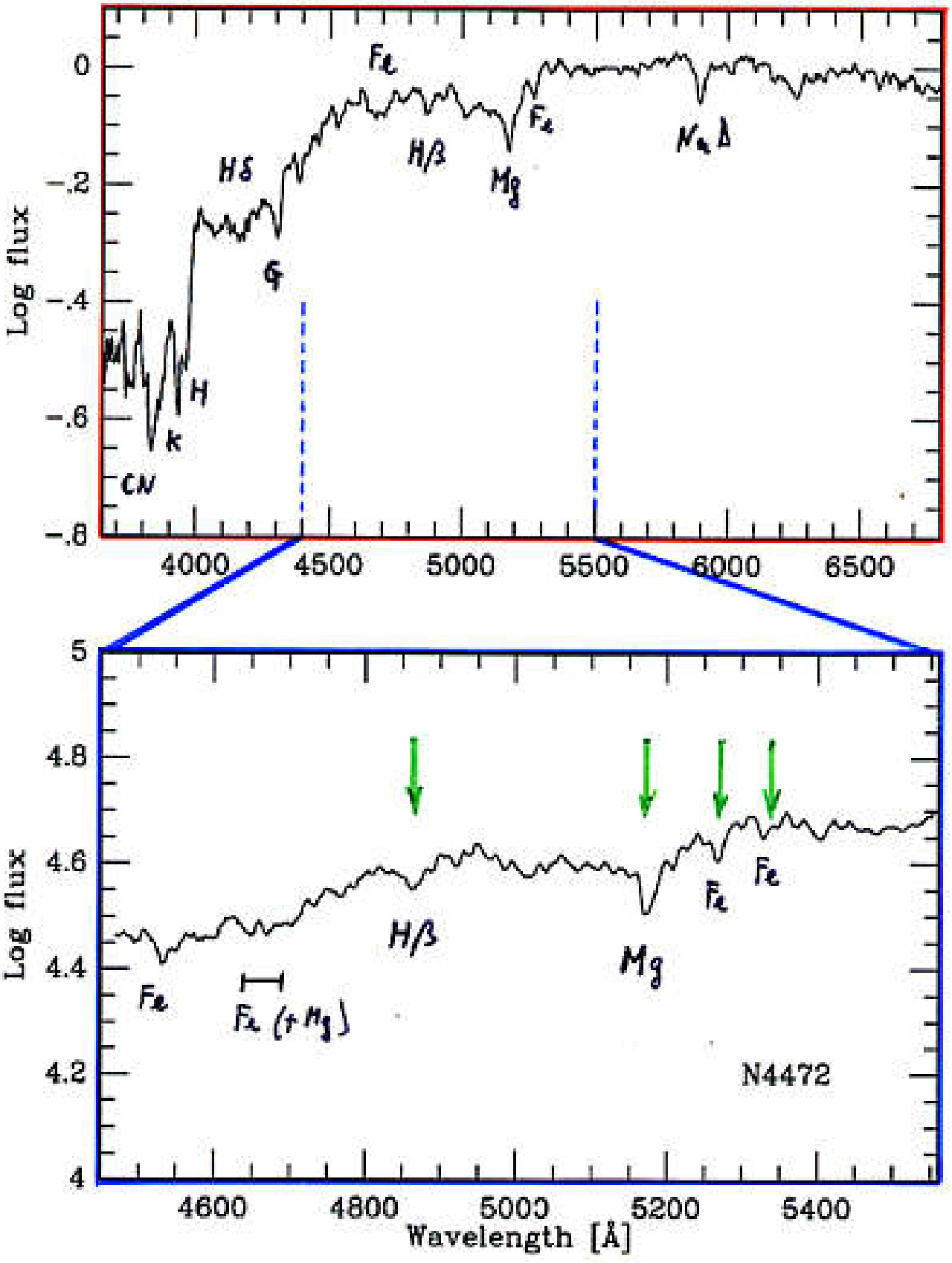

Cosmologia & Look-back time

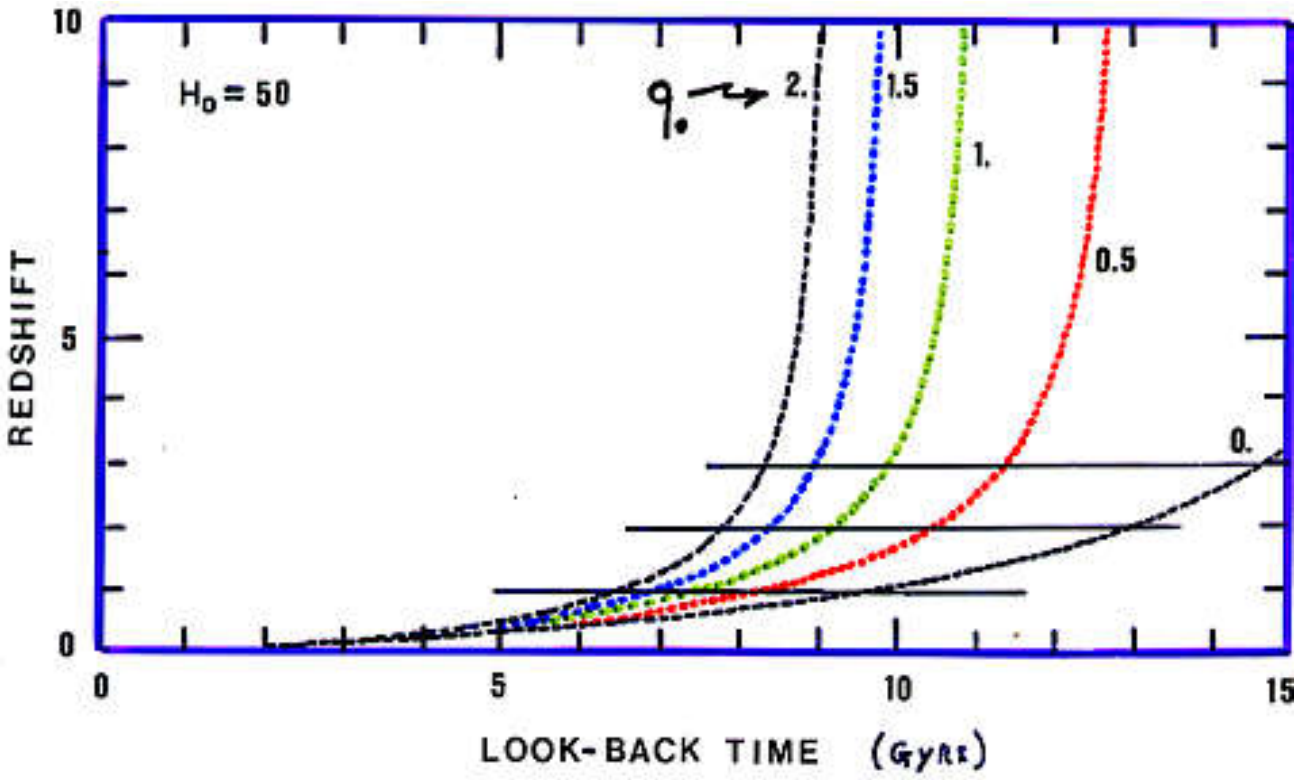

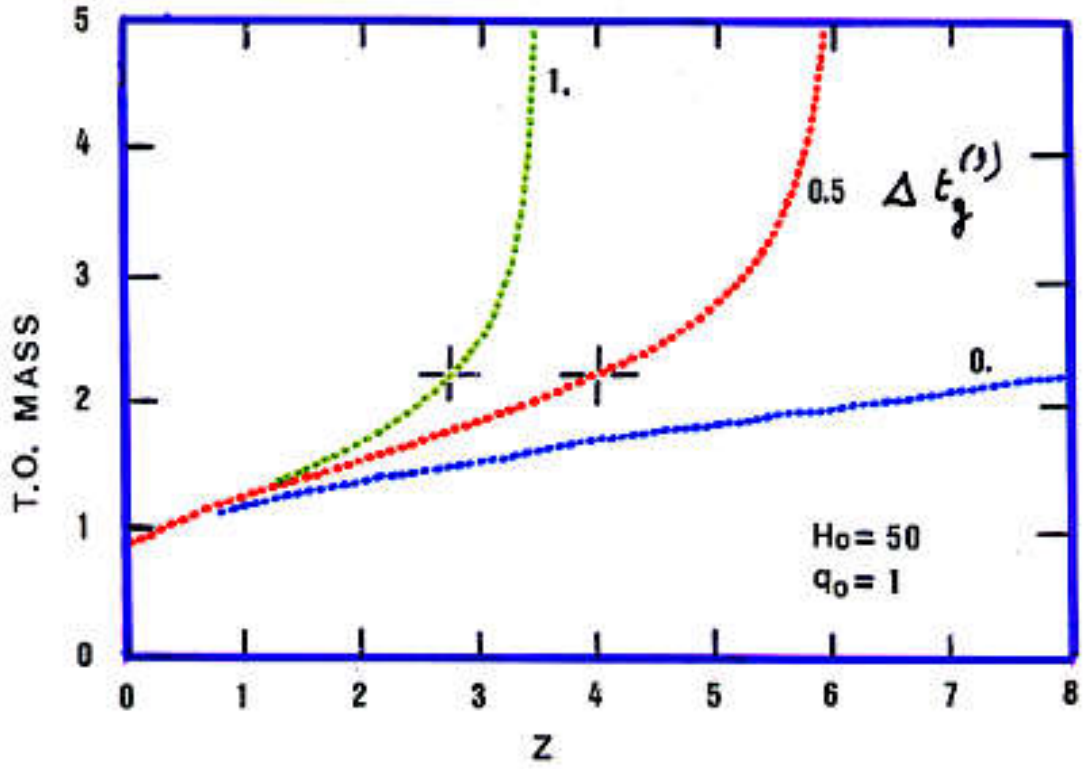

http://en.wikipedia.org/wiki/Distance_measures_(cosmology)

Humason et al. (1956)

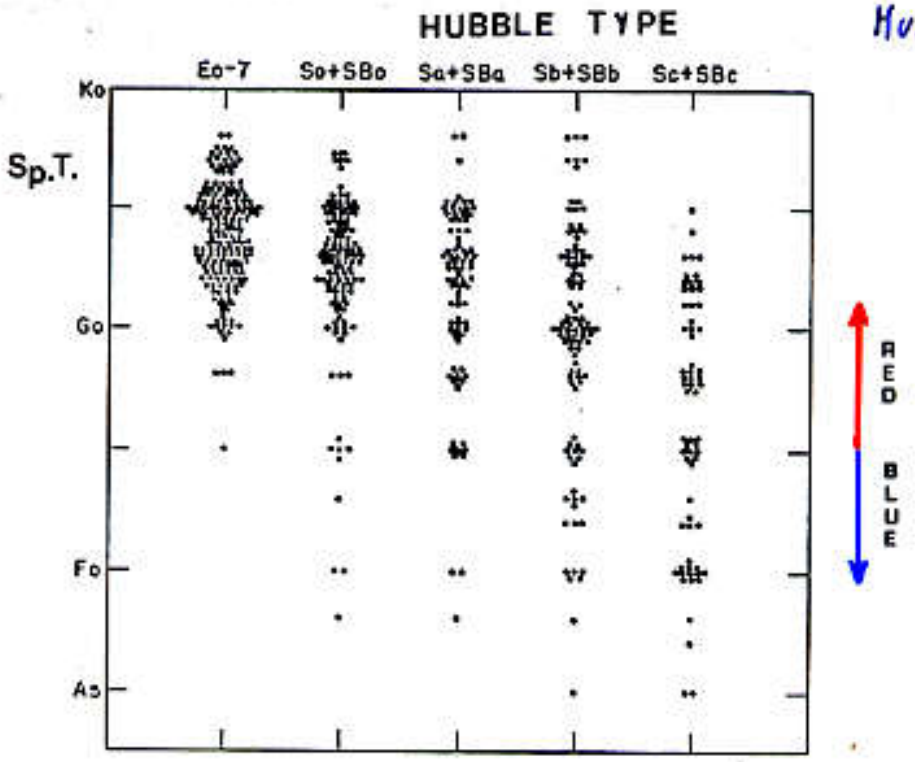

Figure 2. The distribution of spectral type as a function of nebular type for 546 nebulae from Tables I and II.

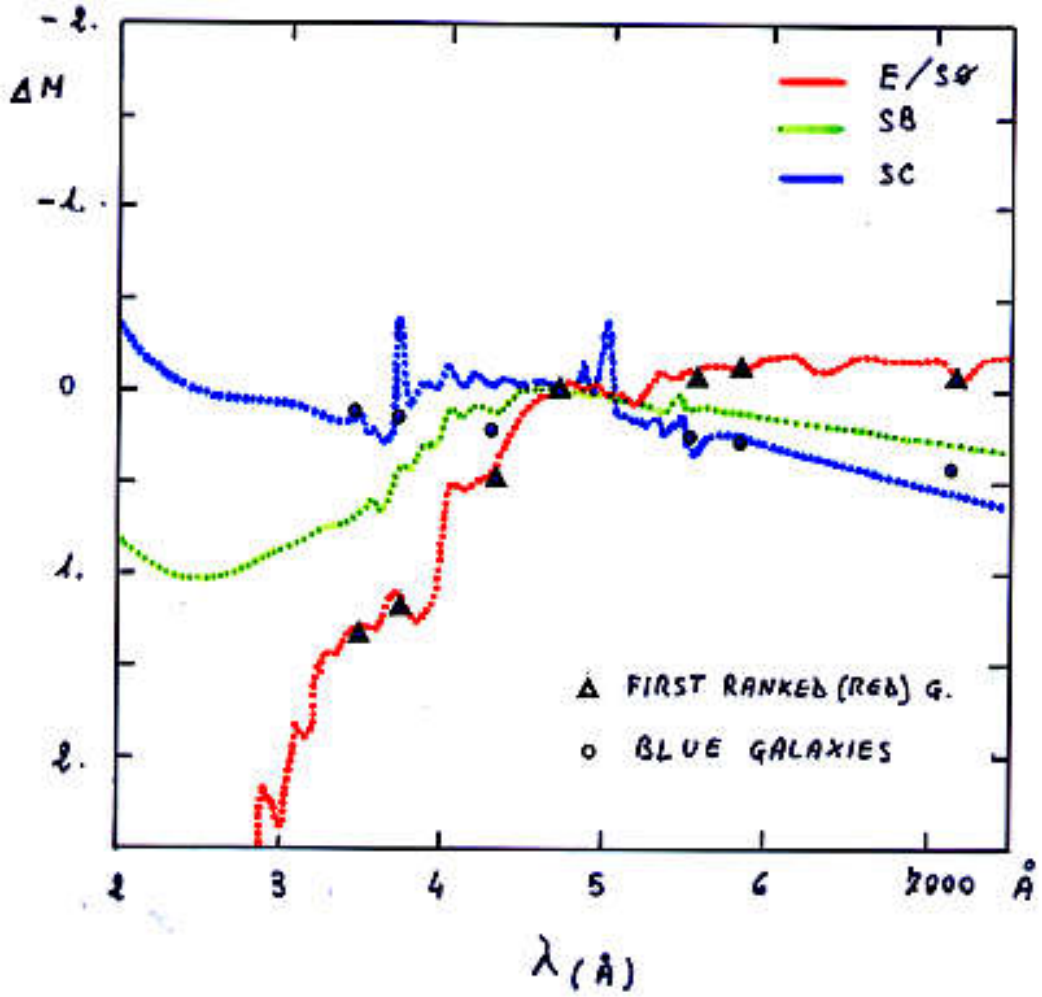

Un diagramma colore-magnitudine tipo (l'ammasso globulare M3)

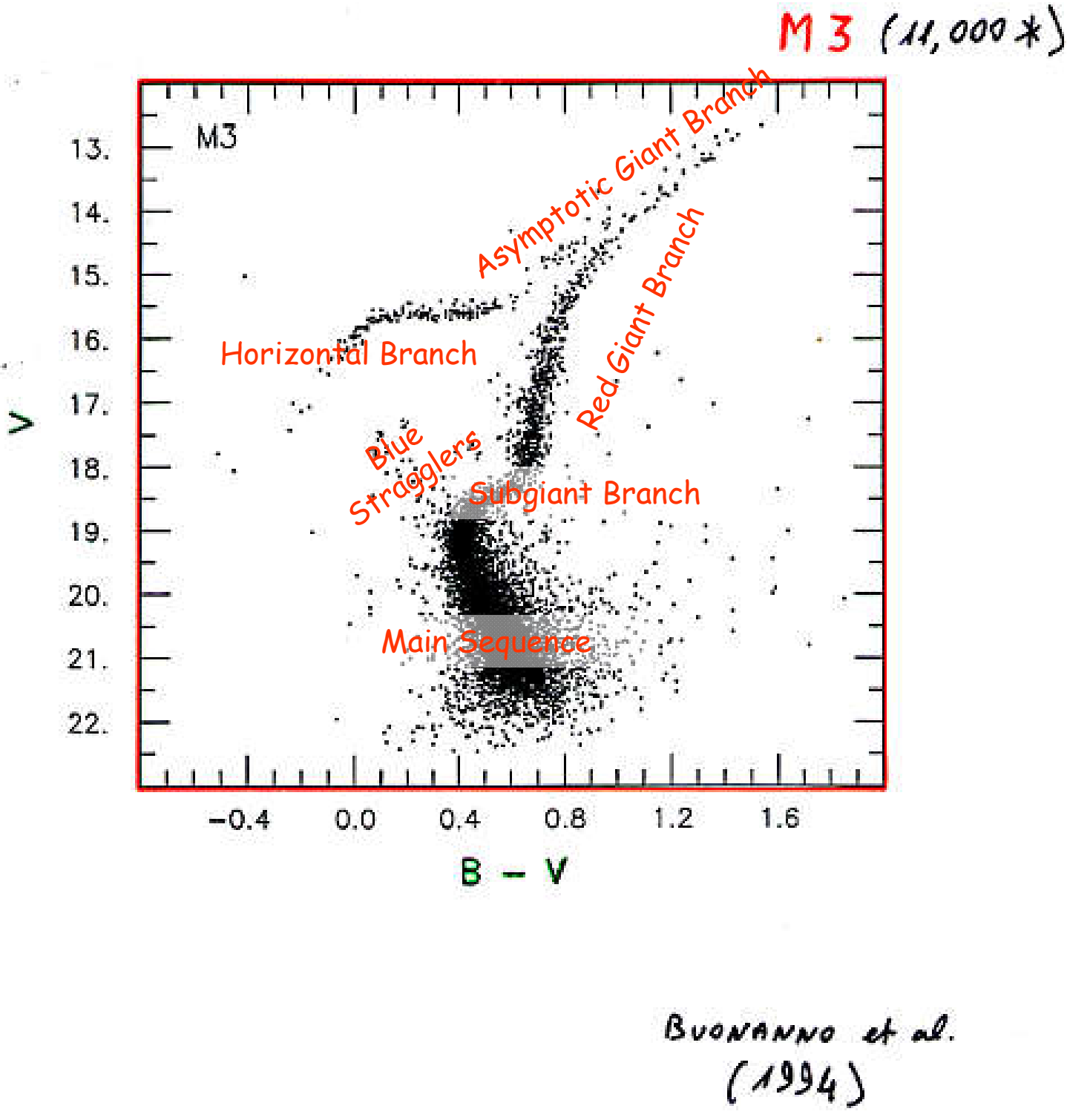

B^{2}FH (1956)

5 October 1956, Volume 124, Number 3223 **SCIENCE**

Origin of the Elements in Stars

F. Hoyle, William A. Fowler,
G. R. Burbidge, E. M. Burbidge

Experimental (*1, 1a*) and observational (*2–6*) evidence has continued to accumulate in recent years in support of the theory (*7–10*) that the elements have been and are still being synthesized in stars. Since the appearance of a new and remarkable analysis by Suess and Urey (*11*) of the abundances of the elements, we have found it possible to explain, in a general way, the abundances of practically all the isotopes of the elements from hydrogen through uranium by synthesis in stars and supernovae. In this article we wish to outline in a qualitative fashion the essentially separate mechanisms which are required in stellar synthesis (*12*).

Thermal Conversion of Pure Hydrogen through Helium to Iron

As long as extremely high temperatures in excess of 5×10^9 degrees Kelvin are not under consideration, the general tendency of nuclear reactions inside stars is to increase the average binding energy per nucleon. For a given temperature and density and for a given time scale of op- in some cases by resonance penetration. Since barrier effects become less severe as the temperature increases, it follows that the binding energies increase with temperature. This will become clear from the following examples.

At temperatures from about 10^7 to 5×10^7 degrees in main-sequence stars, hydrogen is transformed to helium, $4H^1 \rightarrow He^4$, with an average binding energy of 7.07 million electron volts (Mev) per nucleon. We emphasize that the proton-proton sequence of reactions makes possible the production of helium starting only with hydrogen. The recent discovery of the free neutrino as reported by Cowan *et al.* (*1a*) leads to increased confidence in the existence of the primary proton-proton interaction which proceeds through prompt electron-neutrino emission. At temperatures from 10^8 to 2×10^8 degrees in red giant stars, He^4 is transformed principally to C^{12}, O^{16}, and Ne^{20} with an average binding energy of 7.98 Mev per nucleon. The important roles of the ground state of Be^8 and of the second excited state of C^{12} in expediting the primary process of helium fusion, $3He^4 \rightarrow C^{12}$, have recently been

appreciably greater atomic weight than Fe^{56}.

The situation, then, is that a thermal "cooking" of pure hydrogen yields principally He^4 and the α-particle nuclei with $A = 4n$, $Z = 2n$, $n = 3$, 4, 5, 6, 7, 8, 9, and 10 (C^{12} to Ca^{40}), together with nuclei centered around Fe^{56}. These are the most abundant nuclei. Moreover, the relative abundances that have been calculated for these nuclei, and particularly for the 20-odd isotopes of titanium, vanadium, chromium, manganese, iron, cobalt, and nickel, show good agreement with observed abundances. The original equilibrium calculations by Hoyle (*7*) have been considerably improved by taking into account the low-lying excited states of the iron-group nuclei and of the radioactive nuclei which ultimately decay to them, and by statistically weighting each state according to its observed spin or that expected on nuclear shell theory. Typical results for the equilibrium abundances of the chromium isotopes at 3.8×10^9 degrees are indicated in Table 1.

We regard results similar to those presented in Table 1 as giving strong support to the view that the elements under consideration were synthesized inside stars and that they became subsequently distributed in space, either by slow emission from late-type giants or by catastrophic explosion, as for instance in supernovae.

Thermal Reactions of Hydrogen and Helium with Light Elements

More complicated effects arise when the thermal cooking is considered, not of completely pure hydrogen, but of hydrogen adulterated with a small proportion of the elements mentioned in the previous paragraphs. When a second-genera-

Clocks

$L\,t = E$

KELVIN-HELMHOLTZ $\quad E = \dfrac{GM^2}{R}$

$$t_\odot \sim \frac{E}{L} \sim \frac{GM^2}{RL} \sim \frac{6\,10^{-8}\,(2\,10^{33})^2}{7\,10^{10}\;4\,10^{33}}\ \text{sec.}$$

$$t_\odot \sim \frac{6\,10^{25}}{7\,10^{10}\;3\,10^{7}}\ \text{yr} \Rightarrow \boxed{\frac{2}{7}\,10^{8}\ \text{yr}}$$

NUCLEARE $\quad E = \alpha\, Mc^2$, $\alpha \downarrow 0.007$

$$t_\odot \sim \frac{E}{L} \sim \frac{\alpha Mc^2}{L} \sim \frac{7\,10^{-3}\,2\,10^{33}\,9\,10^{20}}{4\,10^{33}}\ \text{sec.}$$

$$t_\odot \sim \frac{63}{2}\,\frac{10^{17}}{3\,10^{7}}\ \text{yr} \sim \frac{63}{6}\,10^{10} \sim \boxed{10^{11}\ \text{yr}}$$

DIPENDENZA DALLA CHIMICA

$$\begin{cases} t \propto \dfrac{M}{L} \\ L \propto \dfrac{M^3/\mu^4}{\tilde{K}} \end{cases} \Rightarrow t \propto \frac{M\tilde{K}}{M^{\frac{3}{2}}/\mu^4} \propto \boxed{\frac{1}{M^2}\left(\frac{\tilde{K}}{\mu^4}\right)}$$

quindi: se $M = fix$ $\quad t \uparrow$ se $Z \uparrow$, $t \downarrow$ se $\gamma \uparrow$

se $t = fix$ $\quad M_{TO} \uparrow$ se $Z \uparrow$, $M_{TO} \downarrow$ se $\gamma \uparrow$

$$
\begin{cases}
1) & \nabla P = -\rho g \Rightarrow \dfrac{P}{R} \propto \rho \dfrac{M}{R^2} \Rightarrow P \propto \rho \dfrac{M}{R} \\
2) & \nabla M = 4\pi R^2 \rho \\
3) & \nabla L = 4\pi R^2 \varepsilon \\
4) & \nabla T = -\dfrac{3\rho k L}{16\pi a c T^3 R^2} \Rightarrow \dfrac{T}{R} \propto \dfrac{\rho L}{T^3 R^2} \Rightarrow T^4 \propto \dfrac{\rho L}{R} \\
5) & P = \dfrac{\rho k T}{\mu H} \Rightarrow P \propto \rho T
\end{cases}
$$

$$
\rho T \propto \rho \frac{M}{R}
$$

$$
\Downarrow
$$

$$
\begin{cases}
T \propto \dfrac{M}{R} \\
T^4 \propto \dfrac{\rho L}{R}
\end{cases}
\Rightarrow \frac{M^4}{R^4} \propto \frac{M}{R^4} L \Rightarrow \boxed{L \propto M^3}
$$

$$
L\, t \propto M
$$

$$
\Downarrow
$$

$$
\begin{cases}
t \propto \dfrac{M}{L} \\
L \propto M^3
\end{cases}
\Rightarrow \boxed{\begin{aligned} t &\propto M^{-2} \\ t &\propto L_{T.O.}^{-2/3} \end{aligned}}
$$

http://en.wikipedia.org/wiki/Stellar_structure

Relazioni di scala per le stelle in Sequenza Principale

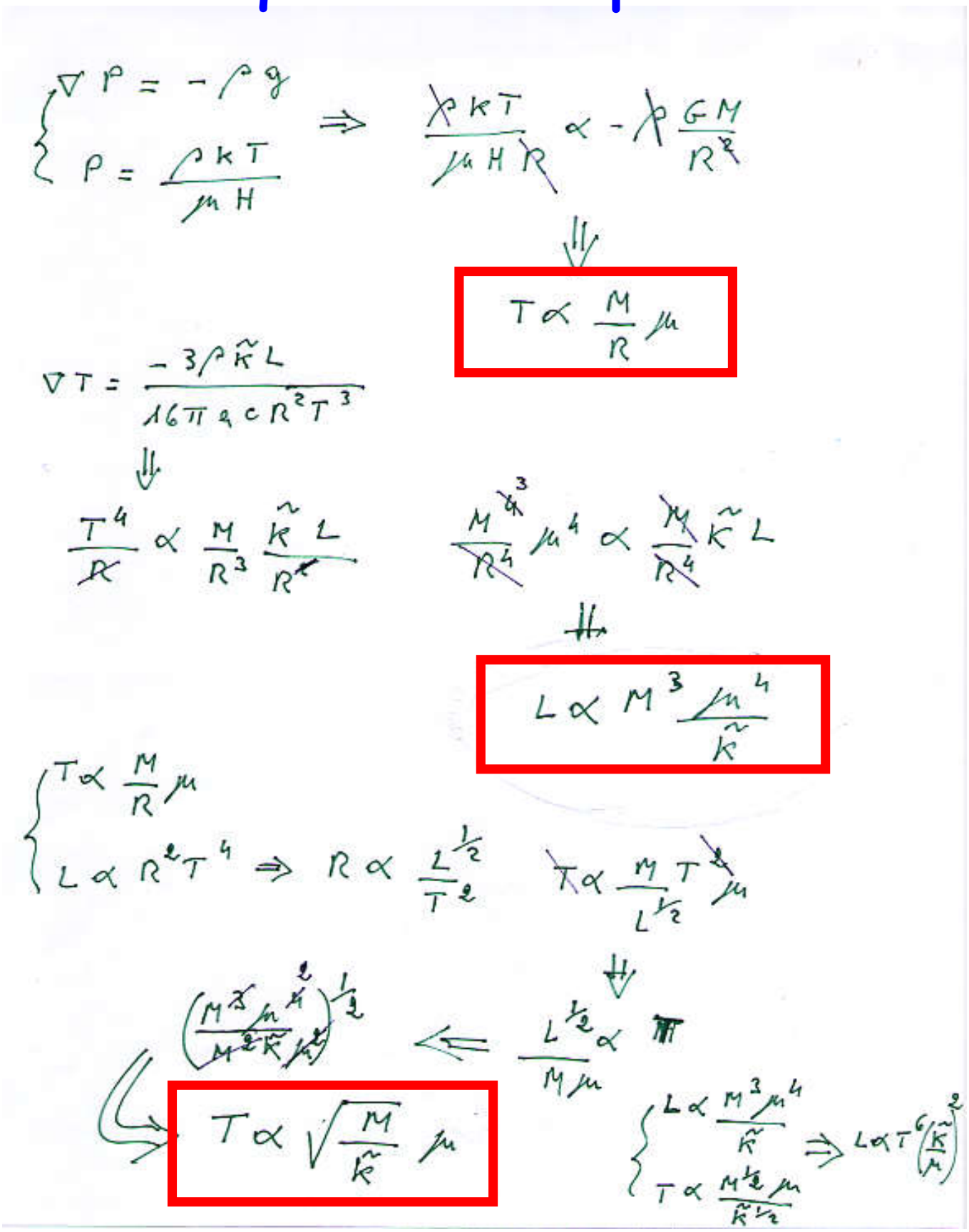

http://en.wikipedia.org/wiki/Mass-luminosity_relation

Il punto di Turn Off come indicatore di eta'

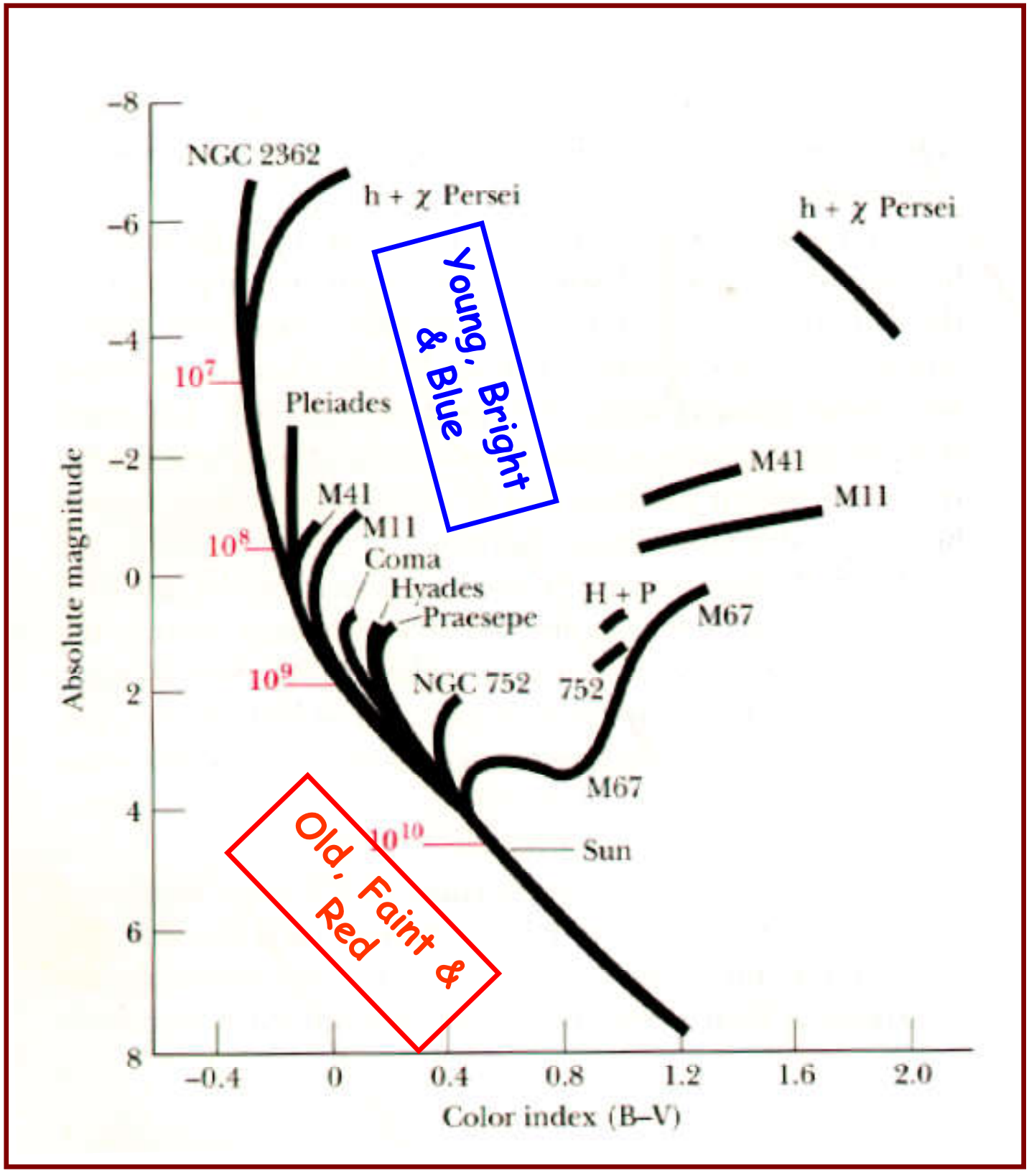

Il punto di Turn Off come indicatore di eta'

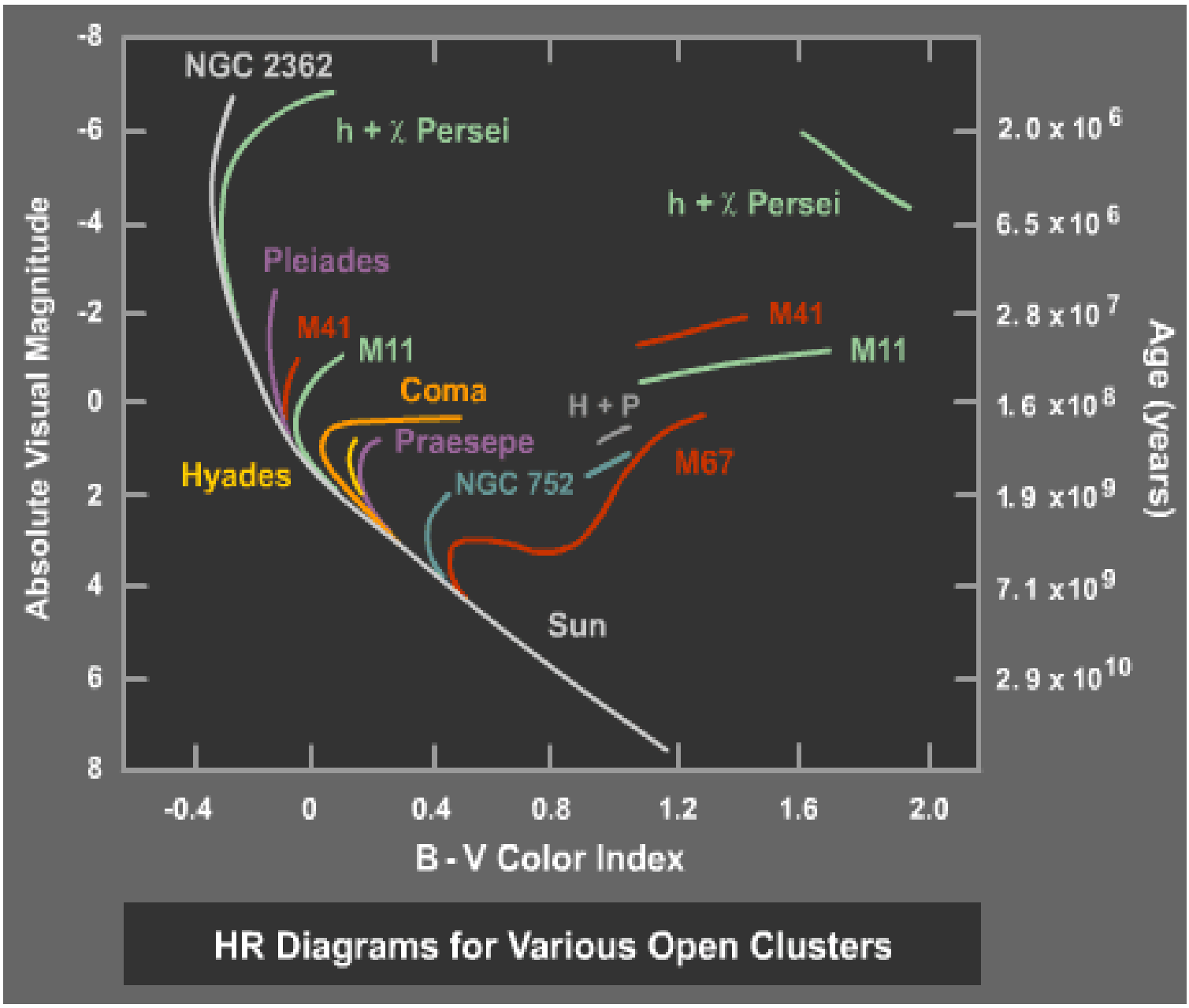

HR Diagrams for Various Open Clusters

The Clock

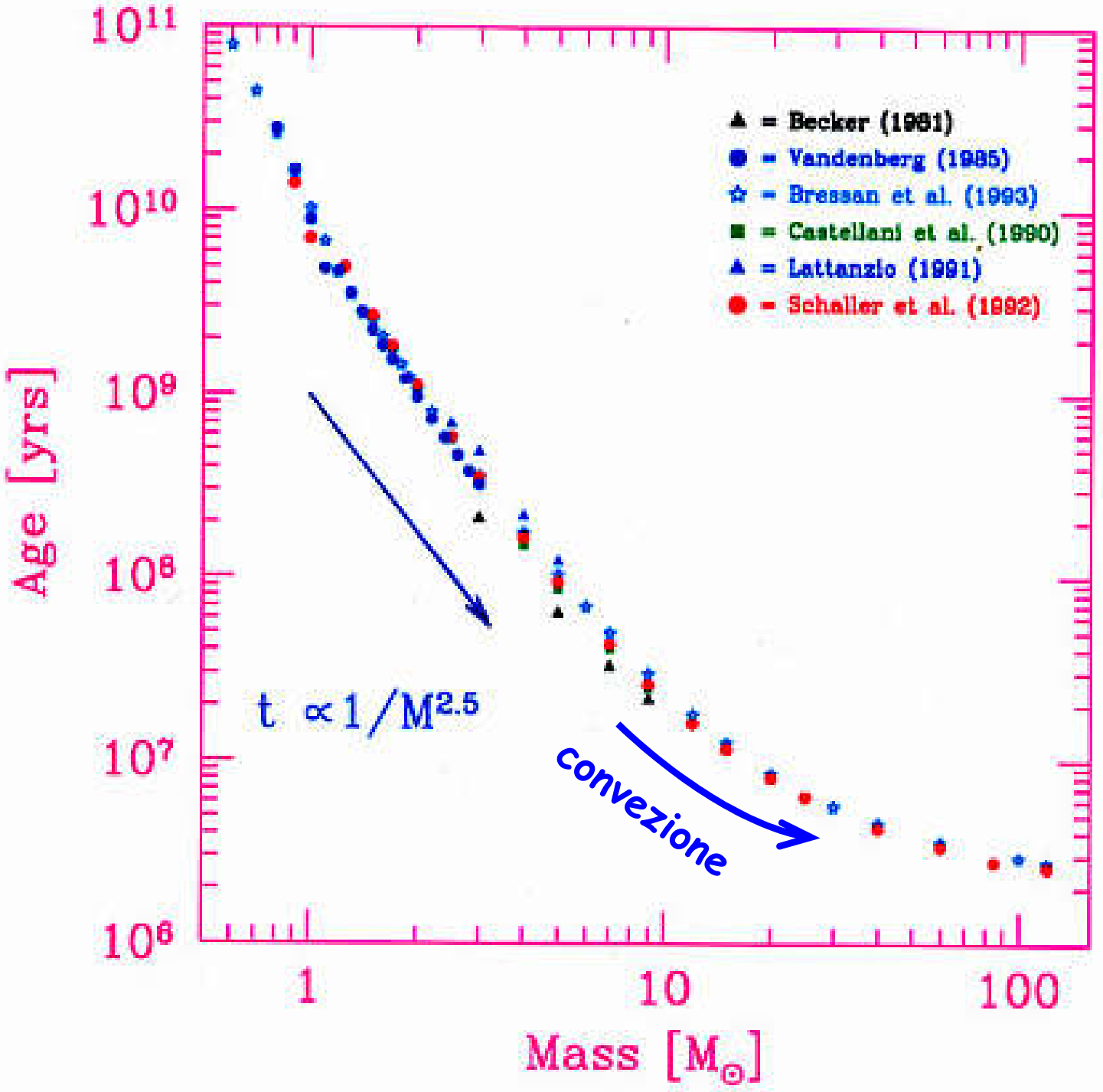
Age [yrs]
10^{11}
10^{10}
10^{9}
10^{8}
10^{7}
10^{6}
1
10
100
Mass [$M_\odot$]
▲ = Becker (1981)
● = Vandenberg (1985)
☆ = Bressan et al. (1993)
■ = Castellani et al. (1990)
▲ = Lattanzio (1991)
● = Schaller et al. (1992)
$t \propto 1/M^{2.5}$
convezione

Peso Molecolare Medio

$$\mu = \frac{\sum n_j m_j}{\sum n_j}$$

$\forall\ j$ = tutte le specie chimiche

GAS NEUTRO

$$\mu_N = \frac{\rho X + \rho Y + \rho Z}{\frac{\rho X}{H} + \frac{\rho Y}{4H} + \frac{\rho Z}{2ZH}} \sim \frac{H}{X + \frac{Y}{4} + \frac{Z}{2Z}}$$

$\frac{Z}{2Z} \sim 0$

PLASMA TOT IONIZZATO

$$\mu_i = \mu_N + \frac{\rho}{\frac{\rho X}{H} + \frac{2\rho Y}{4H} + \frac{2Z\rho Z}{2Z}} = \mu_N + \frac{H}{X + \frac{Y}{2} + \frac{Z}{2}}$$

$$\mu_i = \frac{H}{\left(X + \frac{Y}{4} + \frac{Z}{2Z}\right) + \left(X + \frac{Y}{2} + \frac{Z}{2}\right)} = \frac{H}{2X + \frac{3}{4}Y + \left(1 + \frac{1}{Z}\right)\frac{Z}{2}}$$

$\frac{1}{Z} \sim 0$

$$\mu_i \sim \frac{H}{2X + \frac{3}{4}Y + \frac{Z}{2}}$$

Thermometers & Clocks (effetto della metallicita')

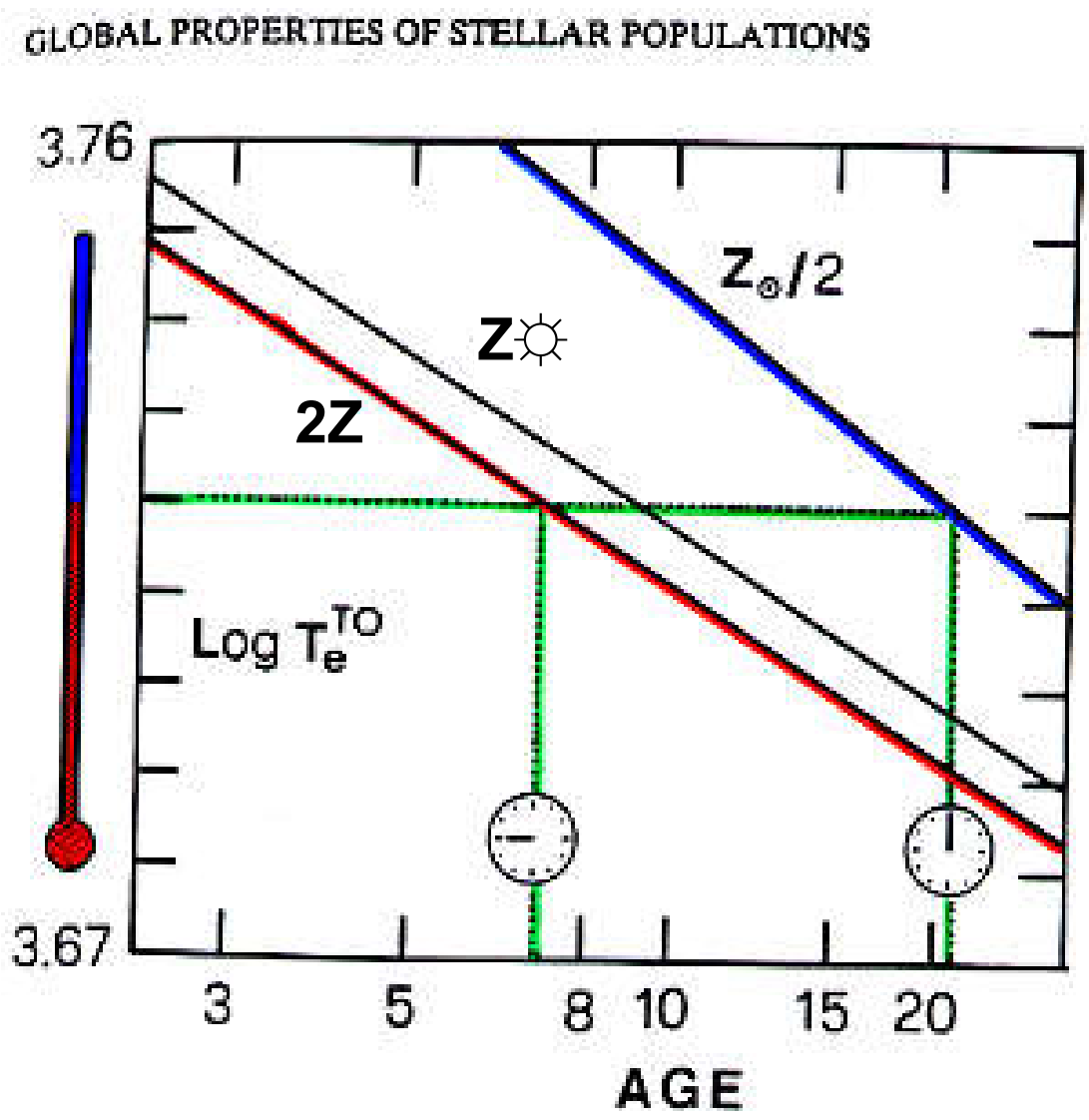

Renzini & Buzzoni (1986)

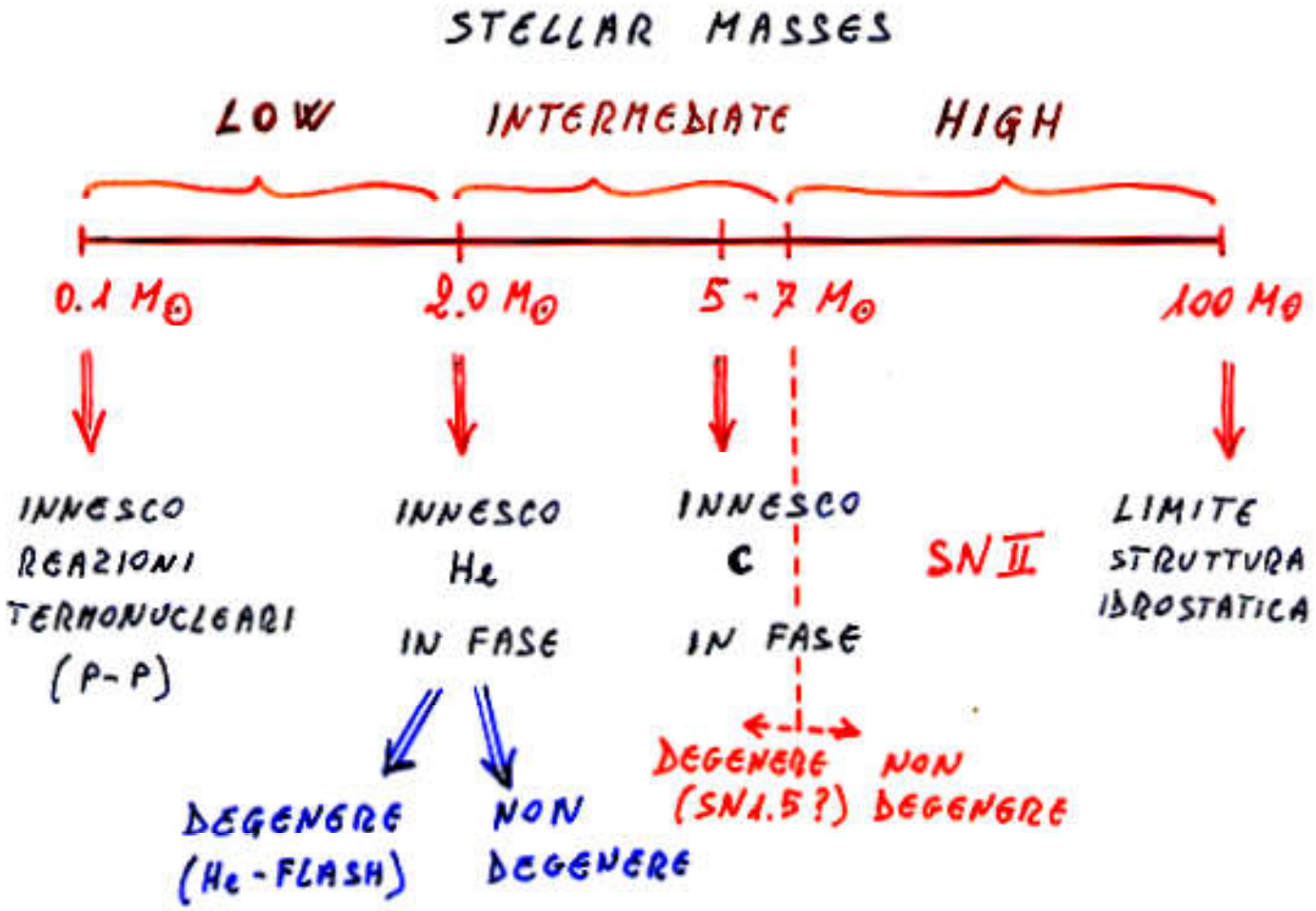

FASE	LOW-MASS	HIGH-MASS
CORE H-BURNING	MS	MS
SHELL H-BURNING	SGB RGB	1-ST GB
CORE He-BURNING	HB	1-ST BLUE LOOP
DOUBLE (MULTIPLE) SHELL BURNING	AGB	2-ND, 3-RD etc. GBs

http://it.wikipedia.org/wiki/Formazione_stellare

L'effetto della "transizione di fase" in RGB

SWEIGART, GREGGIO & RENZINI (1989)

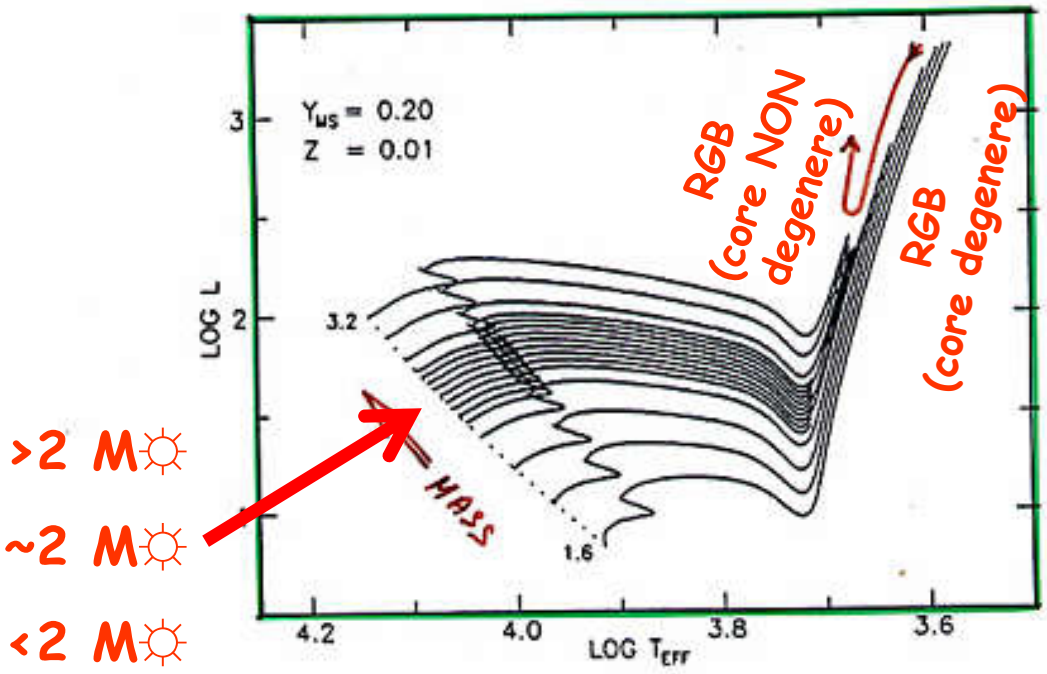

RENZINI & BUZZONI (1986)

GLOBAL PROPERTIES OF STELLAR POPULATIONS

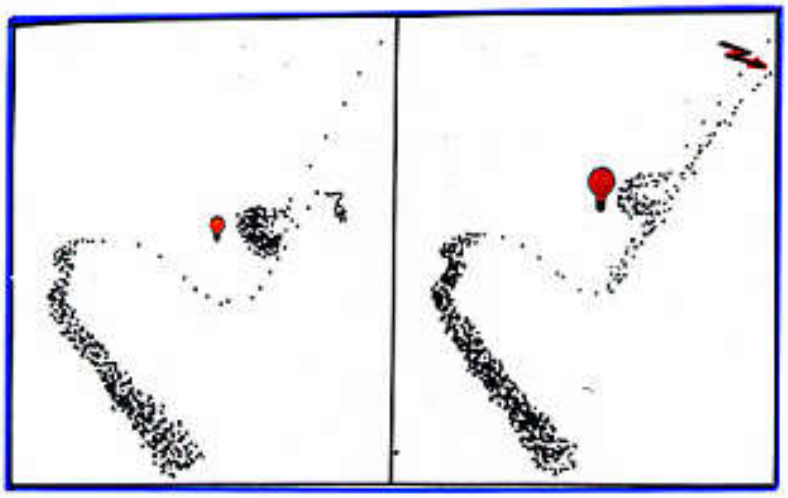

Figure 14. An artist view of the RGB phase transition. On the left panel the HR diagram of a cluster slightly younger than $t(M_{HeF})$. On the right panel the same cluster when slightly older than $t(M_{HeF})$. Note the virtual identity of the main sequences, and, by contrast, the development of the RGB. The plug indicates the point when helium ignites (non degenerately). The jagged arrow indicates the helium flash location. The growing light bulb emphasizes the brightening of the clump giants across the RGB phase transition. The AGB stays nearly the same across the transition.

DISTINCTIVE PARAMETERS IN A STELLAR POPULATION

1) AGE $\Longrightarrow$ t

2) CHEMICAL COMPOSITION $\Longrightarrow$ Z, $[Fe/H]$

3) STAR MASS DISTRIBUTION $\Longrightarrow$ IMF

4) STAR FORMATION HISTORY $\Longrightarrow$ SFR

CANONICAL ASSUMPTIONS

1) IMF $N_{(M)} \propto M_*^{-s}$ $(s = 1.35)$

2) SFR
- $\delta(0)$ → SSP
- $f(t)$ → CSP

Articoli consigliati (vedi Webpage):
http://www.bo.astro.it/~eps/lezioni/lezioni.html

- **SSP Theory (Renzini & Buzzoni 1986)**
- **Galaxy Colors (Buzzoni 2005)**
- **Spectral Properties of Galaxies (Kennicutt 1992)**
- **Energetic & Chemical evolution of Spirals (Buzzoni 2011)**

Come nascono le galassie?

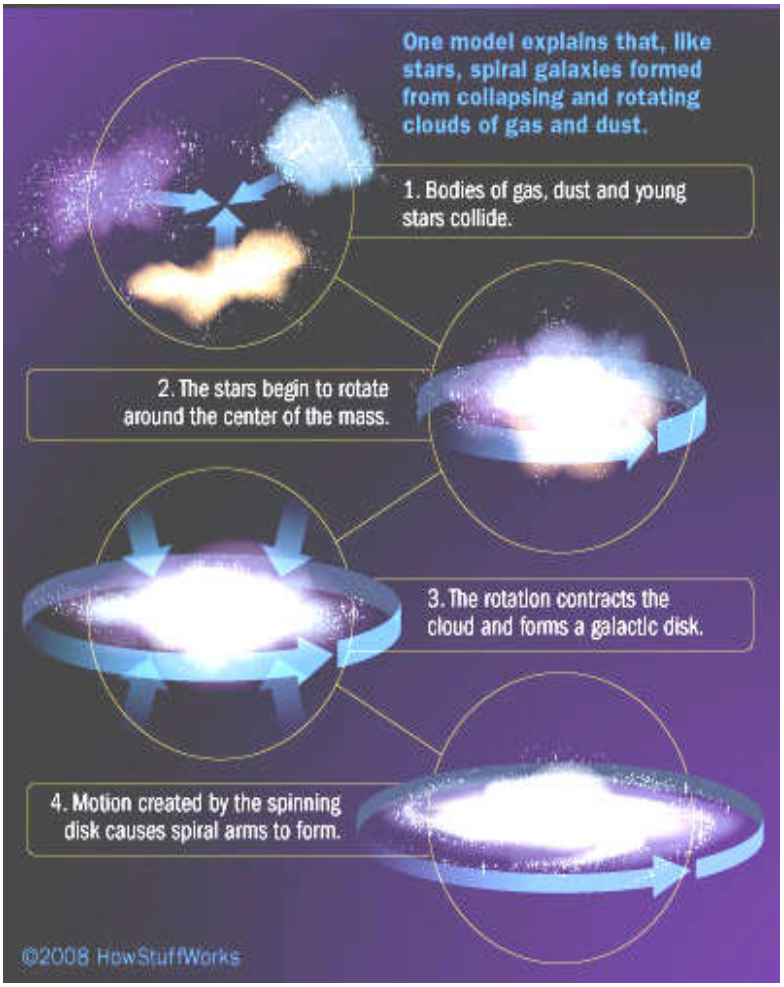

Scenario "monolitico"

(Larson 1974,1975)

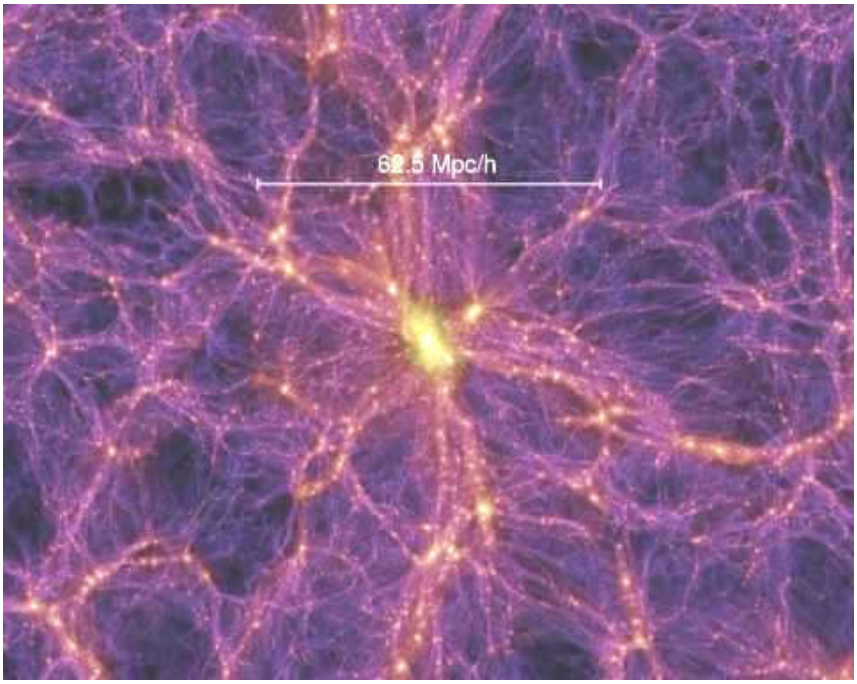

Scenario "gerarchico"

(Kauffmann & White 1993)

http://en.wikipedia.org/wiki/Galaxy_formation_and_evolution

http://en.wikipedia.org/wiki/Dwarf_galaxy_problem

Scenario Gerarchico & Cosmologia "di consenso"

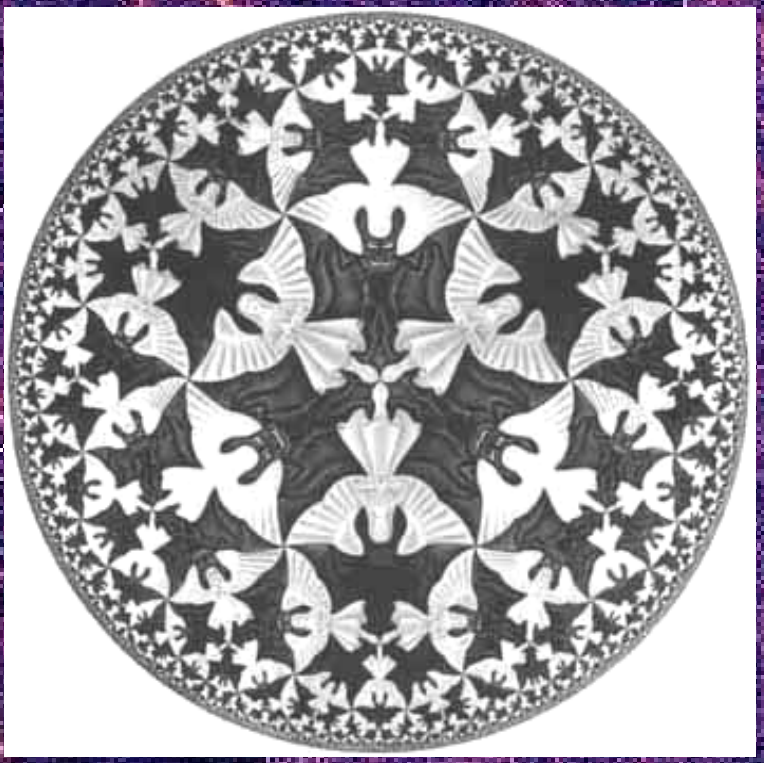

1. Dwarf galaxies must be "older" & metal poor
2. They must "surround" high-mass systems
3. Standard galaxies form "outside in"
4. Ellipticals must be "younger" (i.e. appear at "lower" z) & with a metal-poor bulge
5. Ellipticals could NOT be homologous systems (i.e. Fundamental Plane)

http://it.wikipedia.org/wiki/Via_Lattea

La Via Lattea

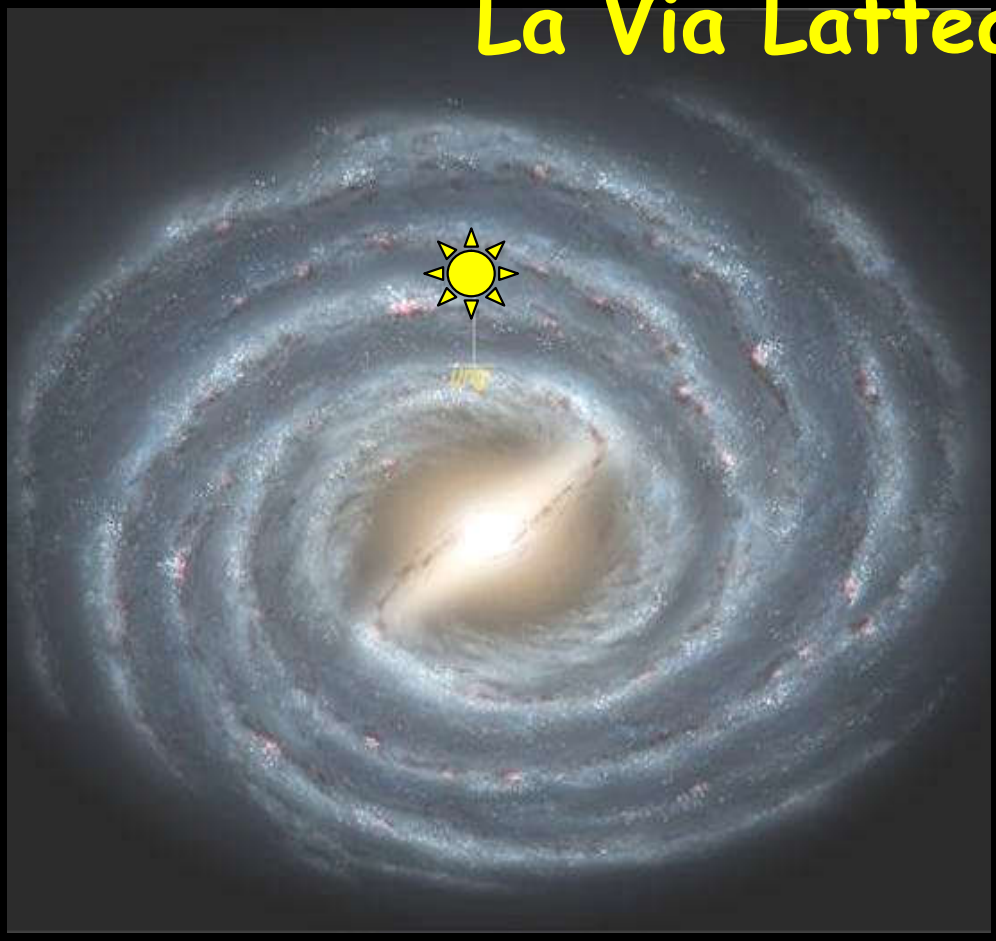

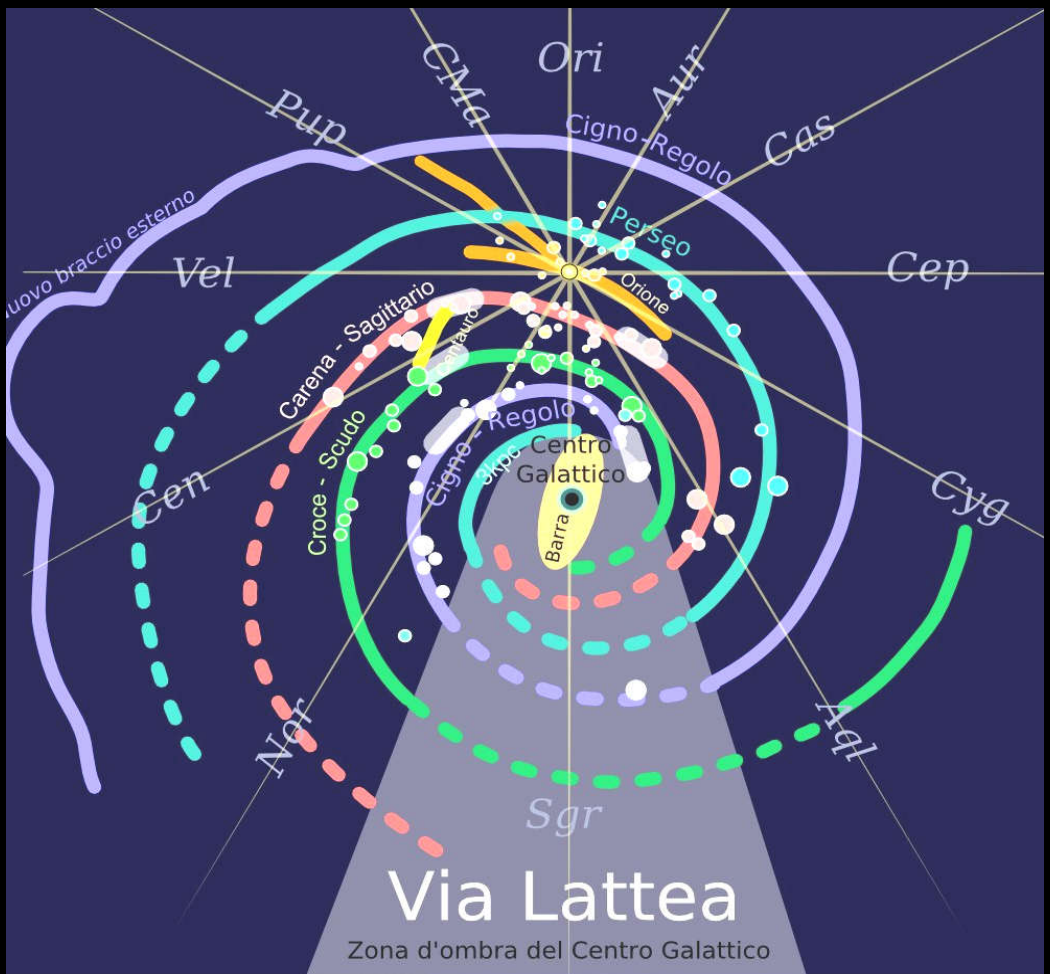

I vari bracci della Via Lattea (schematico)

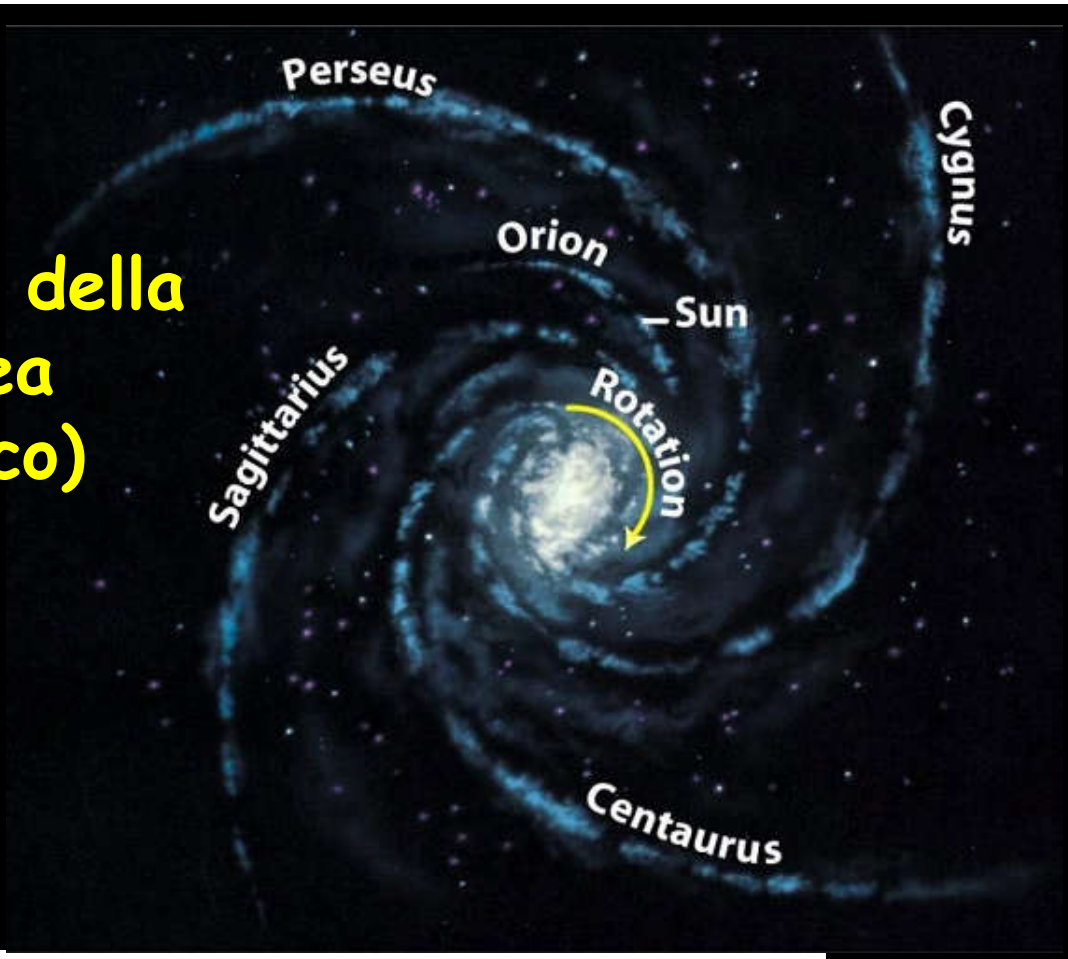

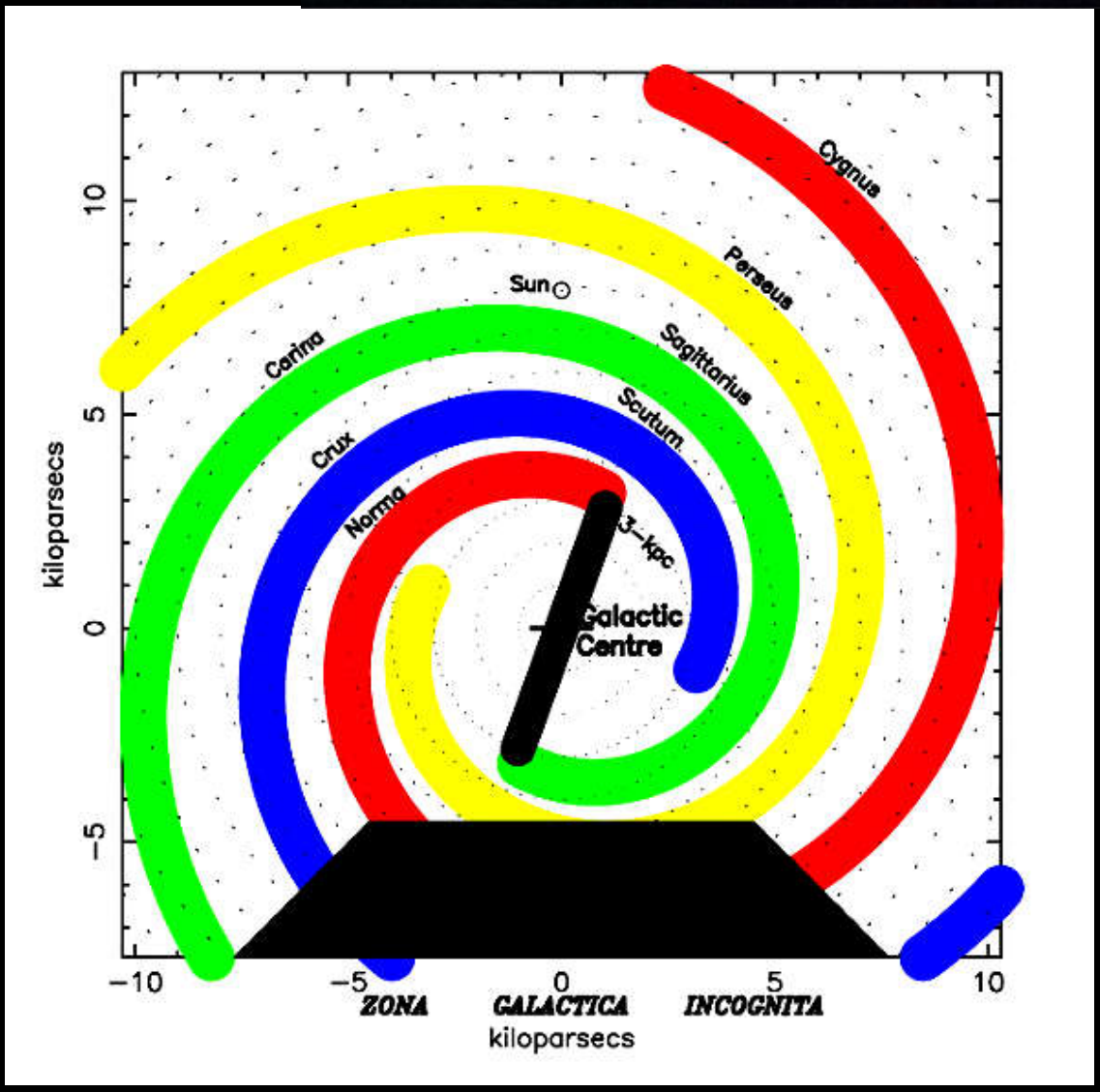

Vallée (2005)

I diversi sistemi stellari nella Via Lattea

Ammassi aperti

Verso il centro galattico

(da "dentro")

(in sezione)

Ammassi globulari

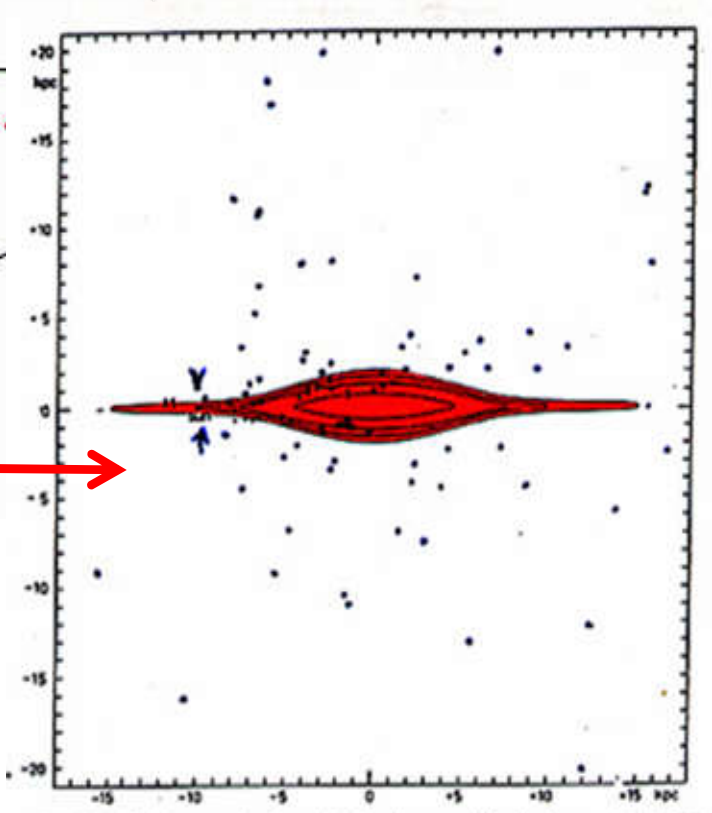

Fig. 23.6: Il *sistema galattico*: distribuzione spaziale degli ammassi globulari, proiettata su di un piano passante per il sole e perpendicolare al piano galattico, ed aree di uguale densità (riferite alle vicinanze del sole). Nel piano galattico è rappresentato, punteggiato, il sottile strato di materia interstellare con popolazione I estrema (braccio della spirale) (secondo J. H. Oort).

http://en.wikipedia.org/wiki/Globular_cluster

Gli ammassi aperti come traccianti dei bracci a spirale

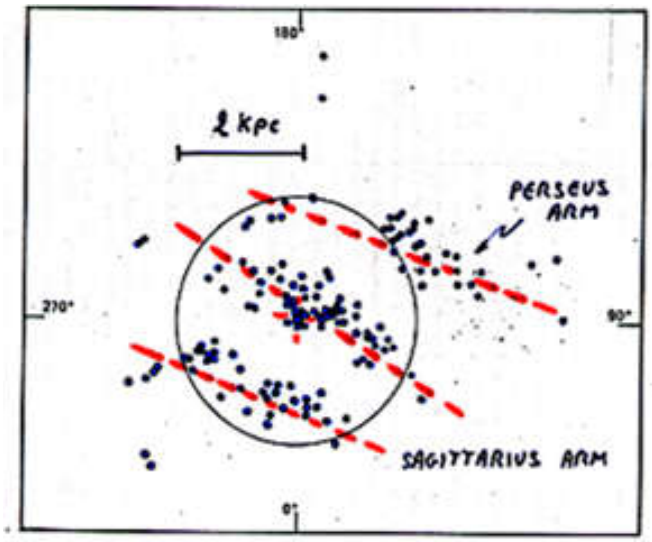

Associazioni O-B (<1Myr)

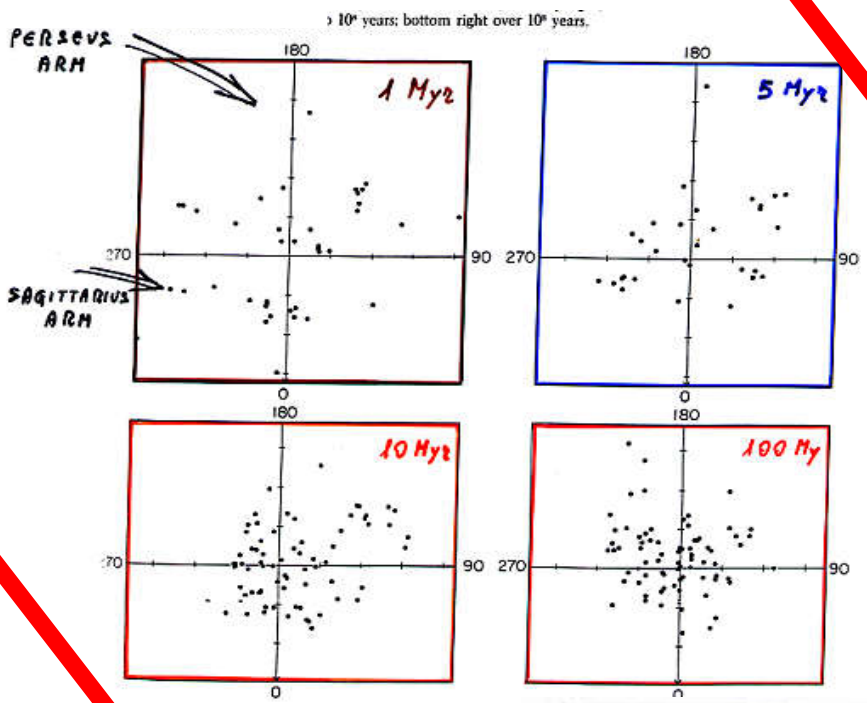

Eta'

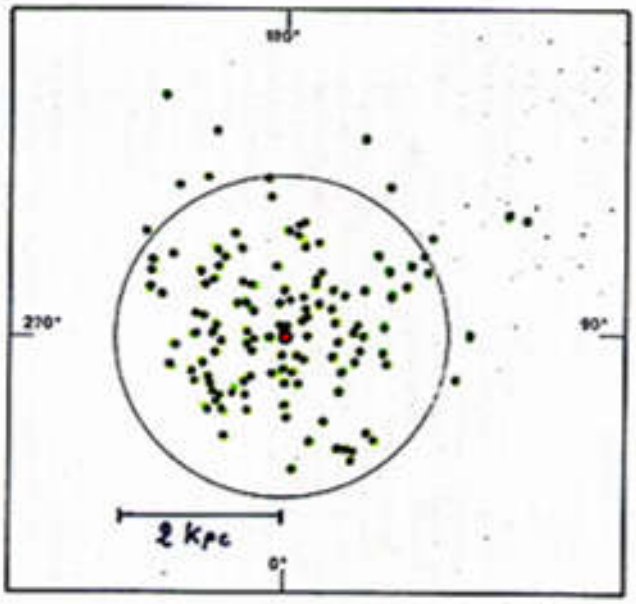

Ammassi aperti (>1Gyr)

http://it.wikipedia.org/wiki/Ammasso_aperto

Risonanze orbitali & genesi delle braccia a spirale

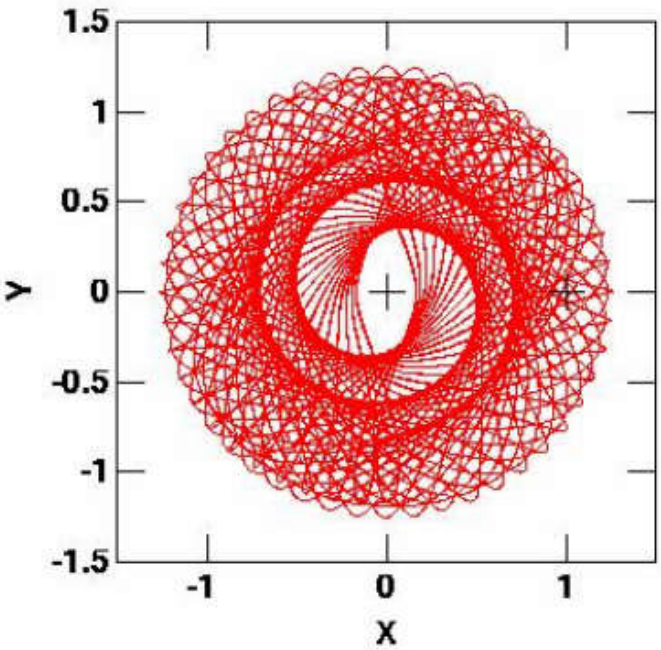

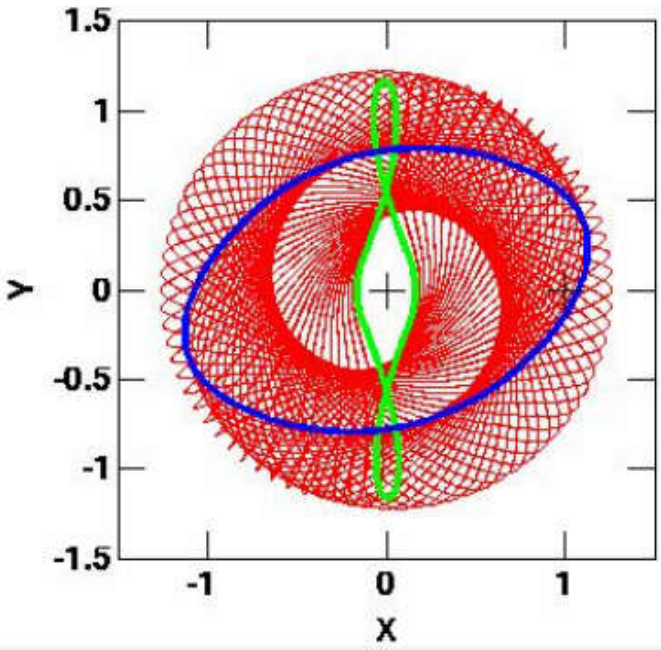

Struck (2015)

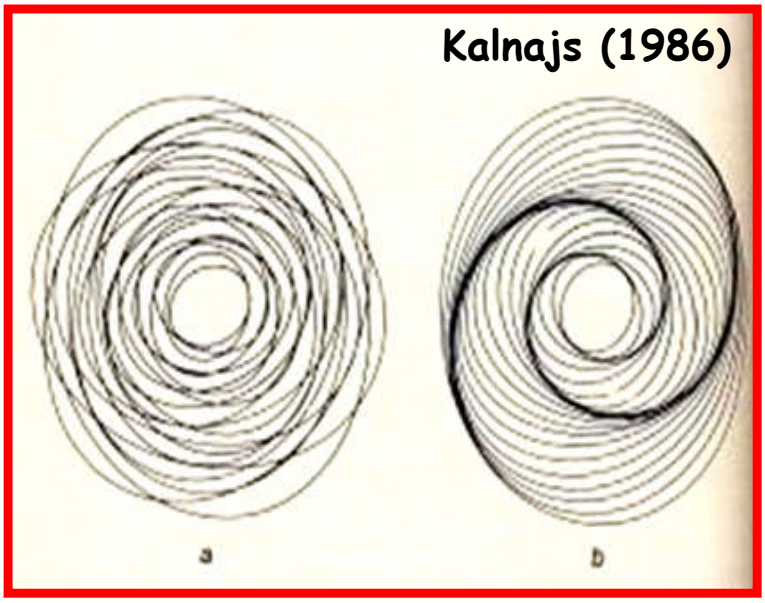

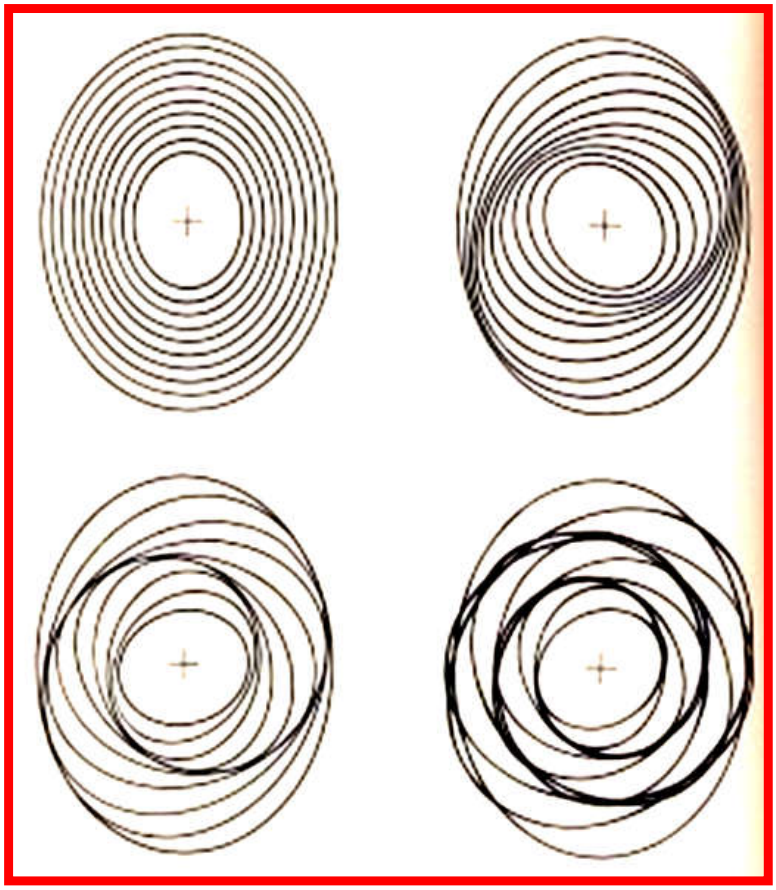

http://en.wikipedia.org/wiki/Density_wave_theory

Il meccanismo di formazione stellare

Il caso di M51

Ottico

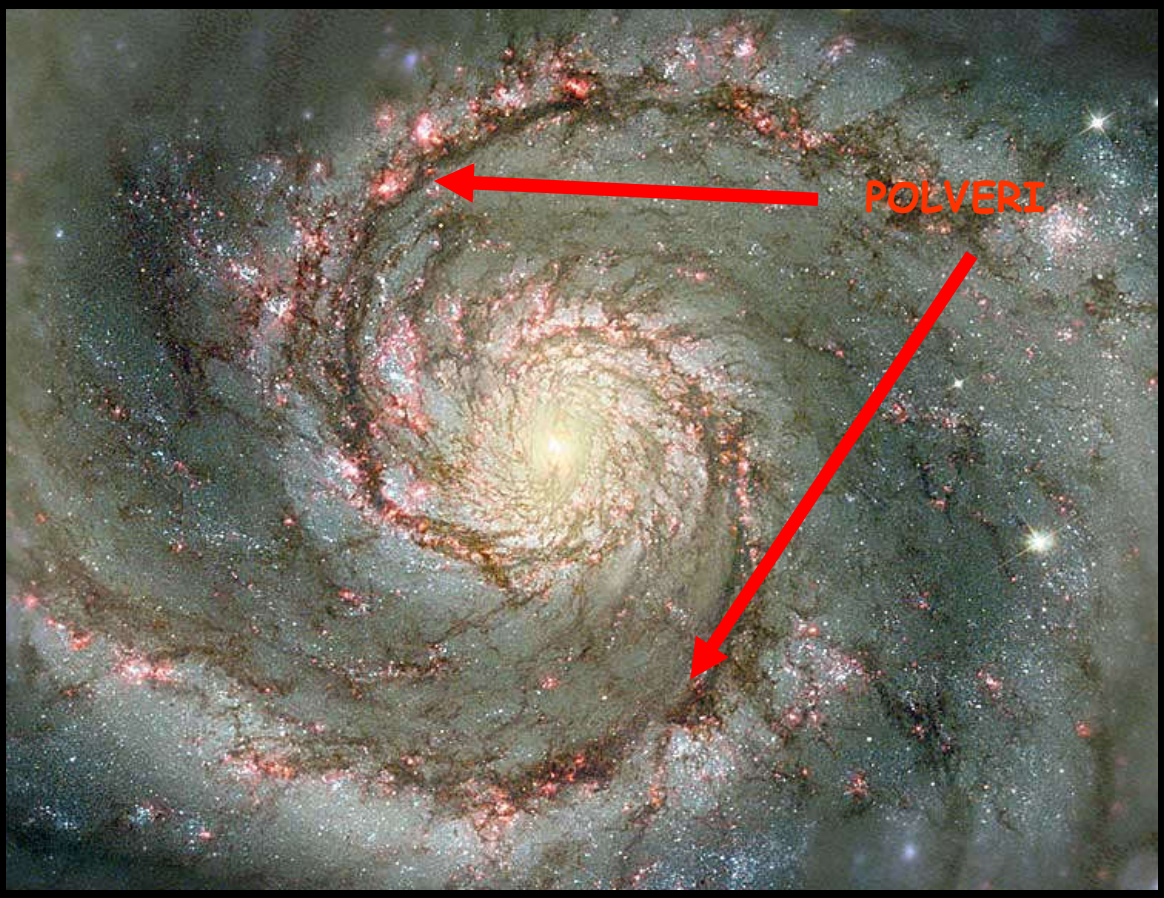

Ultravioletto

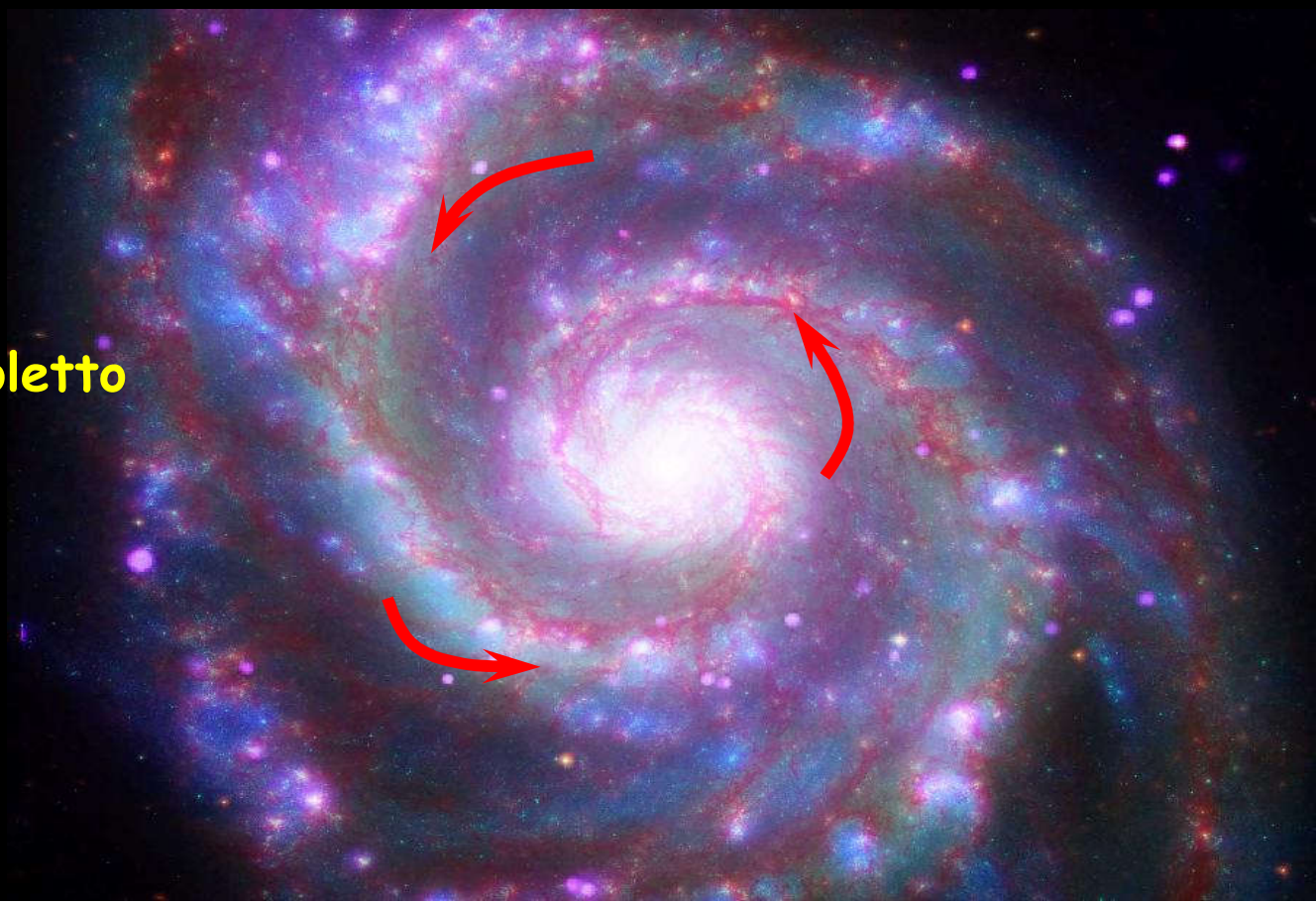

Struttura delle galassie a spirale

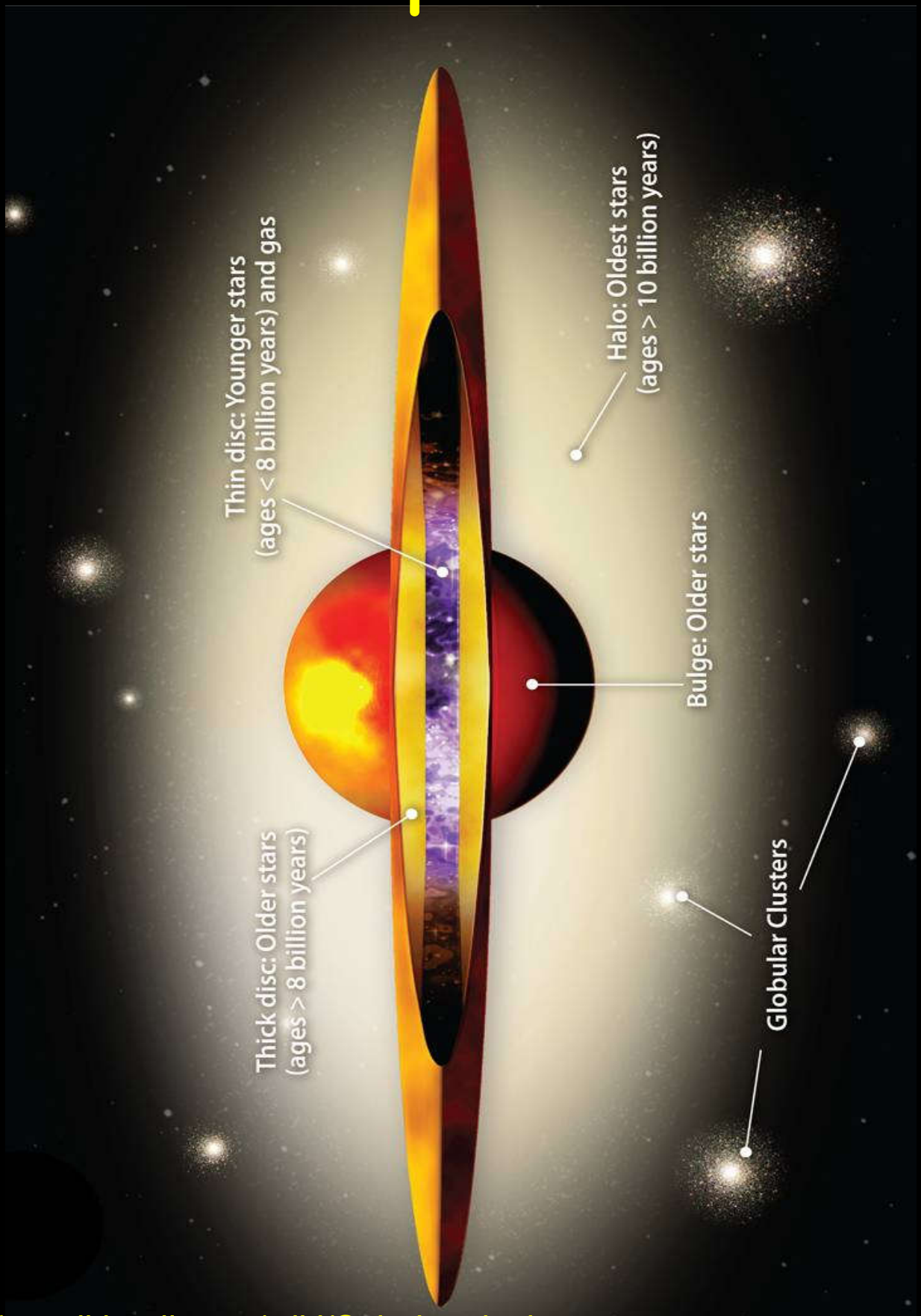

http://en.wikipedia.org/wiki/Spiral_galaxies

Il Diagramma di Bottlinger e la diagnostica delle popolazioni stellari

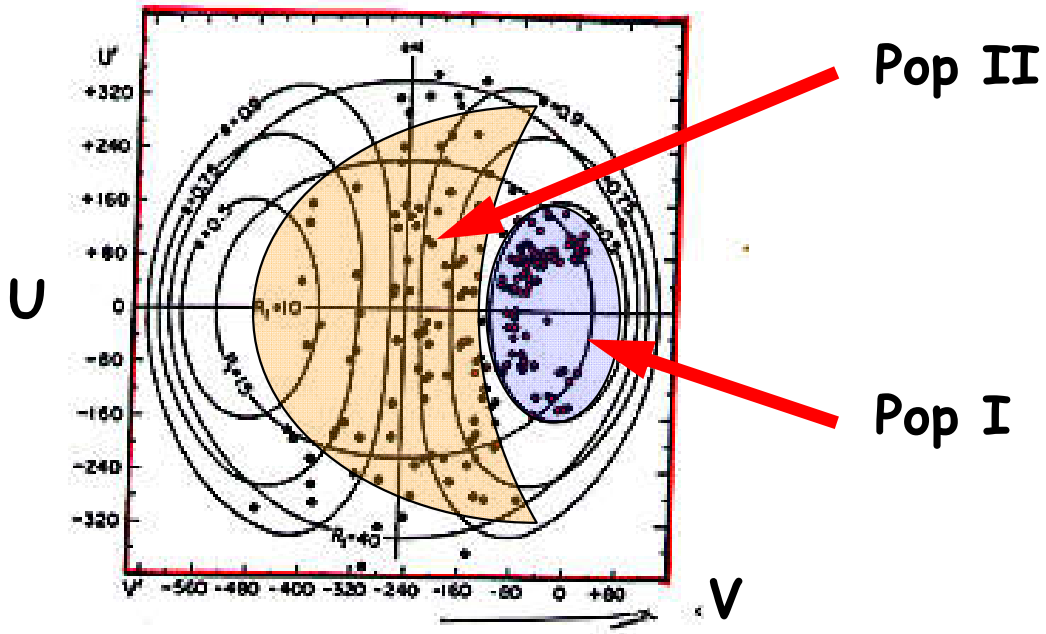

Fig. 23.10: *Diagramma di Bottlinger*. Sono riportate le componenti delle velocità galattiche U' (verso l'anticentro) e V' (nel senso della rotazione) relative ai dintorni del sole. Gli assi ortogonali rappresentano le U e V assolute. Per ogni curva è data l'eccentricità orbitale e e la distanza apogalattica R_1 in kpc. Nel capitolo 27 diremo sulle stelle (segnate con •) aventi un eccesso nell'ultravioletto $\delta\,(U-B) > +0^m.16$, cioè le stelle povere di metalli della popolazione II di « halo ». Queste sono, incidentalmente, stelle veloci con grande velocità spaziale. Con o sono segnate le stelle con $\delta\,(U-B) < +0^m.16$, le quali costituiscono una transizione dalla popolazione II di halo alla popolazione del disco galattico, con orbite meno eccentriche (secondo O. J. Eggen).

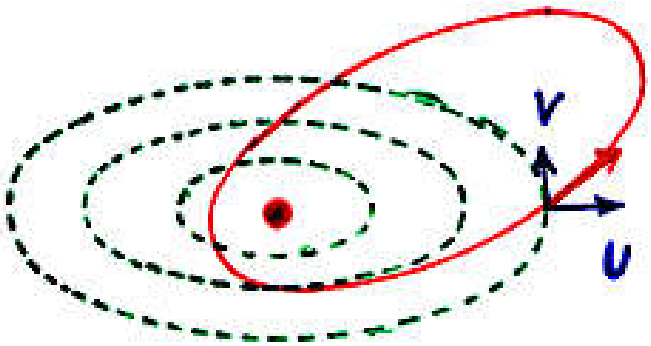

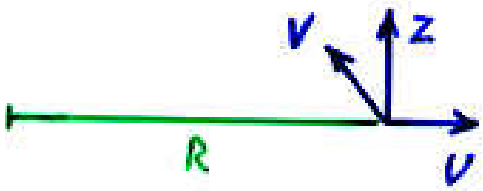

Il Diagramma di Bottlinger - 2

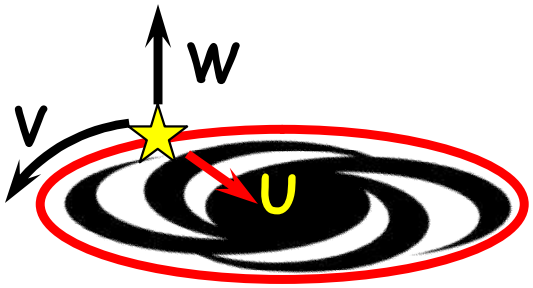

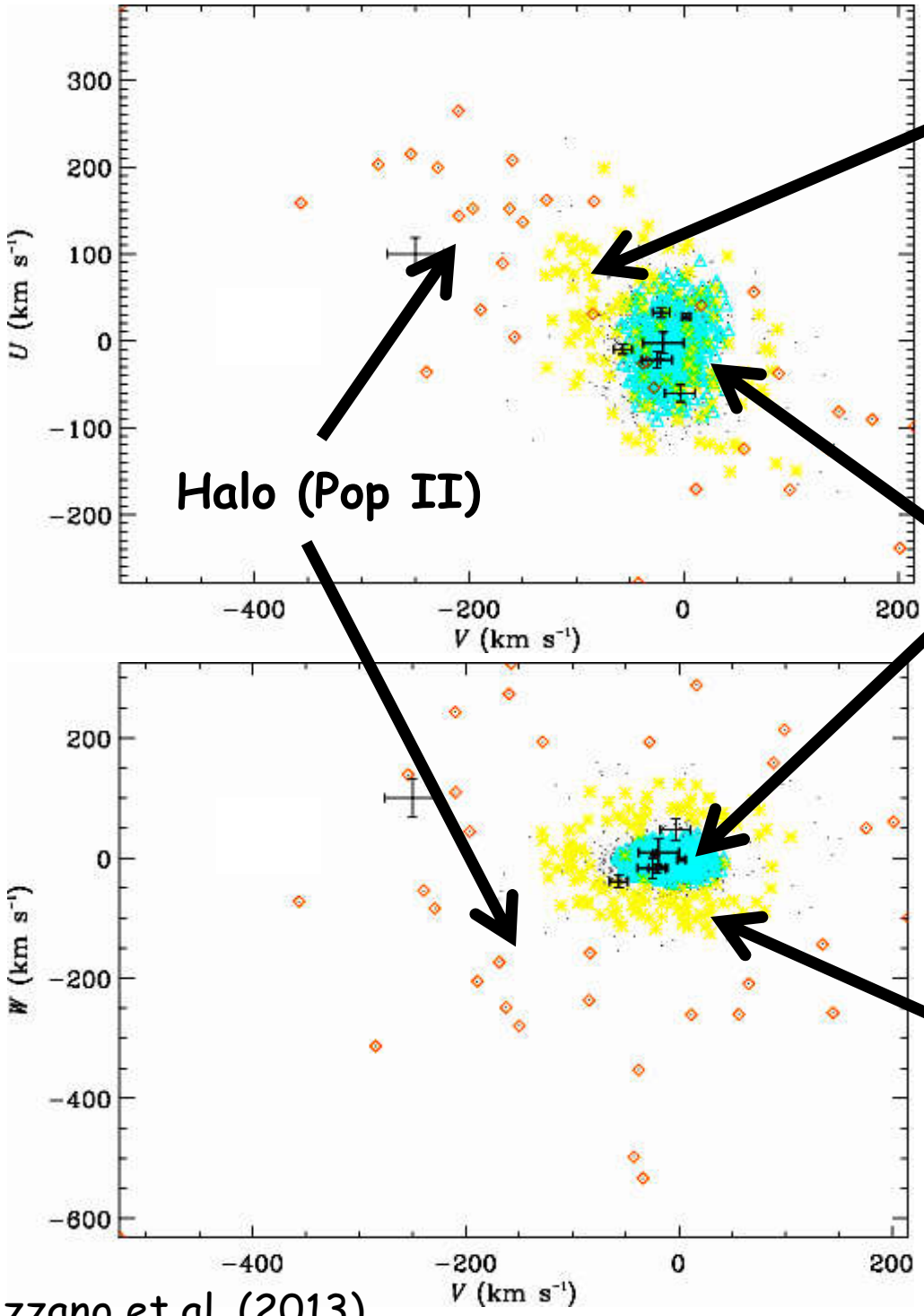

Gazzano et al. (2013)

La struttura verticale del disco

SANDAGE (1982)

SANDAGE & FOUTS (1987)

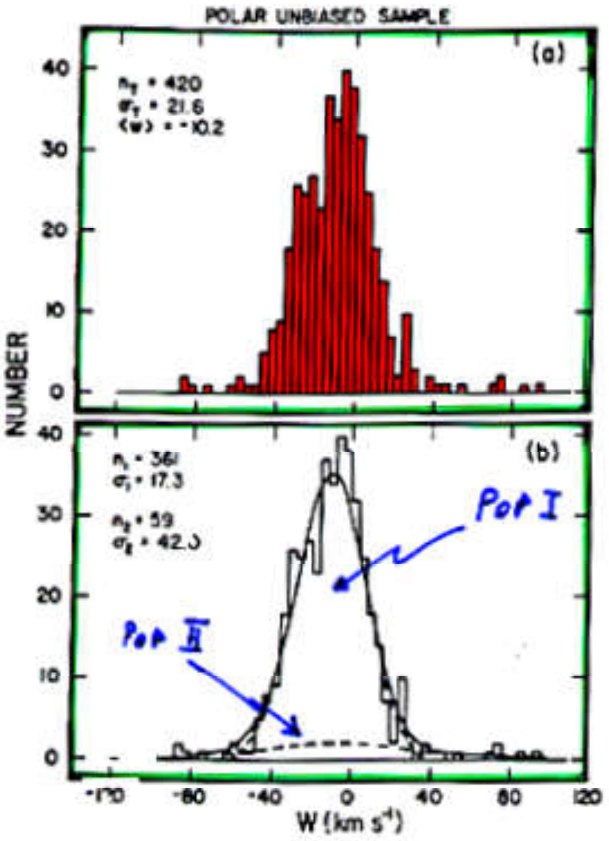

FIG. 2. (Top) Distribution of W velocities from Table VI for the 420-star sample, binned in 4 km s^{-1} intervals. (Bottom) Two-Gaussian fit to the observed distribution. The $\langle W \rangle_2$ and σ_2 values for the high-velocity component have been assumed.

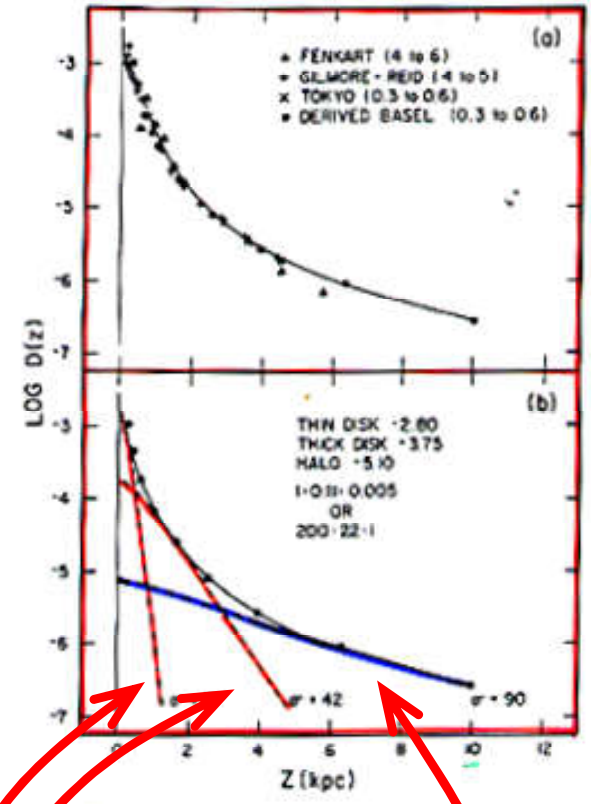

FIG. 3. (Top) The density $D(Z)$ perpendicular to the galactic plane for the four data sets listed in Table II, III, and V. (Bottom) Decomposition of the observed log $D(Z)$ function into three components using the calculated densities shown in Fig. 1.

HALO 1

THICK DISK 22

THIN DISK 200

ρ/ρ_{HALO}

Le orbite delle Pop I e Pop II

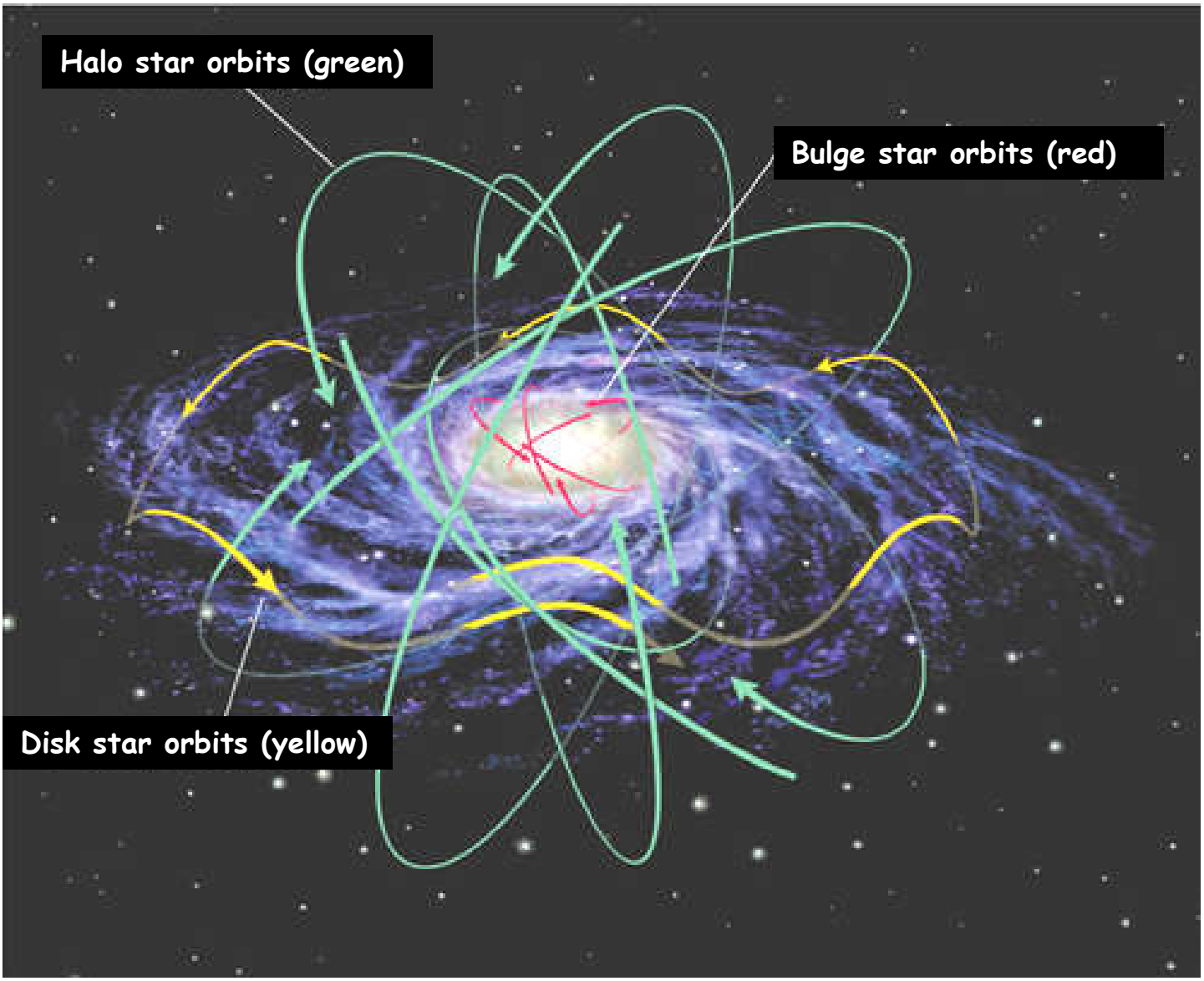

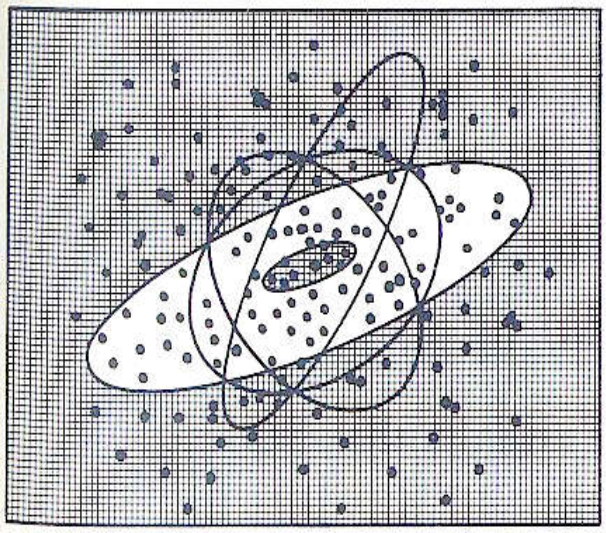

Fig. 11 Schema della costituzione della Galassia. Sono indicate alcune tipiche orbite delle stelle e degli ammassi dell'alone.

Castellani (1986)

Thick & Thin disk: The G-dwarf problem

TWAROG (1980)

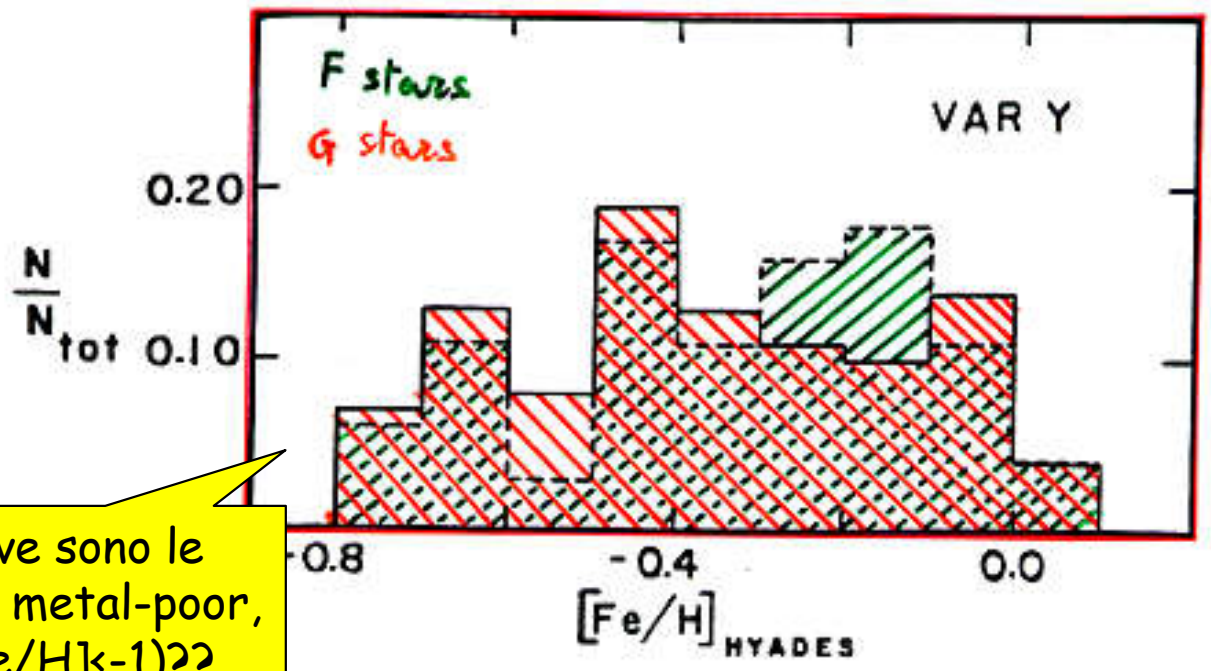

Dove sono le stelle metal-poor, ([Fe/H]<-1)??

FIG. 8.—F dwarf metallicity distribution (*dashed line*) including corrections for stellar evolution and scale height effects which produce a constant SFR compared to the G dwarfs (*solid line*).

TIMMES et al. (1995)

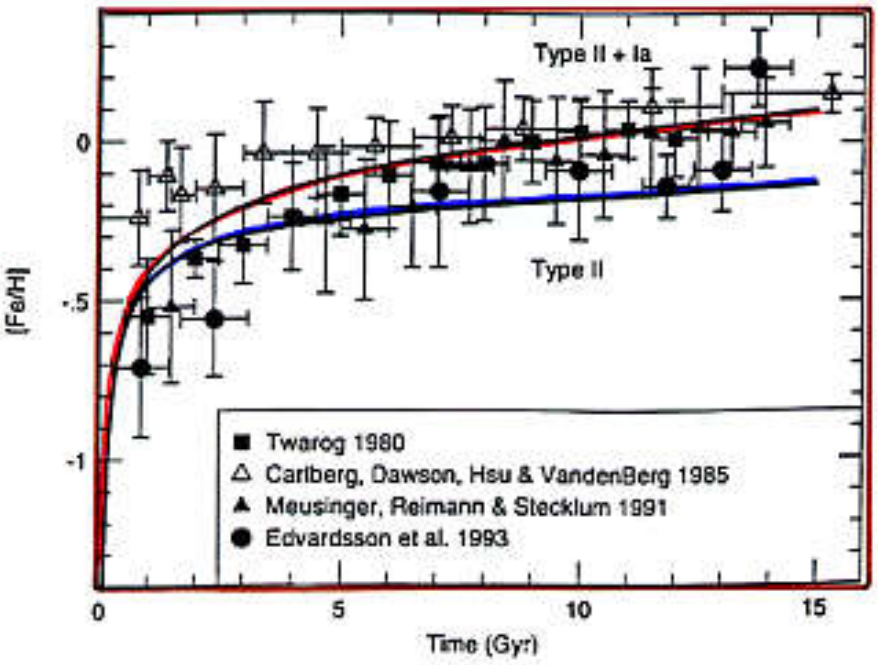

Thick & Thin disk e SFR

PARDI & FERRINI (1994)

SFR

$[M_\odot / pc^2 / yr]$

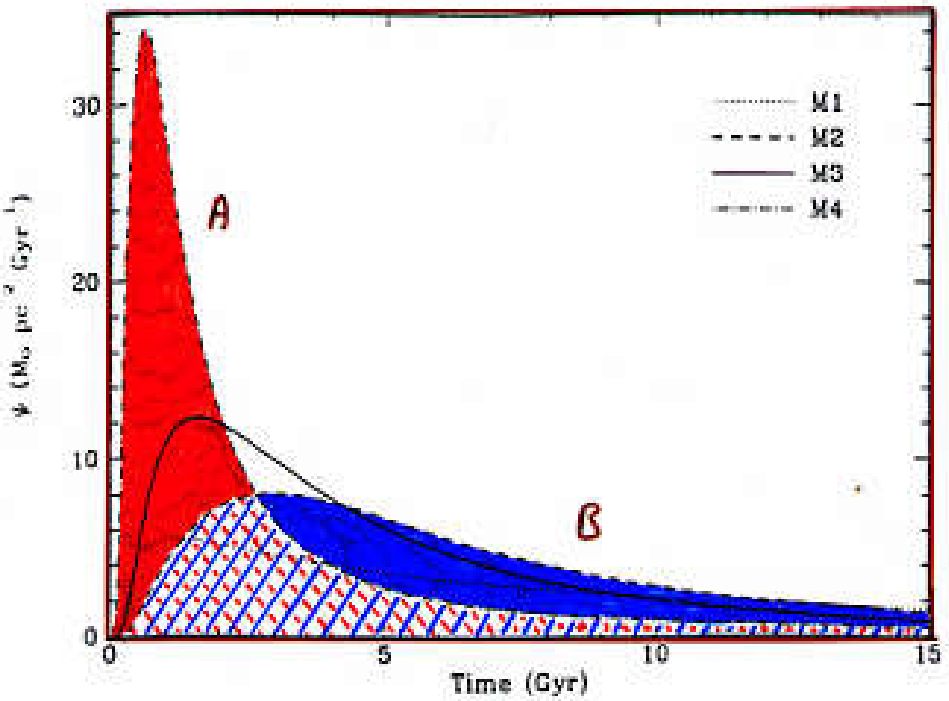

FIG. 3.—SF rate vs. time (M1–M4)

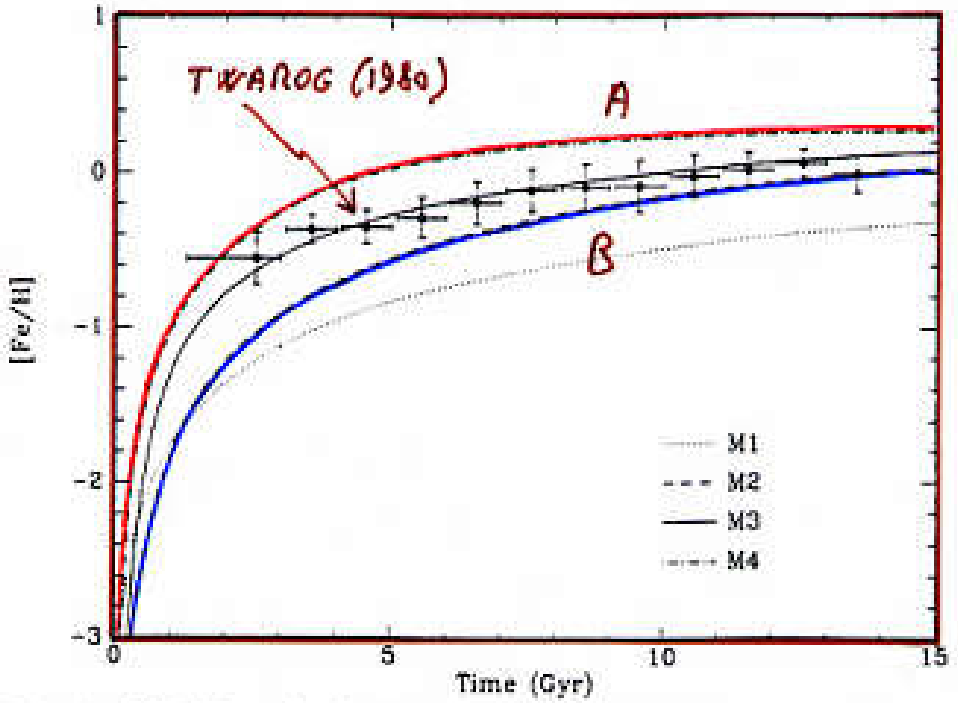

FIG. 4.—[Fe/H] vs. time for the same models of Fig. 3, superposed on data of Twarog (1980).

Hipparcos (1993) (22,000 stars)

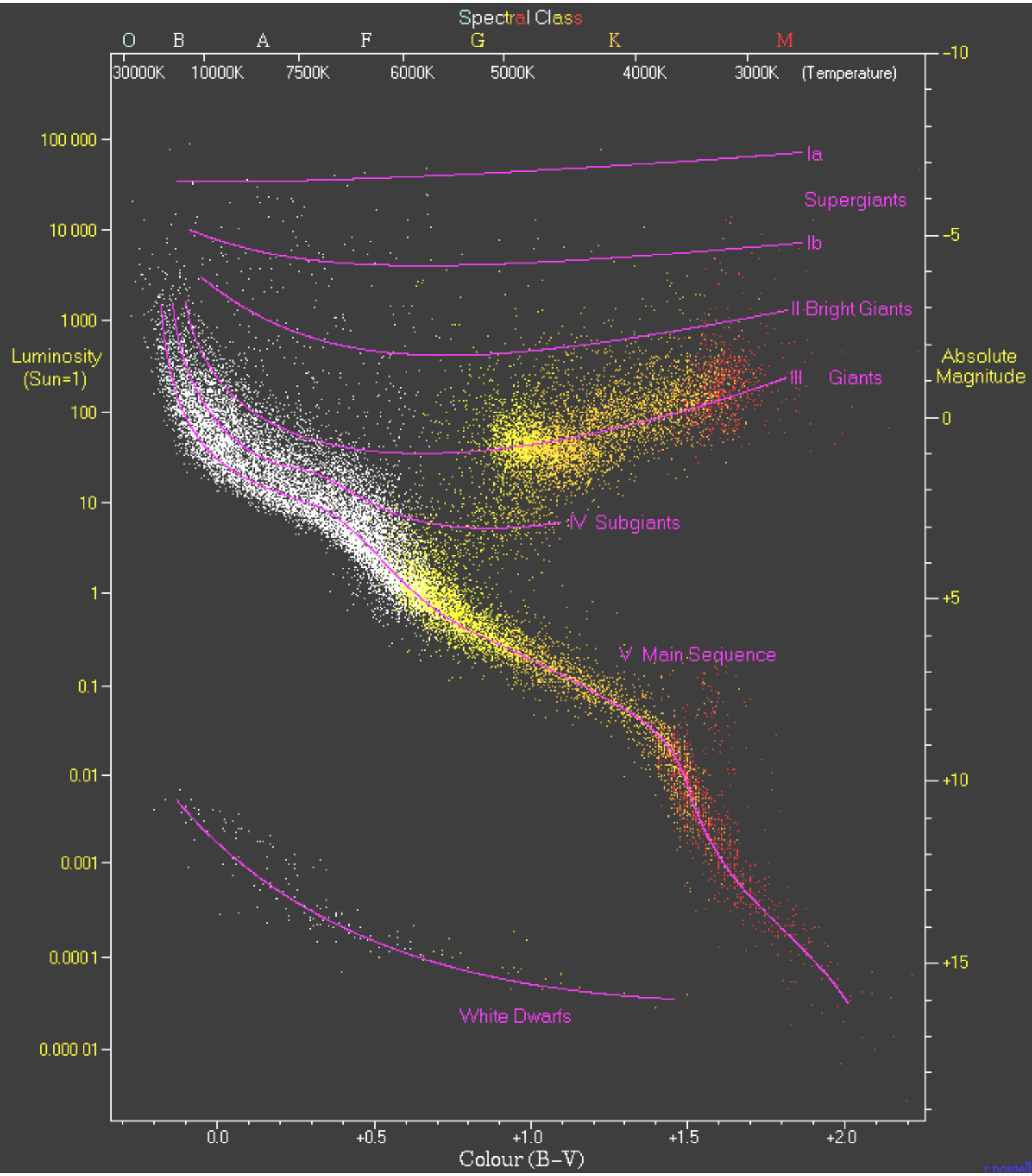

I conteggi stellari e la determinazione della IMF

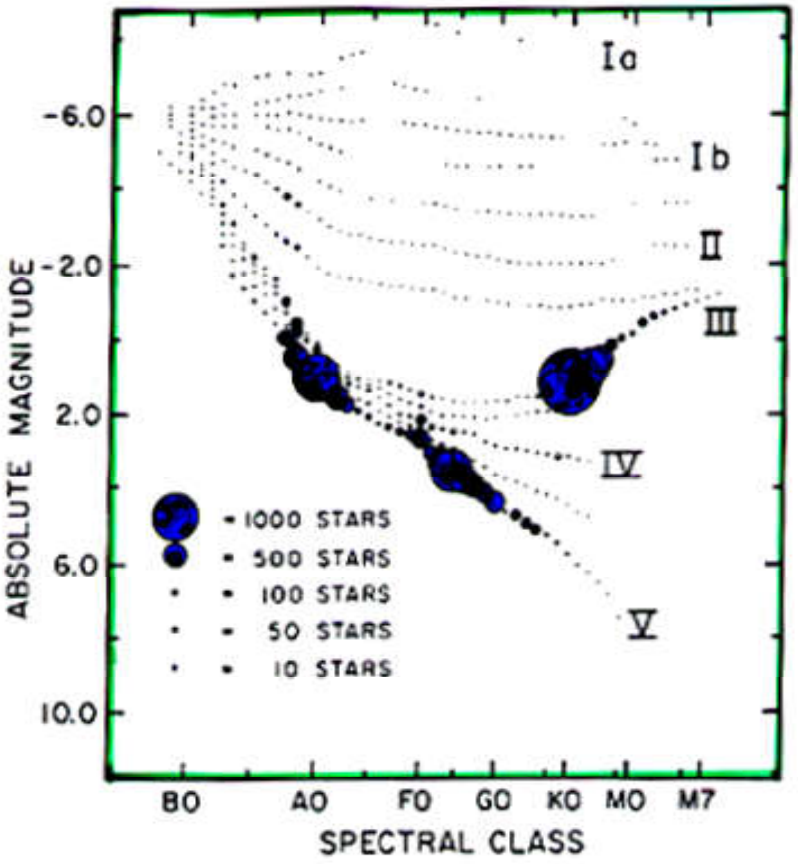

App. Mag. limited

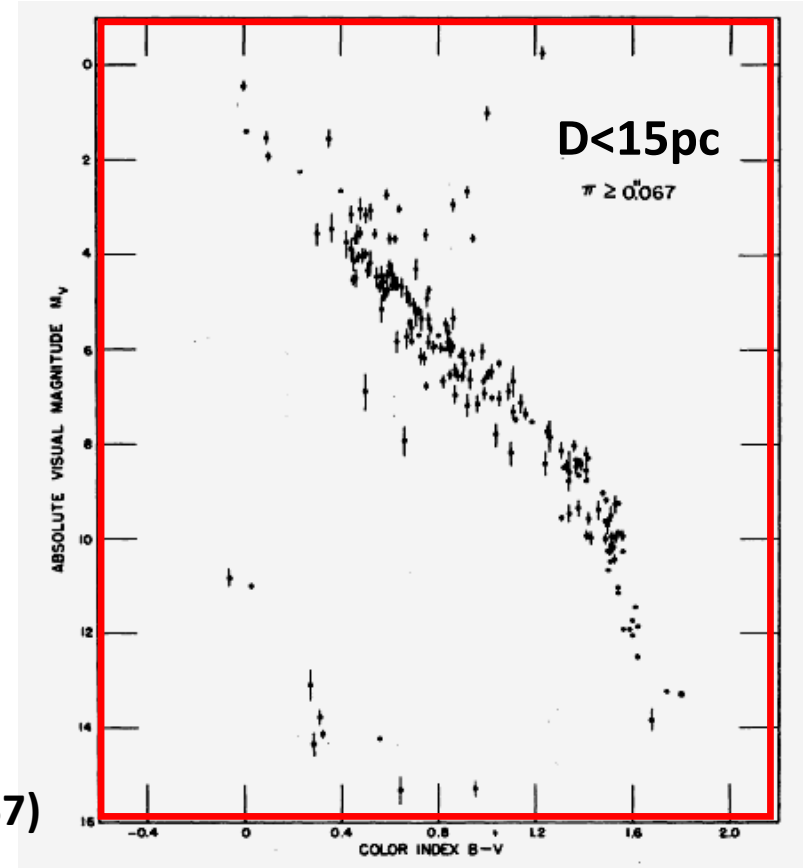

Distance limited

Sandage (1957)

GAIA'S FIRST HERTZSPRUNG-RUSSELL DIAGRAM (~10^6 stars) (2015)

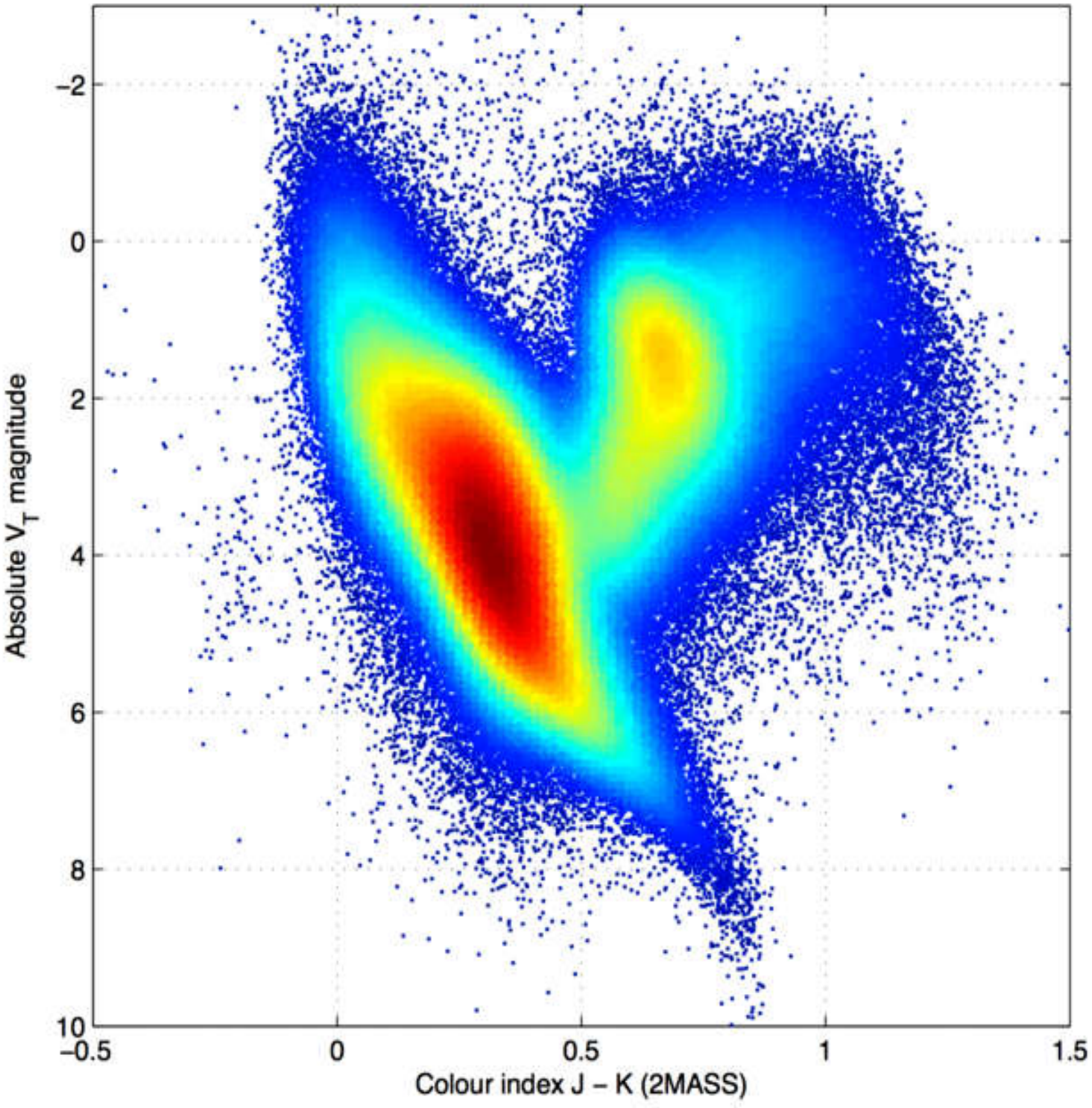

Il diagramma di Hess

Figure 5.2. Schematic Hess diagram for stars in our neighborhood. Numbers of stars per cubic parsec are shown by contours which refer to 20, 200, 2000, and 20,000 stars. The main sequence runs along the ridge. Probably the peak is reached at about the bottom right corner of the diagram, with about 40,000 stars per cubic parsec. Statistics for fainter stars do not permit us to say how fast the slope falls off from there. The contours for white dwarfs are not shown; these stars populate a moderately high ridge, roughly parallel to the main ridge and separated from it by a deep valley.

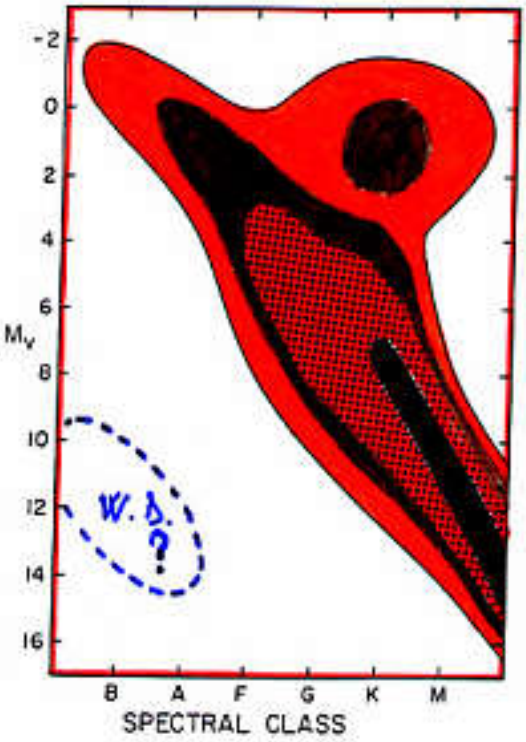

DIAGRAMMA DI HESS

20
200
2000
20,000

$*/Pc^3$

Statistica stellare. Funzione di luminosità

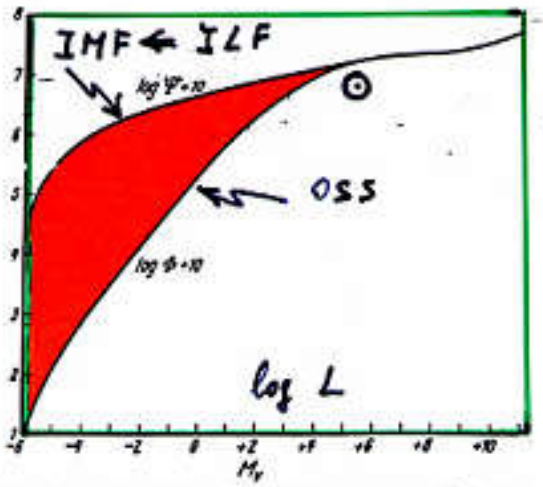

Fig. 26.8: Funzione di luminosità $\Phi(M_v)$ e funzione iniziale di luminosità $\Psi(M_v)$, per stelle della sequenza principale nei dintorni del sole. La Φ e la Ψ dànno rispettivamente il numero osservato di stelle per pc^3 comprese fra $M_v - 1/4$ ed $M_v + 1/4$, e di quelle formatesi a partire dalla formazione della Galassia.

KAPTEYN & VAN RHIJN '20

SALPETER (1953)

Il diagramma di Hess (2)

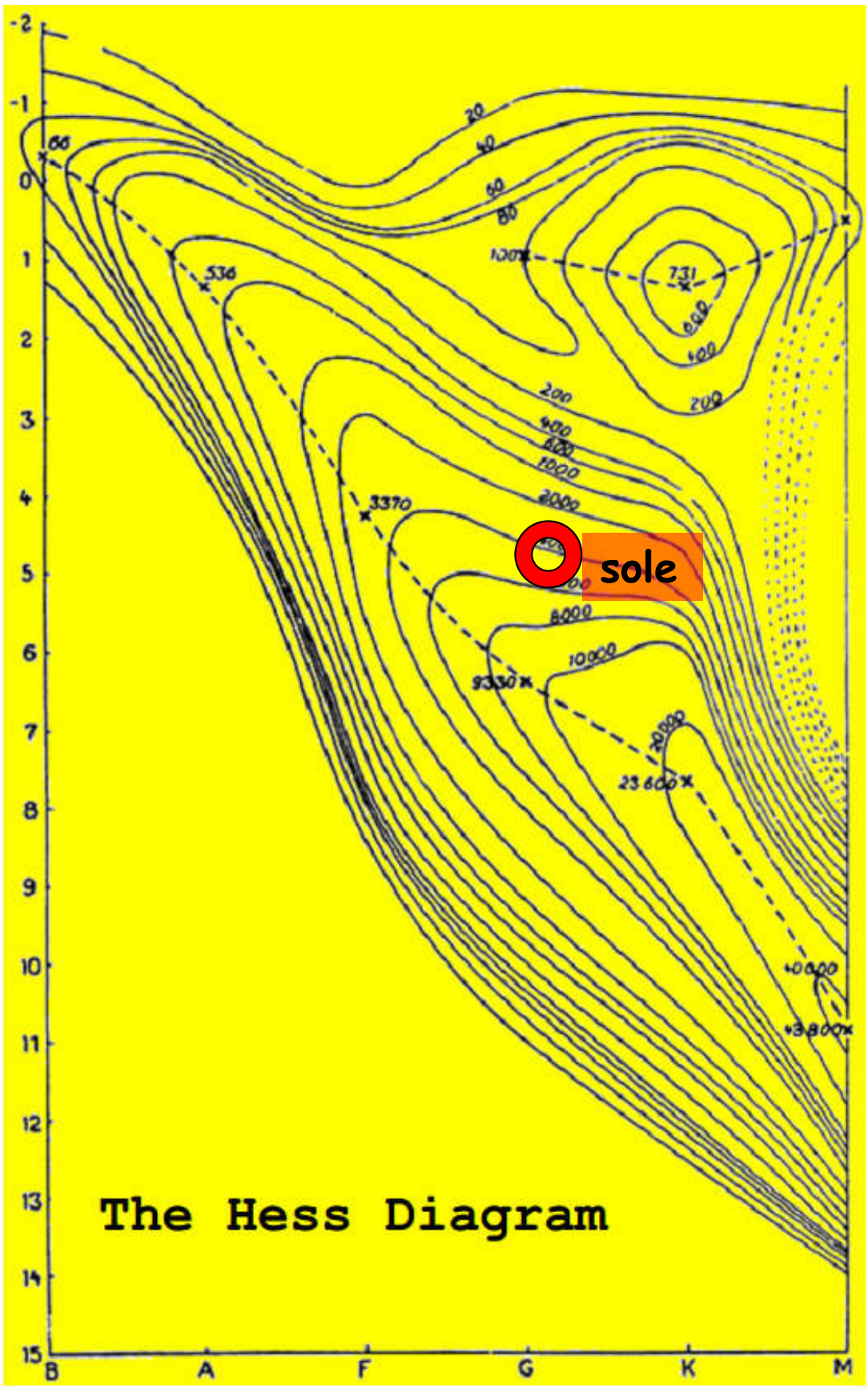

Magnitudine assoluta

Tipo Spettrale

La IMF

PARDI & FERRINI (1994)

SCALO (1987)

RANA (1991)

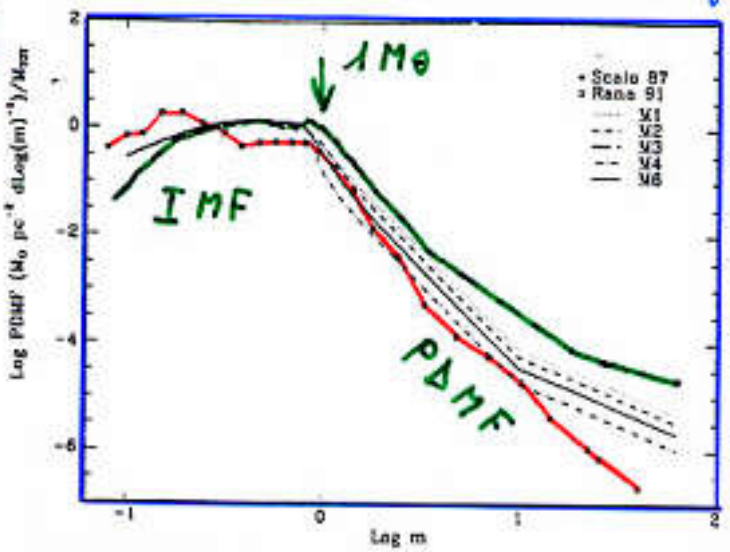

log N

[*/d log M/Pc^3]

FIG. 12.—PDMFs predicted by the model in cases M1–M4 and M6 superposed on data of Scalo (1987 [*triangles*]) and Rana (1991 [*squares*]).

A) $\psi_{(M)} \propto M^{-1.3}$

B) $\psi_{(M)} \propto M^{-2.2}$

C) $\psi_{(M)} \propto M^{-2.7}$

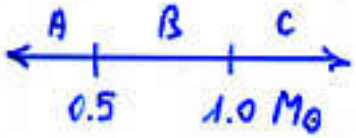

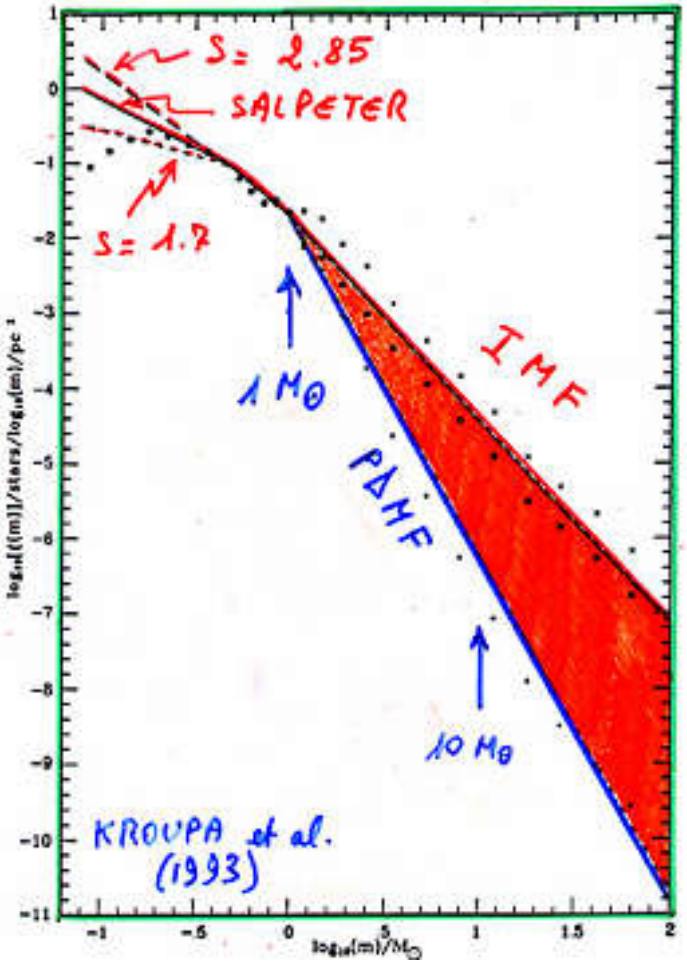

log $\psi_{(M)}$

[*/d log M/Pc^3]

http://en.wikipedia.org/wiki/Initial_mass_function

La IMF (2)

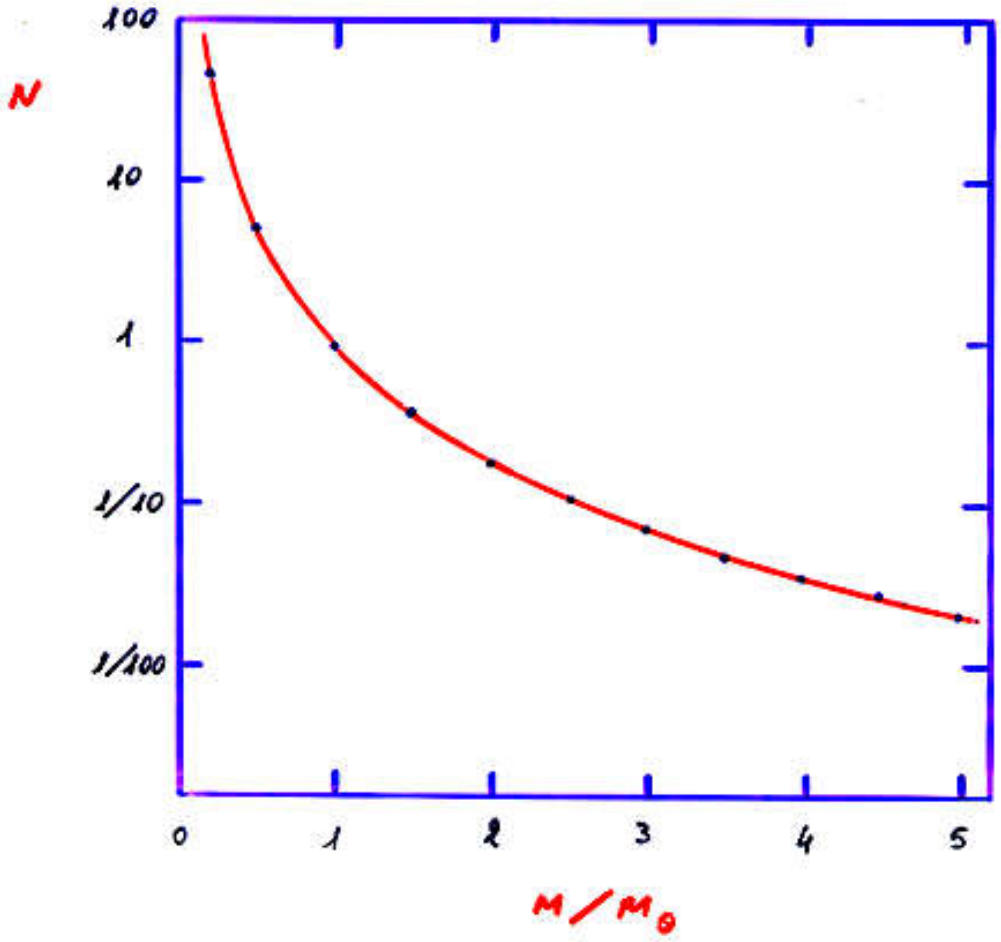

M	L	N
0.1	0.0001	220
0.5	0.06	5
1	1	1
2	16	1/5
5	625	1/40
10	10'000	1/220
50	$6\,10^6$	1/10'000

La IMF negli ammassi globulari galattici

Metal rich Metal poor

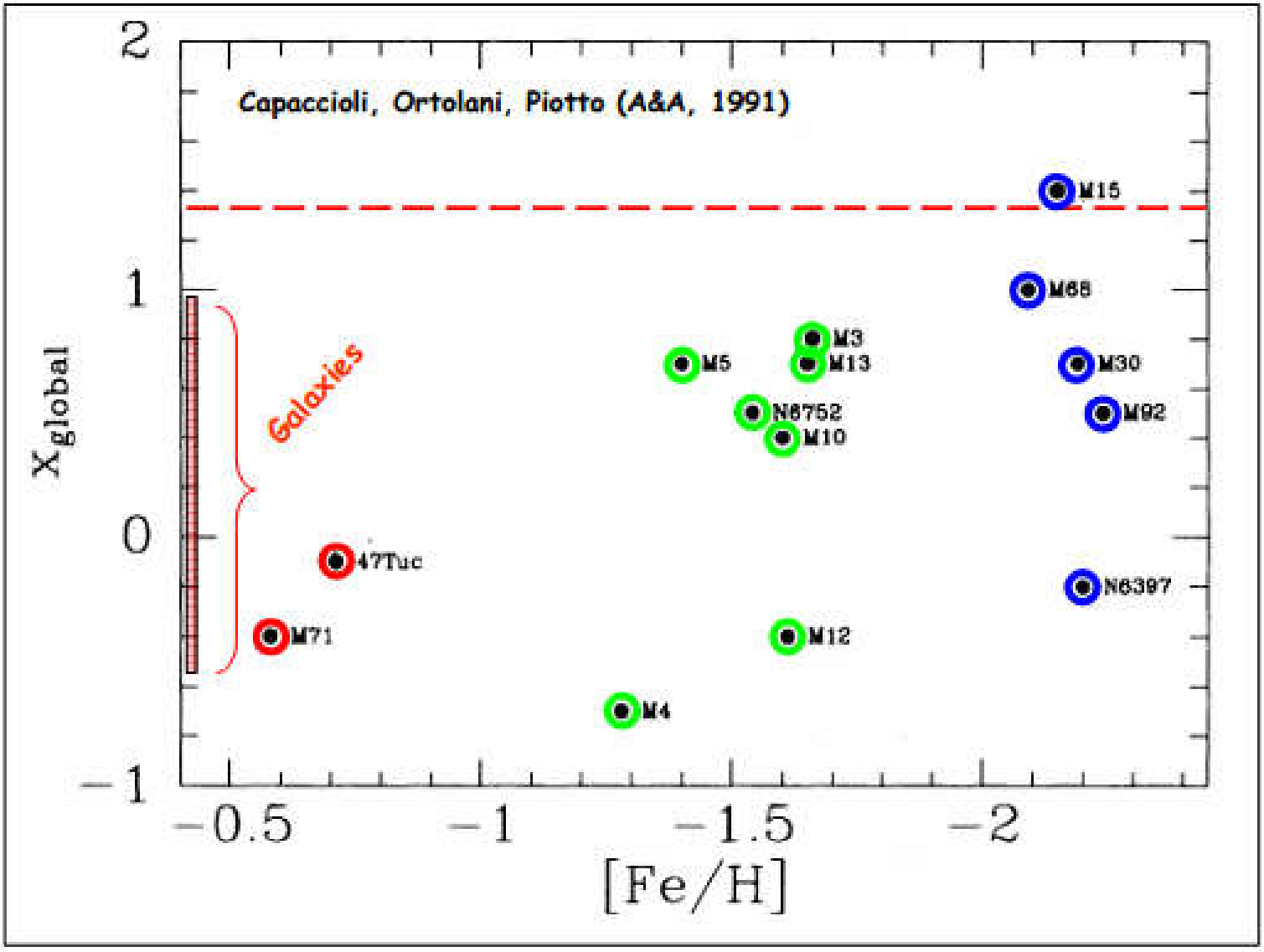

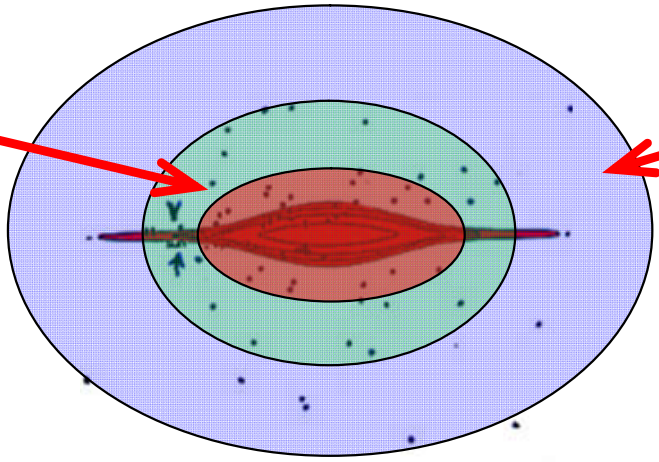

La IMF negli ammassi globulari galattici

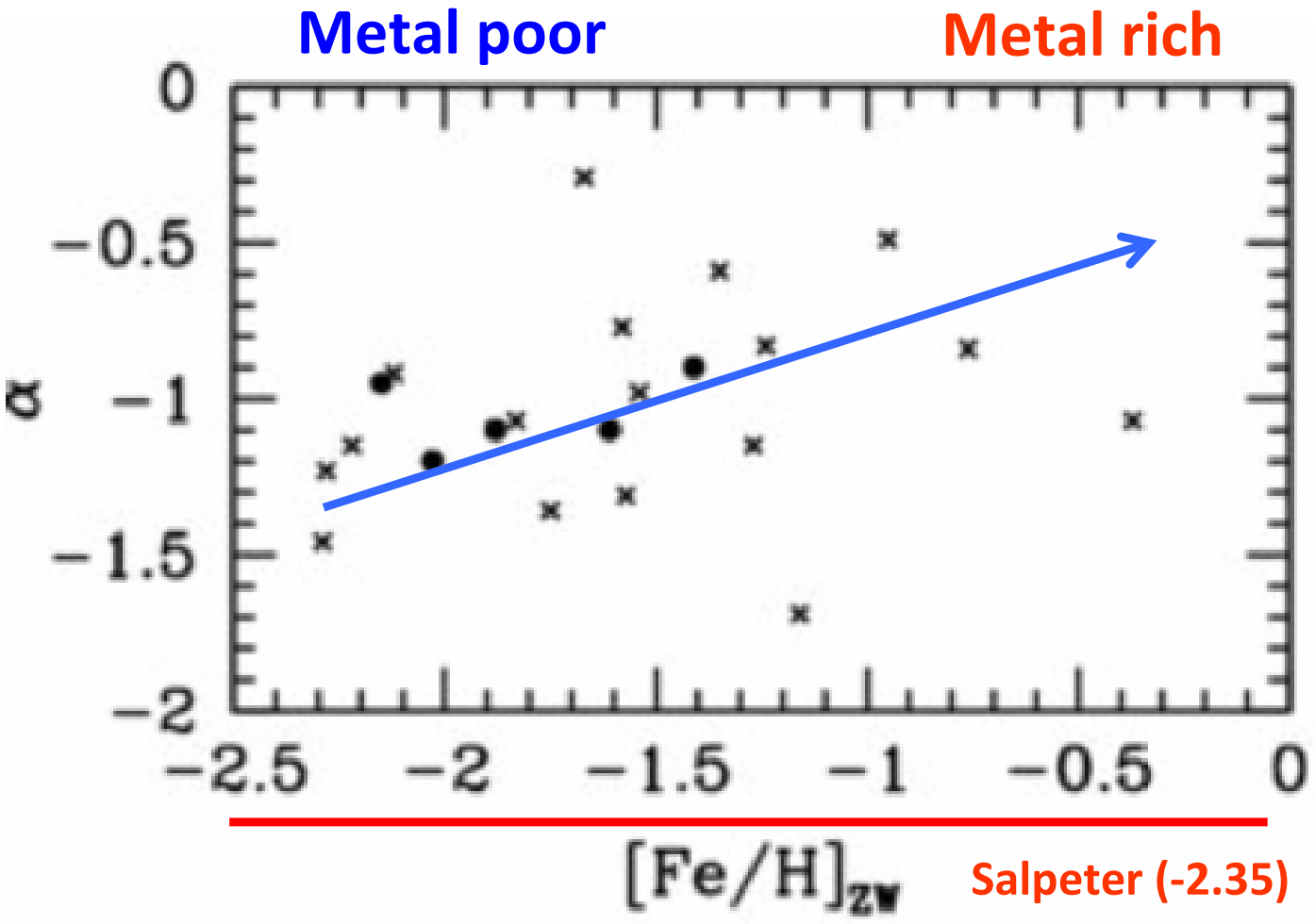

Paust et al. (2010)

Articoli consigliati (vedi Webpage):
http://www.bo.astro.it/~eps/lezioni/lezioni.html

- **Energetic & Chemical evolution of Spirals (Buzzoni 2011)**
- **Milky Way mass (Licquia 2015)**
- **Milky Way mass profile (Taylor 2016)**
- **MW Disk (Sandage 1987)**
- **MW z-shape & Bottlinger Diagrams (Sandage & Fouts 1987)**
- **MW thin disk & Bottlinger Diagrams (Gazzano et al. 2013)**
- **Lindblad orbits (Struck 2015)**
- **Galaxy Colors (Buzzoni 2005)**
- **Galaxy mass assembly (Pan 2015)**
- **IMF (Miller & Scalo 1979)**
- **IMF (Kroupa et al. 1993)**
- **IMF (Kalirai et al. 2013)**
- **IMF (Weidemann 2000)**

Teoria delle Popolazioni Stellari Semplici (SSPs)

Renzini & Buzzoni (1986)

Definition of SSP:

1) A generation of COEVAL stars ($SFR = \delta_0$)
(so that we can define an AGE of the population)

2) Fixed metallicity (unique Z)

Star partition:

MS: $\boxed{N_{(M)} = A\, M^{-s}}$ (IMF)

Post-MS:

$$\Delta M = M_{DYING} - M_{TO} \simeq - \left.\frac{dM}{dt}\right|_{\tau_{PMS}} \simeq M_{TO}\, \frac{\tau_{PMS}}{T}$$

$$\boxed{N_{PMS} = A\, M_{TO}^{-s}\, \Delta M = A\, M_{TO}^{-s}\, \dot{M}_{TO}\, \tau_{PMS}}$$

Massa al Turn Off

Massa finale (Nane Bianche)

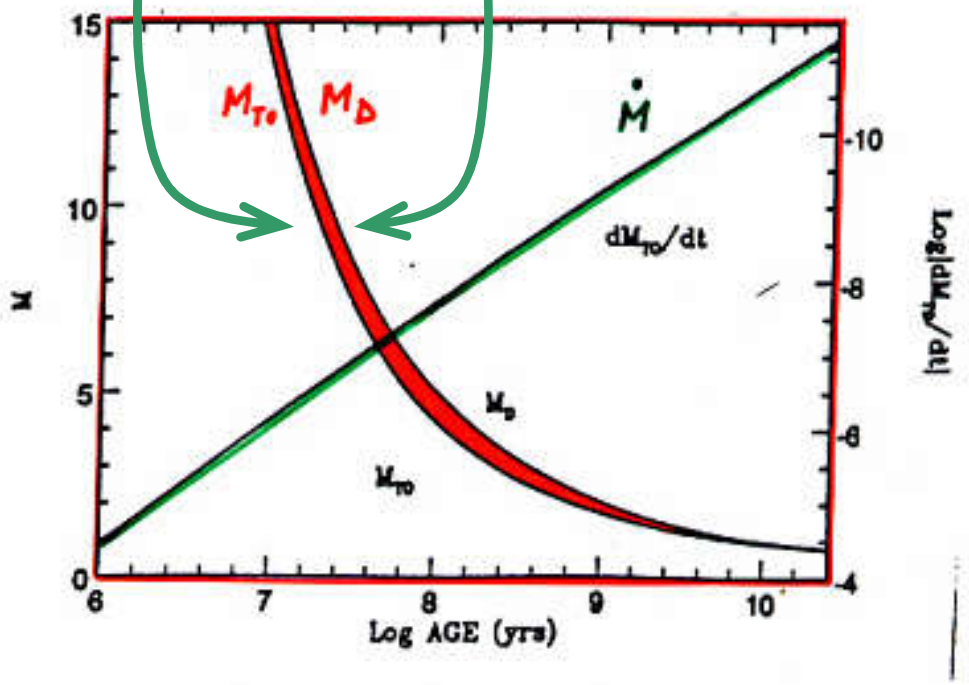

Renzini & Buzzoni (1986)

Flusso evolutivo specifico

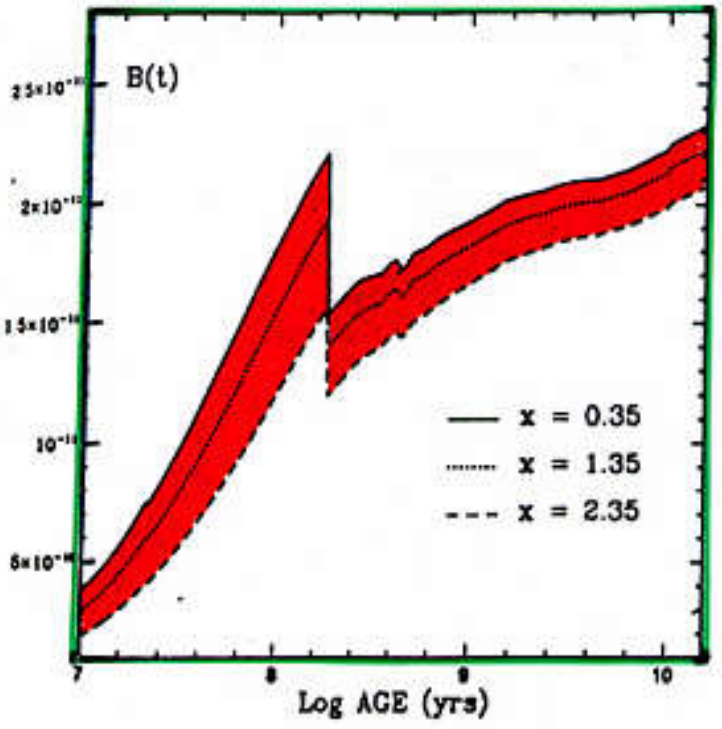

Fig. 1.3: The specific evolutionary flux $B(t)$ as a function of age for three IMF slopes $(1 + x)$.

$2 \cdot 10^{-11}$

B

10^{-11}

B = (b/Ltot)

$$N_{PMS} = \underbrace{A\, M_{TO}^{-s}\, \dot{M}}\; \tau_{PMS}$$

$$l_b = B\, L_{TOT}$$

$$N_{PMS} = B\, L_{TOT}\, \tau_{PMS} = 1.7\, 10^{-11} \left(\frac{L}{L_\odot}\right)\left(\frac{\tau}{yr}\right)$$

$\Downarrow$

specific Evolutionary Flux

LUMINOSITY

$$L_{MS} = A \int_0^{TO} l_* M^{-s} dM \qquad \begin{cases} l_* \propto M^3 \\ t_* \propto M^{-2} \end{cases}$$

$$L_{MS} \simeq \frac{A}{4-s} M_{TO}^{4-s} \qquad (s < 4)$$

$$L_{MS} \propto t^{-\frac{4-s}{2}} \sim t^{-0.85}$$

$$L_{PMS} = \int_{PMS} l_*\, dN = A\, M_{TO}^{-s}\, \dot{M}_{TO} \underbrace{\int_{PMS} l_*\, d\tau}$$

fuel ~ const.

$$L_{PMS} \propto t^{-\frac{3-s}{2}} \sim t^{-0.35}$$

$$\frac{L_{PMS}}{L_{MS}} \propto \frac{t^{-\frac{3-s}{\ell}}}{t^{-\frac{4-s}{\ell}}} \propto \sqrt{t}$$

Conclusion: MS always dominates with decreasing time

Corollary: Total SSP luminosity is a DECREASING function of time

Model evolutionary rate at different bands

$$L_{BOL} \propto t^{-0.75}$$
$$L_B \propto t^{-0.95}$$
$$L_V \propto t^{-0.86}$$
$$L_I \propto t^{-0.75}$$
$$L_K \propto t^{-0.71}$$

$Z = Z_\odot$

$s = 1.35$

Buzzoni (2005)

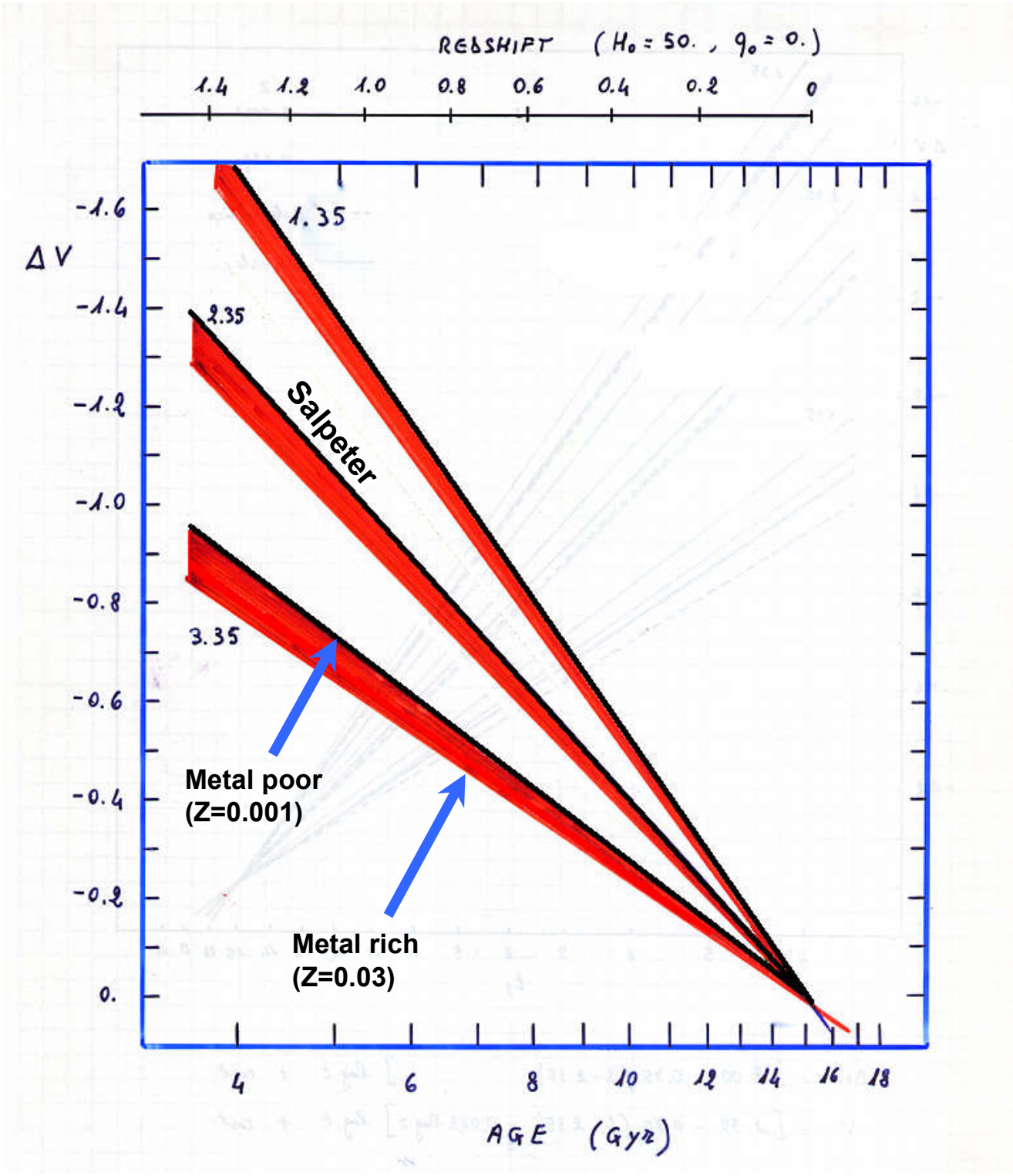

$$t \propto \frac{1}{M^2}\frac{\tilde{k}}{\mu^4}$$

$$L_* \propto M^3 \frac{\mu^4}{\tilde{k}}$$

$$\frac{dt}{t} = -\frac{2}{3}\frac{dL_*}{L_*} + \frac{1}{3}\frac{d\tilde{k}}{\tilde{k}} - \frac{4}{3}\frac{d\mu}{\mu}$$

Quindi, la stessa variazione di luminosita' dL/L, avviene su tempi piu' lunghi (dt/t) se k ↑(ovvero se Z ↑)

SSP
Contributi bolometrici

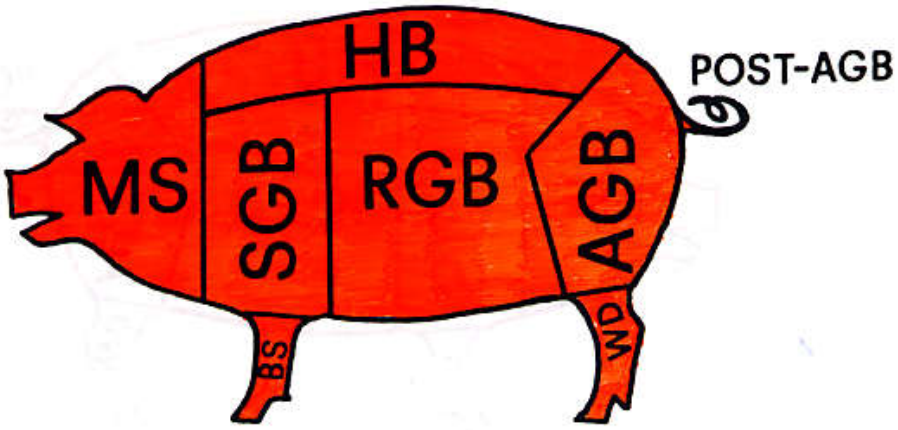

All the cuts of a stellar population.

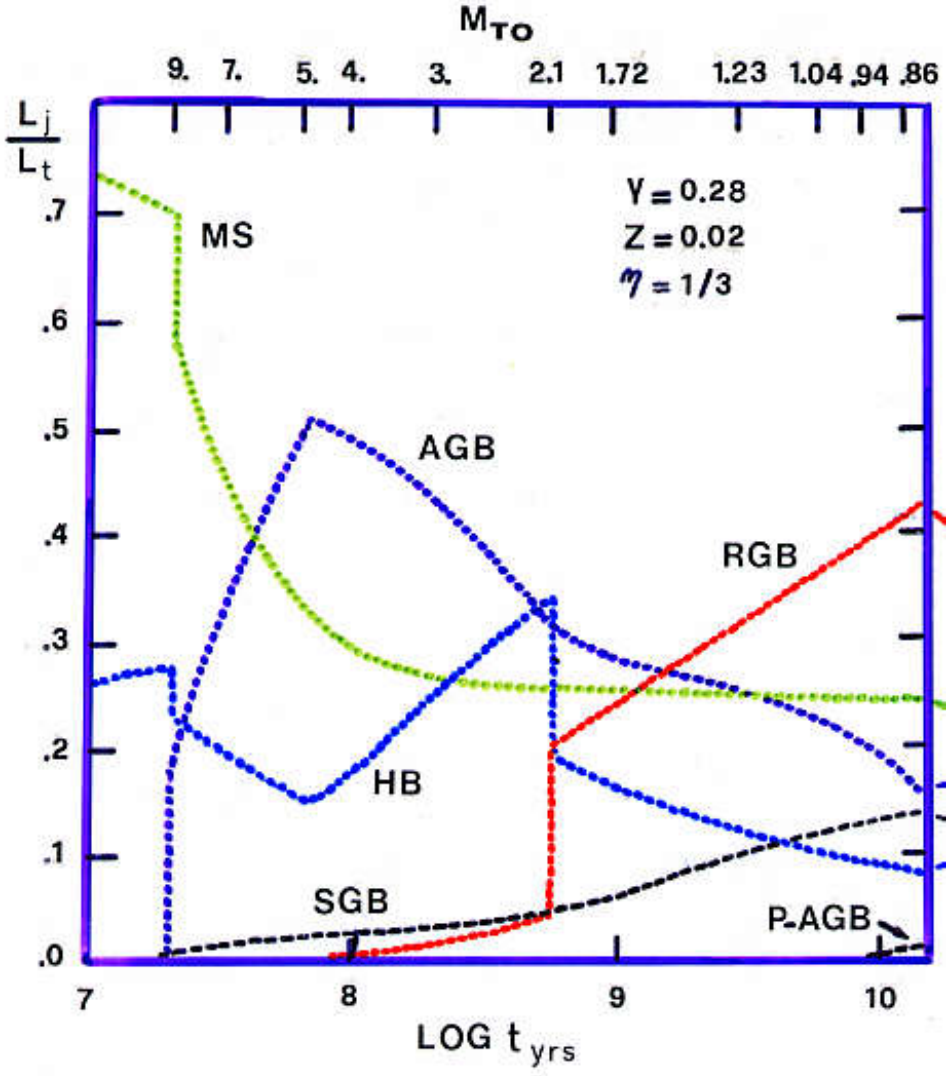

Renzini & Buzzoni (1986)

IMF e Luminosita' totale

Una IMF alla Salpeter permette alla SSP di rilasciare la max luminosita' per unita' di massa

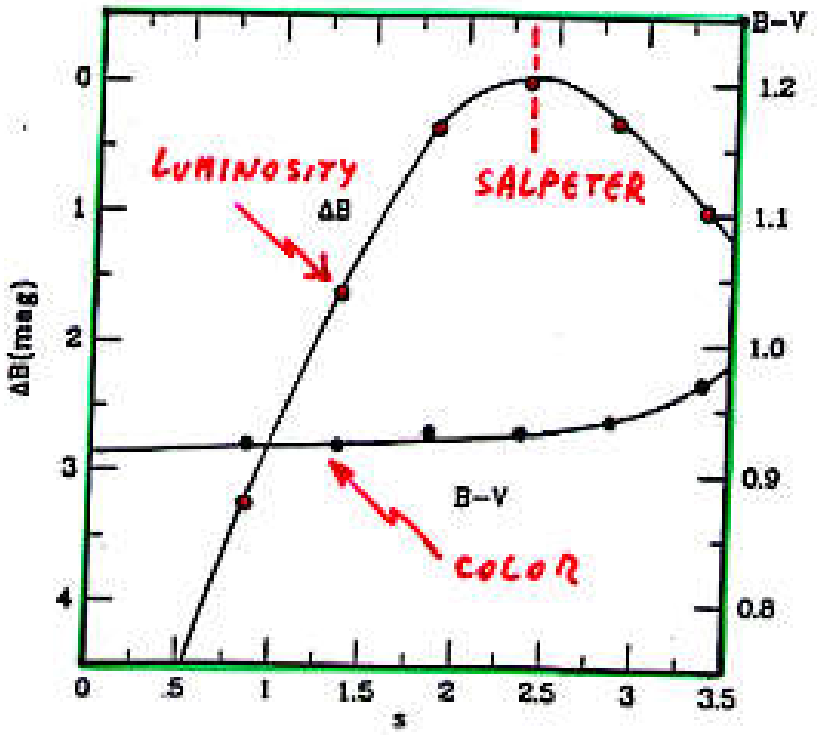

BUZZONI (1995)

$$M_{TOT} = A \int M\, M^{-s} = \frac{A}{2-s}\left[M_u^{2-s} - M_l^{2-s} \right]$$

$s > 2$ DWARF - DOMINATED SSP

$s < 2$ GIANT - DOMINATED SSP

Una IMF alla Salpeter permette alla SSP di rilasciare la max luminosita' per unita' di massa: DIMOSTRAZIONE

$L_{tot} \propto A \dot{M} M_{TO}^{-S}$ Solo "A" e M_{TO}^{-S} dipendono da "S"

$$M_{TOT} = A \int M_*^{-S} M_* dM_* = \frac{A}{2-S} \left[M_*^{2-S} \right]_{low}^{up}$$

Assumiamo $S > 2$ e vediamo se esiste soluzione all'interno di questo dominio

$$\forall\ S>2 \qquad A = \frac{M_{TOT}(2-S)}{M_{low}^{2-S}}$$

$$L_{tot} \propto \frac{M_{TOT}(2-S)}{M_{low}^{2}} \left(\frac{M_{TO}}{M_{low}} \right)^{-S}$$

(non dipende da "S")

$$\left(\frac{L}{M}\right) \propto \frac{1}{M_{low}^{2}} (2-S) \left(\frac{M_{TO}}{M_{low}} \right)^{-S}$$

$$\frac{\partial \left(\frac{L}{M}\right)}{\partial S} = 0 \Longrightarrow -1 \left(\frac{M_{TO}}{M_{low}} \right)^{-S} = (2-S) \ln \left(\frac{M_{TO}}{M_{low}} \right) \left(\frac{M_{TO}}{M_\odot} \right)^{-S}$$

$$2 - S_{MAX} = \frac{1}{\ln \left(\frac{M_{low}}{M_{TO}} \right)}$$

$$S_{MAX} = 2 - \frac{1}{\ln \left(\frac{M_{low}}{M_{TO}} \right)}$$

$M_{low} \sim 0.1\ M_\odot$

$\forall\ M_{TO} \rightarrow 0.01 \lesssim \frac{M_{low}}{M_{TO}} \lesssim 0.1$

$$2.2 \lesssim S_{MAX} \lesssim 2.4$$

Articoli consigliati (vedi Webpage):
http://www.bo.astro.it/~eps/lezioni/lezioni.html

- **SSP Theory (Renzini & Buzzoni 1986)**
- **Energetic & Chemical evolution of Spirals (Buzzoni 2011)**
- **M/L clusters (Girardi et al. 2002)**
- **IMF (Miller & Scalo 1979)**
- **IMF (Kroupa et al. 1993)**
- **IMF (Kalirai et al. 2013)**
- **IMF (Weidemann 2000)**

Evoluzione fotometrica delle SSP: dal bolometrico al monocromatico

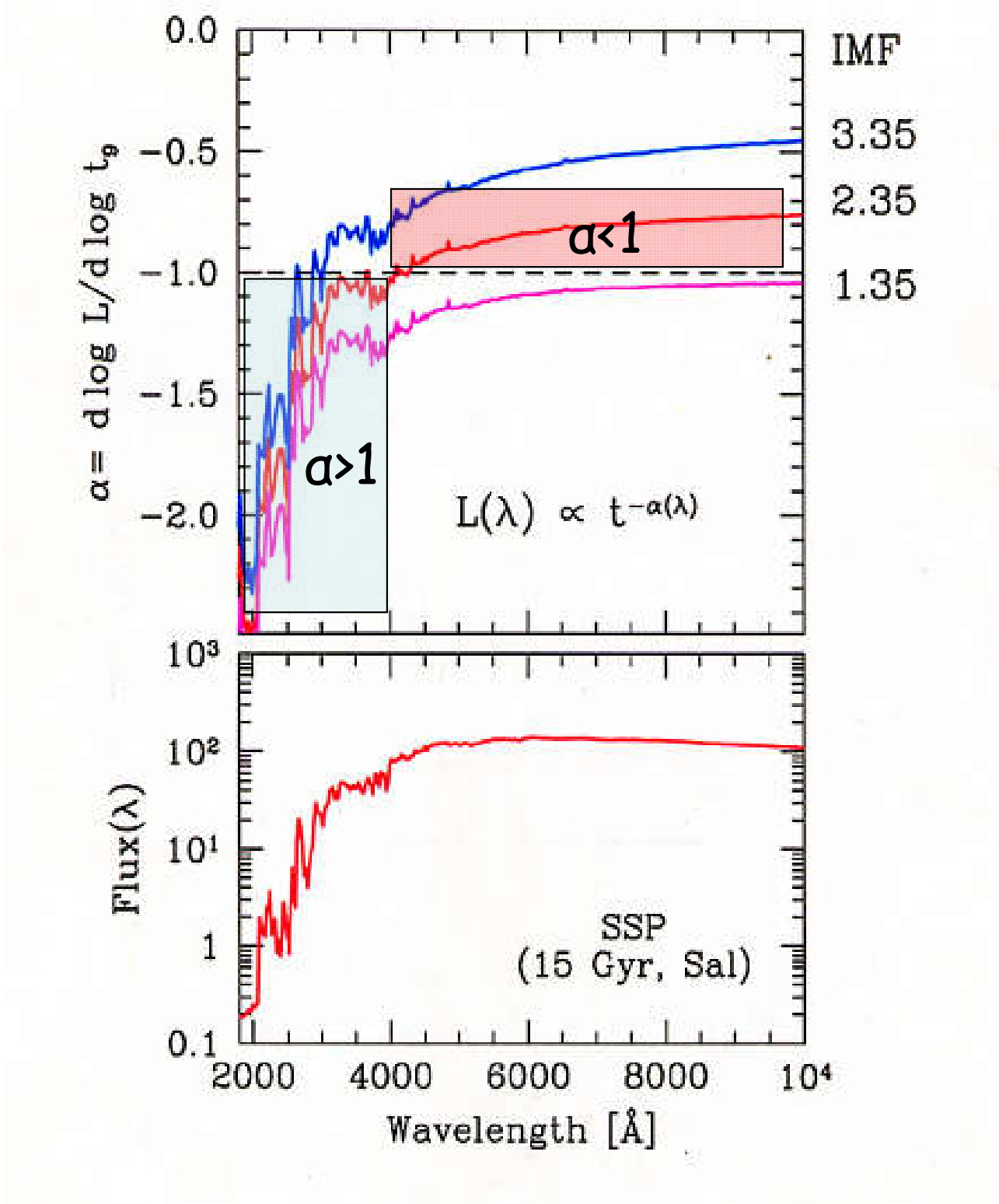

L'evoluzione fotometrica delle SSPs nell'UV avviene piu' veloce di t^{-1} !! Dunque, in una CSP, l'UV traccia la SFR recente.

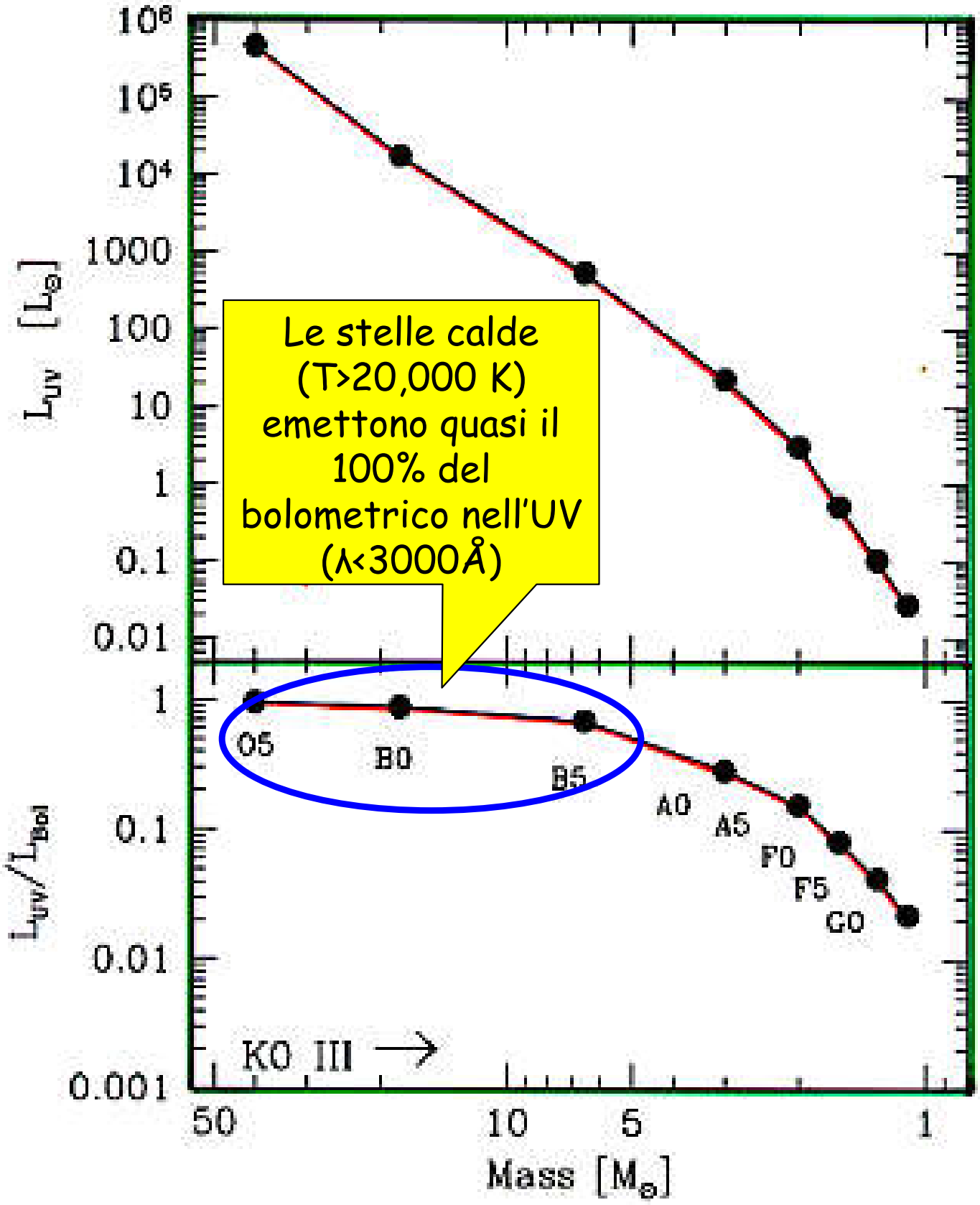

Buzzoni (2002)

$L_{UV} \rightarrow SFR$

Deve esserci corrispondenza lineare fra L_{UV} e SFR

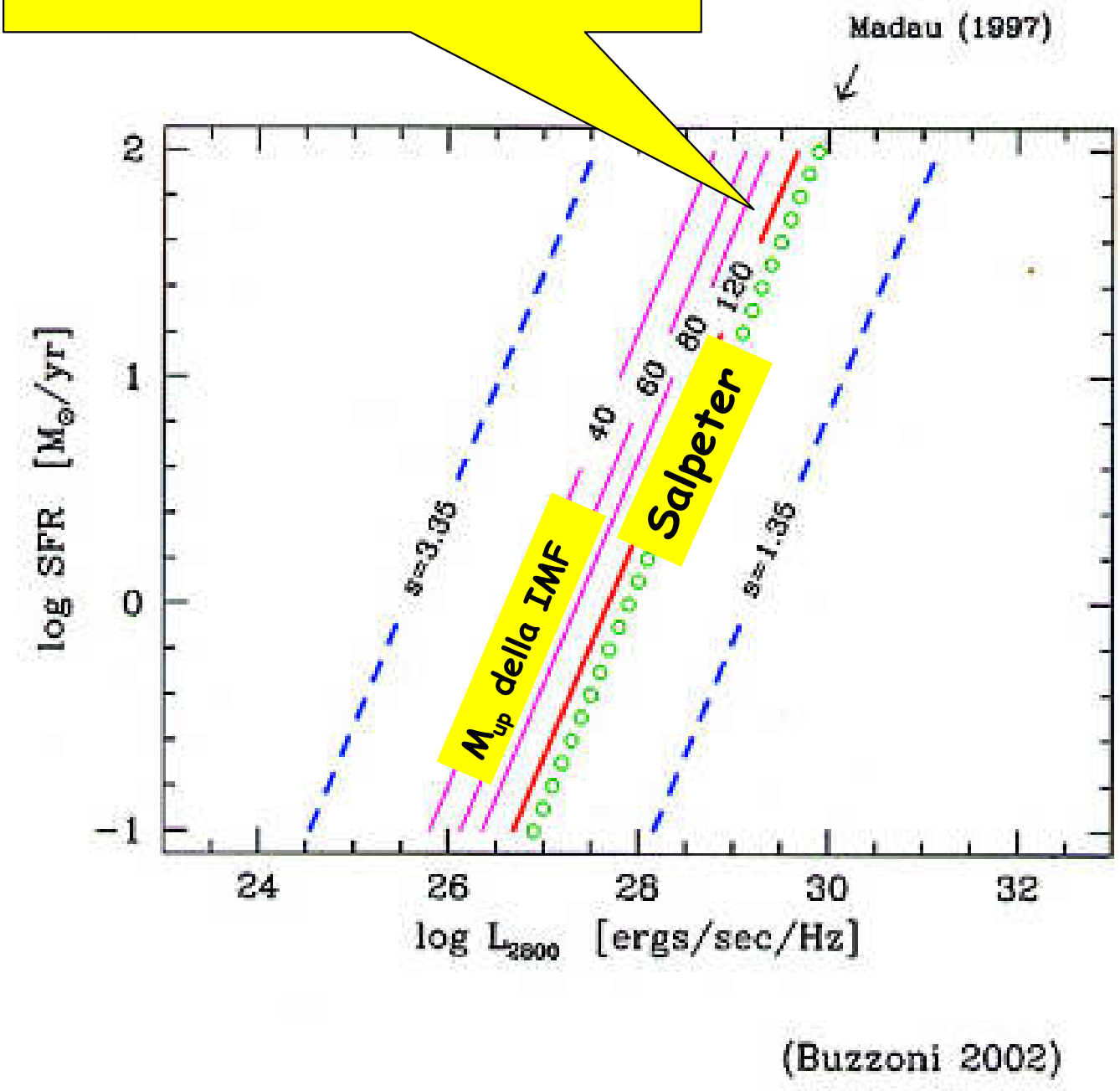

(Buzzoni 2002)

Il "Madau Plot" e la Storia della Formazione Stellare Cosmica

(Madau 1997)

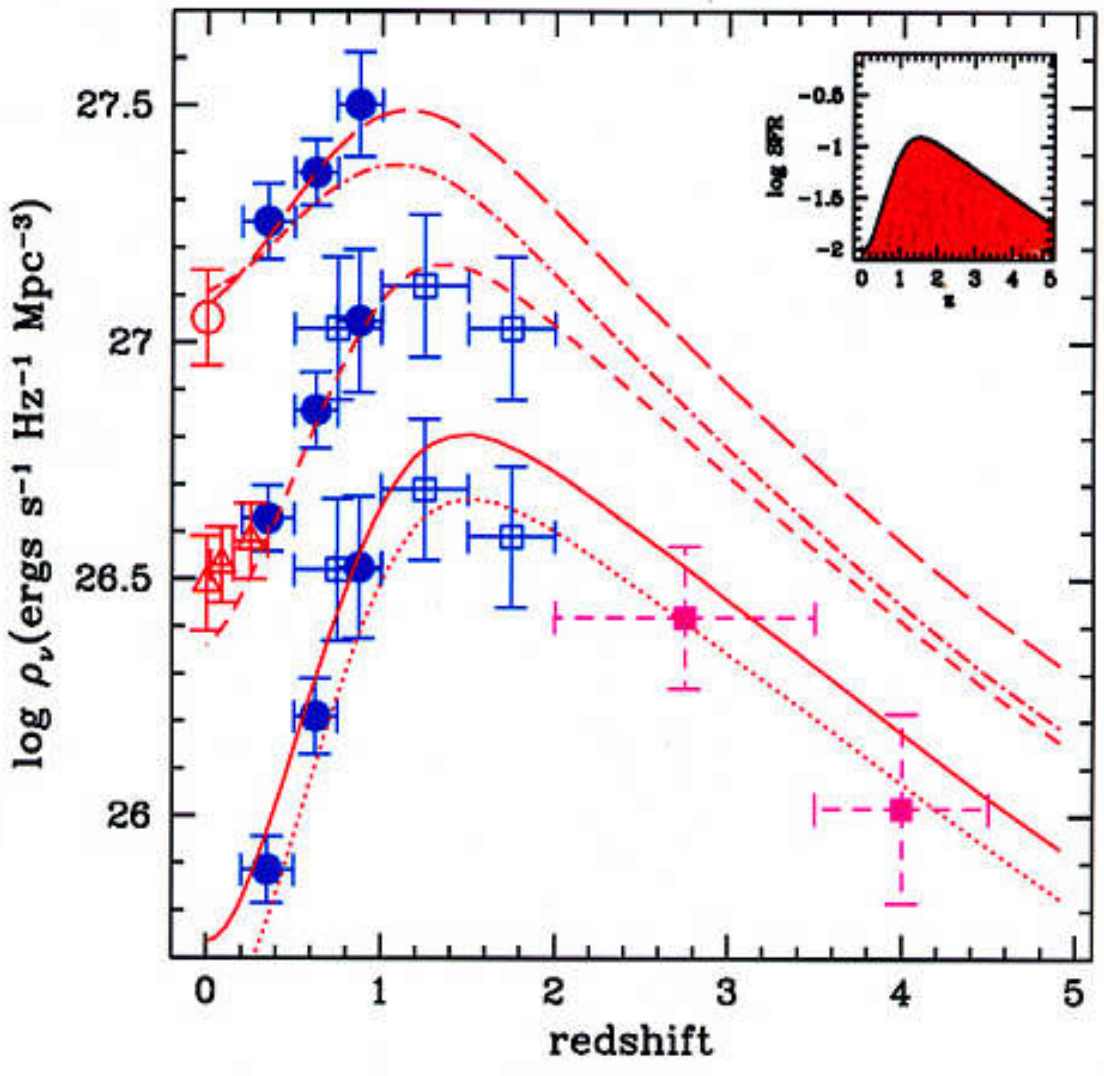

Evoluzione del Madau plot

(includendo incompletezza, assorbimento polveri etc.)

Cosa e' successo qui?

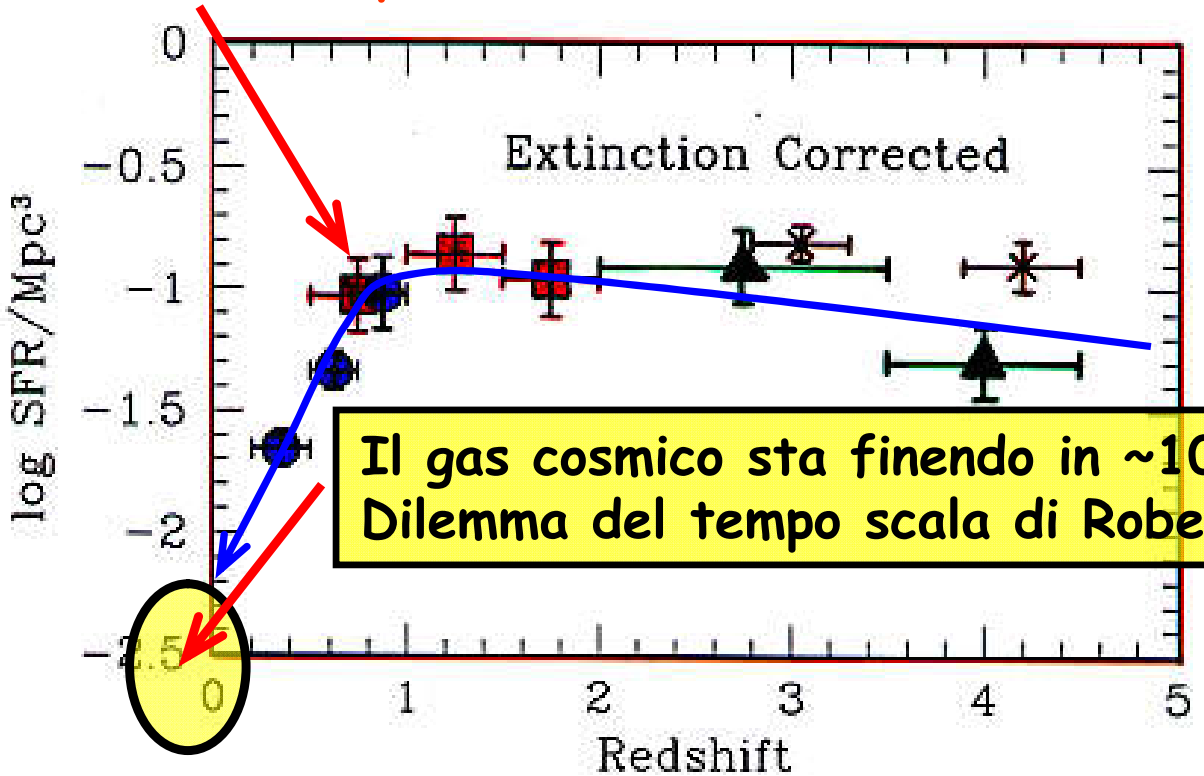

Il gas cosmico sta finendo in ~10^9 yr?
Dilemma del tempo scala di Roberts?

● = LILLY et al. (1996)
■ = CONNOLLY et al. (1997)
▲ = MADAU et al. (1997)
X = STEIDEL et al. (1999)

$(H_0, \Omega_0) = (50, \frac{1}{2})$

Tempo di Roberts: $t_R \sim \frac{f_{gas} M_{gal}}{SFR_{now}}$ **ma (vedi dopo)** $b = \frac{SFR_{now}}{M_{gal}} t_{gal}$

Combinandole: $\frac{t_R}{t_{gal}} = \frac{f_{gas}}{b} \sim \frac{\sim 0.1}{\sim 1}$ **Quindi** t_R **~1-2 Gyr max**

Evoluzione del Madau plot

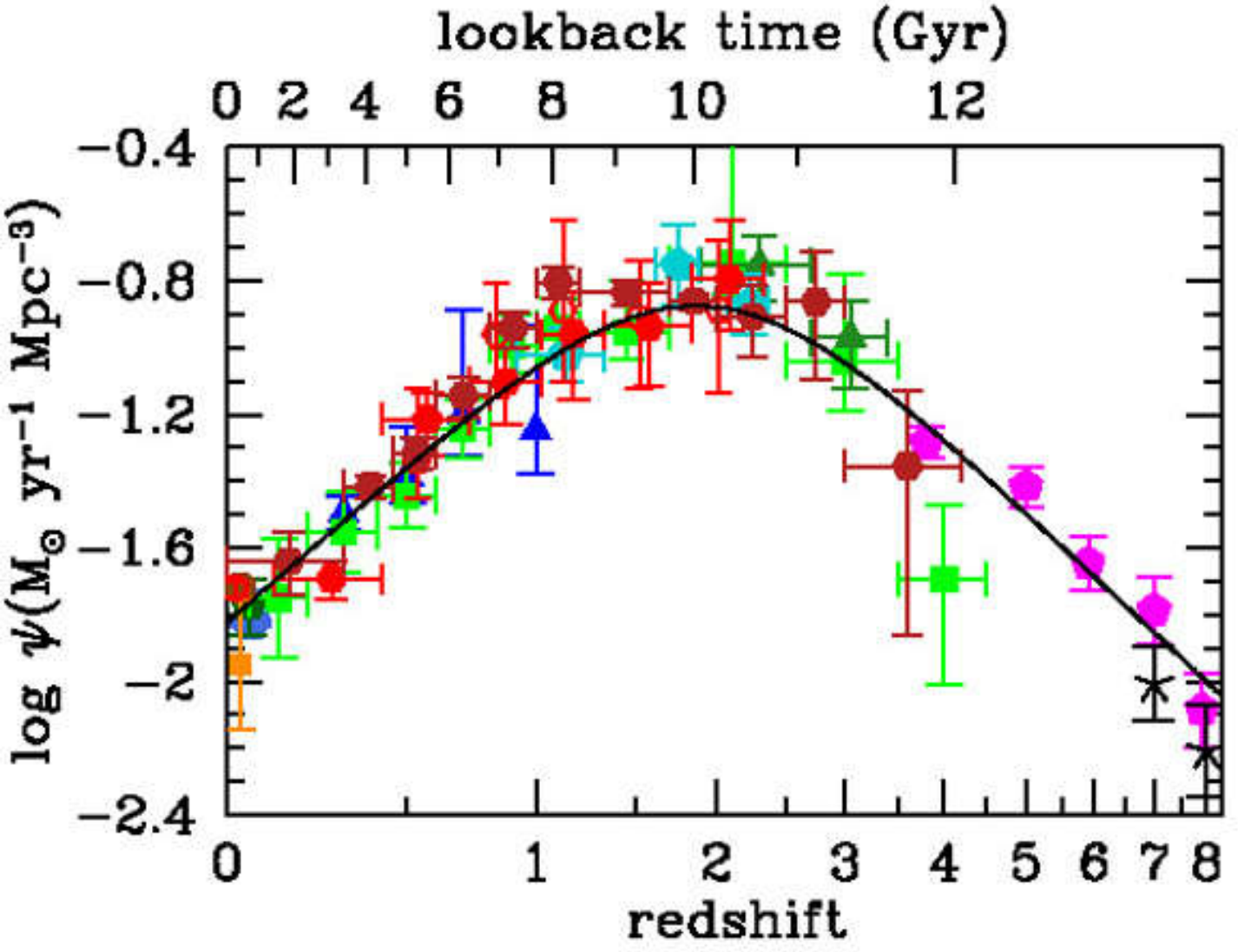

Madau & Dickinson (2014)

Wyder et al. (2005)	blue-gray hexagon	Bouwens et al. (2012ab)	magenta pentagons
Schiminovich et al. (2005)	blue triangles	Schenker et al. (2013)	black crosses
Robotham & Driver (2011)	dark green pentagon	Sanders et al. (2003)	brown circle
Cucciati et al. (2012)	green squares	Takeuchi et al. (2003)	dark orange square
Dahlen et al. (2007)	turquoise pentagons	Magnelli et al. (2011)	red open hexagons
Reddy & Steidel (2009)	dark green triangles	Magnelli et al. (2013)	red filled hexagons
		Gruppioni et al. (2013)	dark red filled hexagons

Articoli consigliati (vedi Webpage):
http://www.bo.astro.it/~eps/lezioni/lezioni.html

- **SSP Theory (Renzini & Buzzoni (1986)**
- **UV Upturn (O'Connell 1999)**
- **Dropout galaxies (Madau 1996)**
- **Madau Plot (1997)**
- **Cosmic SFR (Madau & Dickinson (2014)**
- **Galaxy mass assembly (Pan 2015)**
- **M/L clusters (Girardi et al. 2002)**

Teoria delle Popolazioni Stellari Composite (CSPs)

Buzzoni (2005)

Definition:

$$[CSP] = \int [SSP] \otimes SFR$$

A relevant case: SFR = const

$$\mathcal{L}_{CSP} = \int_0^T L_{SSP}\, dt$$

$L_{SSP} \rightarrow t^{-\alpha}$ $\quad (\alpha < 1)$

$$\mathcal{L}_{CSP}\Big|_T = \frac{T^{1-\alpha}}{1-\alpha} \qquad \mathcal{L}_{CSP} \propto t^{0.15}$$

Conclusion: Total luminosity in a CSP is an INCREASING function of time

Color evolution:

SSP

$$\begin{cases} L_B \propto t^{-\alpha_B} \\ L_V \propto t^{-\alpha_V} \end{cases}$$

CSP

$$\begin{cases} \mathcal{L}_B \propto t^{1-\alpha_B} \\ \mathcal{L}_V \propto t^{1-\alpha_V} \end{cases}$$

SAME LAW!

$$\frac{L_B}{L_V} \propto t^{-(\alpha_B - \alpha_V)}$$

LUMINOSITY EVOLUTION

SSPs
(≈ Ellittiche)

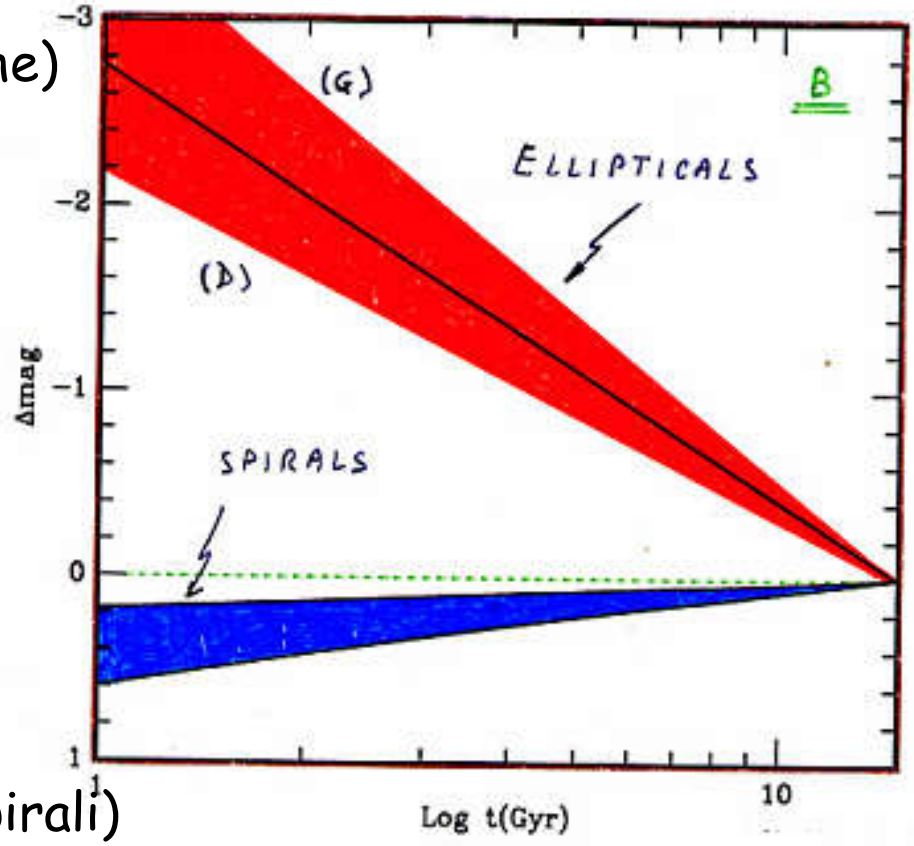

CSPs
(≈ Dischi Spirali)

Ellipticals $L_t \propto t^{-\alpha} \sim t^{-0.8}$

Spirals (disk) $L_t \propto t^{1-\alpha} \sim t^{+0.2}$

Star Formation Rate (Leggi di Schmidt)

$$SFR = -\frac{d f_{gas}}{d t}$$

$$PDMF_{(M,t)} = \int_0^{t \leq T} SFR \times IMF_{(M)}\, dt$$

$\Downarrow$

OBSERVED $\quad 0 \leq t \leq T$

ASSUMED $\quad SFR \propto f_{gas}^{n} \quad n = 2 \quad$ SCHMIDT LAW

$n = 1 \quad SFR = k f = -\dot{f} \quad SFR = k e^{-kt}$

$n = 2 \quad SFR = k f^2 = -\dot{f} \quad SFR = \frac{k}{(1+kt)^2}$

$k = 1/\tau$ (star formation timescale)

$\lim k \to \infty \quad \tau \to 0 \Rightarrow$ SSP

$SFR \to \delta(0)$

Star Formation Rate (Leggi di Schmidt)

Soluzioni:

$n = 1$

$$\begin{cases} SFR = \dot{f}_* = -\dot{f}_{gas} \\ \dot{f}_* = k f_{gas} \end{cases} \rightarrow k f_{gas} = -\frac{d f_{gas}}{dt}$$

$$\frac{d f_{gas}}{f_{gas}} = -k\,dt \quad \text{integro:} \quad f_{gas}(t) = f_{gas}(0)\, e^{-kt}$$

posso assumere $k = \frac{1}{\tau}$ ← tempo scala

Quindi, alla fine ho:

$$\begin{cases} f_{gas} = e^{-kt} \\ SFR = k e^{-kt} \end{cases} \qquad b = \frac{SFR_0}{\langle SFR \rangle} = \frac{k e^{-kt}}{\frac{k}{t}\int_0^t e^{-k\tau} d\tau} = \frac{kt}{e^{+kt} - 1}$$

$0 \leq b \leq 1$

$n = 2$ (Legge di Schmidt canonica)

$$\begin{cases} SFR = -\dot{f}_{gas} \\ SFR = k f_{gas}^2 \end{cases} \rightarrow k f_{gas}^2 = -\frac{d f_{gas}}{dt}$$

$$\frac{d f_{gas}}{f_{gas}^2} = -k\,dt \quad \text{integro:} \quad \frac{1}{f_g(0)} - \frac{1}{f_g(t)} = -kt$$

$$\begin{cases} f_{gas} = \frac{1}{1+kt} \\ SFR = \frac{k}{(1+kt)^2} \end{cases} \qquad b = \frac{k}{(1+kt)^2} \frac{t}{\int \frac{k}{(1+kt)^2}} = \frac{1}{1+kt}$$

$0 \leq b \leq 1$

Star Formation Rate (Power Law)

Soluzione:

Assumo che l'efficienza del meccanismo di formazione stellare sia un parametro intrinseco della galassia, che <u>solo</u> dipende dalla sua morfologia.

Ne consegue che:

$$\begin{cases} SFR = k t^{-\beta} \\ SFR = -\dot{f}_{gas} \end{cases} \rightarrow \quad k t^{-\beta} = -\frac{d f_{gas}}{dt}$$

k ha le dimensioni di $t^{+(\beta-1)}$

$$df_{gas} = -k t^{-\beta} dt \rightarrow 1 - f_{g(t)} = \frac{k}{1-\beta} t^{1-\beta}$$

$$\begin{cases} f_{g(t)} = 1 - \frac{k t^{1-\beta}}{1-\beta} \\ SFR(t) = k t^{-\beta} \end{cases} \qquad b = \frac{k t^{-\beta}}{\frac{k}{t(1-\beta)} t^{1-\beta}} = (1-\beta) \quad \forall t$$

Quindi il Birthrate è indipendente dal tempo.

Il gas si esaurisce in un tempo finito:

$$t_{MAX} = \left(\frac{1-\beta}{k}\right)^{\frac{1}{1-\beta}}$$

SFR & Birthrate

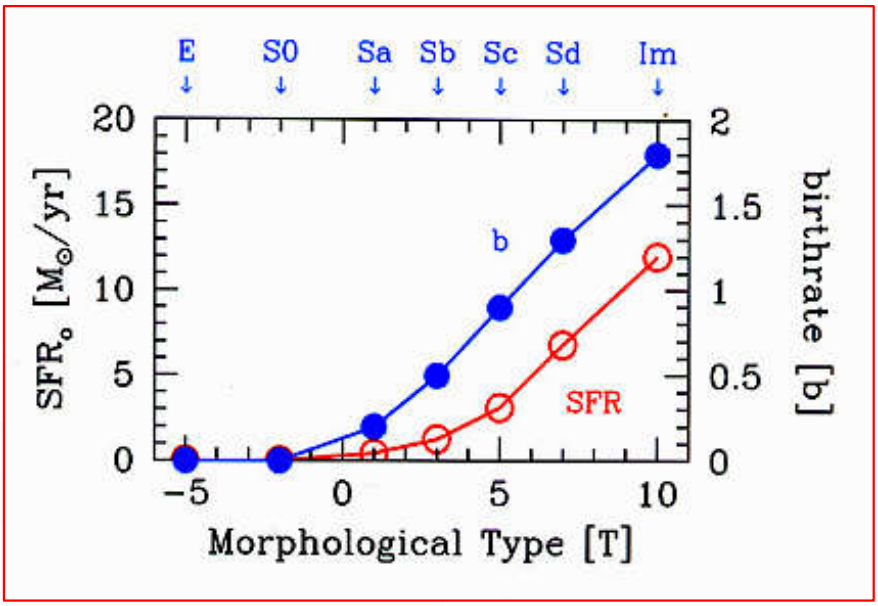

Buzzoni (2002)

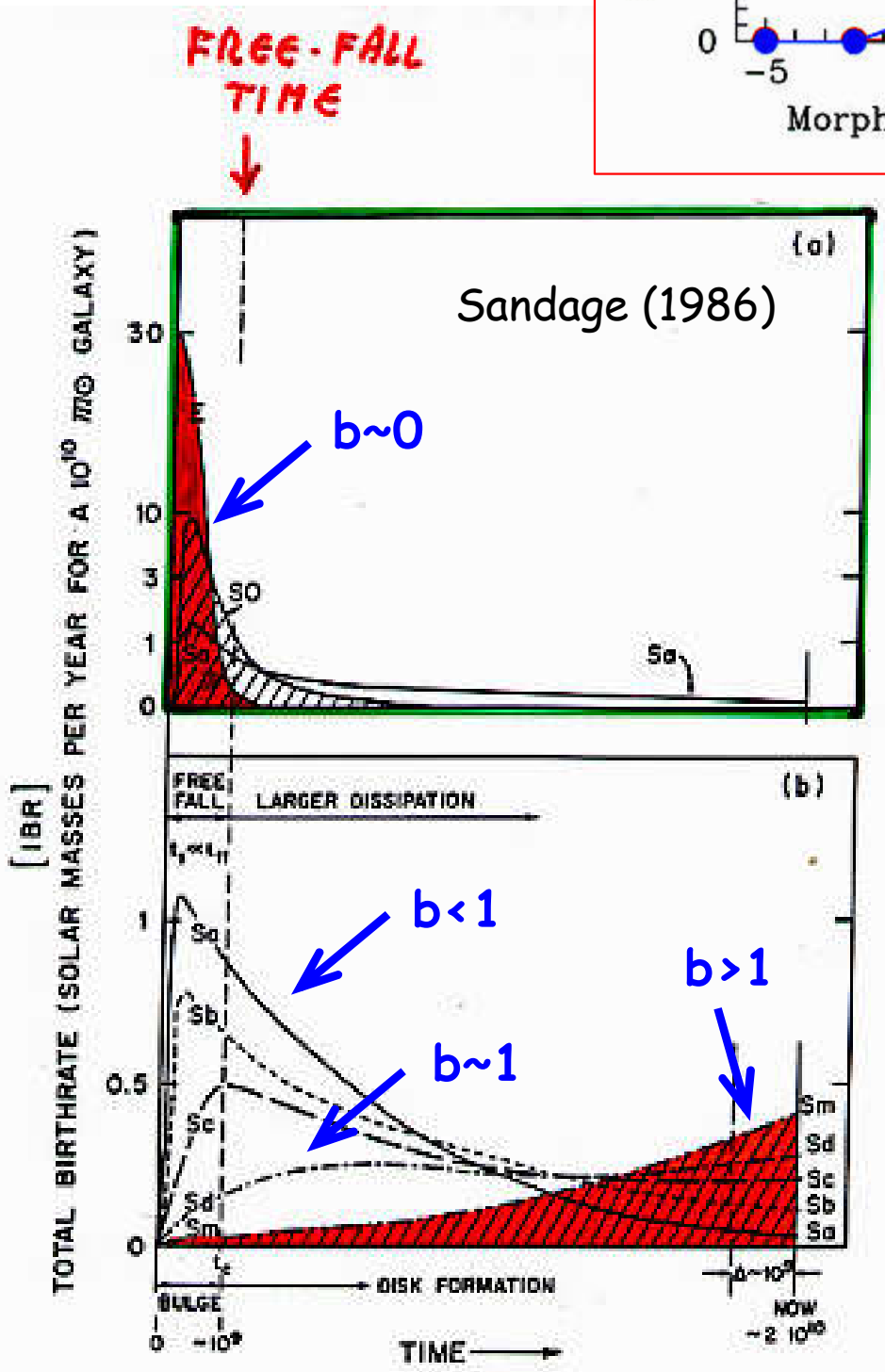

Fig. 10. Same as Fig. 9 with later Hubble types shown in the lower panel. The integral under the Sm curve is shaded for illustration. The curves are only schematic showing the trends that have been established by Gallagher et al. (1984)

Birthrate

$$b = \frac{SFR_o}{< SFR >}$$

Eta' media delle popolazioni e colore integrato delle galassie

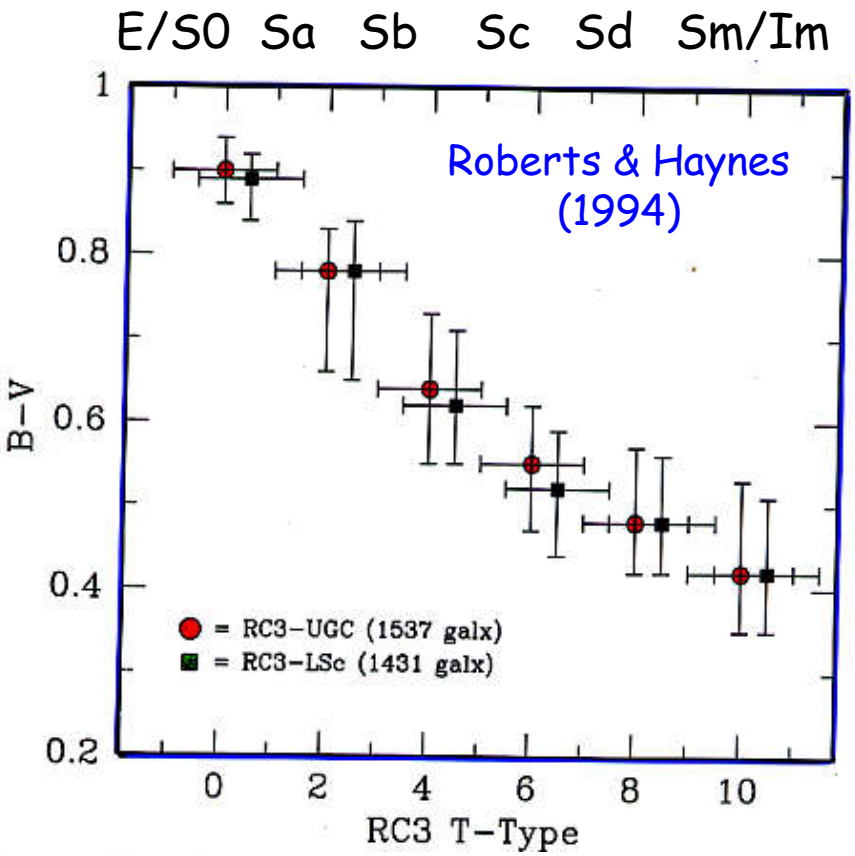

Nel caso di una SFR a legge di potenza:

$$SFR = k\,t^{-\beta}$$

$$\mathcal{L}_{(t)} = k'\int^{t} \tau^{-\alpha}(t-\tau)^{-\beta}\,d\tau = k'\,\frac{\Gamma_{(1-\alpha)}\Gamma_{(1-\beta)}}{\Gamma_{(2-\alpha-\beta)}}\,t^{1-\alpha-\beta}$$

$$b = \frac{SFR(t)}{\langle SFR\rangle} = \frac{k\,t^{-\beta}(1-\beta)\,t}{k\,t^{(1-\beta)}} = (1-\beta) \quad \forall\, t$$

Età media delle SSP componenti (pesata con la luminosità)

$$\langle t\rangle = \frac{k'\int \tau\,\tau^{-\alpha}(t-\tau)^{-\beta}\,d\tau}{k'\int \tau^{-\alpha}(t-\tau)^{-\beta}\,d\tau} = \frac{\int \tau\,\mathcal{L}_{(\tau)}}{\mathcal{L}_{(t)}}$$

Ricordando che $\Gamma_{(1+n)} = n!\,\Gamma_{(n)}$

$$\langle t\rangle = \frac{\Gamma_{[1+(1-\alpha)]}\,\Gamma_{(1-\beta)}}{\Gamma_{[2+(1-\alpha)-\beta]}}\,\frac{\Gamma_{(2-\alpha-\beta)}}{\Gamma_{(1-\alpha)}\,\Gamma_{(1-\beta)}}\,\frac{t^{2-\alpha-\beta}}{t^{1-\alpha-\beta}}$$

$$\boxed{\langle t\rangle = \frac{1-\alpha}{2-\alpha-\beta}\,t}$$

$$\boxed{\frac{\langle t\rangle}{t} \ll 1 \quad \text{se} \quad b \gg 0}$$

Birthrate & Downsizing

Buzzoni (2011) – Marino et al. (2009)

GALEX

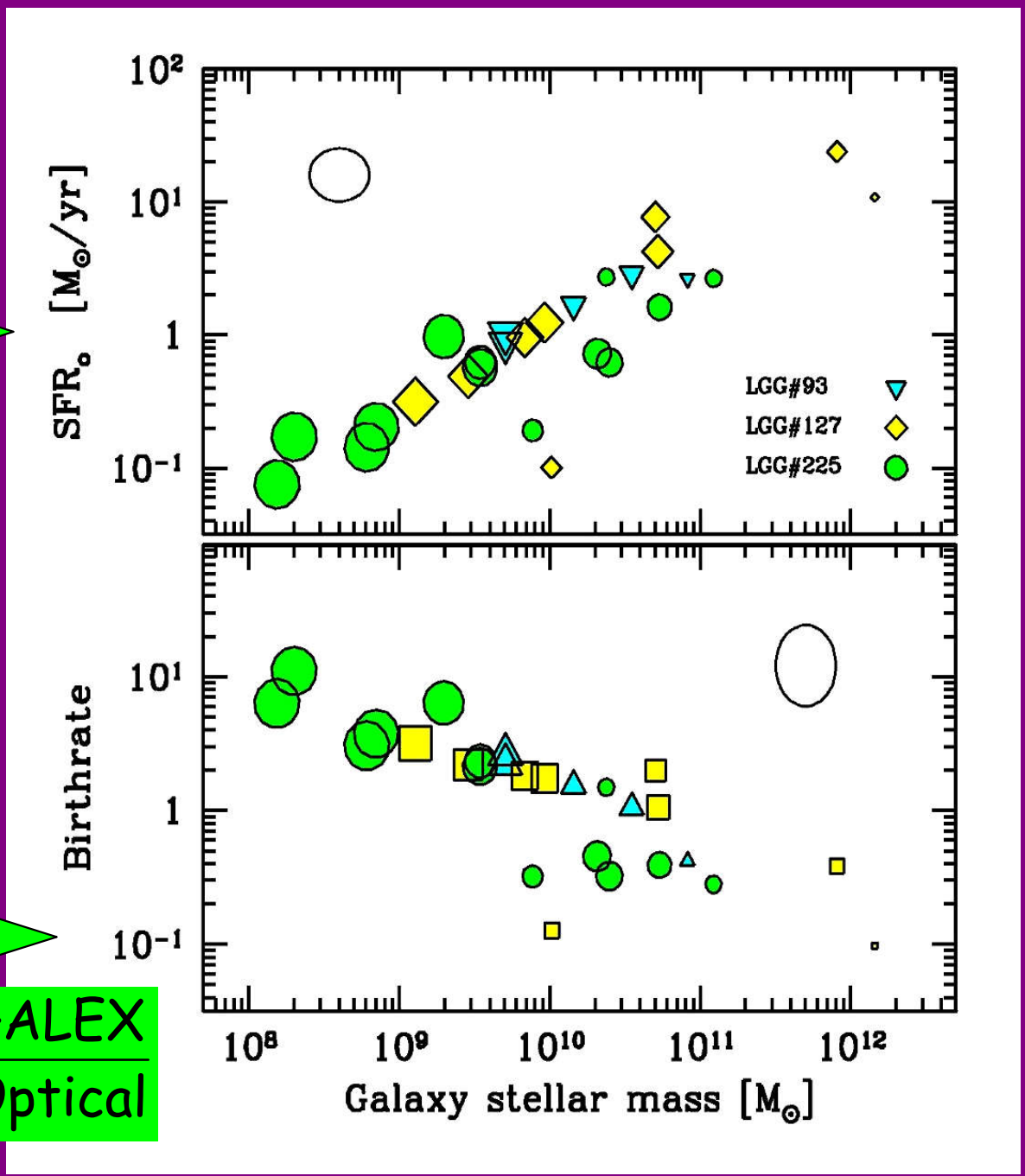

$$b = \frac{SFR}{\langle SFR \rangle} = \frac{GALEX}{Optical}$$

Gas fraction & ISM Metallicity

Kuzio de Naray et al. (2004)

Garnett (2002)

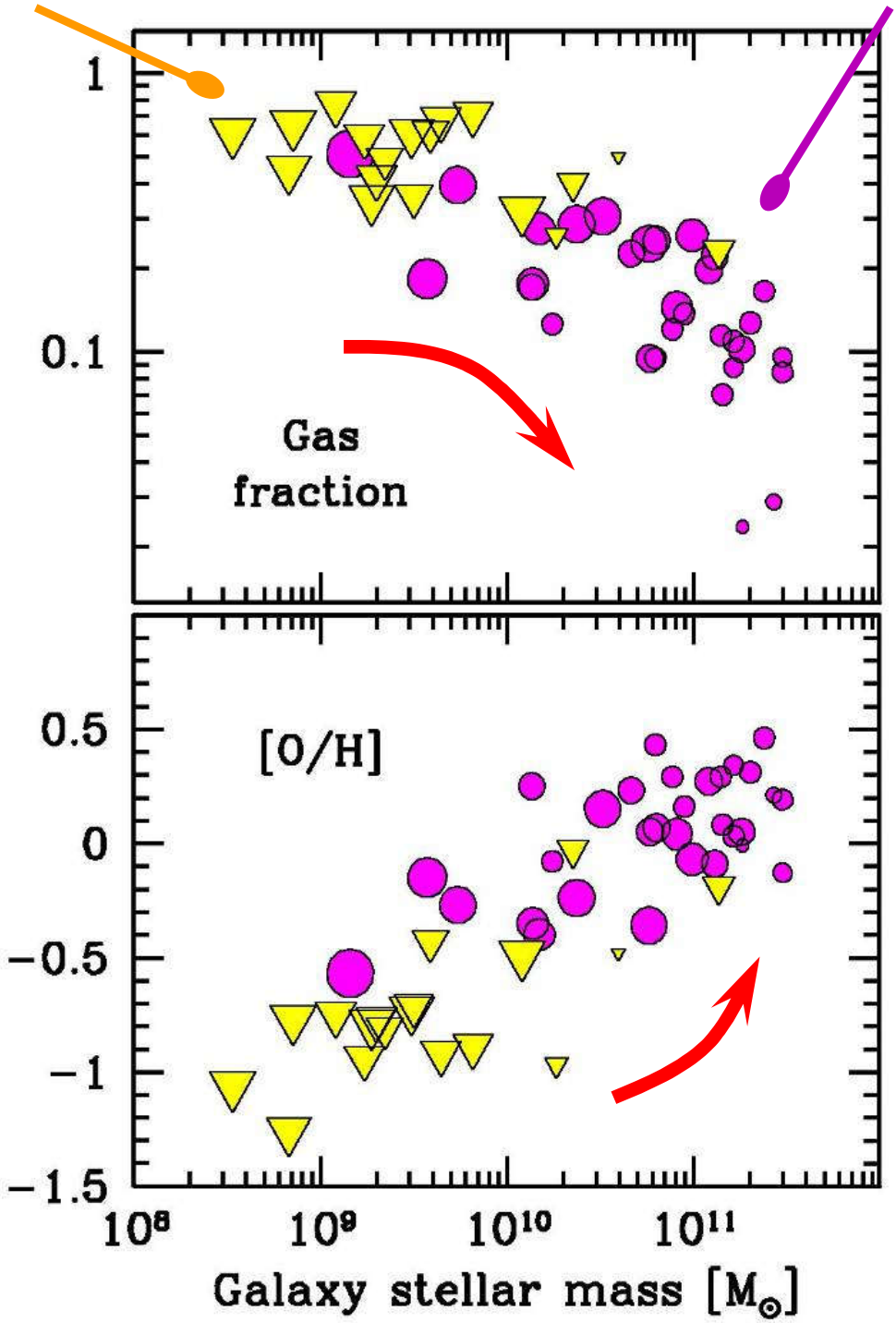

The Roberts time
(hurry up: the party is over!)

Tempo di Roberts: $t_R \sim \frac{f_{gas} M_{gal}}{SFR_{now}}$ ma (vedi dopo) $b = \frac{SFR_{now}}{M_{gal}} t_{gal}$

Combinandole: $\frac{t_R}{t_{gal}} = \frac{f_{gas}}{b} \sim \frac{\sim 0.1}{\sim 1}$ **Quindi** t_R ~1-2 Gyr max

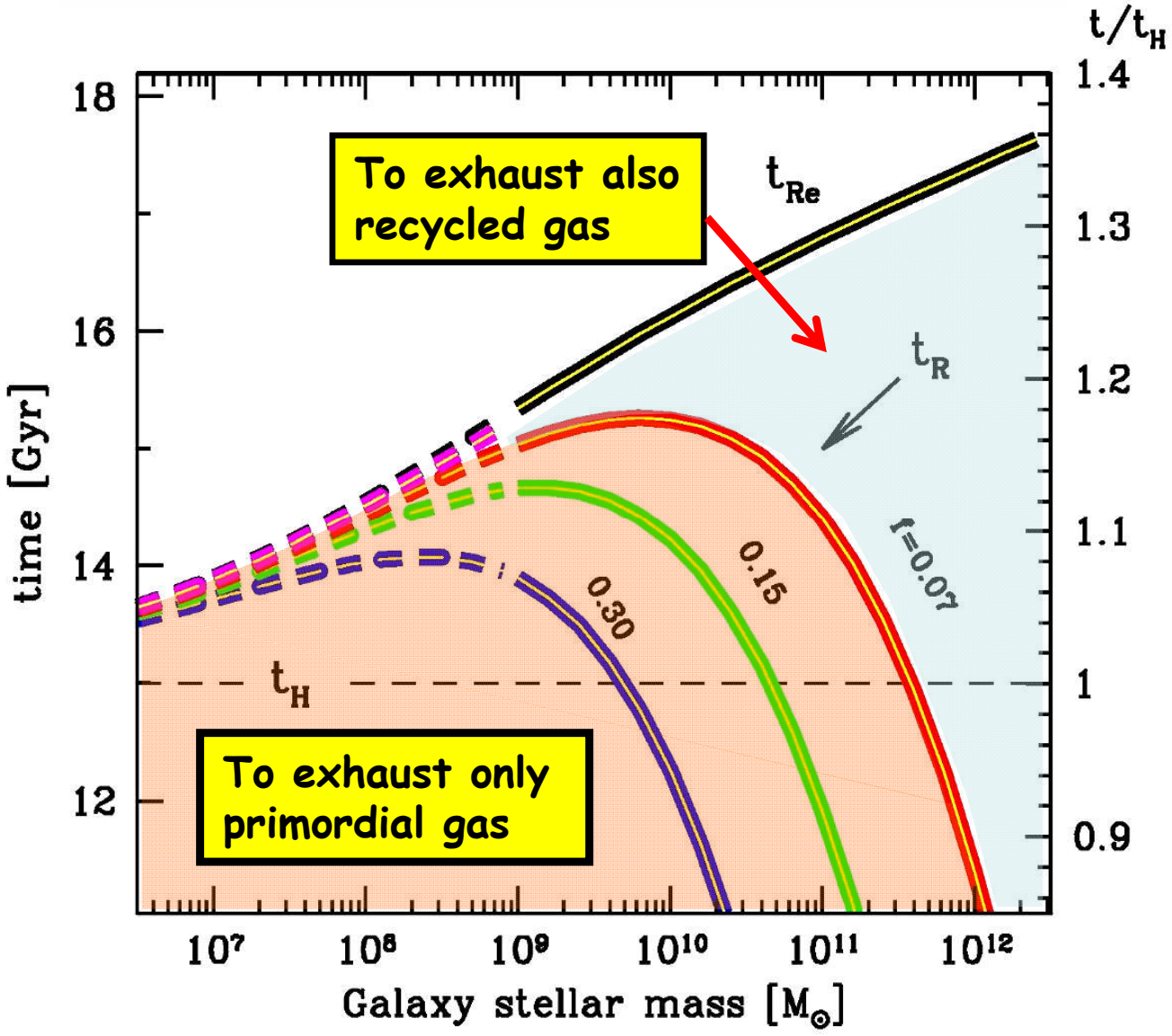

We are (so embarrassingly) close to the final death of galaxies as star-forming systems in the Universe!!

Energetica nucleare e rapporto M/L delle galassie

METAL ABUNDANCE

$$X + Y + Z = 1$$

HYDROGEN HELIUM "OTHERS"

$$\left[\frac{Fe}{H}\right] = \log\frac{Fe}{Fe_\odot} - \log\frac{H}{H_\odot}$$

IF $Fe \propto Z$

$$\left[\frac{Fe}{H}\right] = \log\frac{Z}{0.017} - \log\frac{1-Z-Y}{0.71} \approx \lg Z + 1.8$$

$$(X, Y, Z)_\odot = (0.70, 0.28, 0.017)$$

$1\,gr\ H \rightarrow 1\,gr\ Z$ — ENERGETICS

$6.6\ 10^{18}$ ergs

IN A GALAXY: $M_Z \sim 2\ 10^9\ M_\odot \sim 4\ 10^{42}\ gr$

$$M_Z = \frac{\int L \times t}{6.6\ 10^{18}} \sim \frac{\langle L\rangle\ 10^{10}\,yr}{6.6\ 10^{18}\ ergs}$$

$\langle L\rangle \sim 2.2\ 10^{10}\ L_\odot$ $\frac{M}{L} \leq 5$ in primordial galx

Energetica nucleare e tempi scala evolutivi

Atomic Number	Element Symbol	Element Name	Atomic Weight
1	H	Hydrogen	1.00794
2	He	Helium	4.002602
3	Li	Lithium	6.941
4	Be	Beryllium	9.012182
5	B	Boron	10.811
6	C	Carbon	12.0107
7	N	Nitrogen	14.0067
8	O	Oxygen	15.9994
9	F	Fluorine	18.9984032
10	Ne	Neon	20.1797
11	Na	Sodium	22.989770
12	Mg	Magnesium	24.3050
13	Al	Aluminium	26.981538
14	Si	Silicon	28.0855
15	P	Phosphorus	30.973761
16	S	Sulfur	32.065
17	Cl	Chlorine	35.453
18	Ar	Argon	39.948
19	K	Potassium	39.0983
20	Ca	Calcium	40.078
21	Sc	Scandium	44.955910
22	Ti	Titanium	47.867
23	V	Vanadium	50.9415
24	Cr	Chromium	51.9961
25	Mn	Manganese	54.938049
26	Fe	Iron	55.845

H+He burning

Supernovae I/II

Energetica nucleare e tempi scala evolutivi

H burning: 4 H ⟶ 1 He

4 x 1.00794 u ⟶ 4.002602 u + ε/c²

$$E = \frac{4.03176 - 4.002602}{4.002602} c^2 = 6.6 \cdot 10^{18} erg / gr$$

He burning: 4 He ⟶ 1 C^{12}

3 x 4.002602 u ⟶ 12.0107 u + ε/c²

$$E = \frac{12.007806 - 12.010700}{12.010700} c^2 = 0.2 \cdot 10^{18} erg / gr$$

4 He ⟶ 1 O^{16}

4 x 4.002602 u ⟶ 15.9994 u + ε/c²

$$E = \frac{16.010408 - 15.994000}{15.994000} c^2 = 0.9 \cdot 10^{18} erg / gr$$

Analytic fundamentals

Luminosity of a Composite Stellar Population:

$$\mathcal{L}_{CSP} = \int \ell_{SSP} \otimes SFR \; dt$$

Output energy after "t" years:

$$\mathcal{E}(t) = \int_0^t \mathcal{L}_{CSP}(\tau) d\tau$$

Analytic fundamentals (2)

Metal enrichment:

$$\frac{M_{yZ}}{M^*} = \frac{K^{-1}\varepsilon}{\int SFR} = \frac{\varepsilon_o}{KM_o}\left(\frac{t}{t_o}\right)^{0.23}$$

"Yield Metallicity" of processed mass scales with time as a power law:

$$Z \propto \frac{M_{yZ}}{M^*} \propto \left(\frac{t}{t_o}\right)^{0.23}$$

Mass energetic exploitation does (nearly) NOT depend on the galaxy SFR:

$$\mathcal{F} = \frac{\varepsilon_o}{KM_o}$$

~ 10 -13%

The Age-metallicity relation (AMR)

Buzzoni (2011)

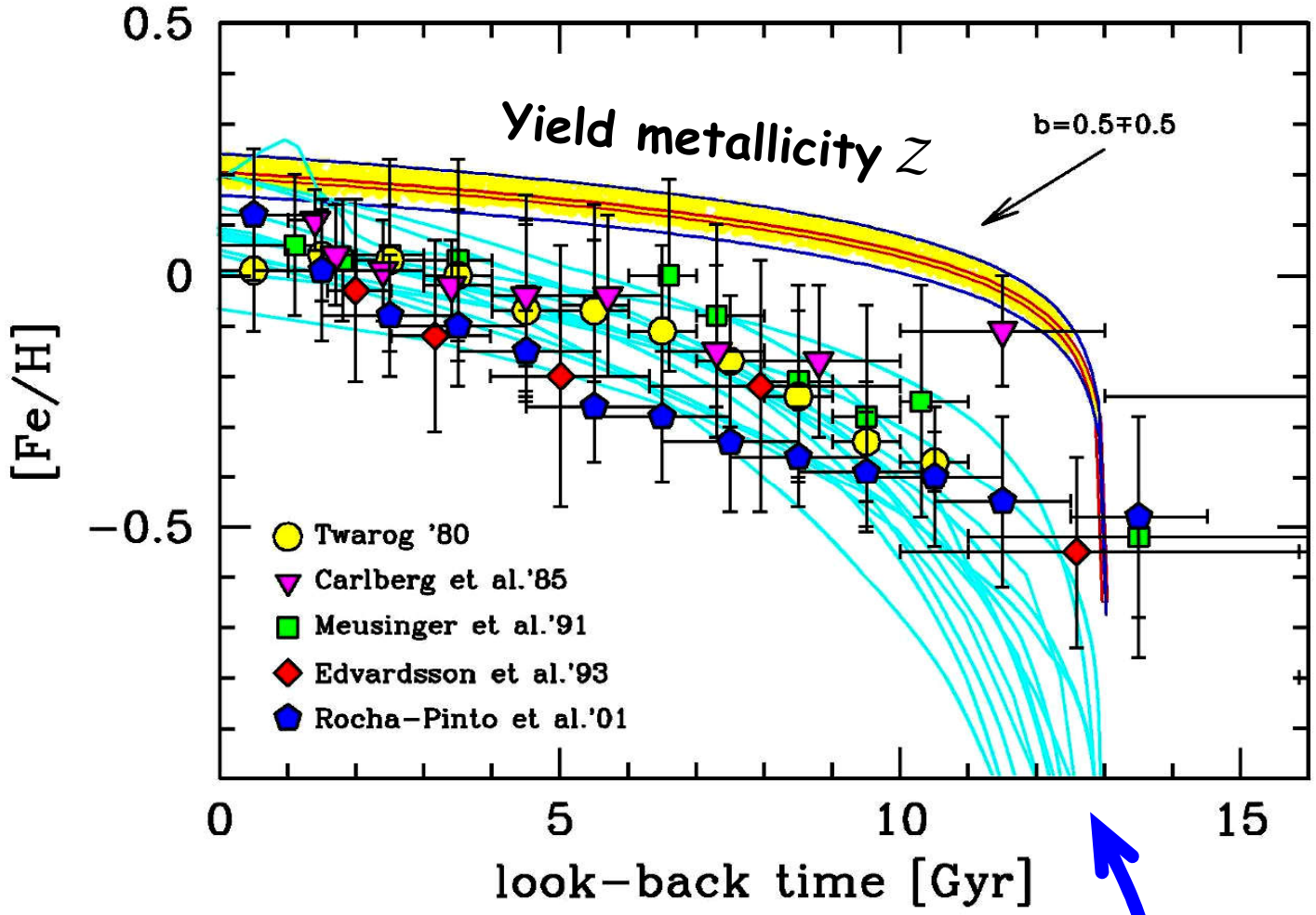

"explicit" chemical evolution (models)

Matteucci & Francois 89 // Wyse & Silk 89 // Carigi 94 // Pardi & Ferrini 94 // Prantzos & Aubert 95 // Timmes et al. 95 // Giovagnoli & Tosi 95 // Pilyugin & Edmunds 96 // Mihara & Takahara 96 // Chiappini,et al. 97 // Portinari et al. 98 // Boissier & Prantzos 99 // Alibes et al. 01

SURFACE BRIGHTNESS Σ_B

SURFACE DENSITY σ_T

GAS (HI)

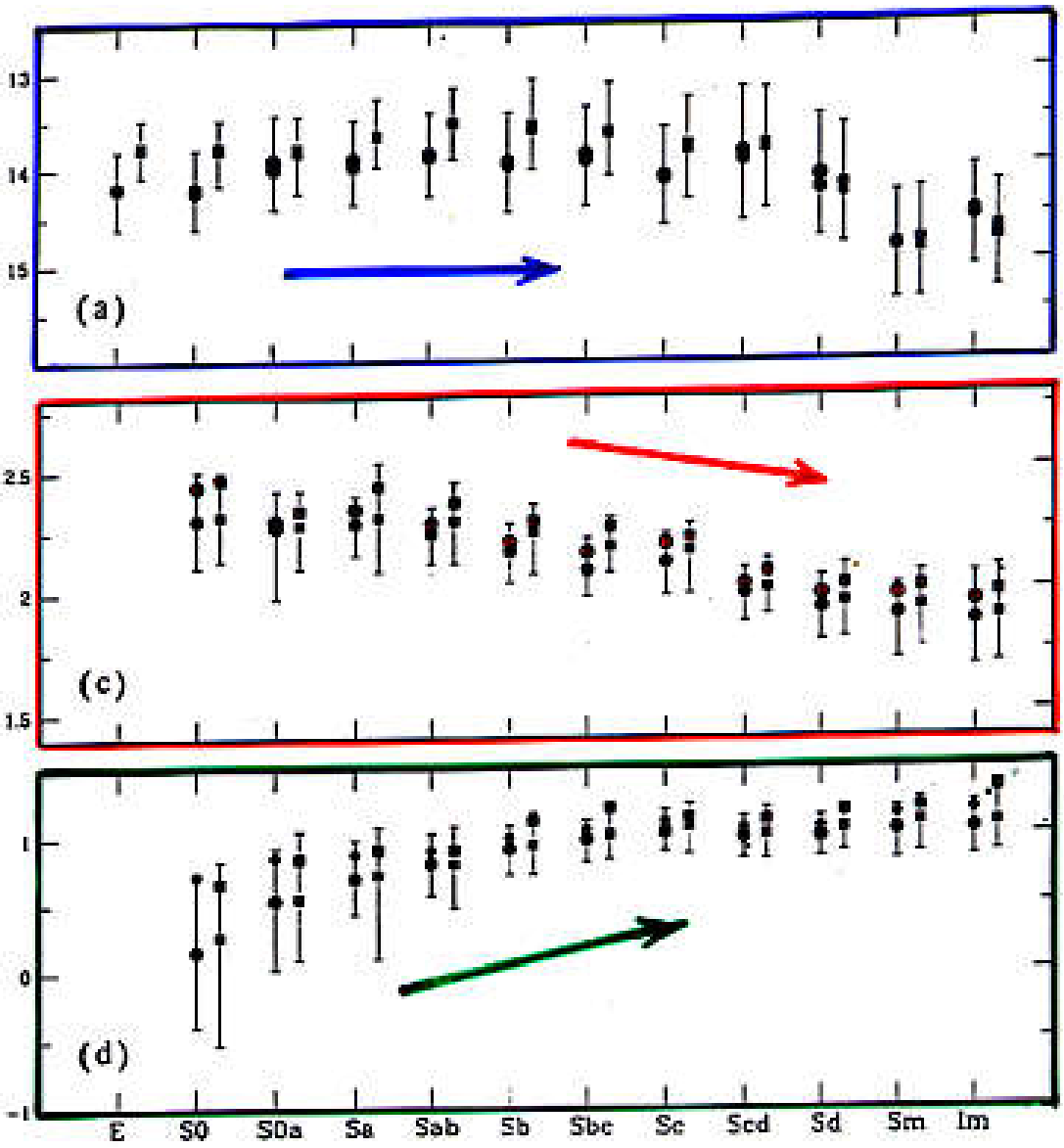

E Sø Sa Sb Sc Sd I

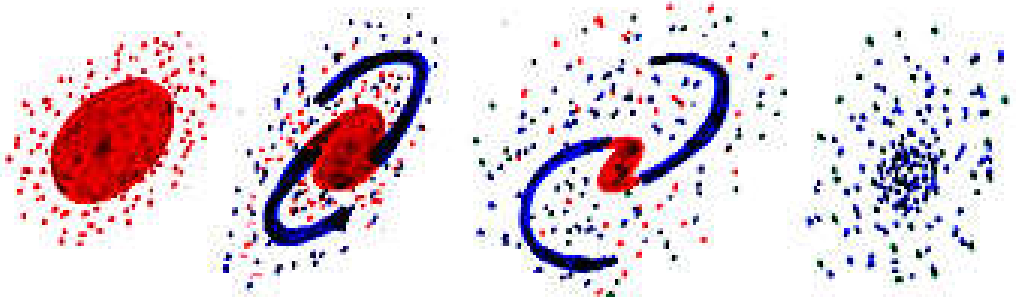

Classificazione Morfologica di Hubble

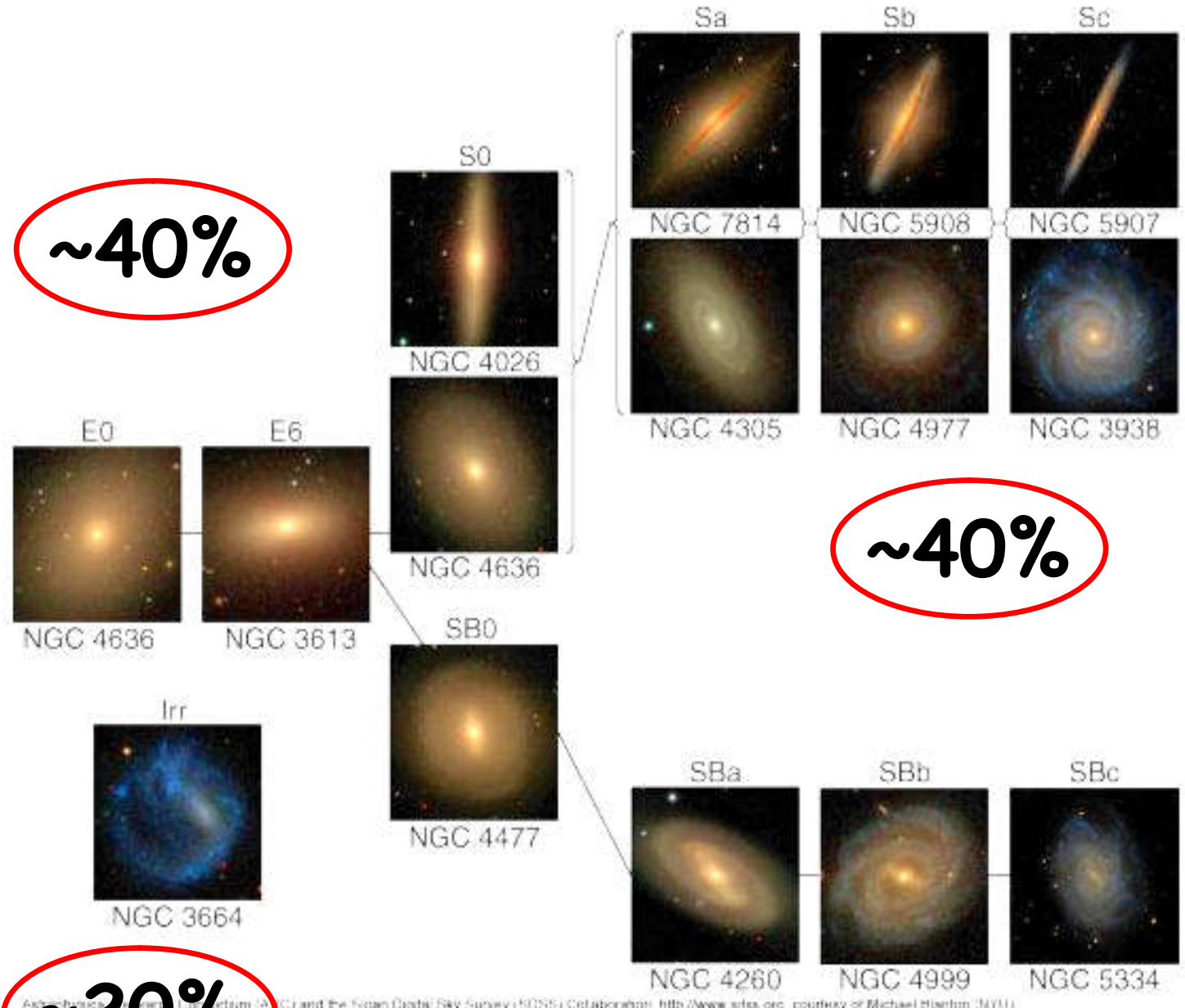

http://en.wikipedia.org/wiki/Galaxy_morphological_classification

Distribuzione galattica e tipo morfologico (Segregazione morfologica)

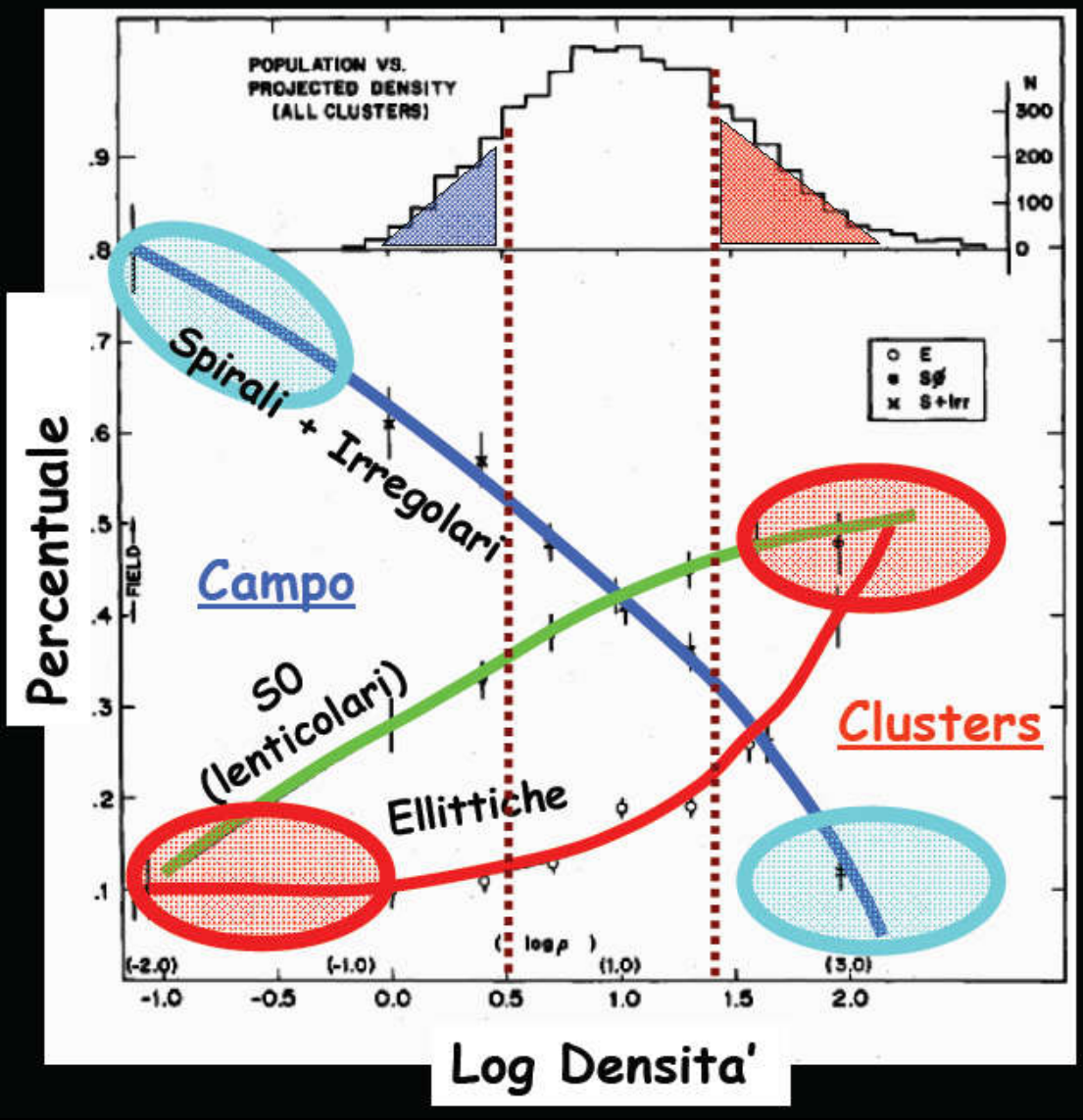

Dressler (1980)

Il Gruppo Locale

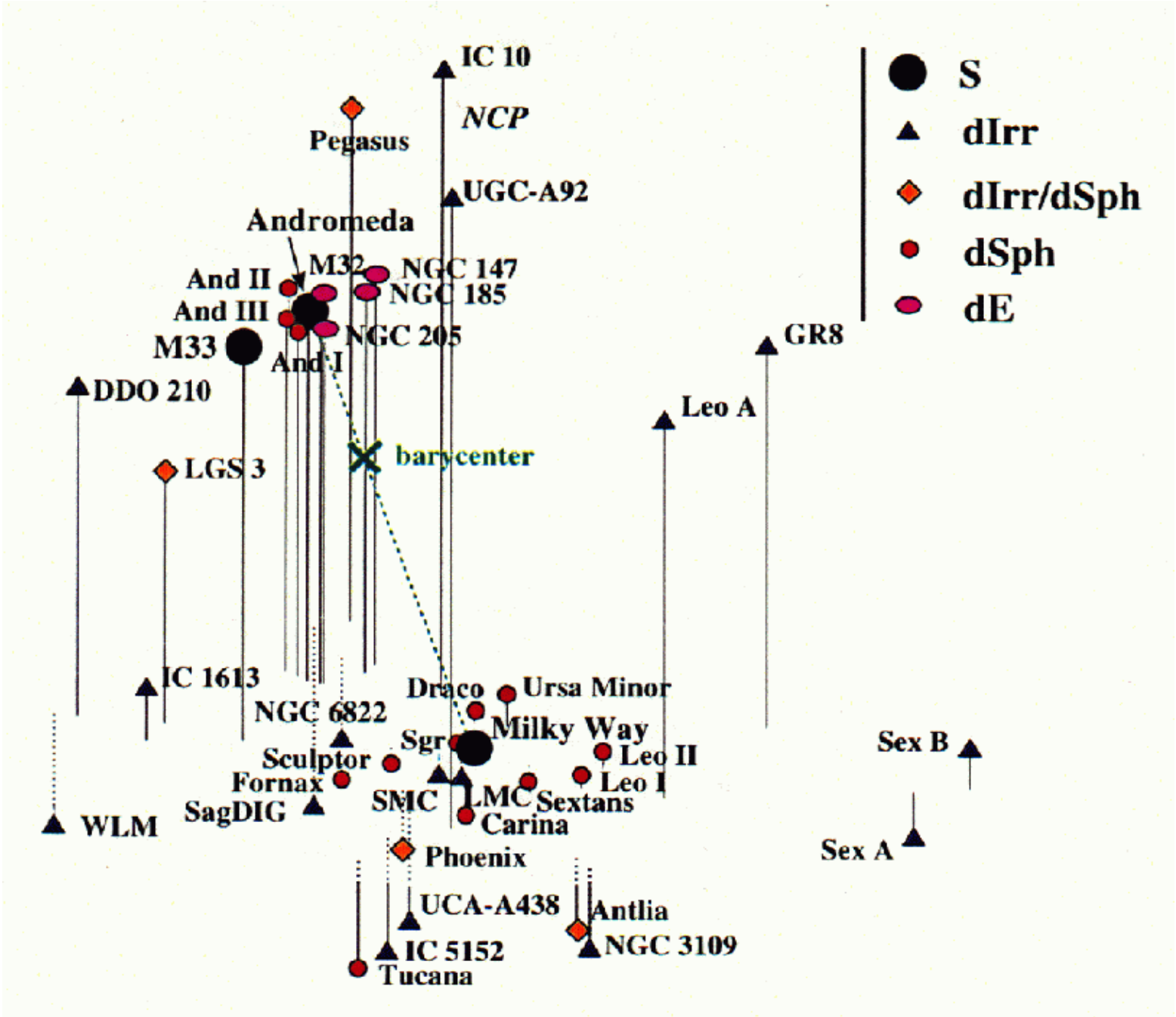

http://it.wikipedia.org/wiki/Gruppo_Locale

Galassie Ellittiche

NGC 5044
(~120 Milioni a.l.)

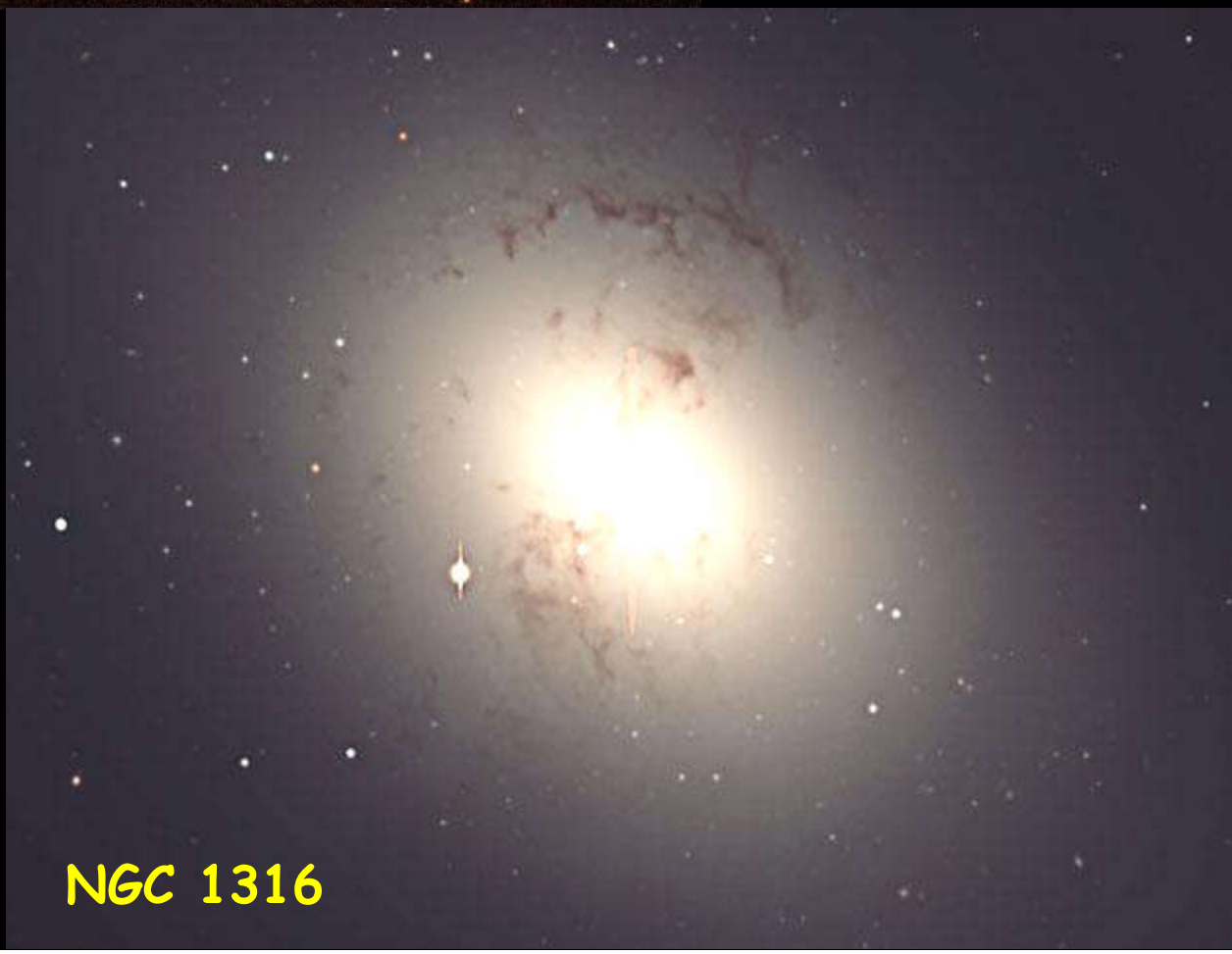

NGC 1316

Galassie ellittiche

M104
El Sombrero

NGC 1300
(69 Milioni a.l.in Eridano)

Galassie a spirale

Galassie Irregolari

NGC 55 (~LMC)
6 Milioni a.l.

Sferoidali nane

La sferoidale nana in Fornax (Gruppo Locale)

Gli Ammassi di Galassie

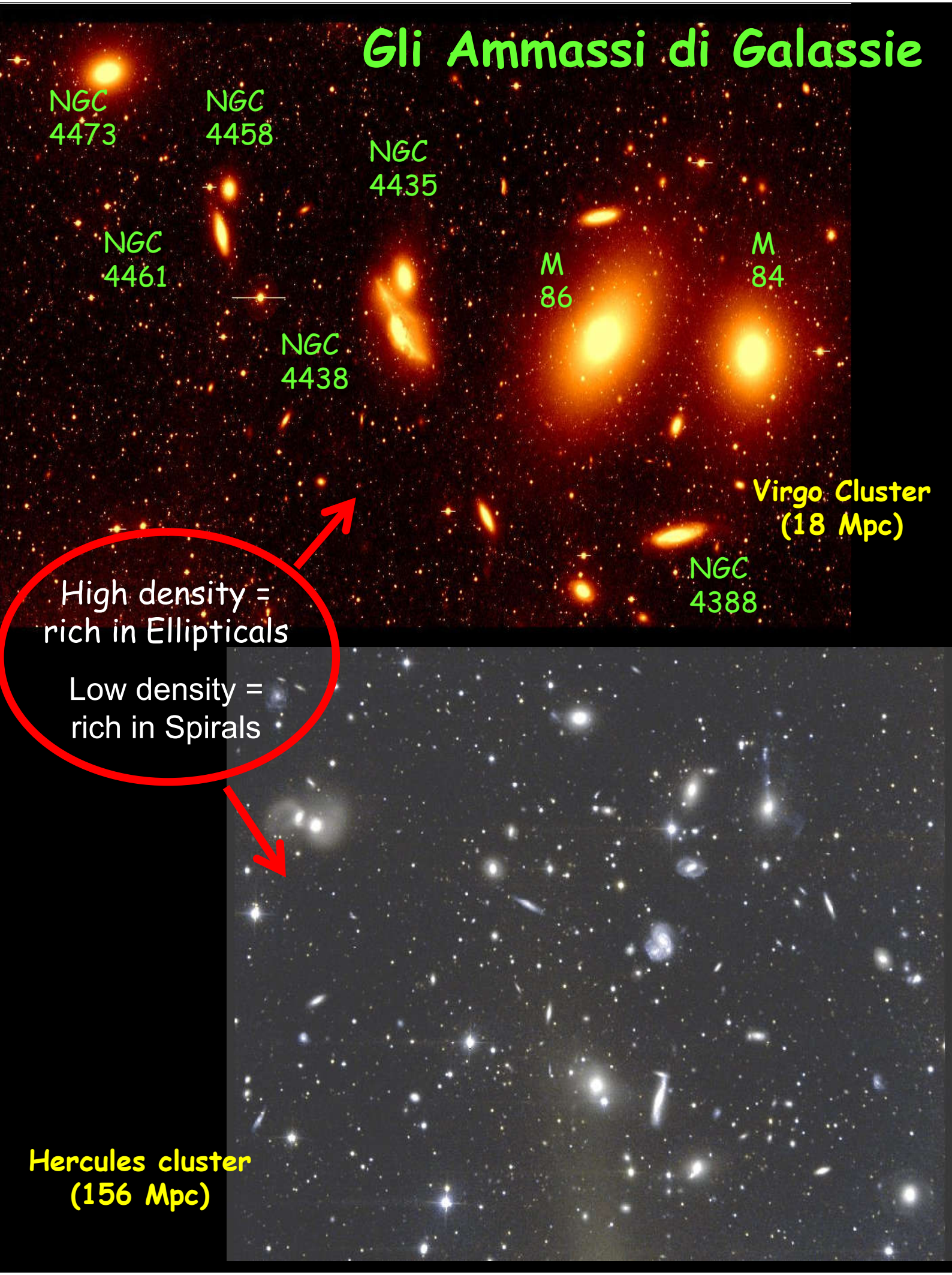

Lo spettro delle Ellittiche

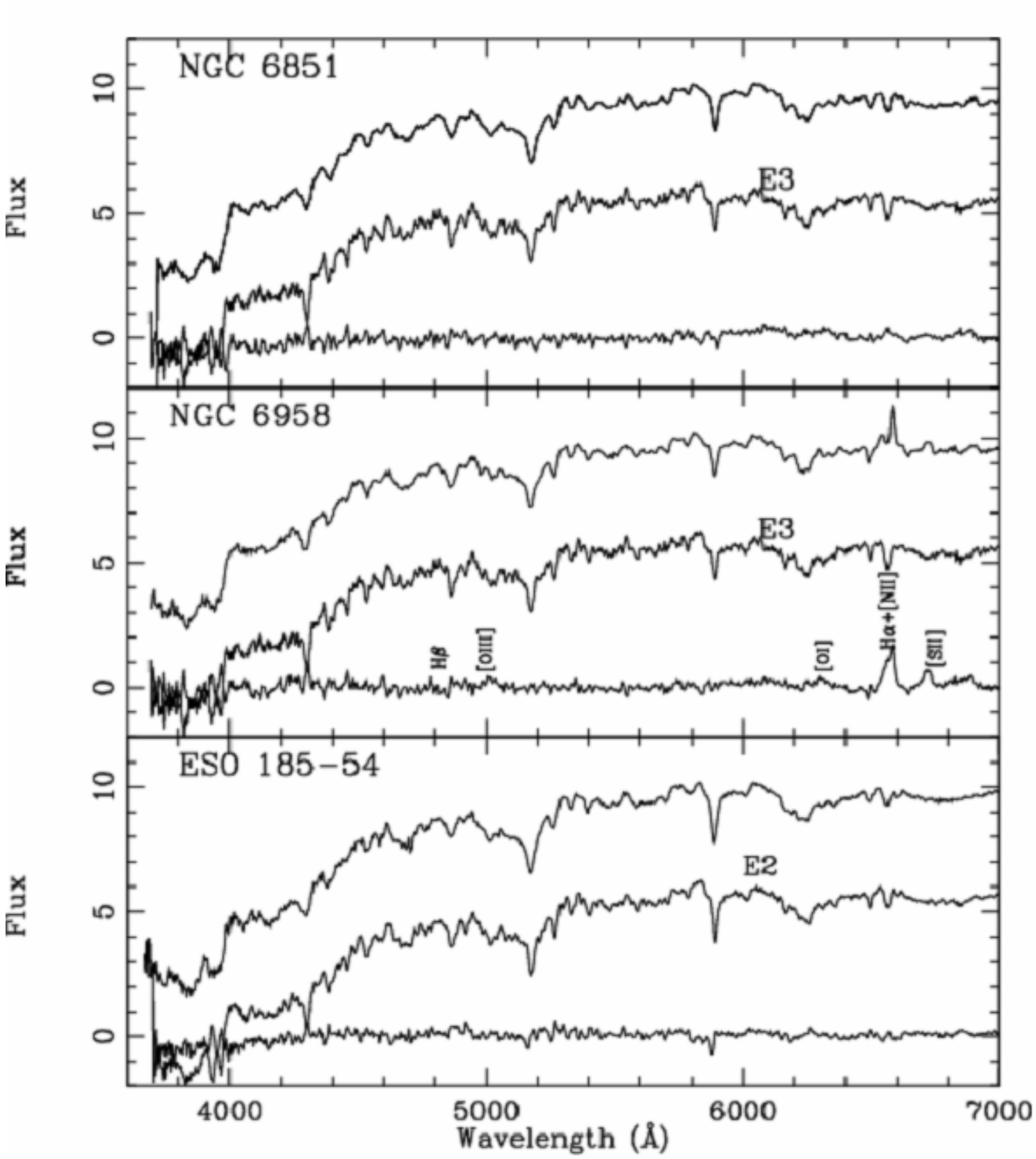

Lo spettro delle Spirali

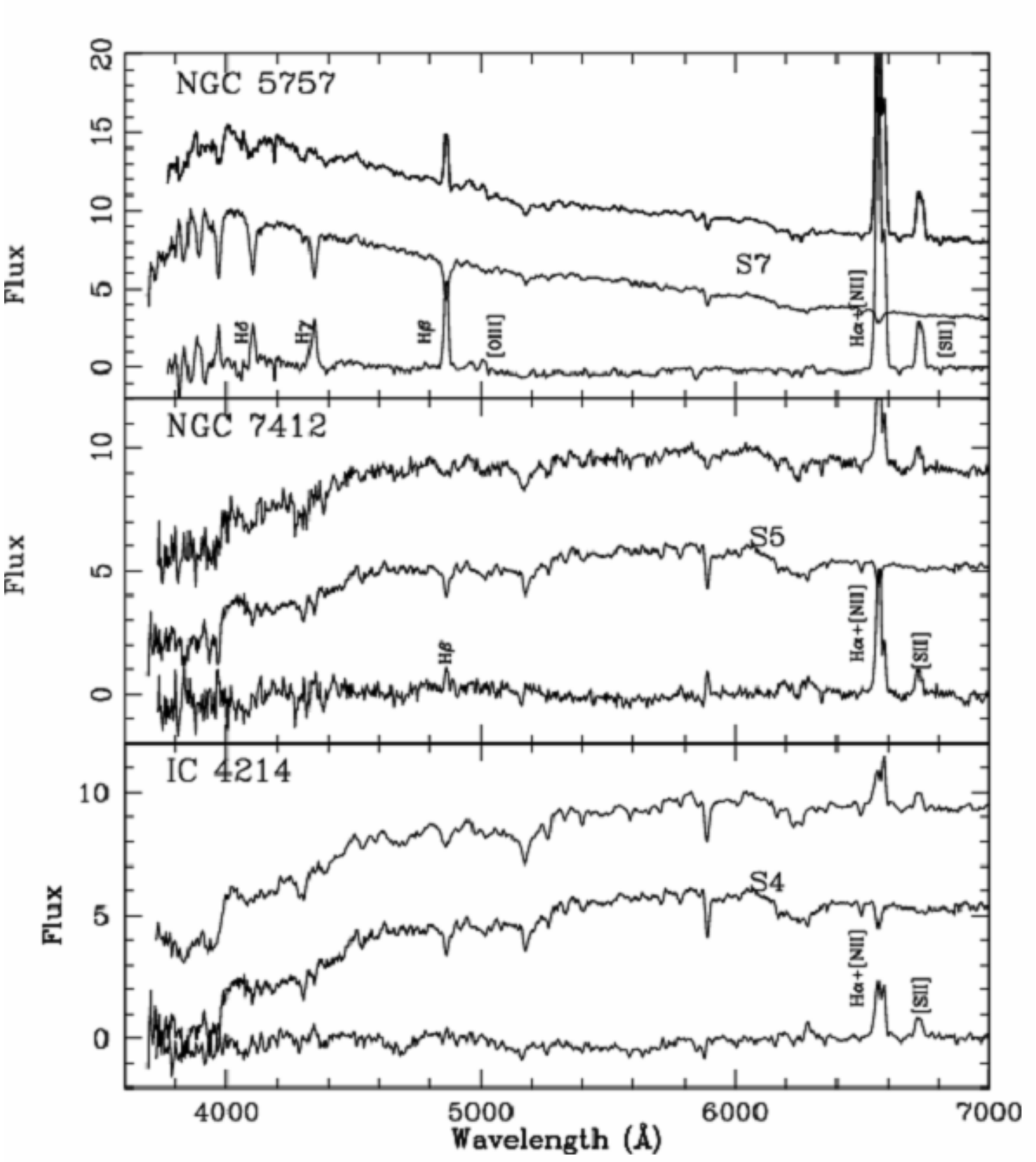

Articoli consigliati (vedi Webpage):
http://www.bo.astro.it/~eps/lezioni/lezioni.html

- **Galaxy Colors (Buzzoni 2005)**
- **Energetic & Chemical evolution of Spirals (Buzzoni 2011)**
- **Spectral Properties of Galaxies (Kennicutt 1992)**
- **Galaxy Spectral Atlas (Kennicutt 1992)**
- **SFR & Hubble Sequence (Kennicutt 1988)**
- **SFR in the MW (Kennicutt & Evans 2012)**
- **SFR (Ryder & Dopita 1994)**
- **SFR (Schmidt 1959)**
- **M/L clusters (Girardi et al. 2002)**
- **Galaxy mass assembly (Pan 2015)**

L'emissione UV nelle SSPs: l'UV Upturn nelle galassie ellittiche

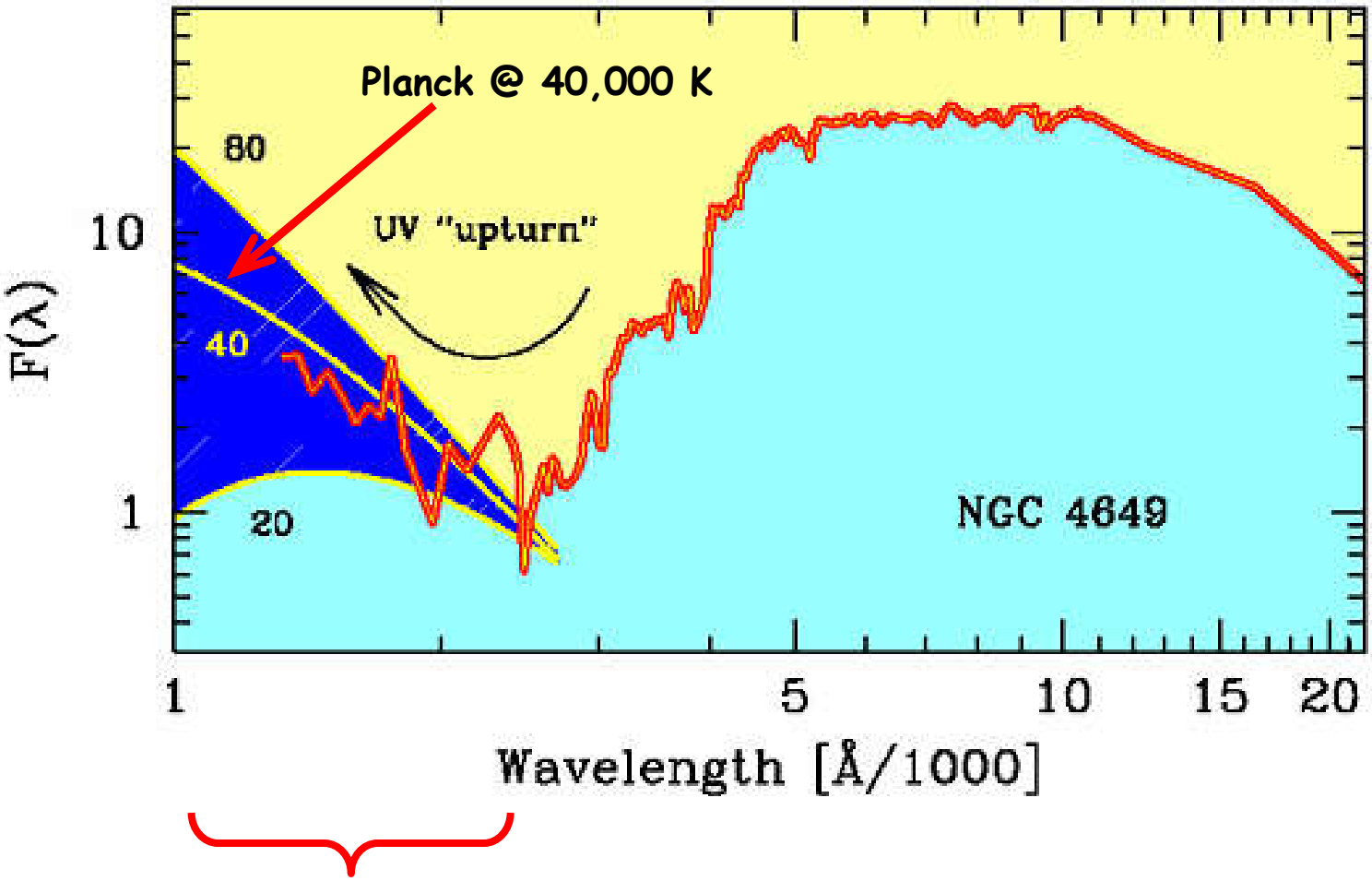

$$\left[\frac{\text{Integrale Planck}}{\text{Bolometrico}}\right] =$$

20,000	40,000	80,000 K
1.4%	**2.1%**	**6.0%**

Il meccanismo della Massa di core in HB

Castellani (1991)

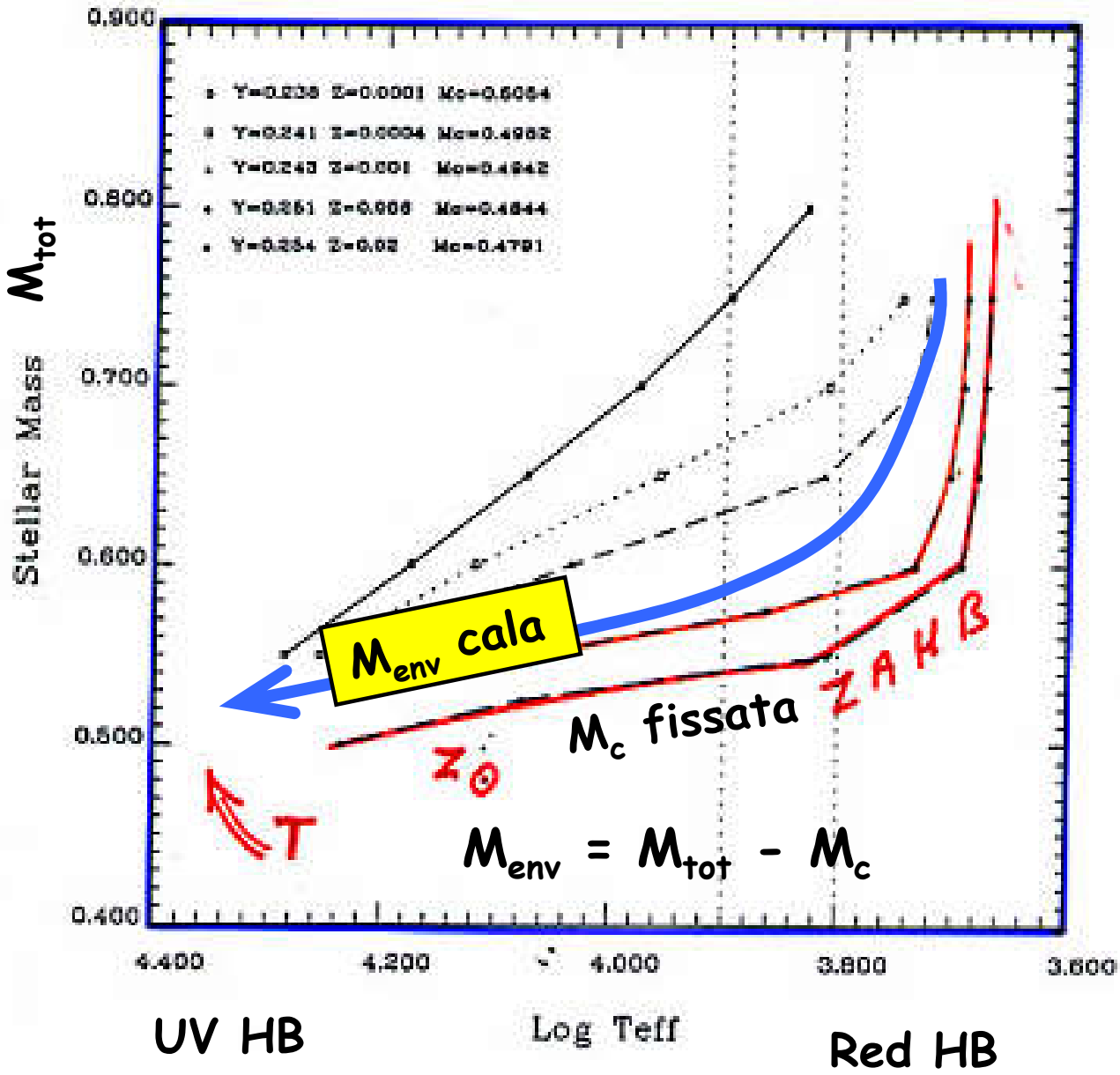

M_{env} cala se
1) Aumenta Mc (= Y ↑ perche' Z↑)
2) Aumenta la "mass loss" (= Z↑ ??)

Evoluzione spettrale dell'UV upturn

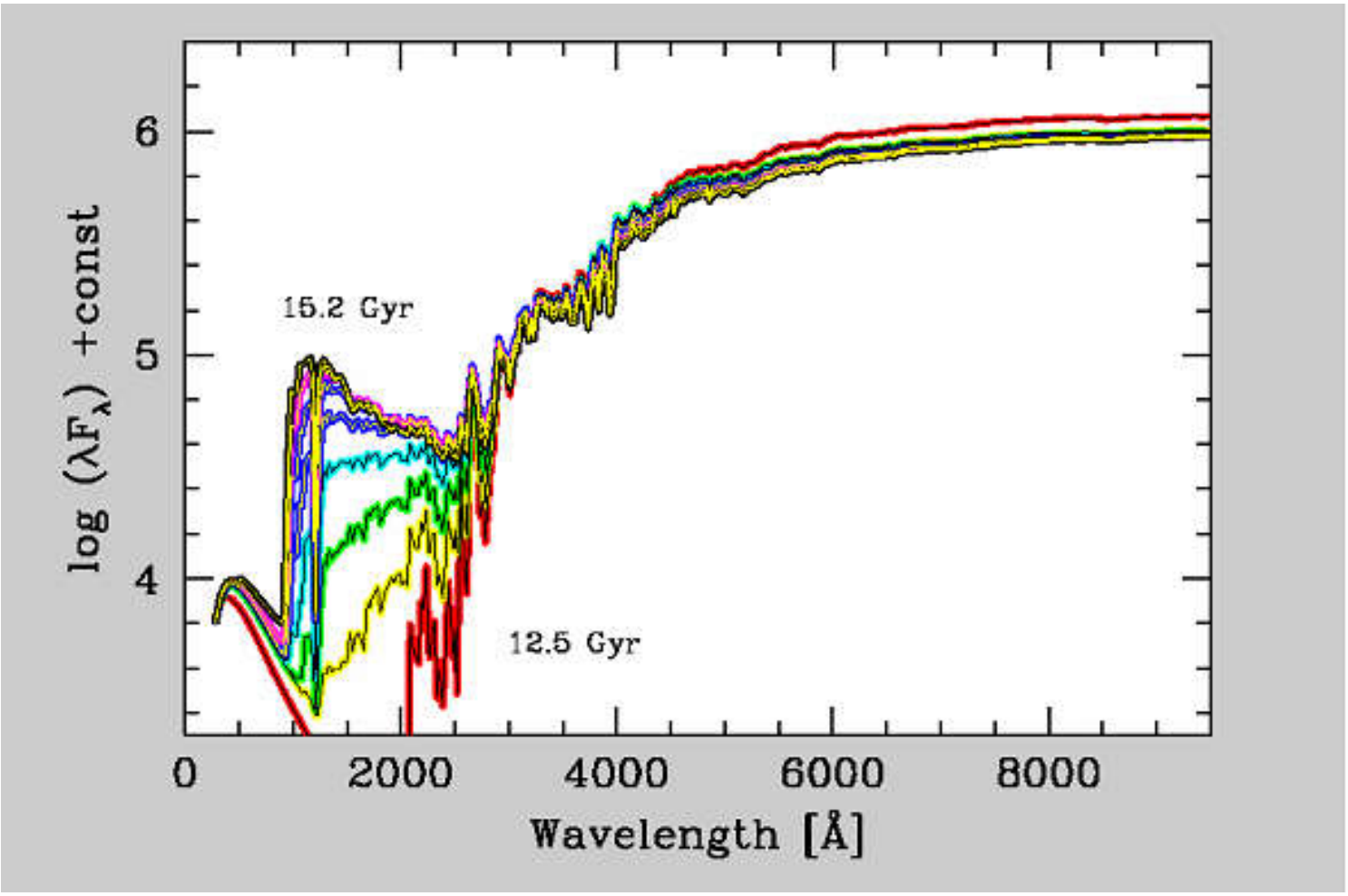

A parita' di efficienza del meccanismo che modula M_{env}, se aumenta M_{TO} possiamo aspettarci che aumenti anche M_{HB}. Siccome la T_{HB} e' molto sensibile a M_{HB}, se t ↑ allora M_{TO} ↑ e M_{HB} ↑. Quindi M_{env} ↑ e T↓. Quindi il Braccio Orizzontale tende velocemente al rosso e l'UV upturn scompare:

$$\frac{dt}{t} \approx -2\frac{dM_{TO}}{M_{TO}} \approx -2\frac{dM_{HB}}{M_{HB}}. \text{ Se } \frac{dM_{HB}}{M_{HB}} \approx 0.1 \Rightarrow \frac{dt}{t} \approx 0.2$$

Quindi, andando indietro di circa 2-3 Glyr (z~0.2-0.3) l'effetto dovrebbe scomparire.

M. CASTELLANI et al. (1994)

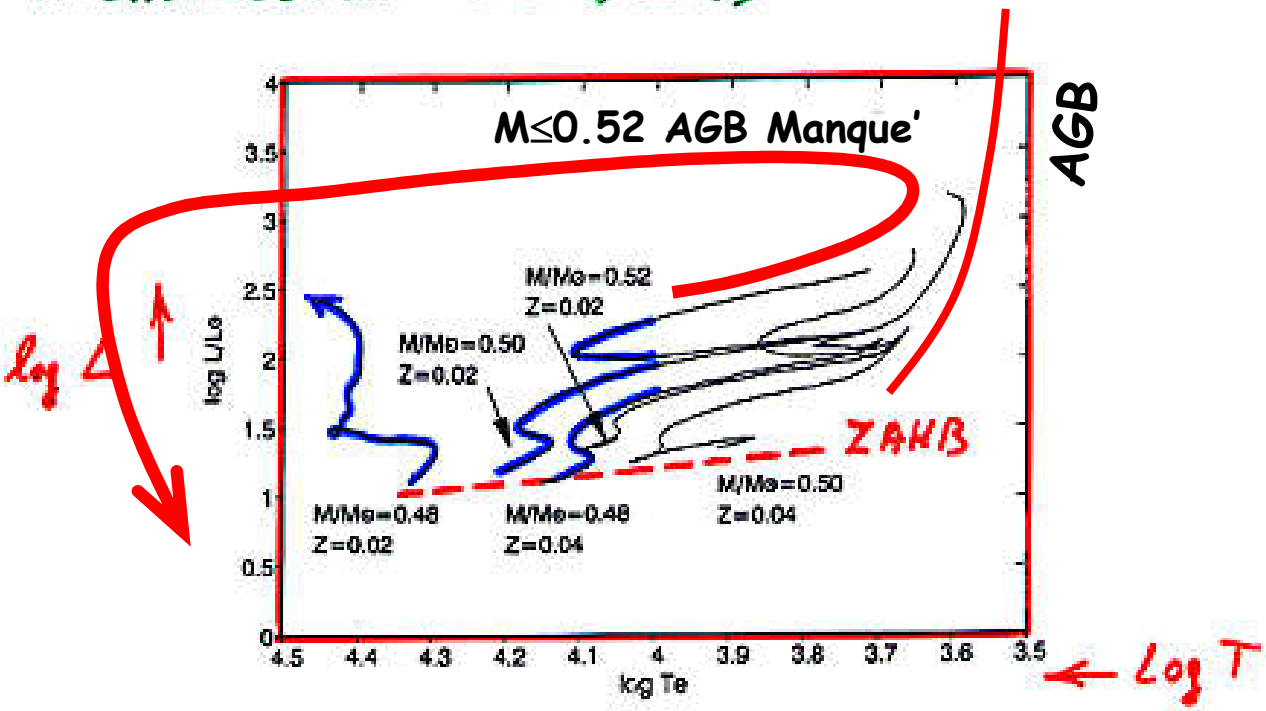

FIG. 1.—The H-R diagram of the models evolved at constant mass covering the central He-burning phase and (in some models) the initial He shell-burning phases.

V. CASTELLANI & TORNAMBÉ (1982)

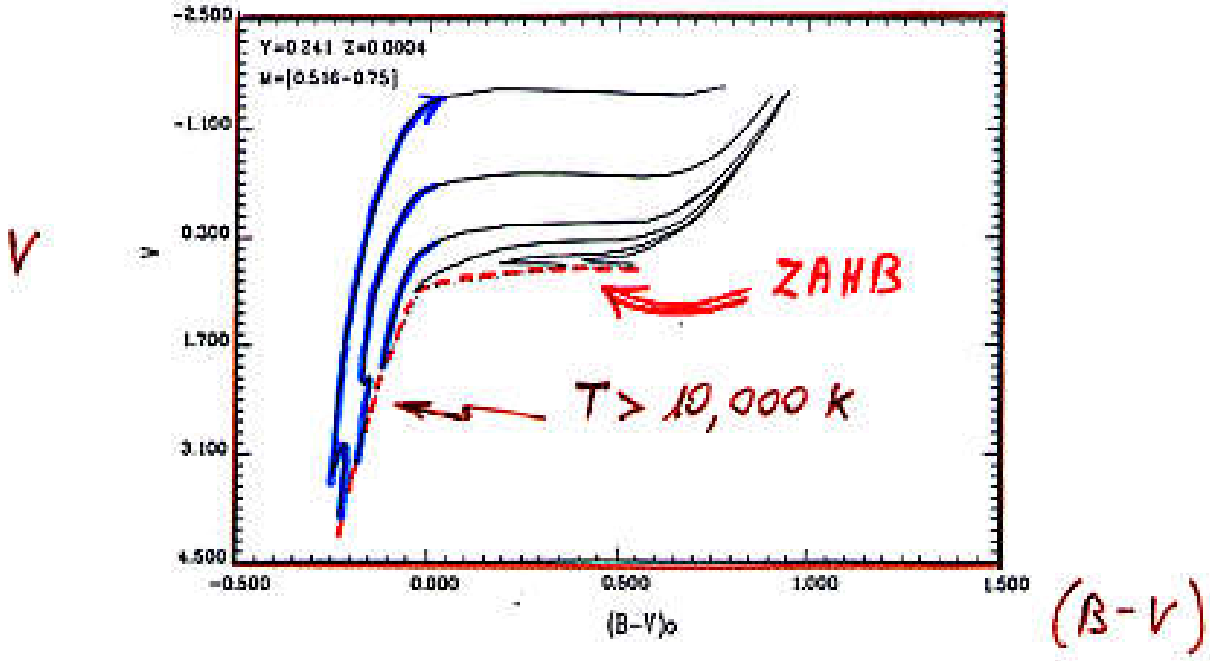

Fig. 5. The evolutionary paths in the V, $B-V$ plane of HB models with $Z = 0.0004$ and for selected values of the stellar mass in the labeled range of masses

Articoli consigliati (vedi Webpage):
http://www.bo.astro.it/~eps/lezioni/lezioni.html

- **SSP Theory (Renzini & Buzzoni 1986)**
- **Galaxy Colors (Buzzoni 2005)**
- **UV Upturn (O'Connell 1999)**
- **Upturn (Brown 2003)**
- **Upturn (Yi & Yoon 2004)**
- **UV Upturn (Ali et al. 2018)**
- **Balmer break (Hamilton 1985)**
- **Lick indices (Worthey et al. 1994)**

Le Nebulose Planetarie

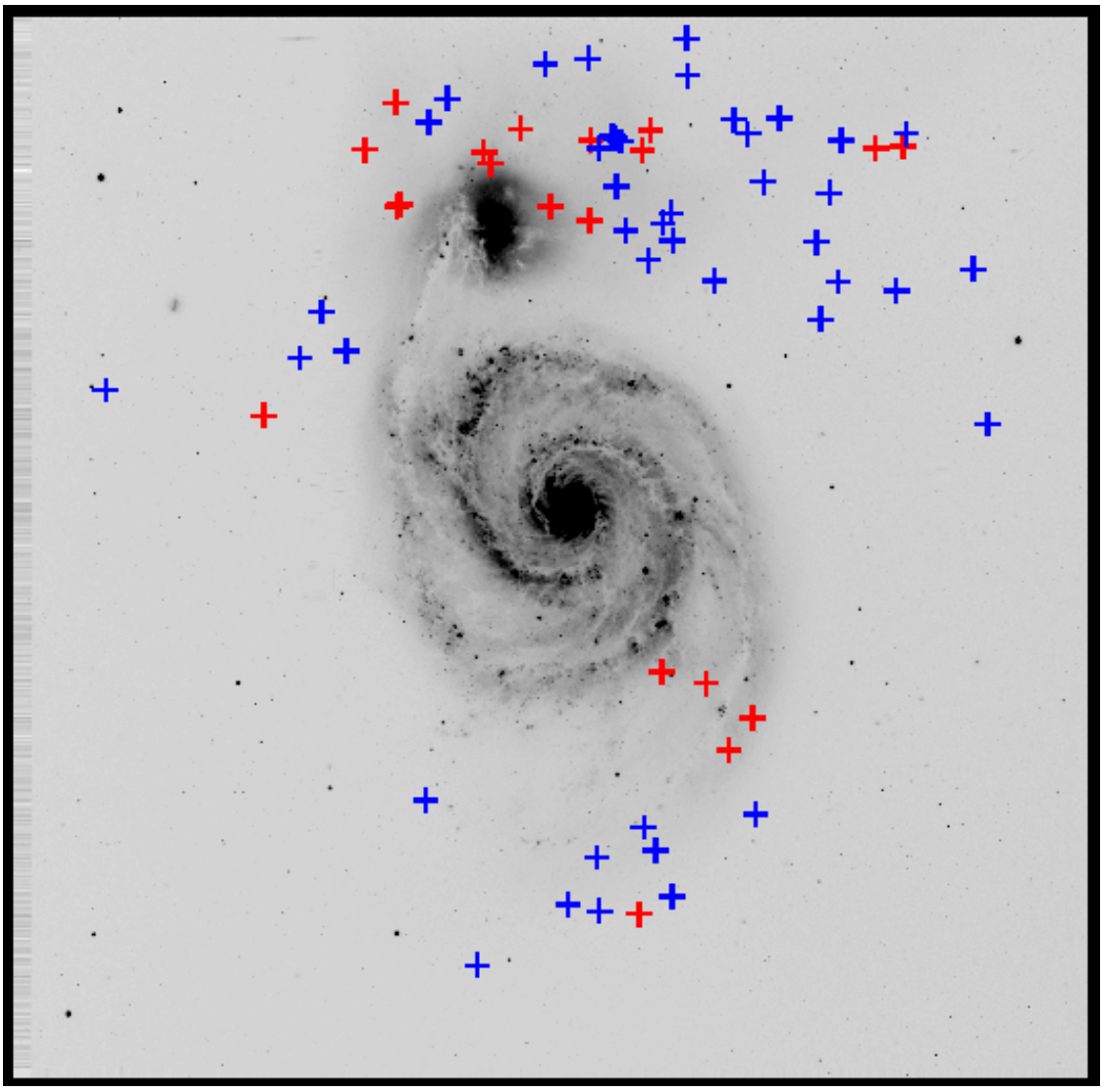

Feldmeier, Ciardullo & Jacoby (1997)

Planetary Nebulae follow Luminosity not surface brightness!

Stars can exist at great distances from luminous galaxies

Il censimento delle PNe nelle galassie del Gruppo Locale

Magrini et al. 2003 A&A 407 51

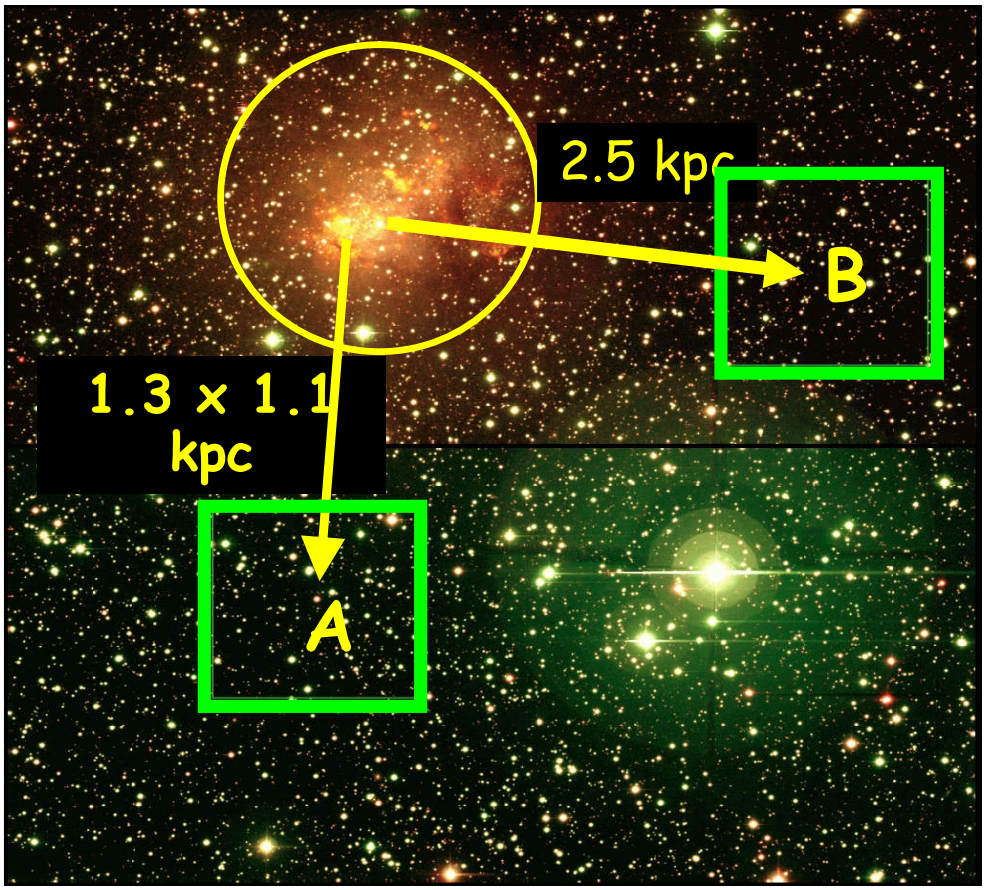

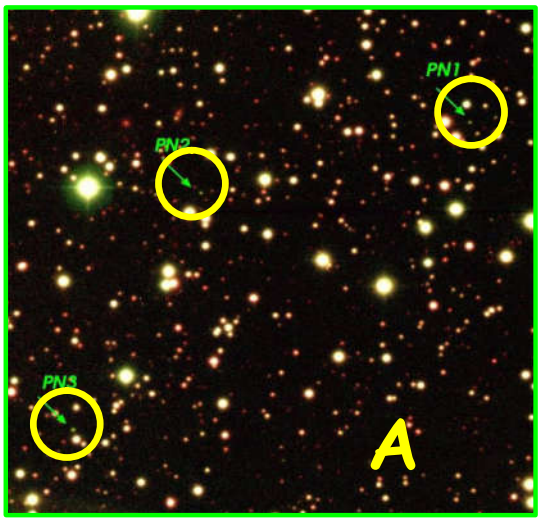

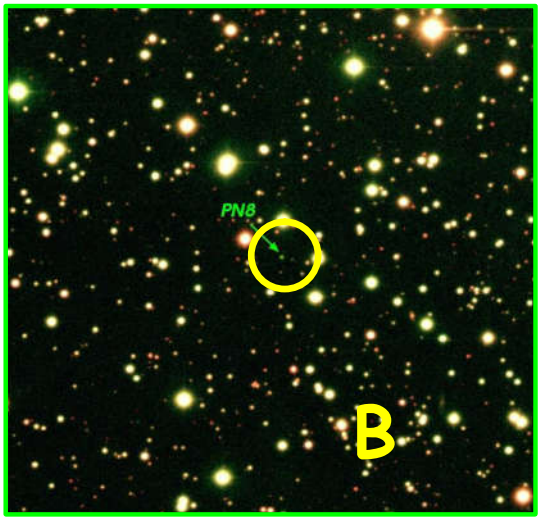

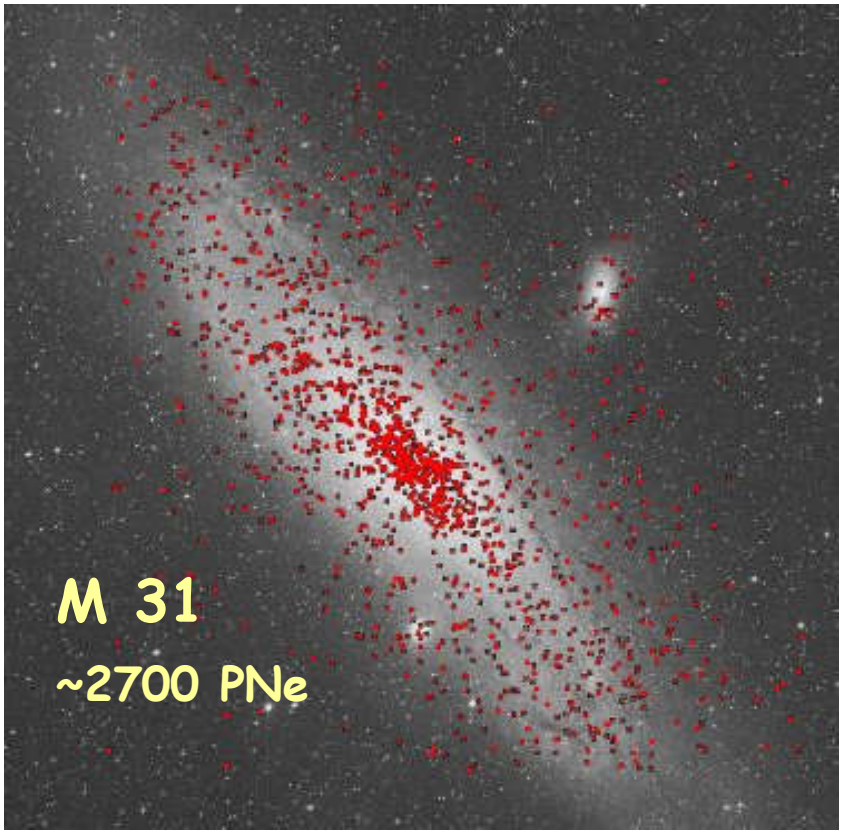

Planetarie intra-galattiche nell'Ammasso della Vergine

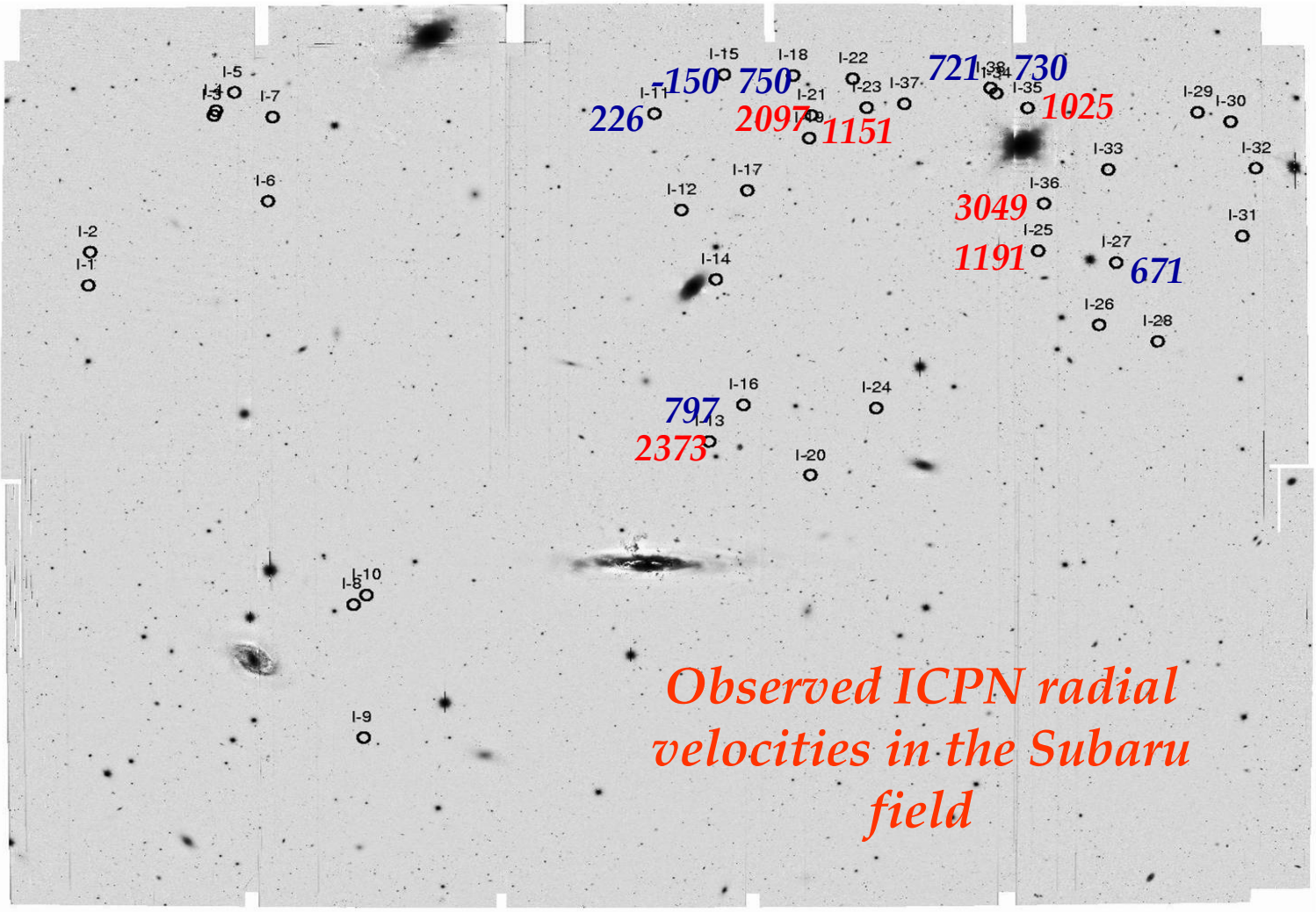

(Arnaboldi et al. 2002)

$$N_{PN} = BL_{tot}\tau_{PN} \quad \Longrightarrow \quad \alpha = \frac{N_{PN}}{L_{tot}} = B\tau_{PN}$$

quindi $\alpha = \frac{N_{PN}}{L_{tot}} \approx 2\times10^{-11}\times3\times10^{4} = 6\times10^{-7}$

Ovvero, 1 PN campiona: $L_{tot} \approx \frac{1}{\alpha} \approx 1.7\times10^{6} L_{sun}$

[OIII]-g *vs.* Ha-r color-color diagrams

NGC 205

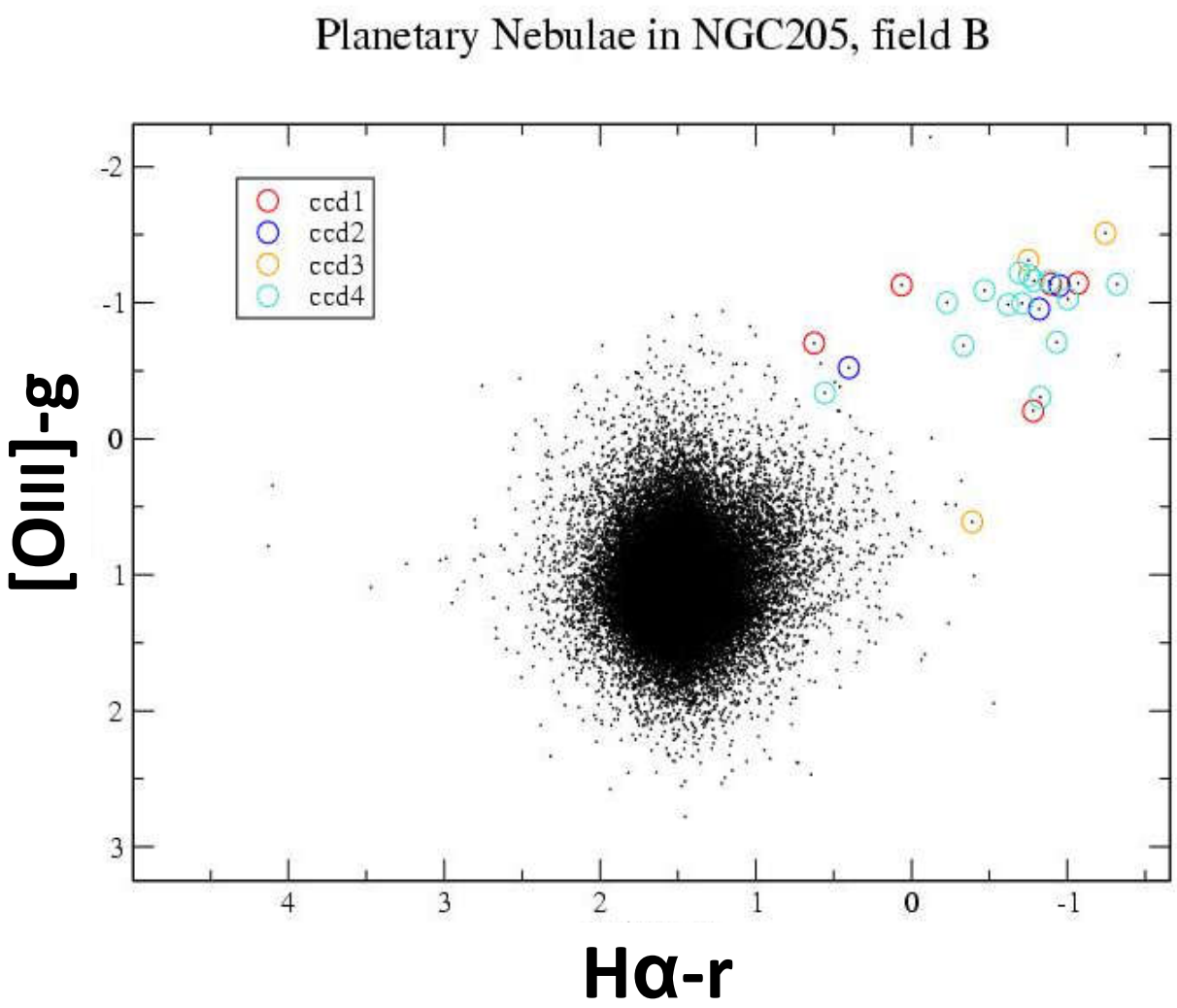

PNe e Intra-Cluster Luminosity (ICL)

(Ciardullo et al. 2003)

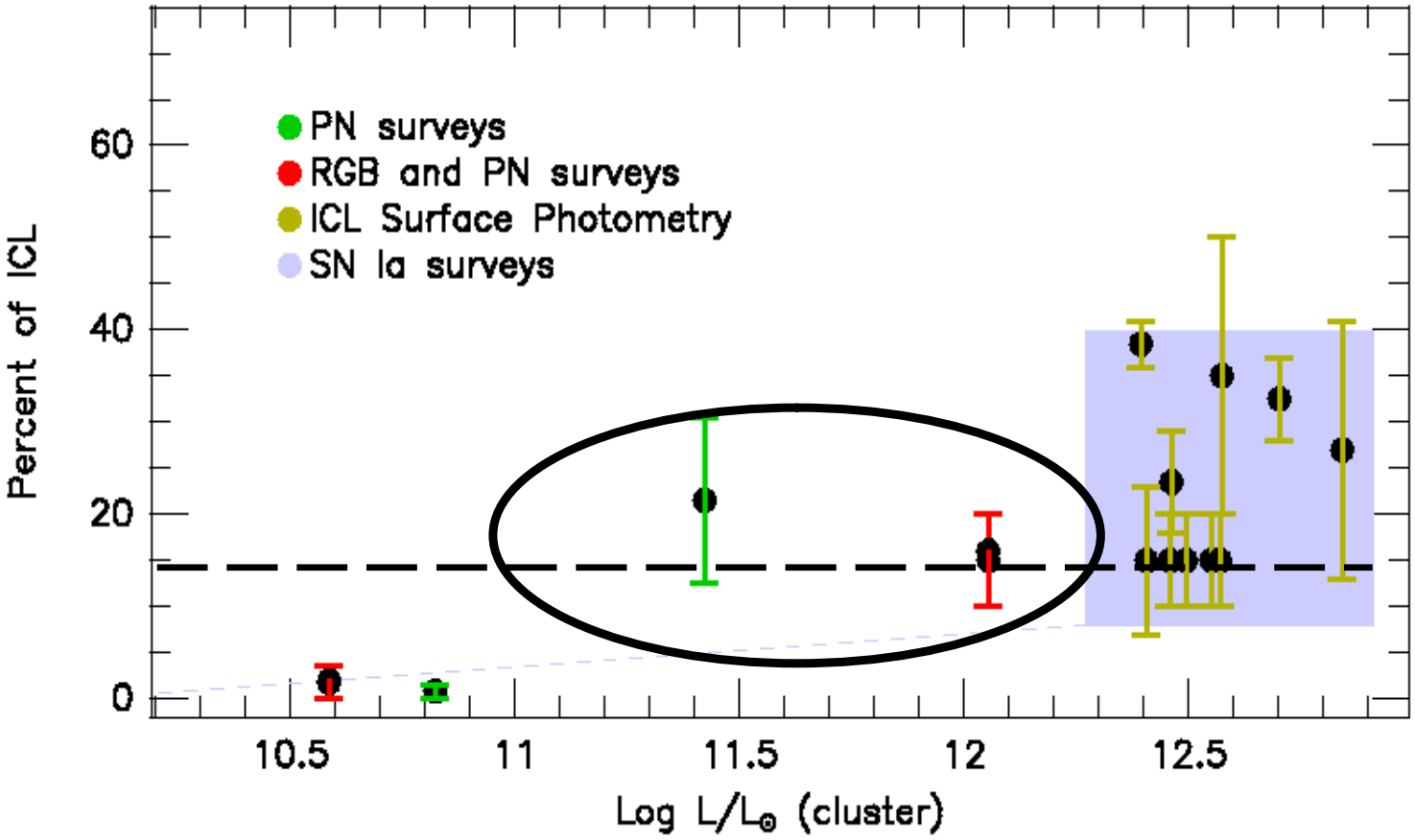

Per l'Ammasso della Vergine, si valuta una ICL dell'ordine del 15% della L dell'intero ammasso.

Tempi scala di visibilita' delle PNe

Buzzoni, Arnaboldi & Corradi (2006)

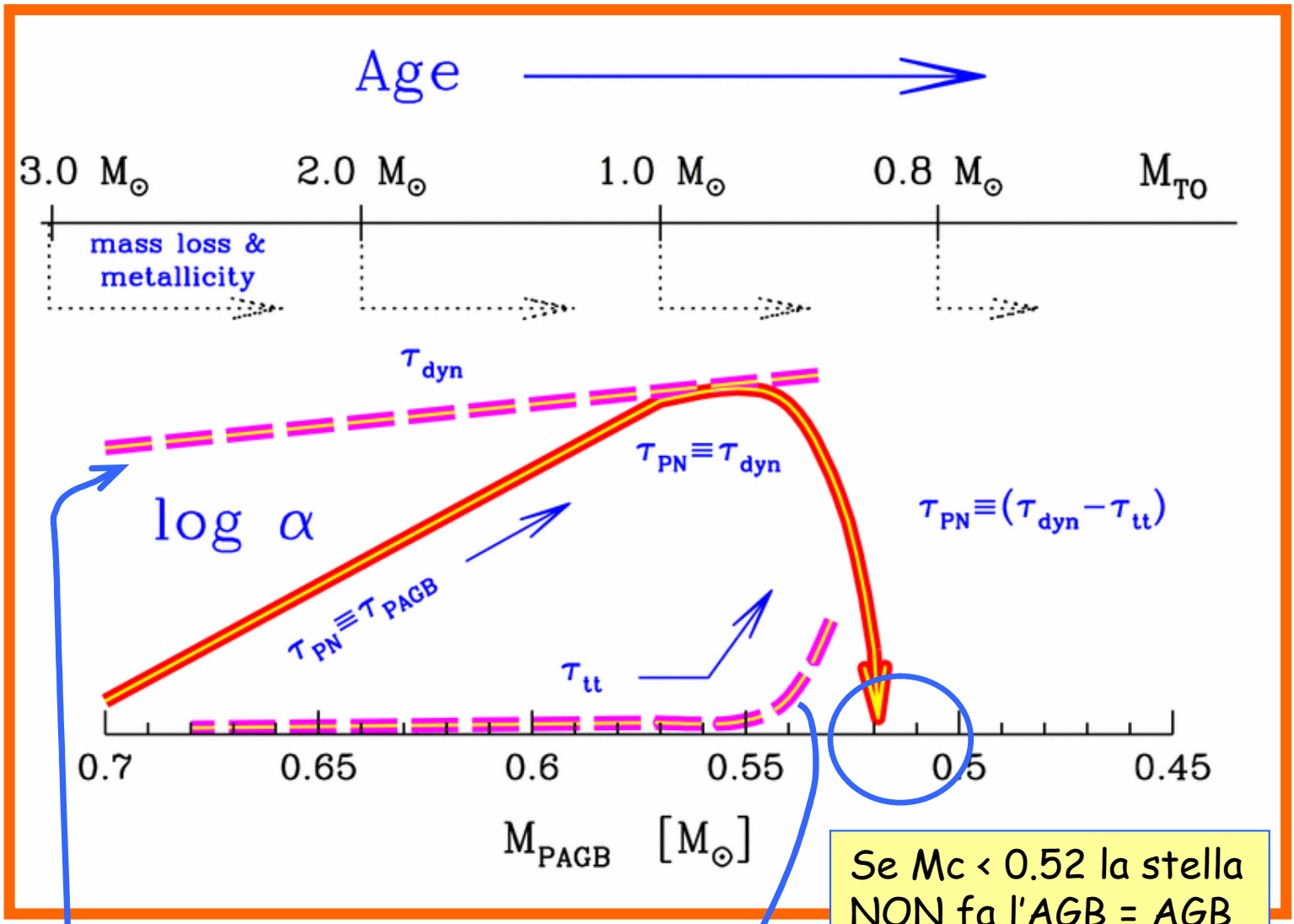

Se Mc < 0.52 la stella NON fa l'AGB = AGB Manque' e quindi non ci sono PNe

Tempo dinamico (evaporazione inviluppo) V~10 km/sec

Tempo di transizione da AGB freddo a T~50,000 K

Massa iniziale e finale delle stelle

Formula di Reimers (1975)

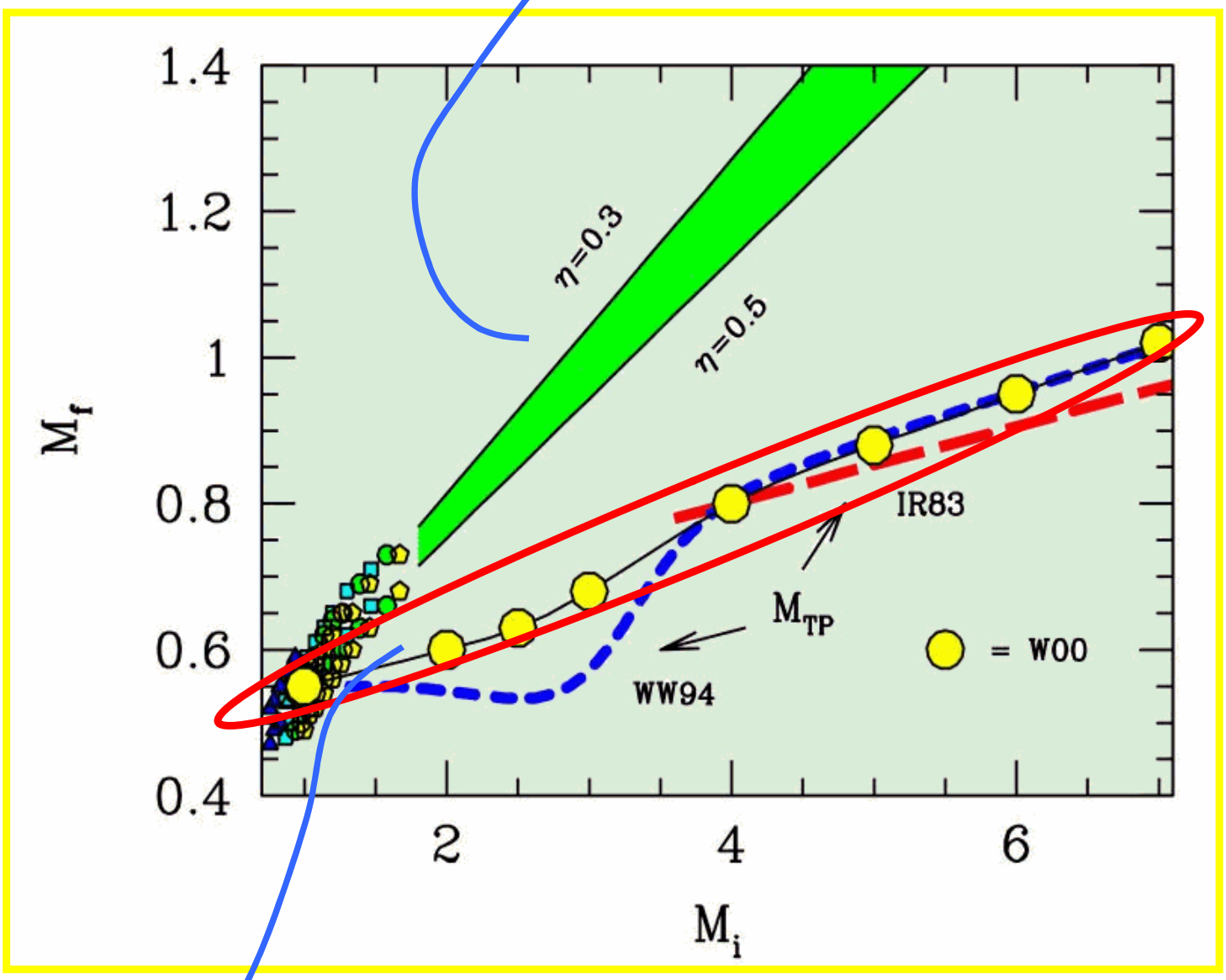

Buzzoni, Arnaboldi & Corradi (2006)

Osservazione empirica di Weidemann (2000) dagli ammassi aperti Galattici, dove $M_i = M_{TO}$, e $M_f = M_{WD}$

Si vede che le PNe devono avere sempre una massa << $1M_{sun}$

PNe e UV upturn nelle galassie ellittiche

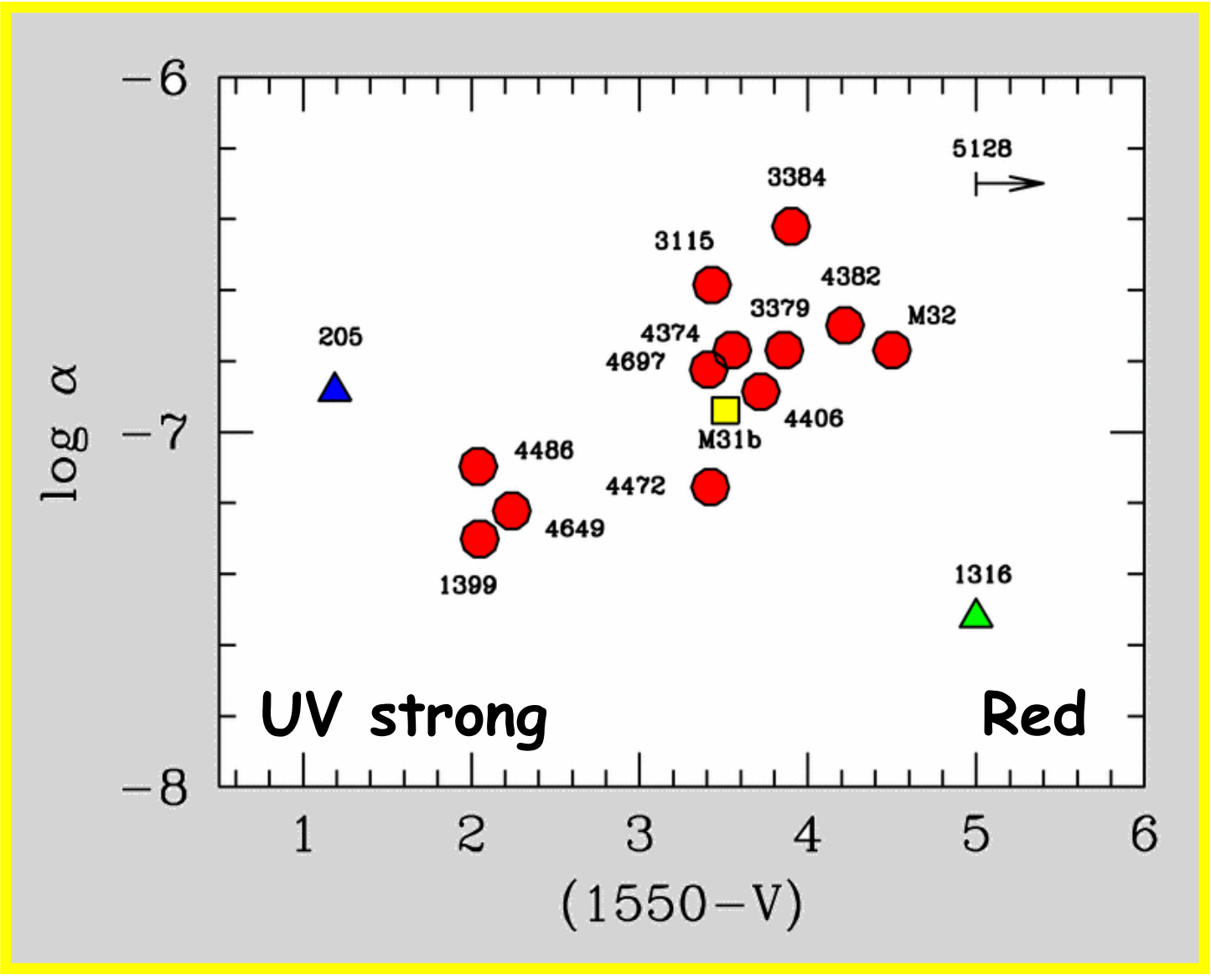

Buzzoni, Arnaboldi & Corradi (2006)

Un forte UV da stelle HB implica molte stelle AGB manque' e quindi α↓

Articoli consigliati (vedi Webpage):
http://www.bo.astro.it/~eps/lezioni/lezioni.html

- **SSP Theory (Renzini & Buzzoni 1986)**
- **ICM & Planetary Nebulae (Arnaboldi 2003)**
- **Extragalactic Planetary Nebulae (Feldmeier 2003)**
- **Planetary Nebulae (Buzzoni et al. 2006)**
- **IMF (Weidemann 2000)**
- **M/L clusters (Girardi et al. 2002)**

Entropia Fotometrica

What a Photometric Entropy theory is for?

Entropy is a measure of the intrinsic "variance" of a stellar aggregate along the different spectral range of observation.

- Surface-brightness Fluctuations
- Crowding
- Diagnostics from Narrow-band Spectroscopy

Some Fundamentals

$$p(x) = \frac{e^{-\lambda}\,\lambda^{x}}{x!} \quad \text{for } \lambda > 0 \text{ and } x = 0, 1, 2\ldots$$

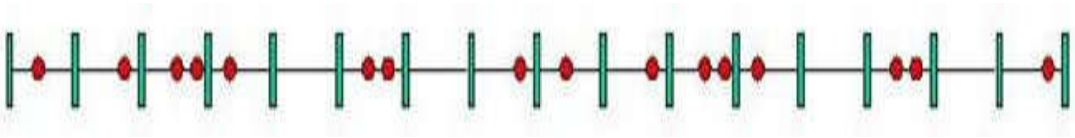

1, 2, 3, ... N_{tot}

→ N= 1± 1 for each cell $L_{tot} = \Sigma\, \ell_* = N_{tot}\, \ell_*$

$\sigma(N_{tot}) = \sqrt{\Sigma 1} = \sqrt{N_{tot}}$ $\sigma(L_{tot}) = \sqrt{\Sigma \ell_*^2} = \ell_* \sqrt{N_{tot}}$

$\sigma(L_{tot})/L_{tot} = 1/\sqrt{N_{tot}}$

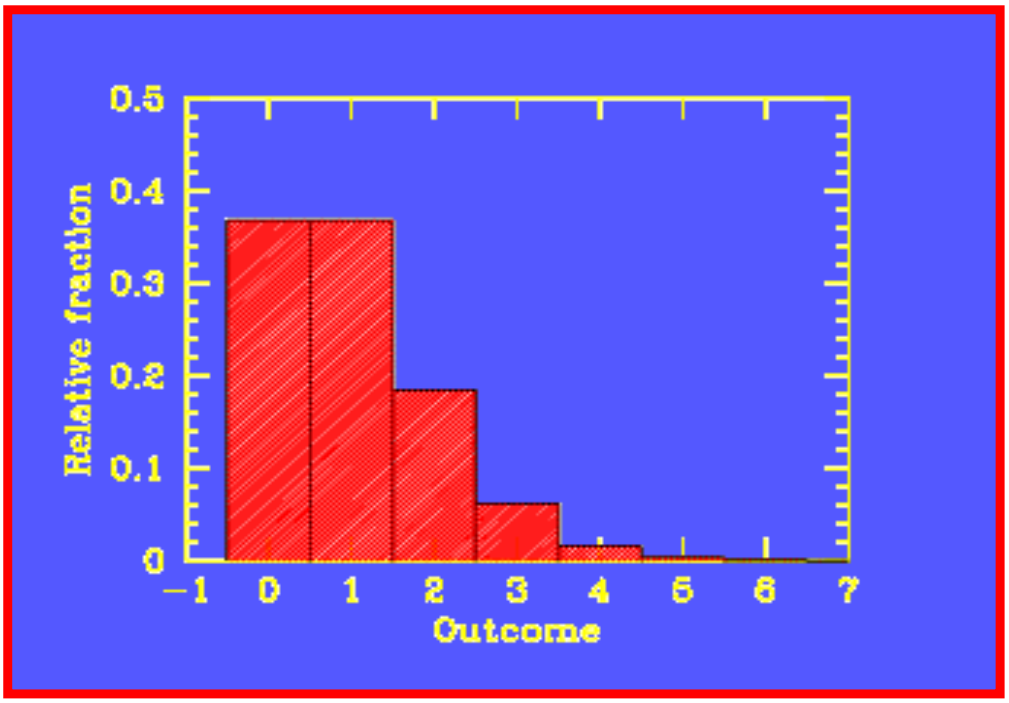

More generally, if ℓ_* is NOT a constant, we can still define

$$\sigma(L_{tot})/L_{tot} = 1/\sqrt{N_{eff}}$$

where, always,

$$N_{eff} \leq N_{tot}$$

N_{eff} will depend on λ as ℓ_* depends on λ

$$S = \text{Log}\,(N_{eff}/N_{tot})$$

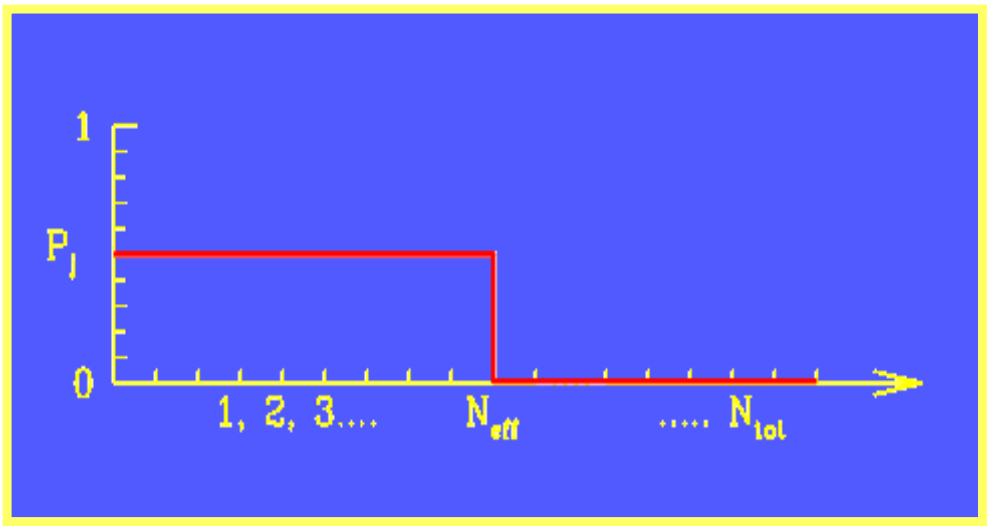

Quite importantly,

$$S = S(\lambda)$$

In order to fix N_{eff} (and Entropy) we need a photometric argument

$$\sigma^2(L_{tot}) \,/\, L_{tot} = \Sigma \ell_*^{\,2} \,/\, \Sigma \ell_* = \ell_{eff}$$

At every λ, it must be:

$$N_{eff} \times \ell_{eff} = L_{tot}$$

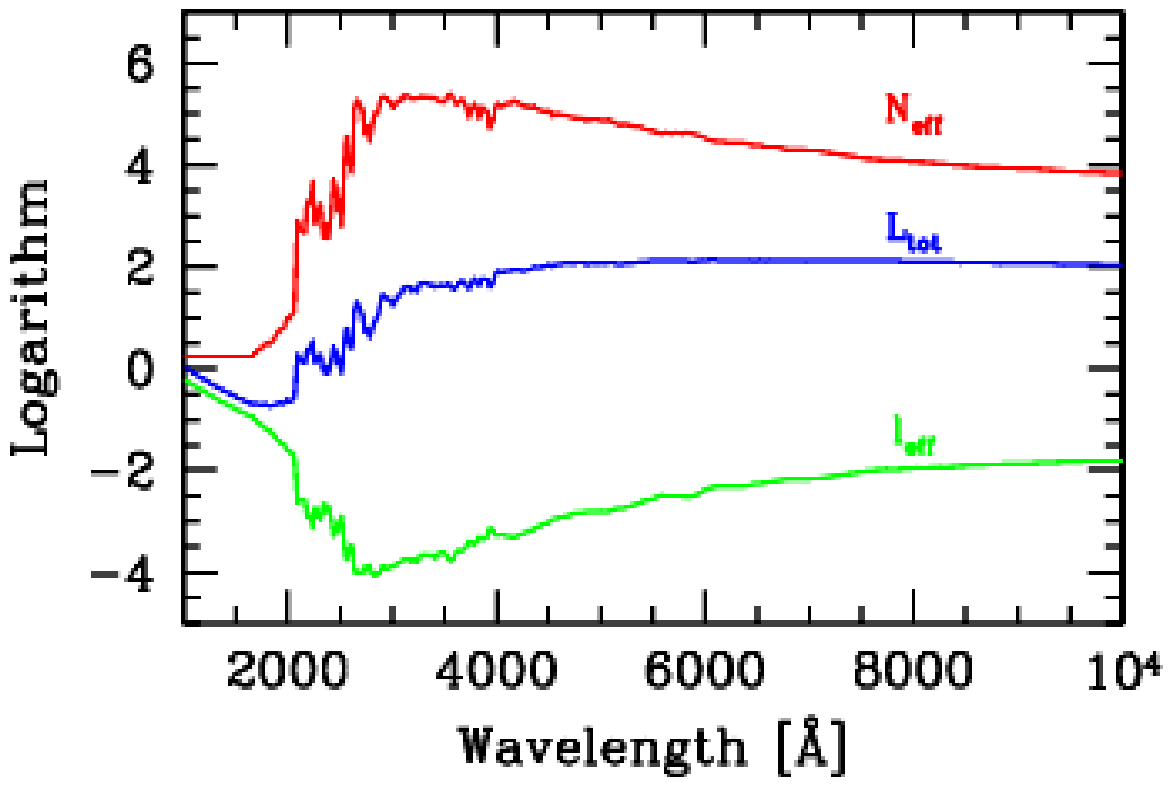

Buzzoni (1993), A&Ap, 275, 433

Cerviño et al. (2002), A&Ap, 381, 51

Teoria dettagliata

CASO A) N stelle di fissata luminosità l_*

$$L_{TOT} = \sum^{N} l_* = N\, l_*$$

$$\sigma_{L_{TOT}} = \left(\sum^{N} \sigma_j^2\right)^{\frac{1}{2}} \qquad \forall * \quad n = 1 \pm 1 \quad (\text{Poisson})$$

$$\left(\sum (l_* 1)^2\right)^{\frac{1}{2}} \rightarrow \left(N\, l_*^2\right)^{\frac{1}{2}} \rightarrow l_* \sqrt{N}$$

Quindi $$\boxed{\frac{\sigma_L}{L_{TOT}} = \frac{l_* \sqrt{N}}{l_* N} = \frac{1}{\sqrt{N}}}$$

CASO B) N stelle tutte diverse

$$L_{TOT} = \sum^{N} l_j = N \langle l \rangle \qquad \text{dove } \langle l \rangle = \frac{\sum l_j}{N}$$

$$\sigma_{L_{TOT}} = \left(\sum l_j^2\right)^{\frac{1}{2}} = \sqrt{N}\, \langle l^2 \rangle \qquad \text{dove } \langle l^2 \rangle = \frac{\sum l_j^2}{N}$$

media quadratica

$$\frac{\sigma_{L_{TOT}}}{L_{TOT}} = \frac{\sqrt{N}\, \langle l^2 \rangle^{\frac{1}{2}}}{N \langle l \rangle} = \frac{K}{\sqrt{N}} \qquad \text{dove } K = \left[\frac{\langle l^2 \rangle}{\langle l \rangle^2}\right]^{\frac{1}{2}}$$

$K \geq 1$ perché $\langle l \rangle^2 < \langle l^2 \rangle$

$$\frac{K}{\sqrt{N}} = \frac{1}{\sqrt{N_{eff}}} \Rightarrow \boxed{\frac{N_{eff}}{N} = \frac{1}{K^2}}$$

Quindi è sempre $N_{eff} \leq N$

Definiamo

ENTROPIA FOTOMETRICA:

$$S = -2 \log K = \log \frac{N_{eff}}{N}$$

Analisi della varianza

$$\sigma^2_{L_{TOT}} = \sum l_j^2$$

$$\frac{\sigma_L^2}{L_{TOT}} = \frac{N\langle l^2\rangle}{N\langle l\rangle}$$ → Questo rapporto ha le dimensioni di una luminosità

quindi $$l_{eff} = \frac{\langle l^2\rangle}{\langle l\rangle} = \frac{\sum l^2}{\sum l}$$

Che relazione c'è fra N_{eff} e l_{eff} ?

$$N_{eff} \cdot l_{eff} = \frac{N}{k^2}\frac{\langle l^2\rangle}{\langle l\rangle} = \frac{N\cancel{\langle l^2\rangle}\langle l\rangle \cancel{k}}{\cancel{\langle l^2\rangle}\langle l\rangle} = N\langle l\rangle \downarrow N\frac{\sum l}{N}$$

Quindi $$N_{eff} \times l_{eff} = L_{TOT}$$

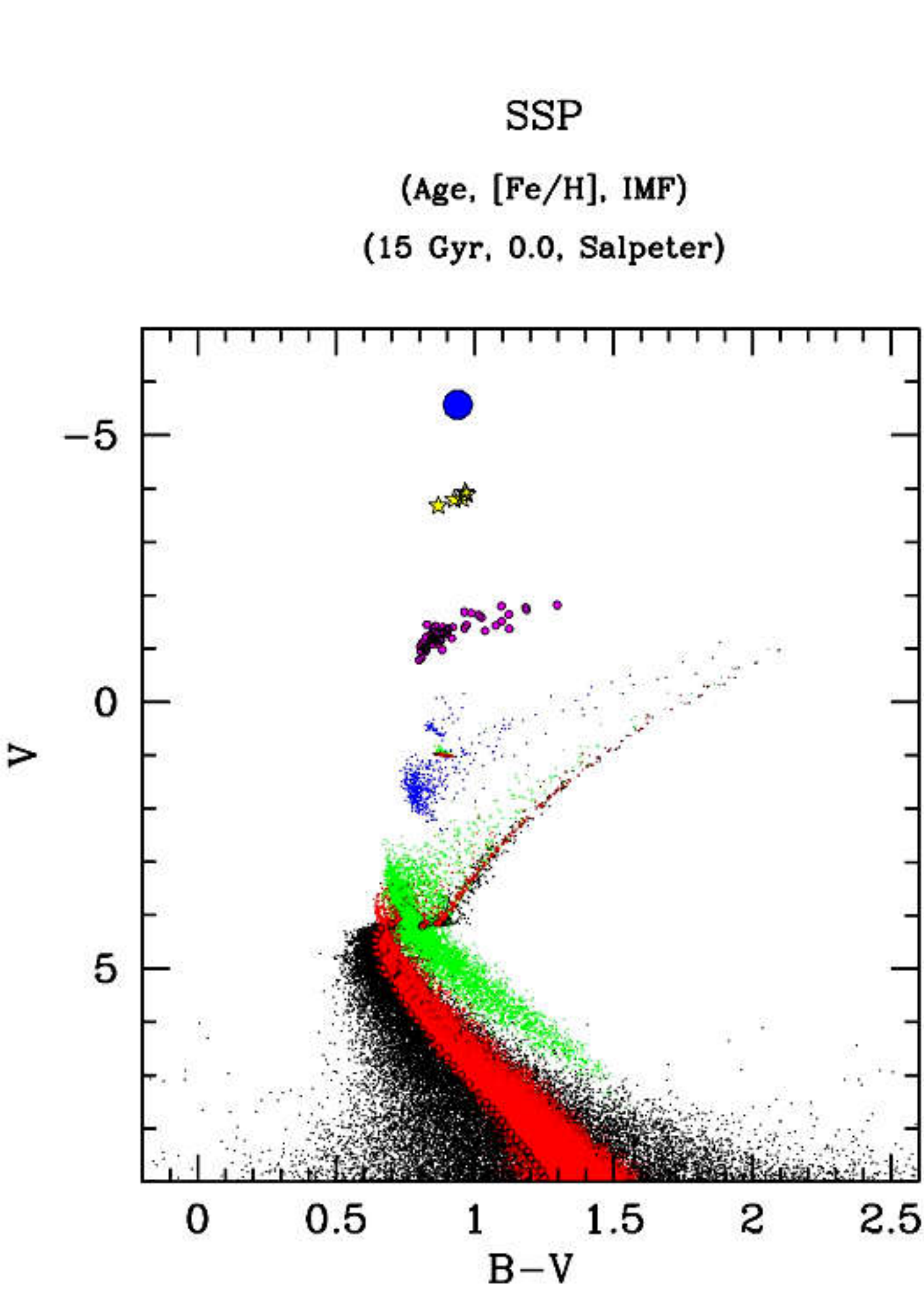
SSP
(Age, [Fe/H], IMF)
(15 Gyr, 0.0, Salpeter)
−5
0
5
V
0
0.5
1
1.5
2
2.5
B−V

Surface-Brightness Fluctuations: an alternative approach for the case of M53

First application of the theory to galx's: Tonry & Schneider (1988) and Tonry (1991)

$$\sigma^2(L_{tot}) \,/\, L_{tot} = \Sigma \ell_*^{\,2} \,/\, \Sigma \ell_* = \ell_{eff}$$

Theory: Population synthesis models → ℓ_{eff} ← Observations

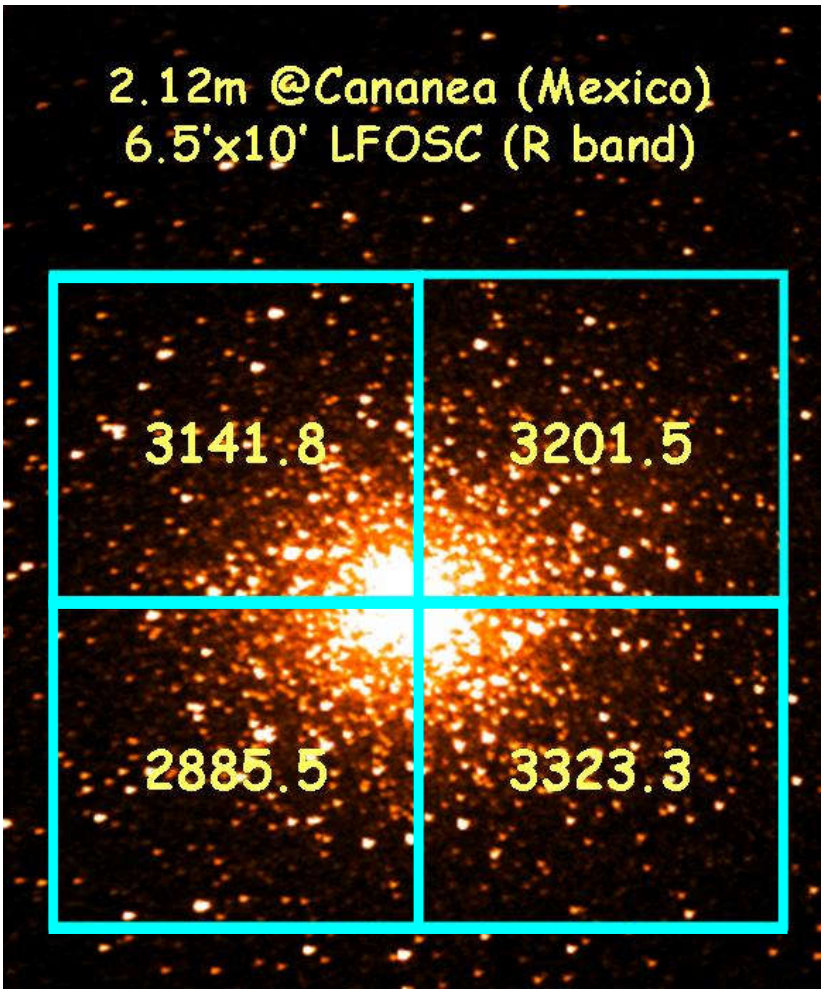

$$L_{(quad)} = 3138 \pm 184$$

Luminosity Sampling and Intrinsic Color Fluctuations

$$\Delta mag = \sigma(L_{tot})/L_{tot} = 1/\sqrt{N_{eff}}$$

$$\sigma\,(B-V) = [\sigma(B)^2 \pm \sigma(V)^2\,]^{1/2} = (1/\,N_{eff}^{B} \pm 1/\,N_{eff}^{V})$$

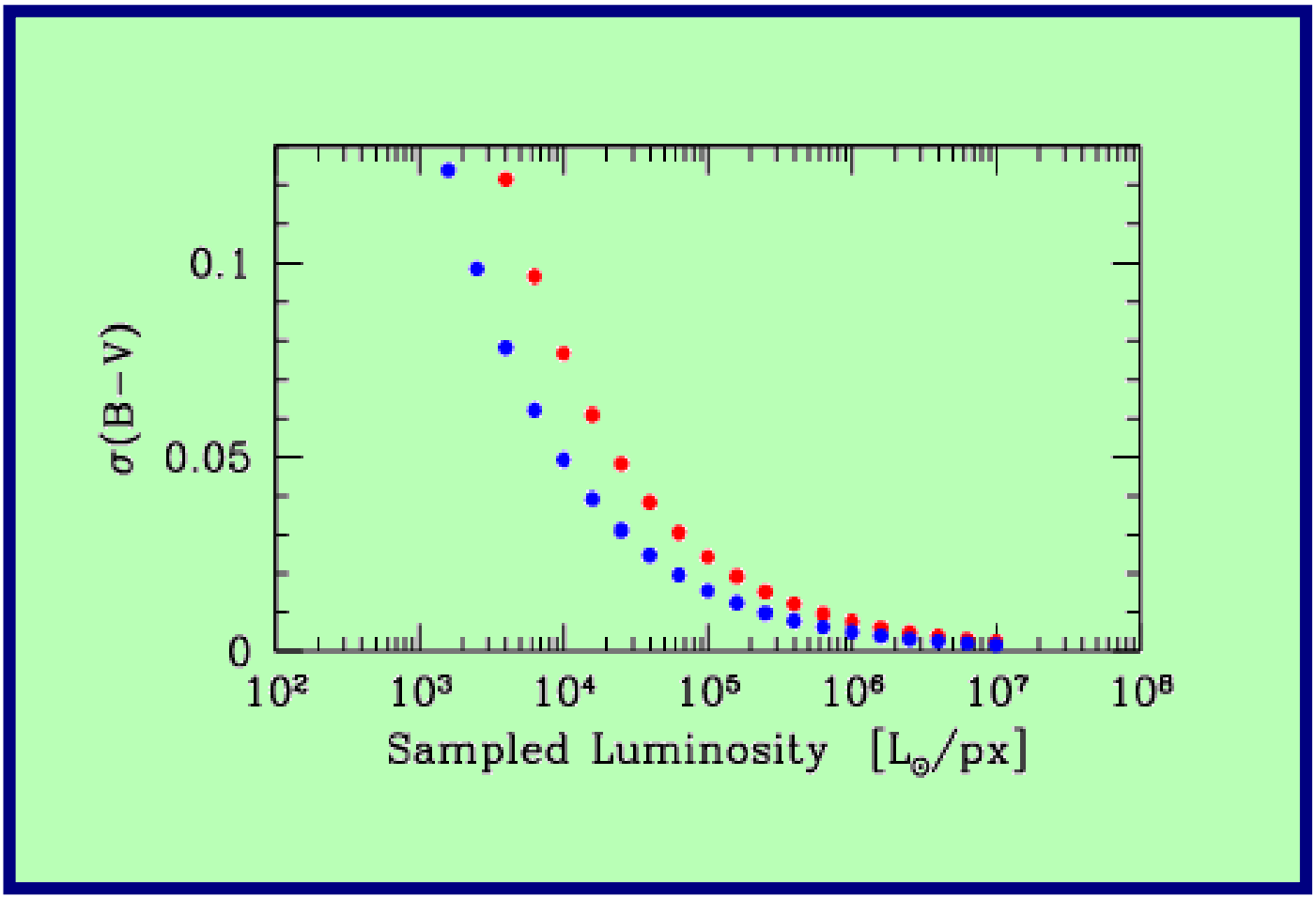

Crowding & Optical opacity

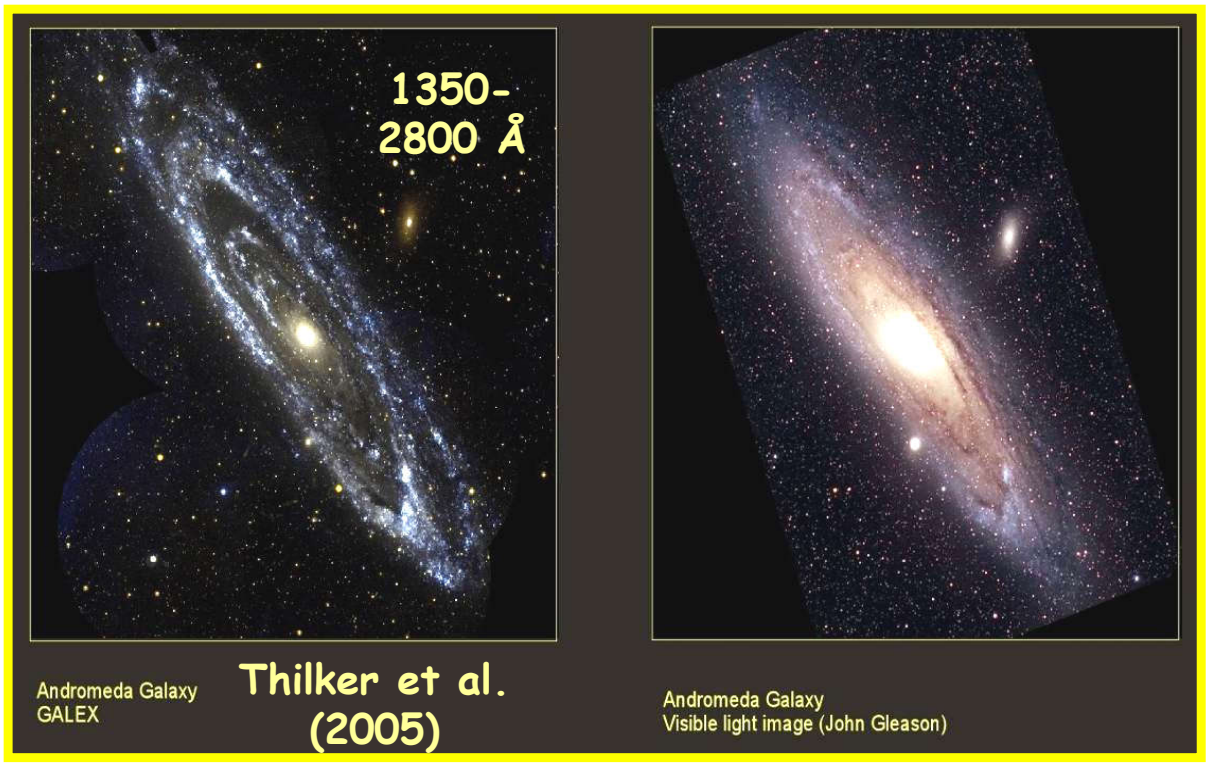

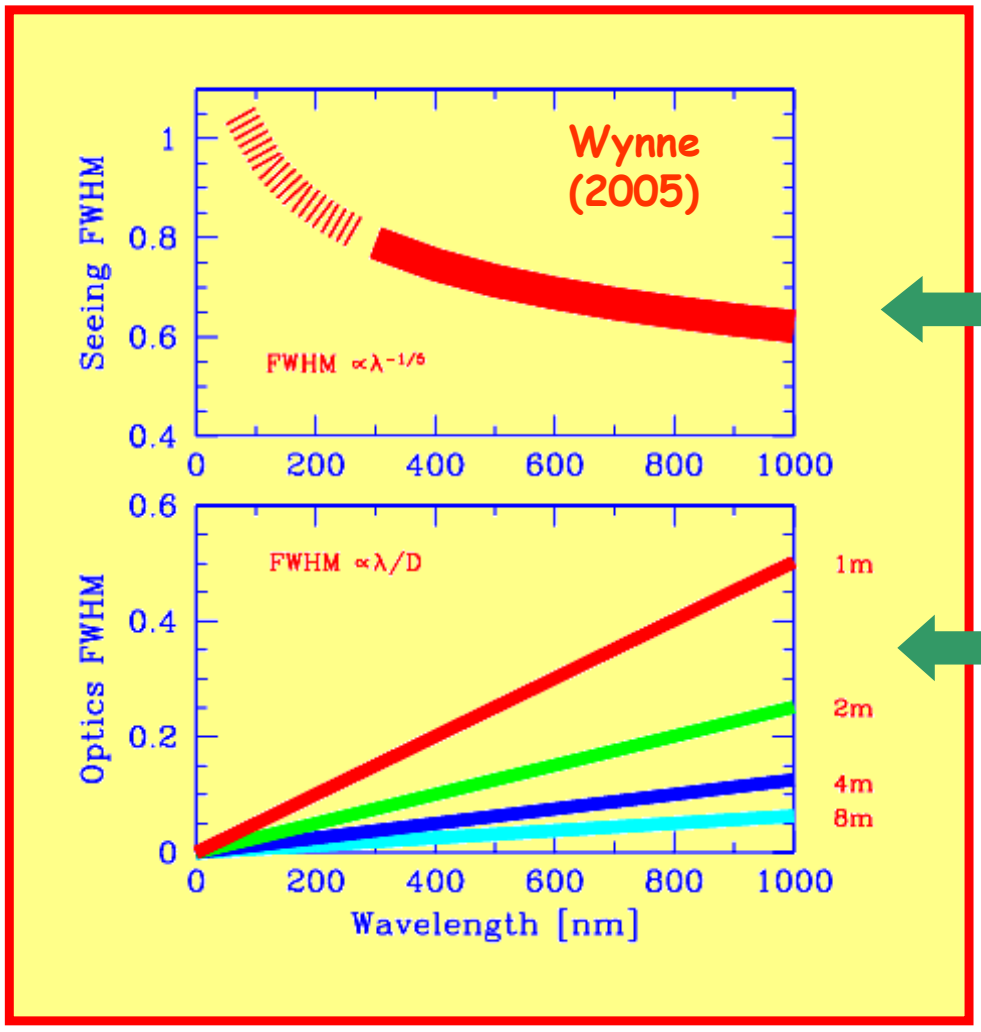

Seeing

Diffraction

Oligarchy vs. Democracy

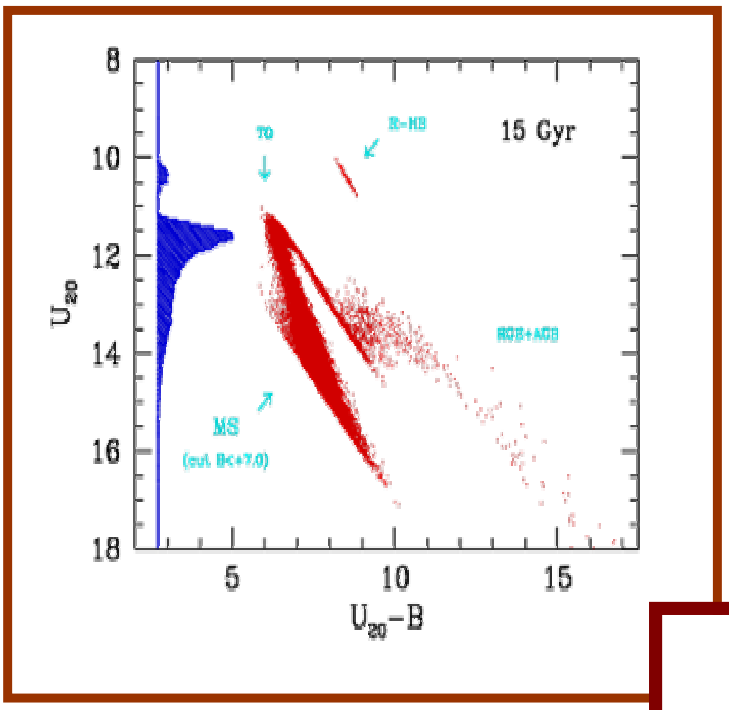

2000 Angstroms

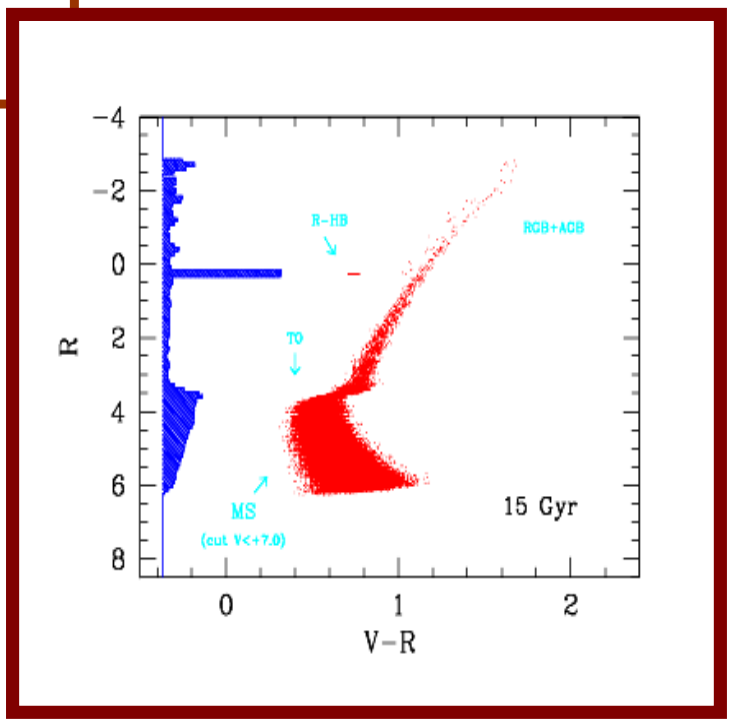

7000 Angstroms

Recovering the Age-Metallicity degeneracy

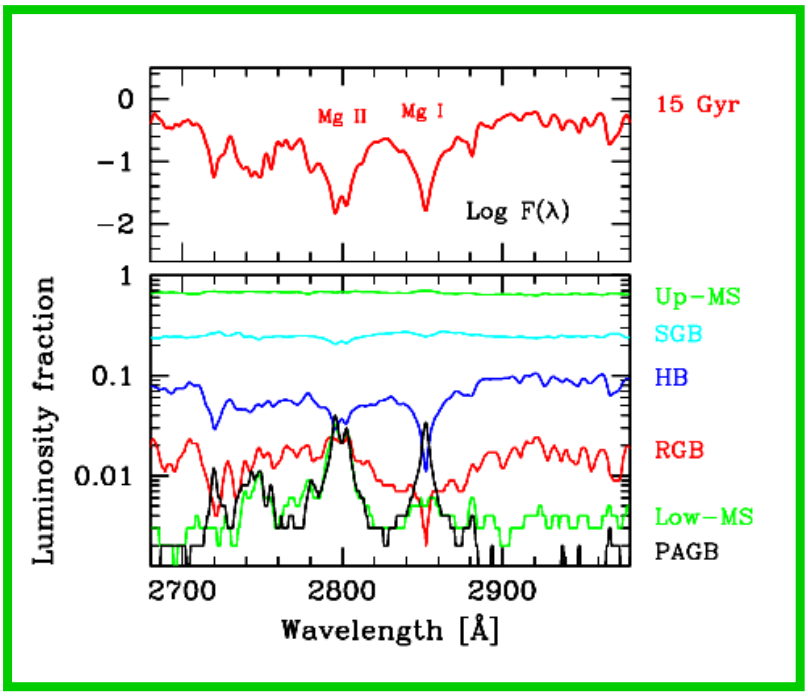

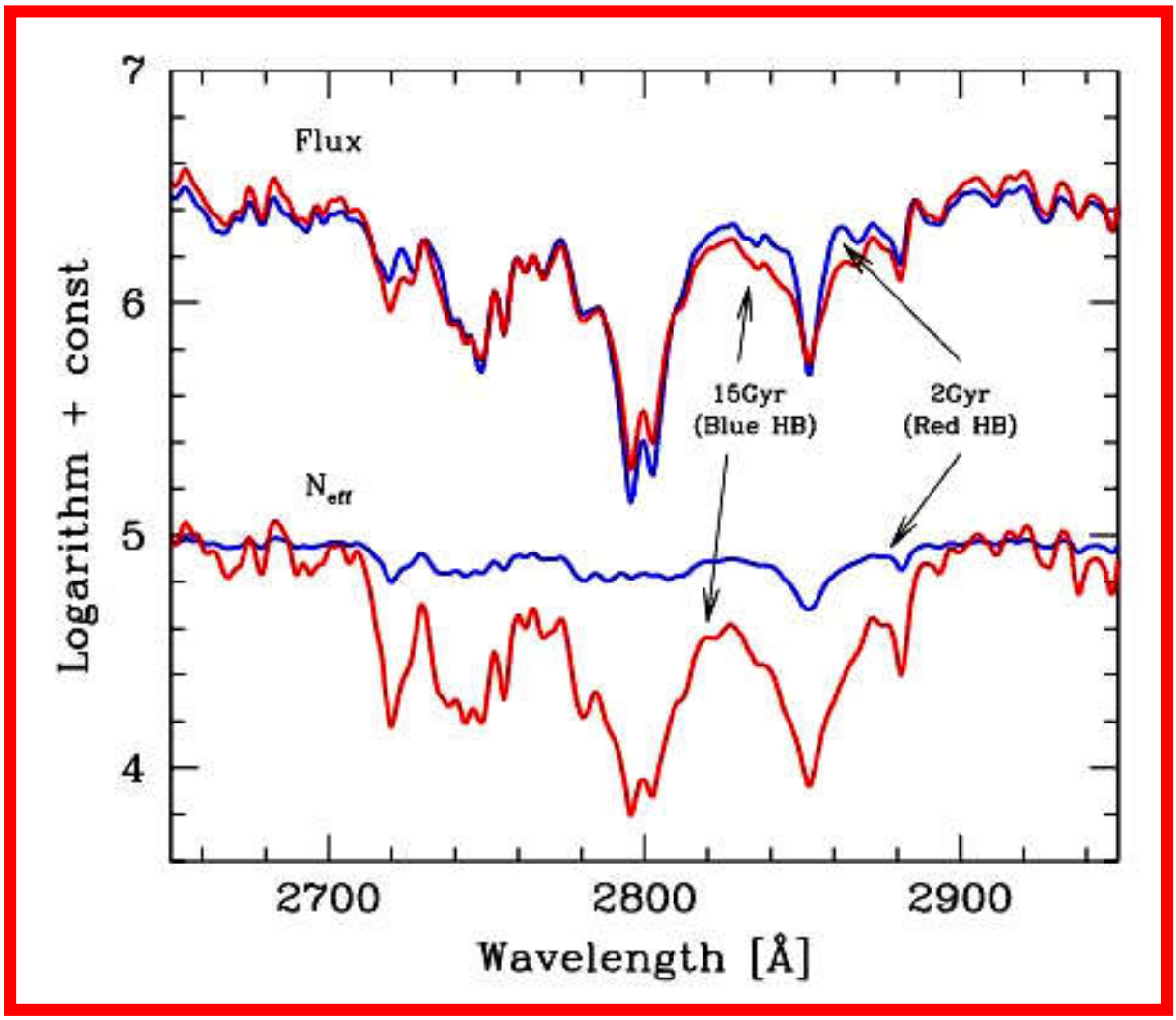

Articoli consigliati (vedi Webpage):
http://www.bo.astro.it/~eps/lezioni/lezioni.html

- **SBF (Buzzoni 1993)**
- **SBF (Tonry & Schneider 1988)**
- **SBF & Photometric Entropy (Buzzoni 2005)**
- **SBF & Photometric Entropy (Cerviño & Luridiana 2005)**

I principi della spettroscopia (Diffrazione & Interferenza)

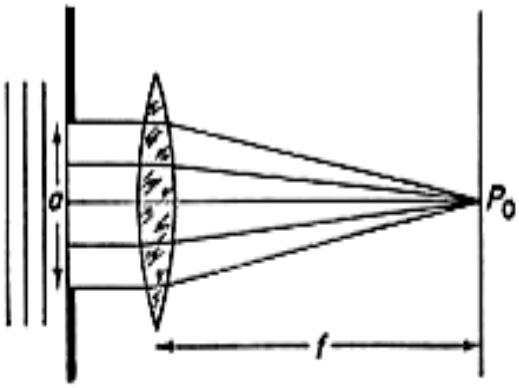

Figura 2. *Massimo centrale nella diffrazione di Fraunhofer.*

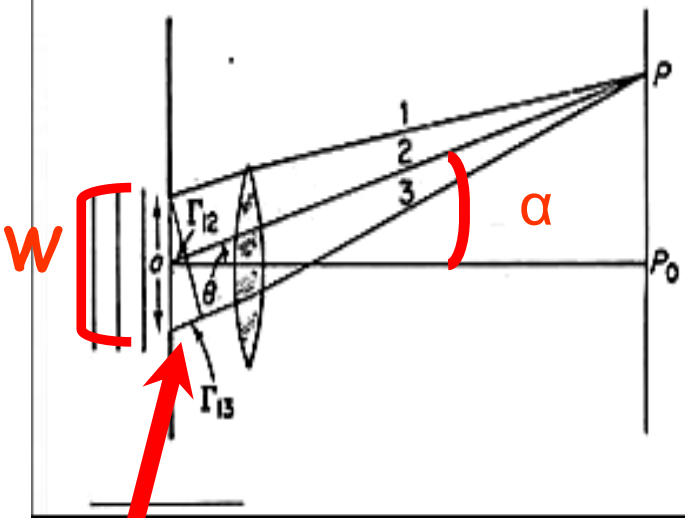

Figura 3. *Diffrazione di Fraunhofer.*

$$\frac{W}{2}\sin\alpha = \frac{m}{2}\lambda \quad \Longrightarrow \quad \alpha \cong m\frac{\lambda}{W}$$

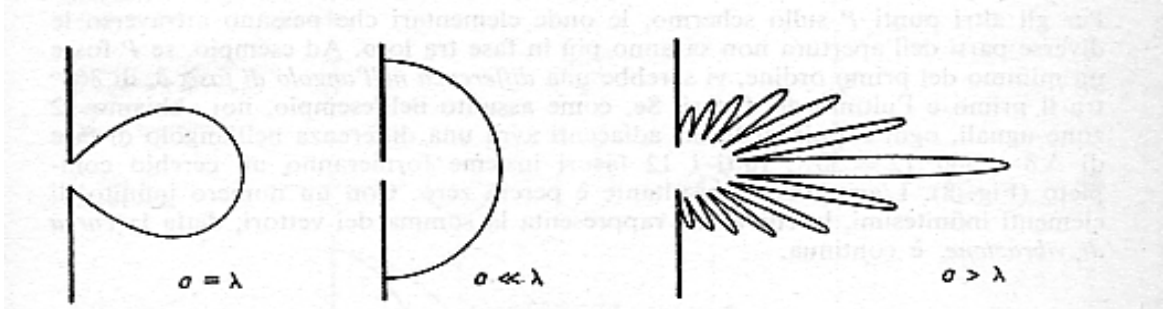

Figura 5. *Distribuzioni d'intensità dietro un'apertura di larghezza* a = λ *(a sinistra), dietro un'apertura estremamente piccola (al centro), e dietro un'apertura più larga (a destra).*

Risoluzione vs. Dispersione

$$\alpha_{\min} \cong m\frac{\lambda}{W}$$

Risoluzione

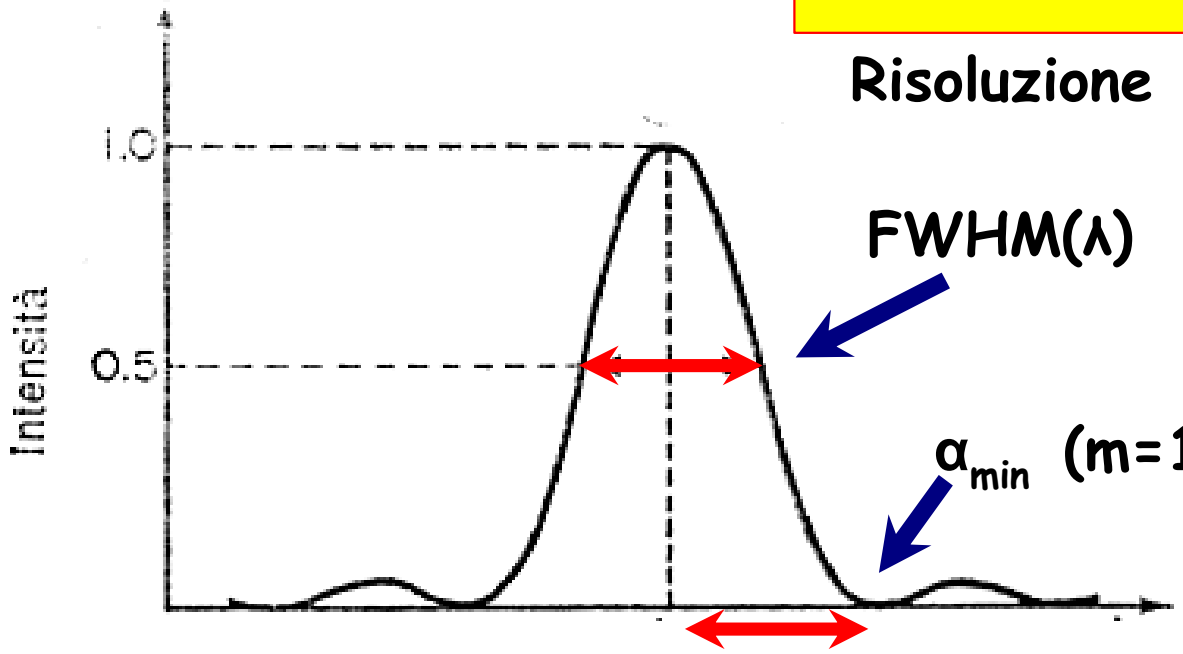

sin(α) ~ α

$$\alpha_{\max 1} \approx 1.5\frac{\lambda}{W}$$

$$\Delta\alpha_1 \approx \frac{1.5}{W}\Delta\lambda$$

Dispersione

$$\frac{\Delta\alpha_1}{\alpha} \approx 1.5\frac{\Delta\lambda}{\lambda}$$

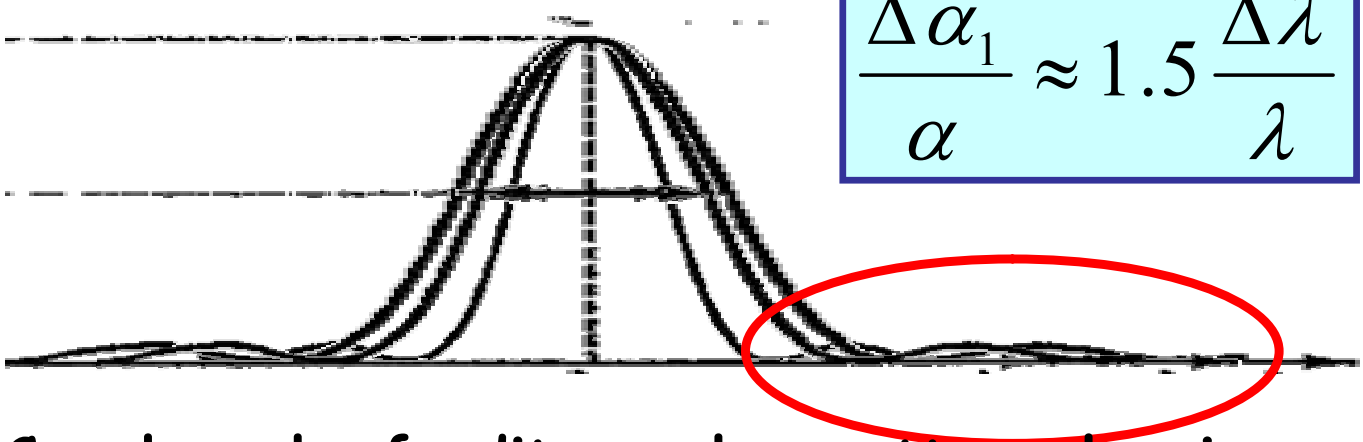

Con la sola fenditura, lo spettro al primo ordine sarebbe totalmente confuso dalla figura di diffrazione all'ordine zero, e quindi inutilizzabile

Reticoli di diffrazione

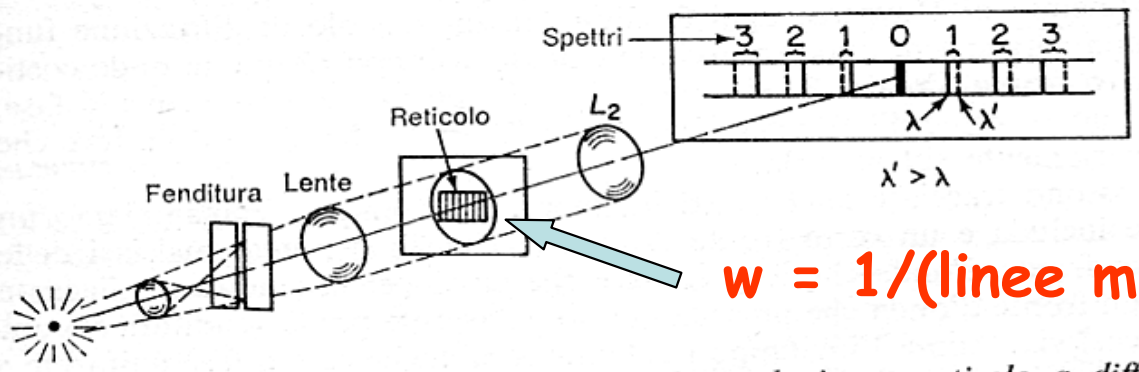

Figura 2. *La formazione di una riga spettrale in un reticolo a diffrazione. Viene mostrato lo spettro di una sorgente che emette su due lunghezze d'onda λ e λ′.*

risoluzione

$$\alpha_{\min} \cong m\frac{\lambda}{W}$$

dispersione

$$\Delta\alpha_1 \approx \frac{1.5}{w}\Delta\lambda$$

"Grism"
(per rifrazione)

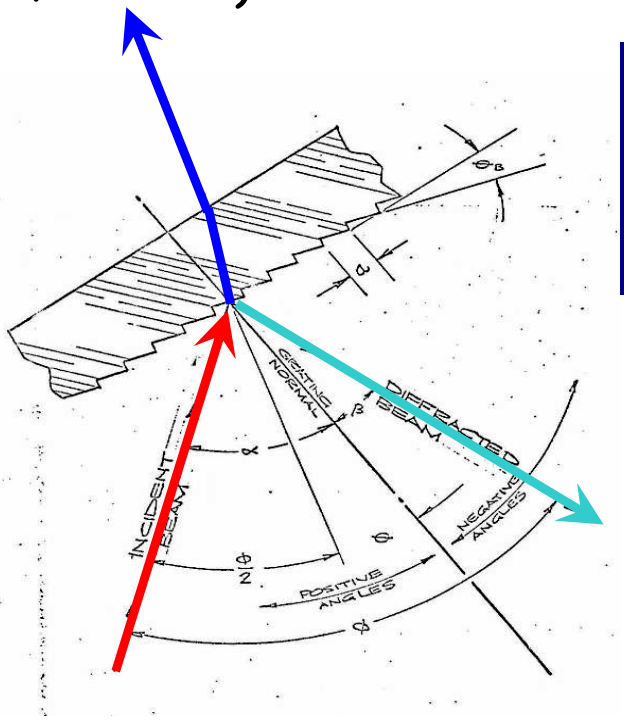

$$\frac{\Delta\alpha}{\alpha} \approx 1.5\left(\frac{W}{w}\right)\frac{\Delta\lambda}{\lambda}$$

"Grid"
(per riflessione)

Quindi:

1) l'ampiezza della fenditura determina la RISOLUZIONE

2) La frequenza di linee del grism/grid determina la DISPERSIONE

Gli spettrografi a riflessione

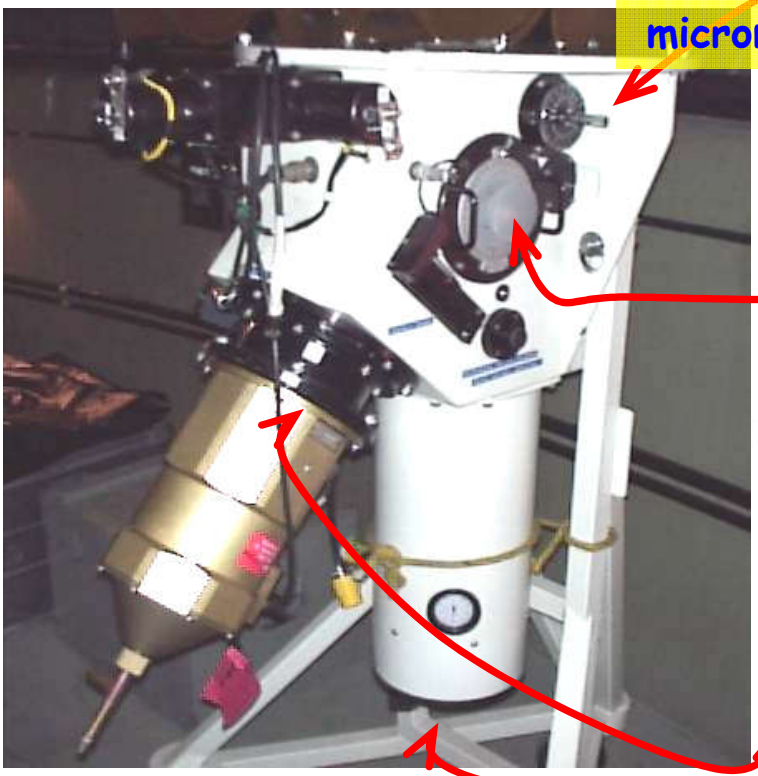

Böller & Chivens

Gli spettrografi a fibre ottiche

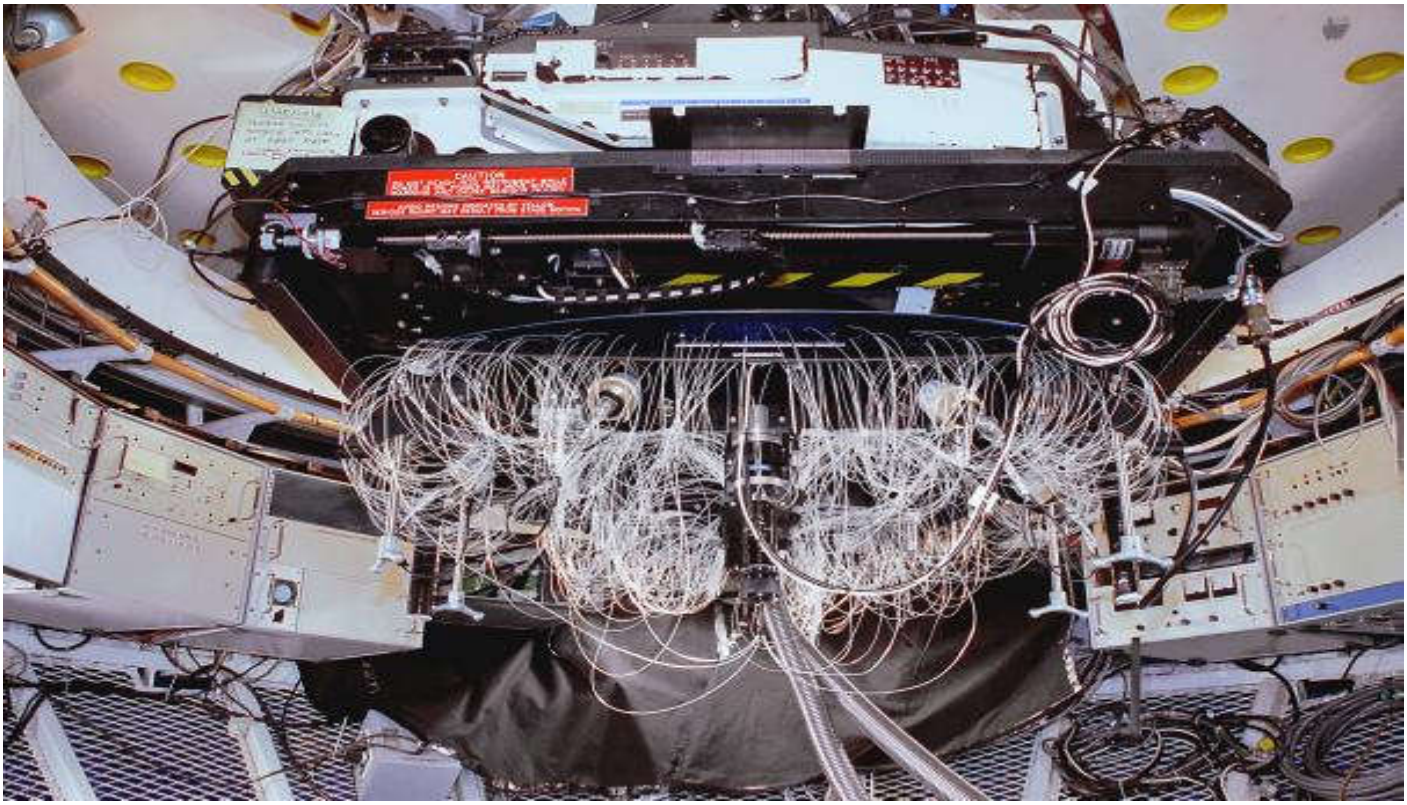

Hydra @KPNO (3.8m) USA

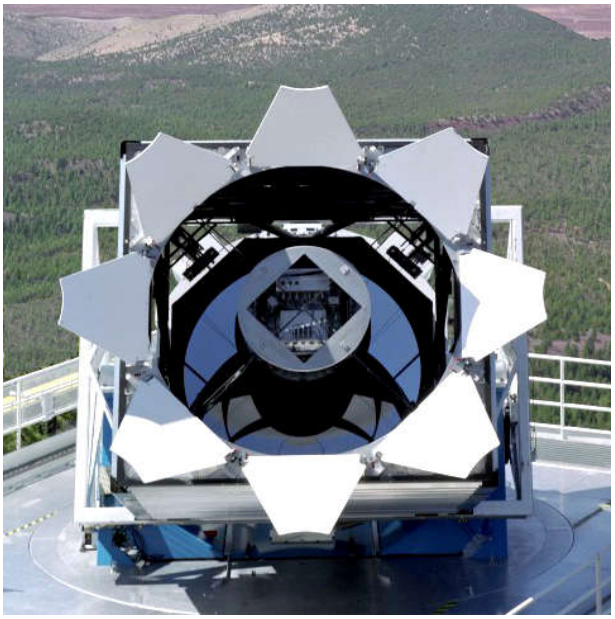

The Sloan Digital Sky Survey's 2.5-meter telescope at Apache Point Observatory, New Mexico

Spettrografi da "banco"

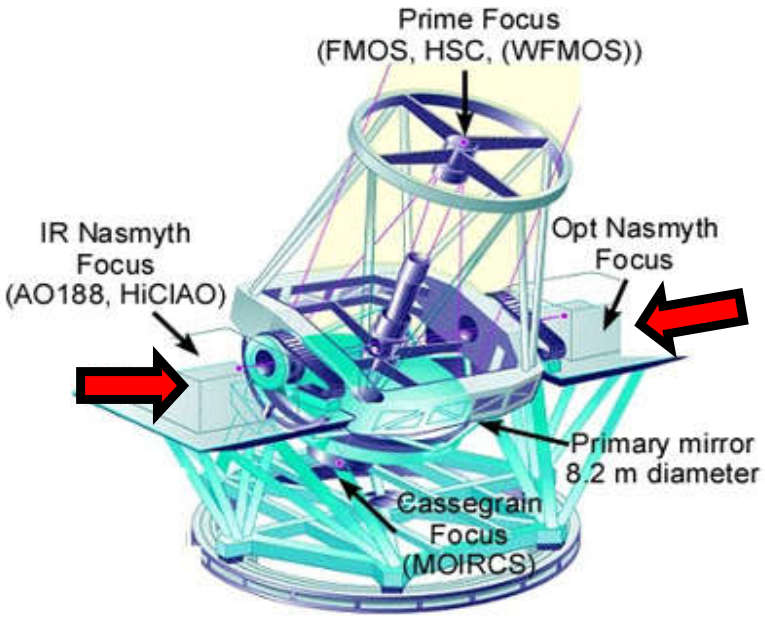

Subaru (8.3m) Japan

Autofib@WHT (4.2m) UK

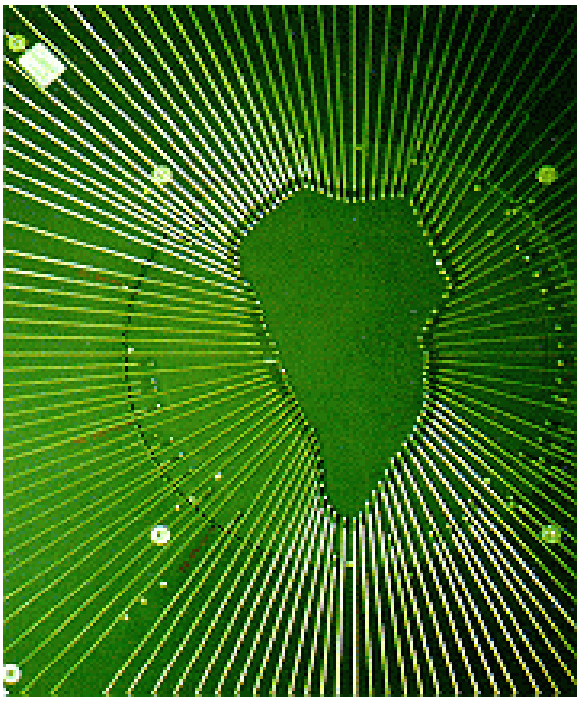

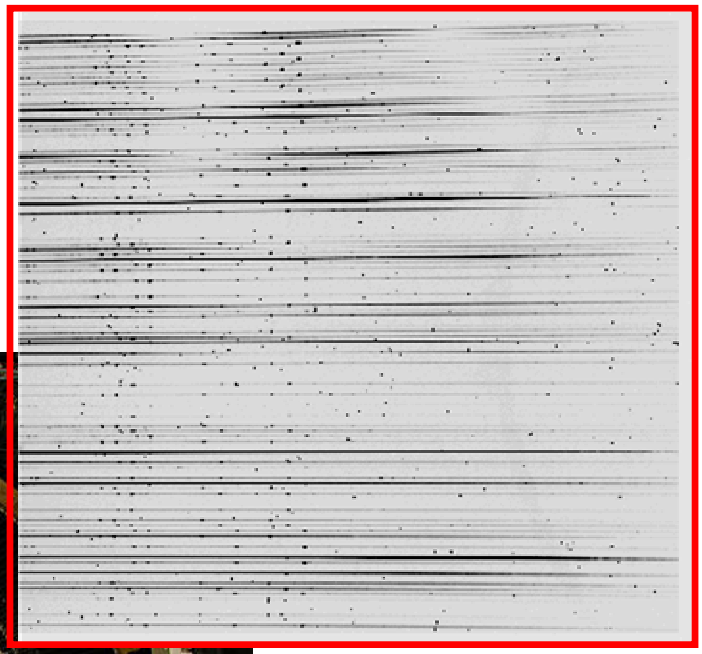

HECTOSPEC@MMT (6.5m)
Arizona (USA)

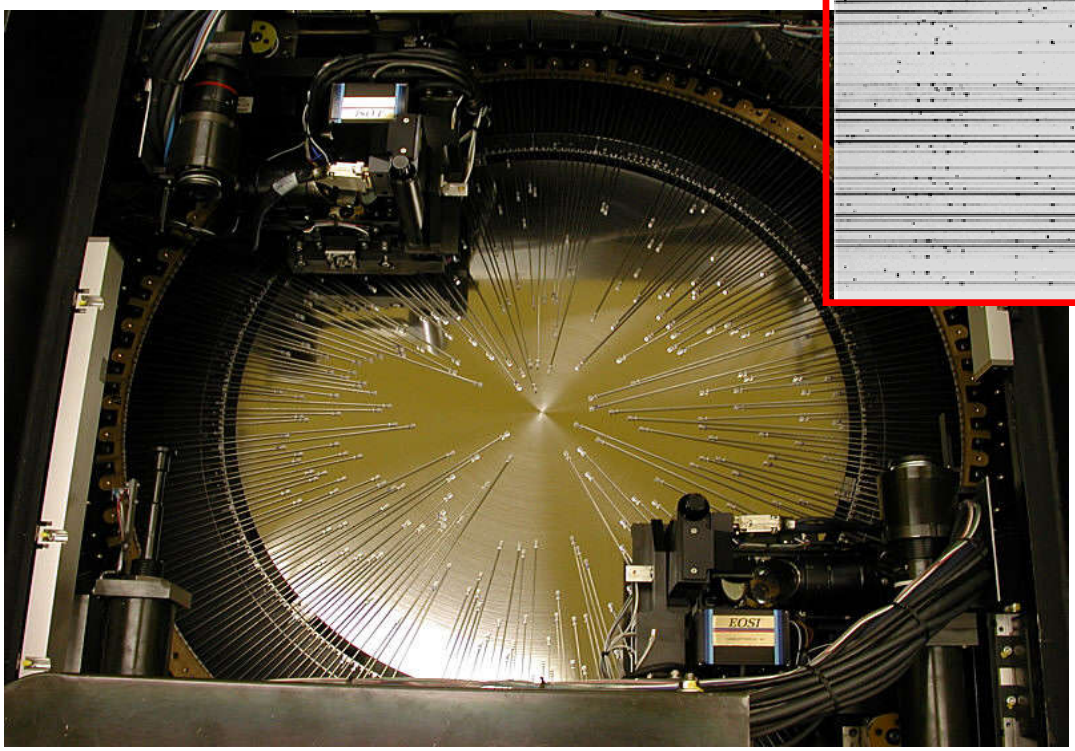

Esempio di uscita spettrografo a fibre

Le camere FOSC

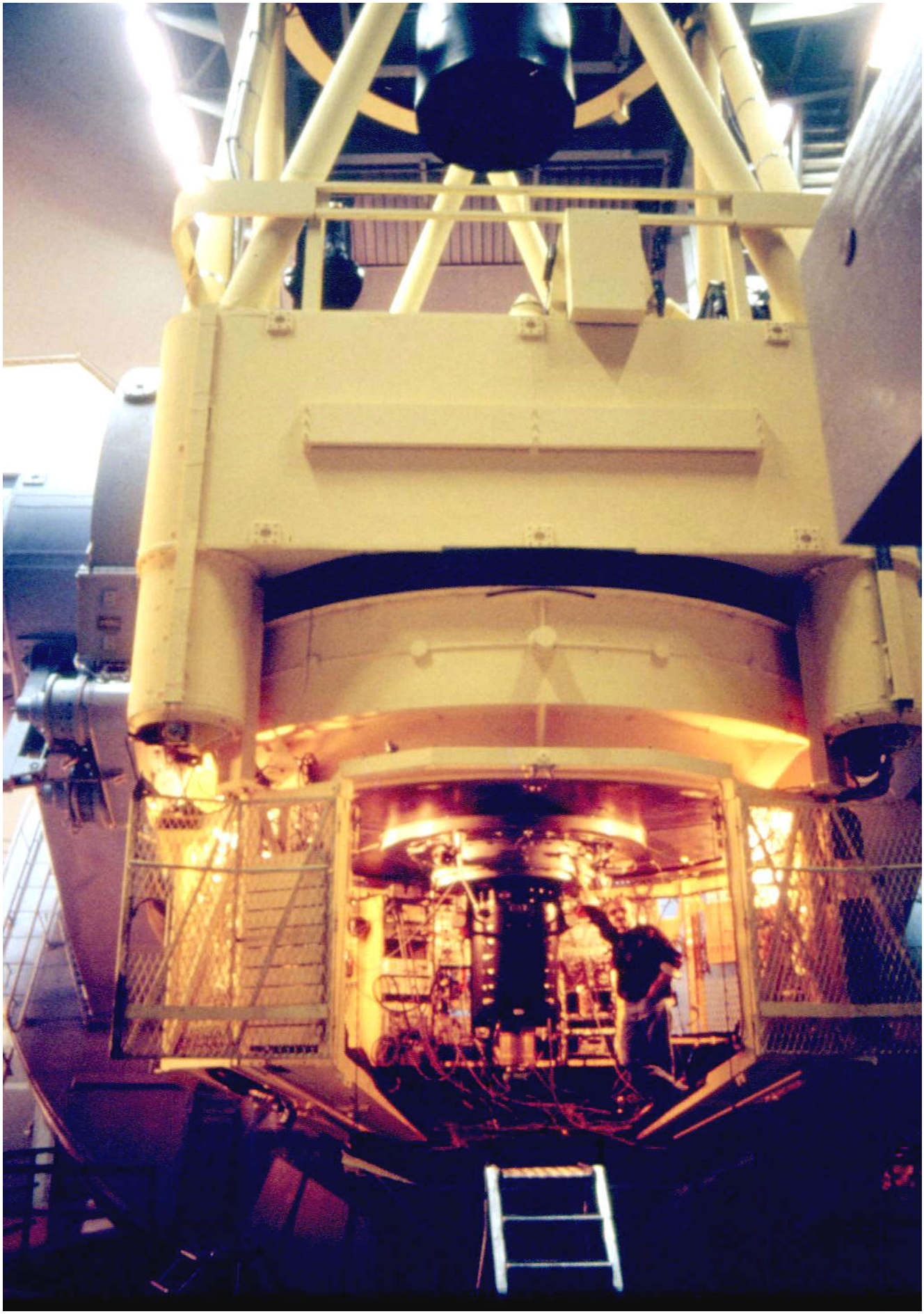

Spettroscopia "MOS" (multiobject)

Spectral resolution

FWHM ~ 2.5 ÷10Å

Resolving power

$$R = \frac{\lambda}{\Delta\lambda} = 500 \Leftrightarrow 2000$$

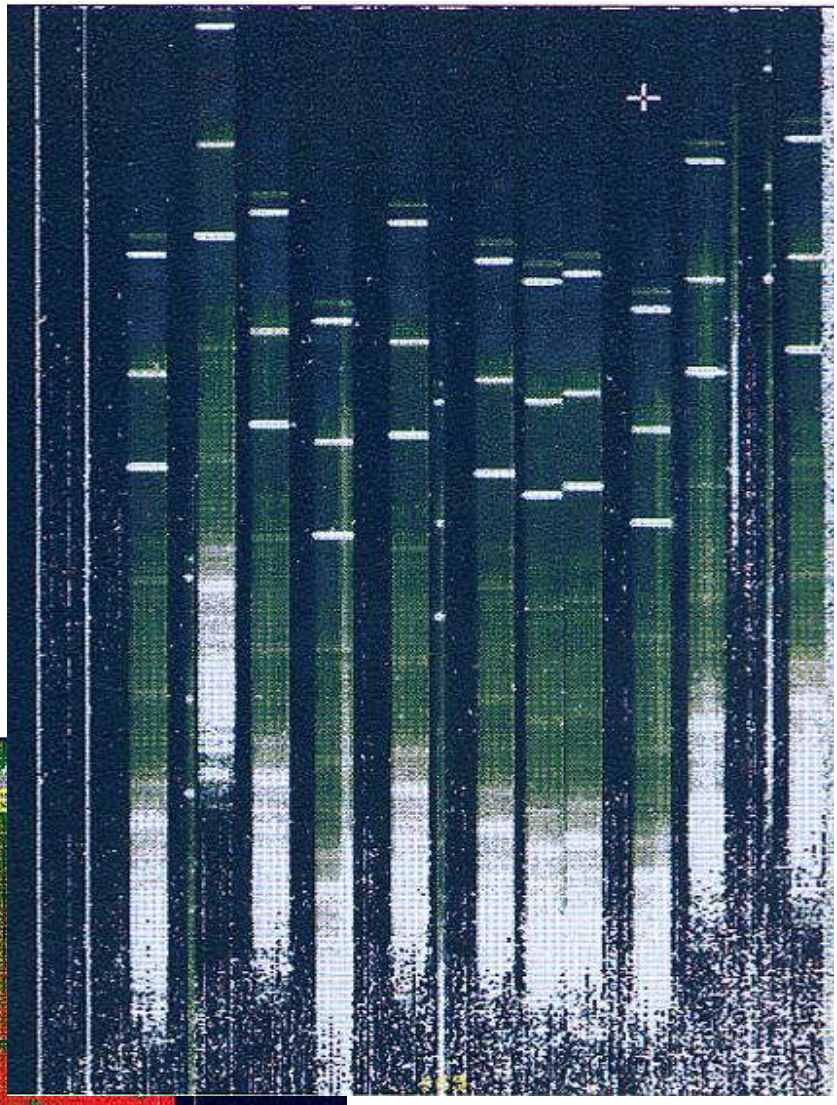

Esempio di uscita spettrografo MOS FOSC

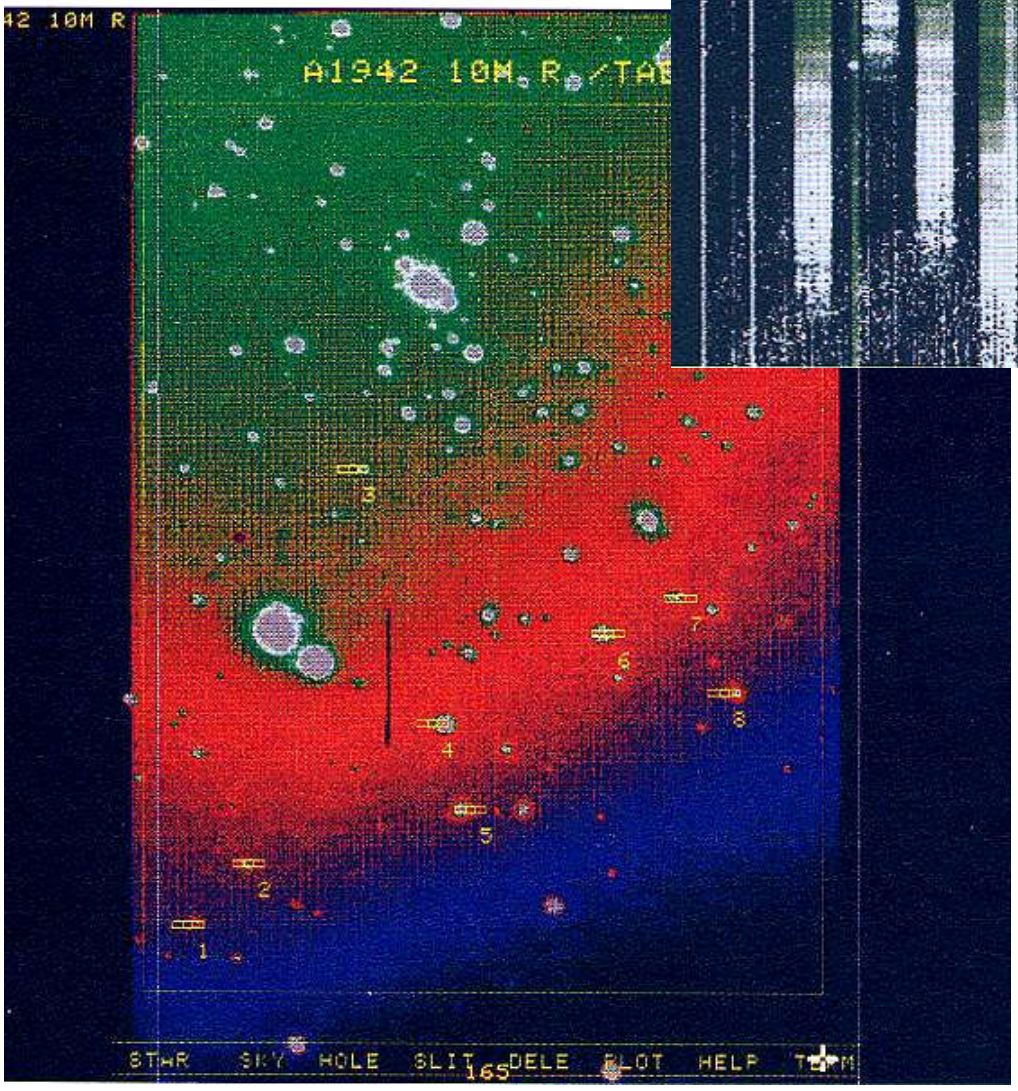

Pre-imaging
(per vedere gli oggetti da puntare)

VIMOS@VLT (ESO) 8.2m, Chile

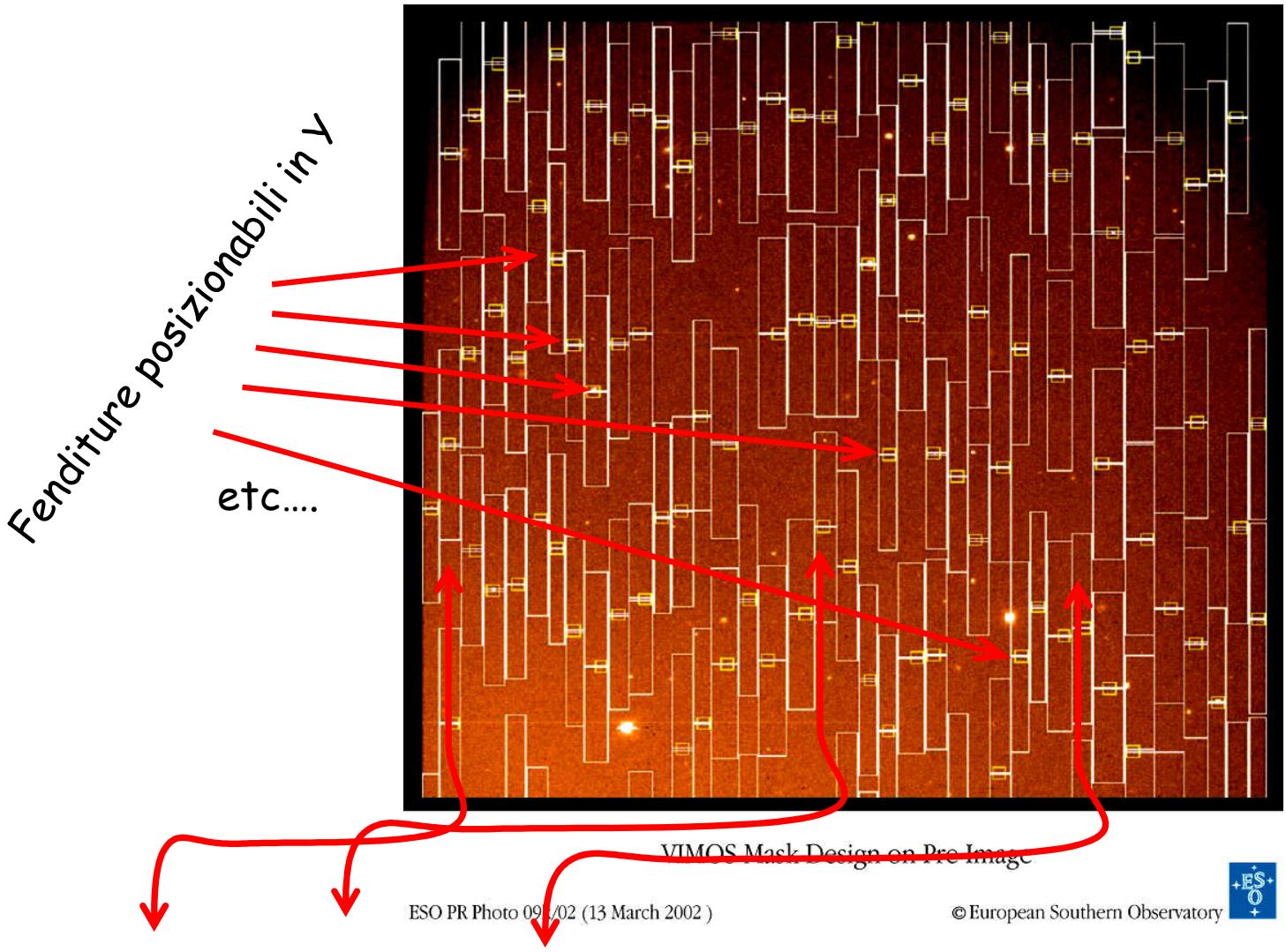

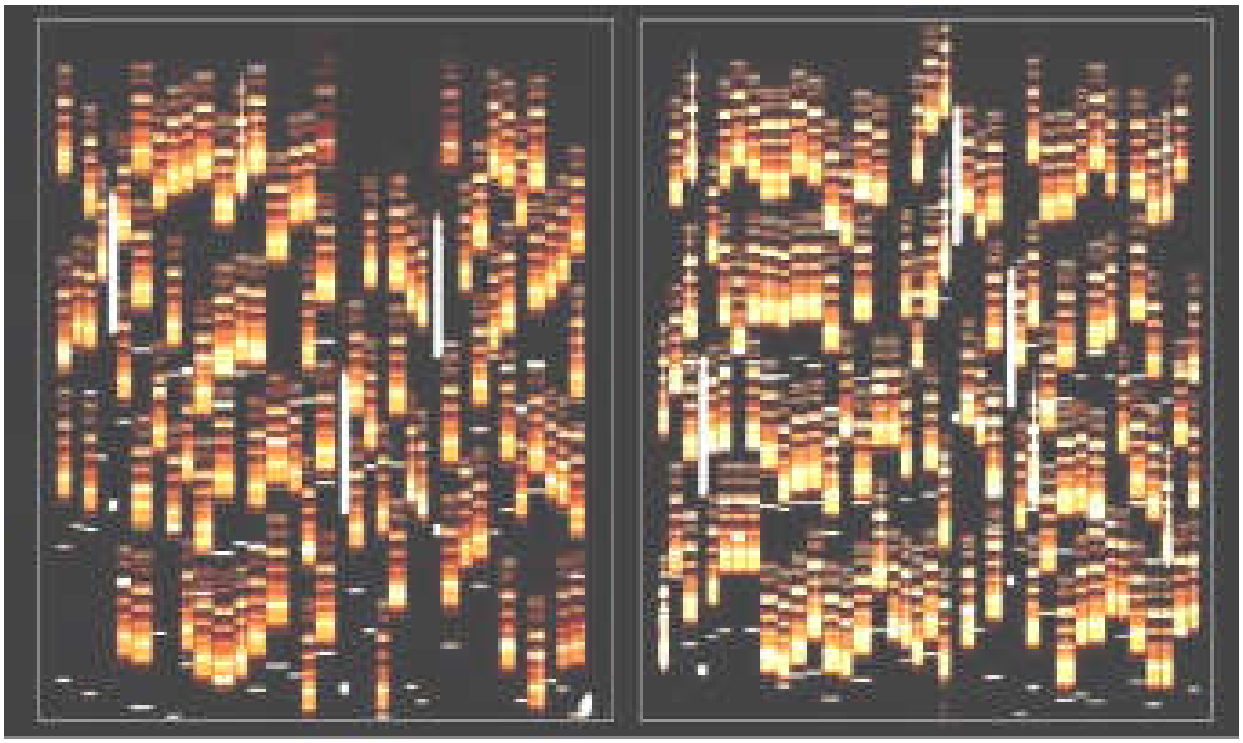

Legge di Wien : $\lambda_{\max} T \propto const$

$$\frac{\lambda_{\max}}{5500} = \frac{5780}{T_K} \longrightarrow \lambda_{\max} \approx \frac{3\,10^7}{T_K} \text{ [Å]}$$

T_K		λ_{max}	[eV]
100,000		300 Å	raggi γ
10,000		3000 Å	UV
6,000		5000 Å	Ottico
3,000		10,000 Å	MIR
1,000		30μm Å	FIR

Equipartizione dell'energia :

$$E \approx 3kT = 4.2\ 10^{-16} T_K \approx h\nu = \frac{hc}{\lambda}$$

$$\langle \lambda \rangle \approx \frac{hc}{kT} = \frac{6.6\ 10^{-27} \times 3\ 10^{10}}{4.2\ 10^{-16} T_K (10^{-8})} = \boxed{\frac{4.7\ 10^7}{T_K}} \text{ [Å]}$$

$$T_K \approx 2400 \; E_{eV}$$

Il potenziale di ionizzazione dell'H e' di 13.6eV. Quindi sono necessarie temperature superiori a circa 35,000 K

Gruppo	1	2	13	14	15	16	17	18
Periodo								
1	H 13.59844							He 24.58741
2	Li 5.39172	Be 9.32263	B 8.29803	C 11.26030	N 14.53414	O 13.61806	F 17.42282	Ne 21.56454
3	Na 5.13908	Mg 7.64624	Al 5.98577	Si 8.15169	P 10.48669	S 10.36001	Cl 12.96764	Ar 15.759
4	K 4.34066	Ca 6.11316	Ga 5.99930	Ge 7.899	As 9.8152	Se 9.75238	Br 11.81381	Kr 13.99961
5	Rb 4.17713	Sr 5.69484	In 5.78636	Sn 7.34381	Sb 8.64	Te 9.0096	I 10.45126	Xe 12.12987
6	Cs 3.89390	Ba 5.21170	Tl 6.10829	Pb 7.4167	Bi 7.2855	Po 8.41671	At 9.2	Rn 10.74850
7	Fr 4.0712	Ra 5.27892						

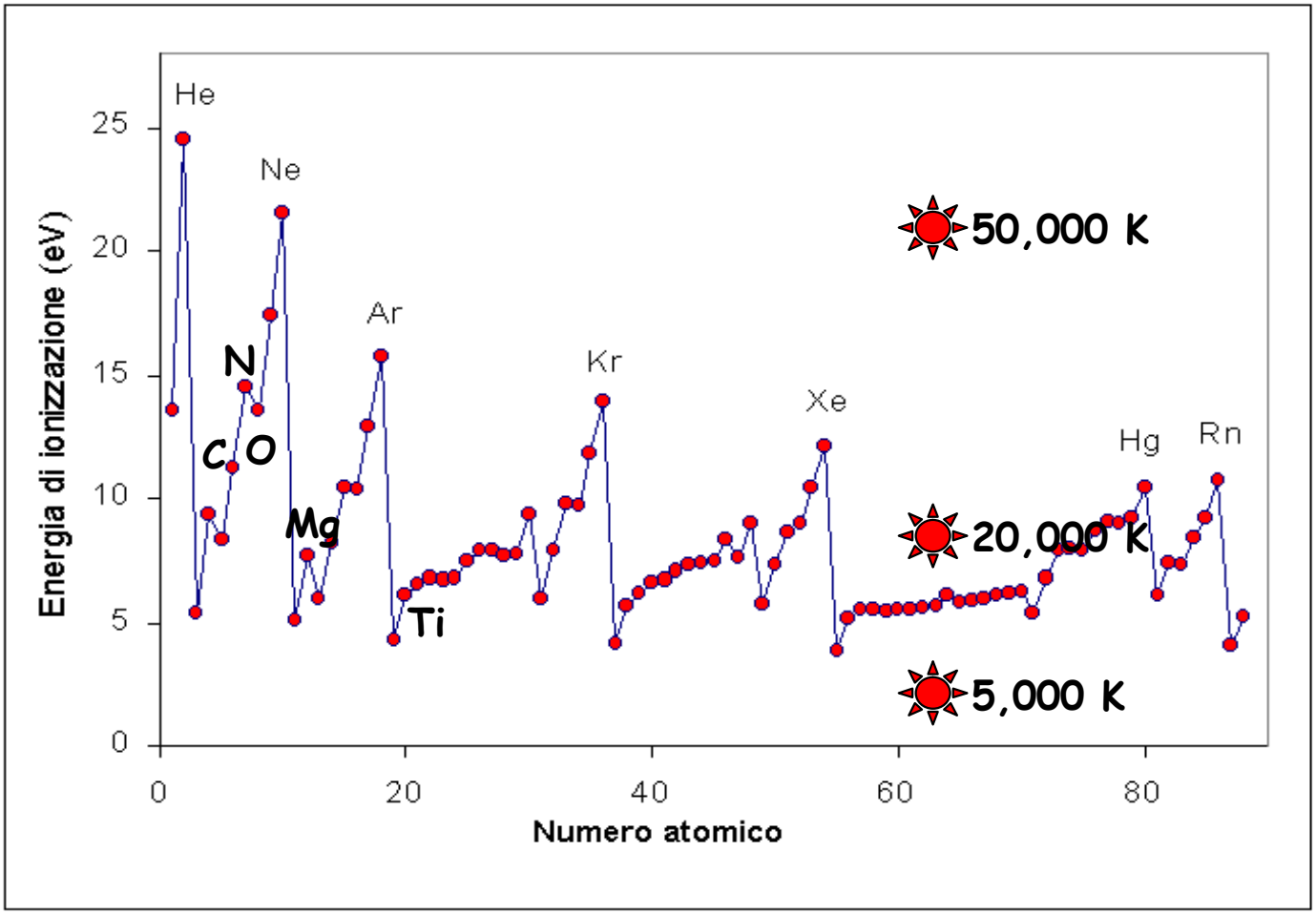

Molecole

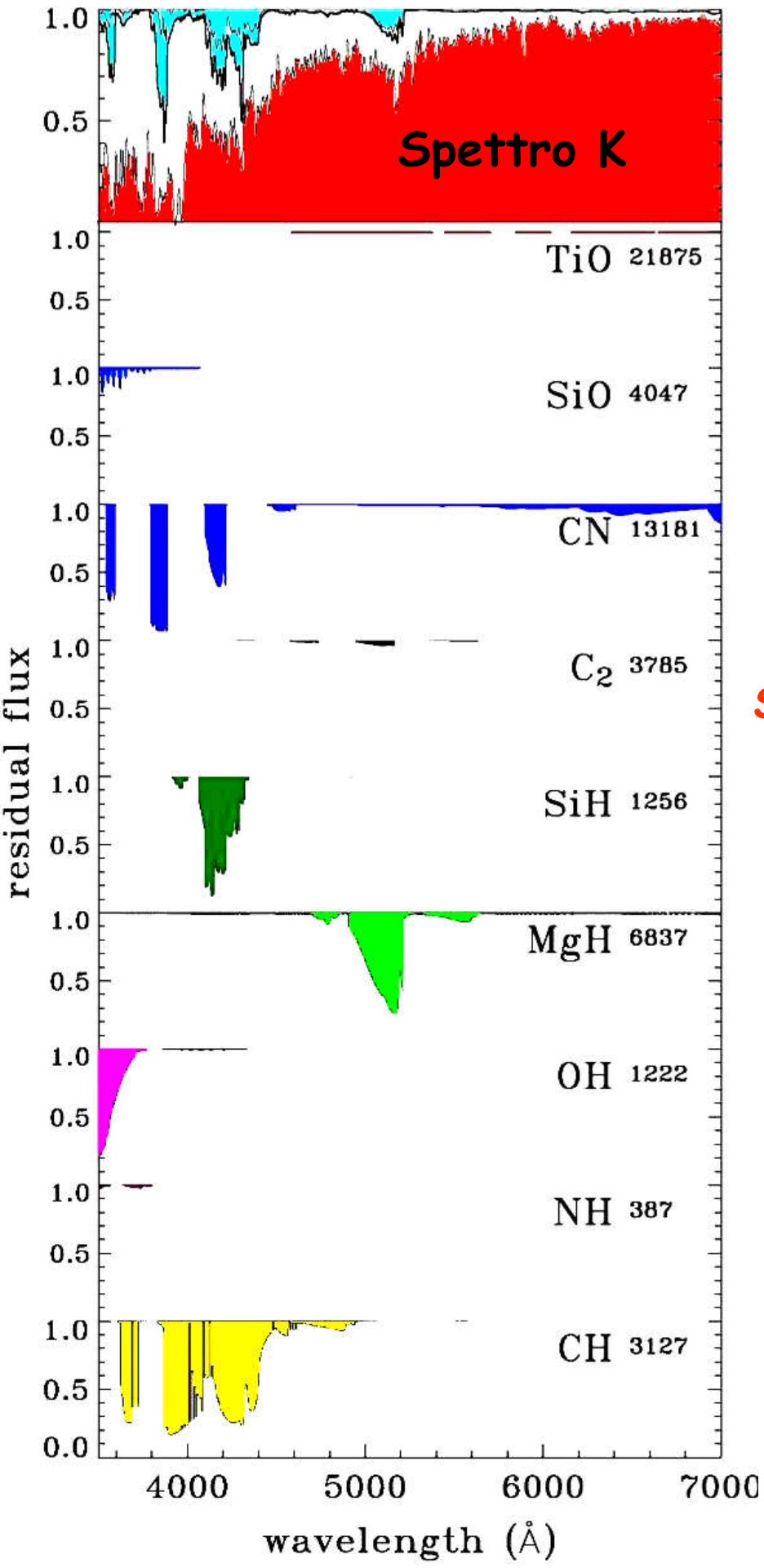

4000 > Teff > 3000 K

Diatomic molecules
(i.e. TiO, SiO,CN, SiH, MgH, OH, CH….)

3000 K > Teff

Triatomic molecules
(Water!)

Emissione & Assorbimento

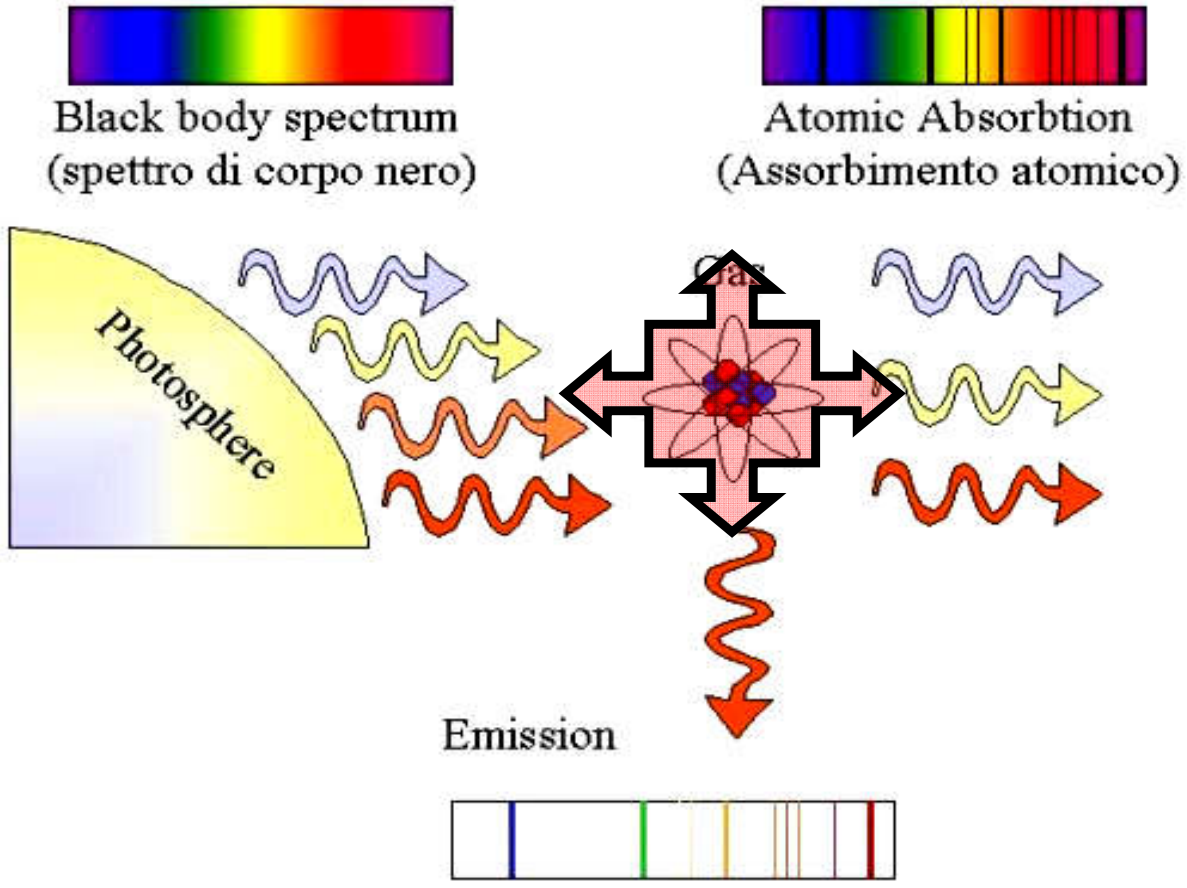

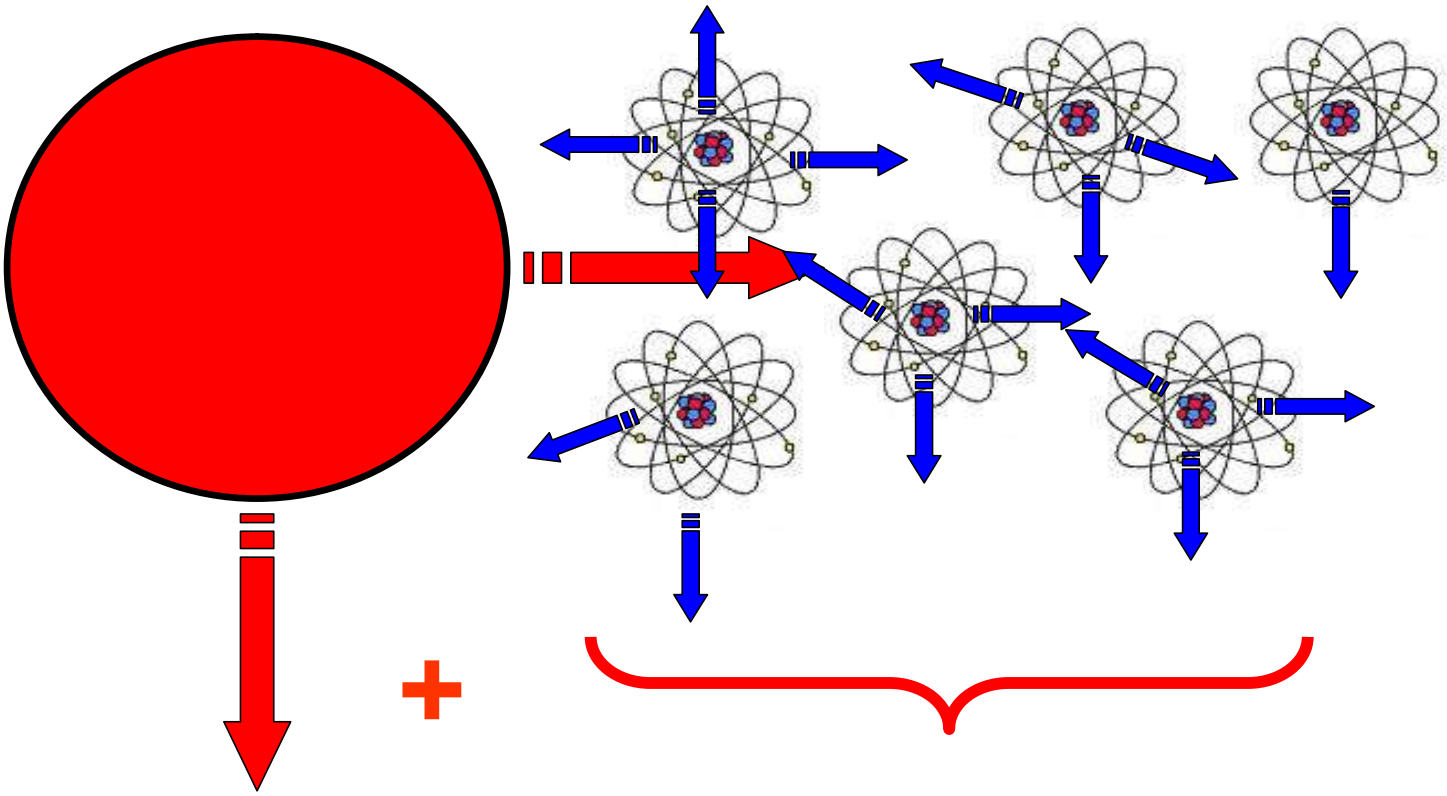

Effetti della rotazione (emissione)

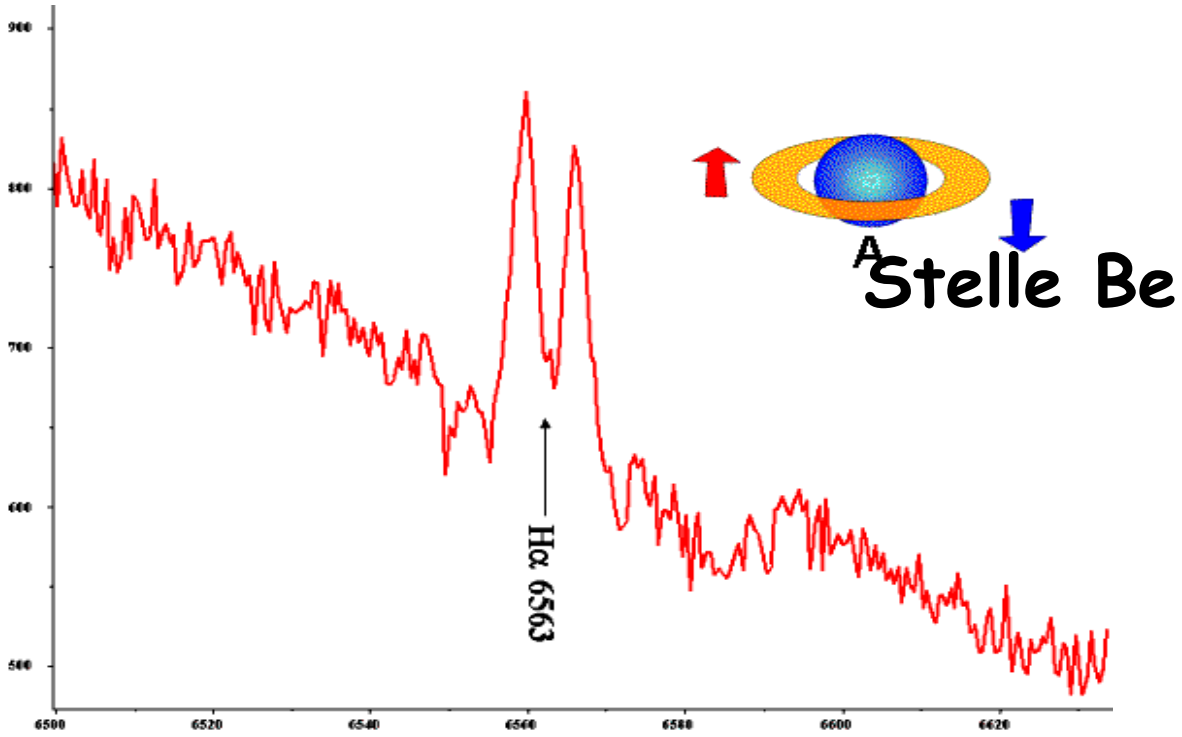

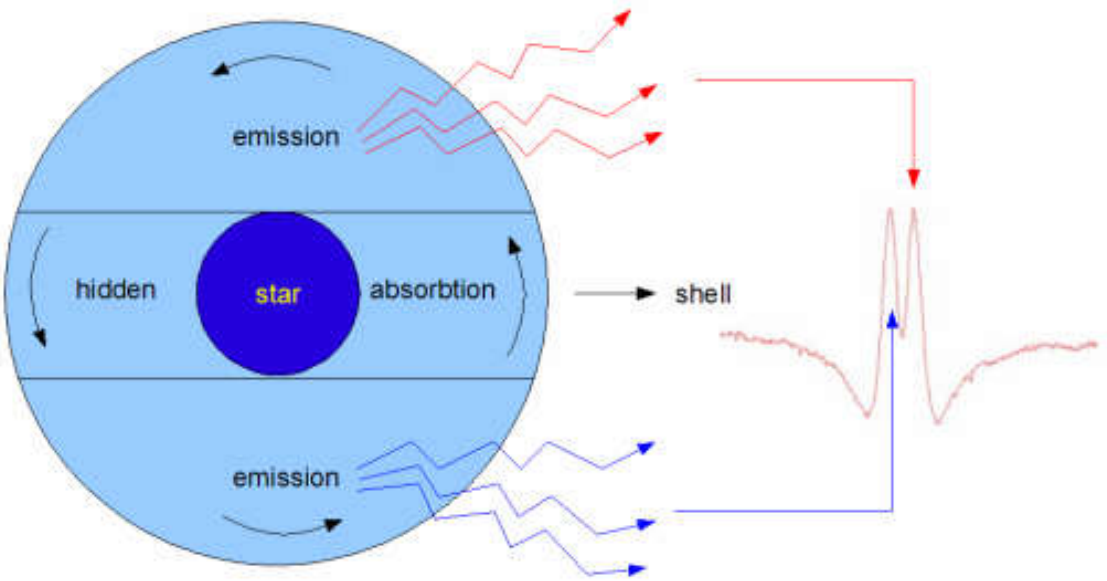

Effetti della rotazione (emissione)

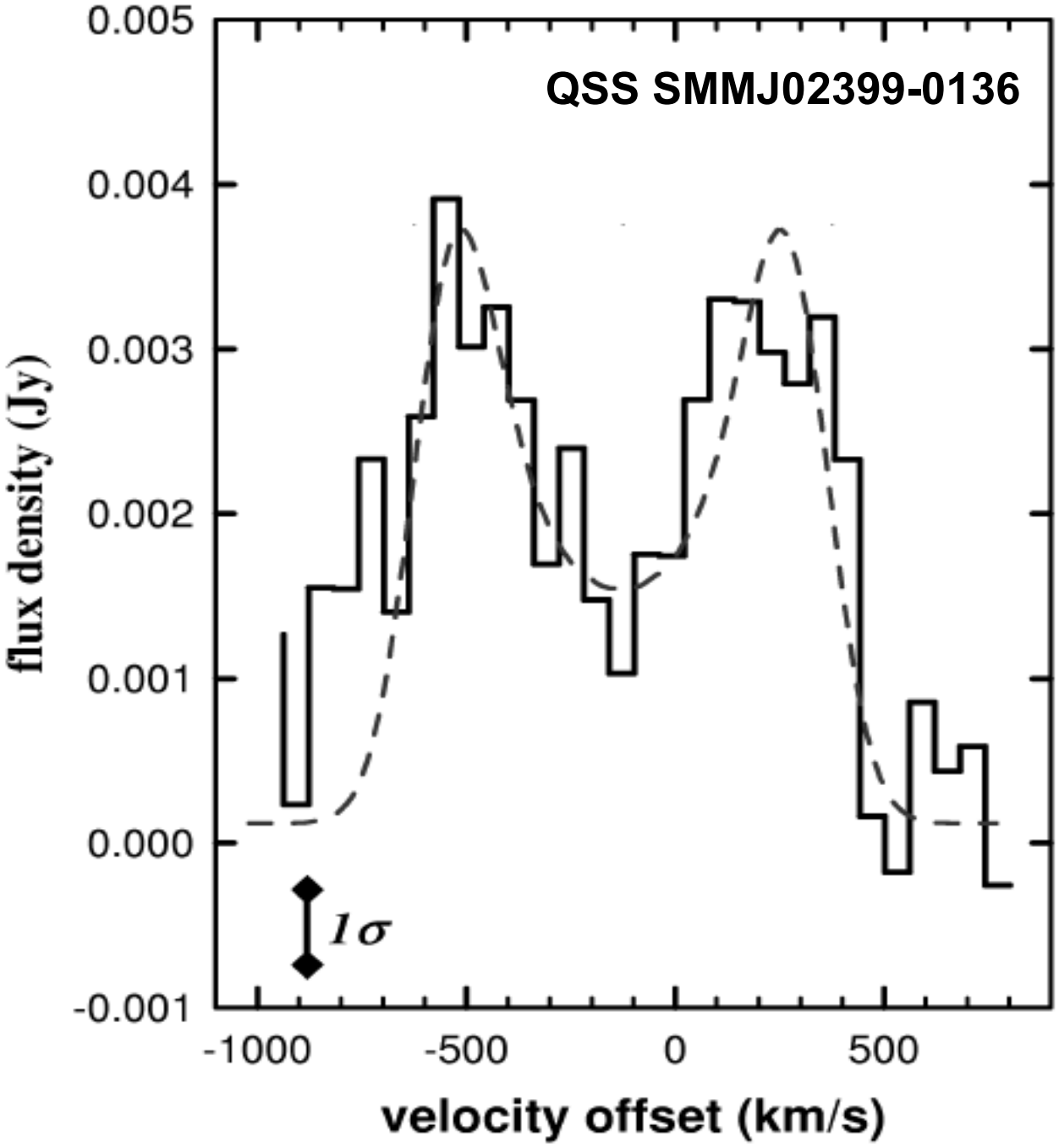

"SMMJ02399-0136 appears to contain a massive molecular ring/disk which rotates about a buried type 2 QSO. Its dynamical mass of $>3.10^{11}$ Msun within a radius of 8 kpc"

A Very Massive Submillimeter Galaxy at z = 2.8 (Genzel et al. 2003)

Effetti della rotazione (assorbimento)

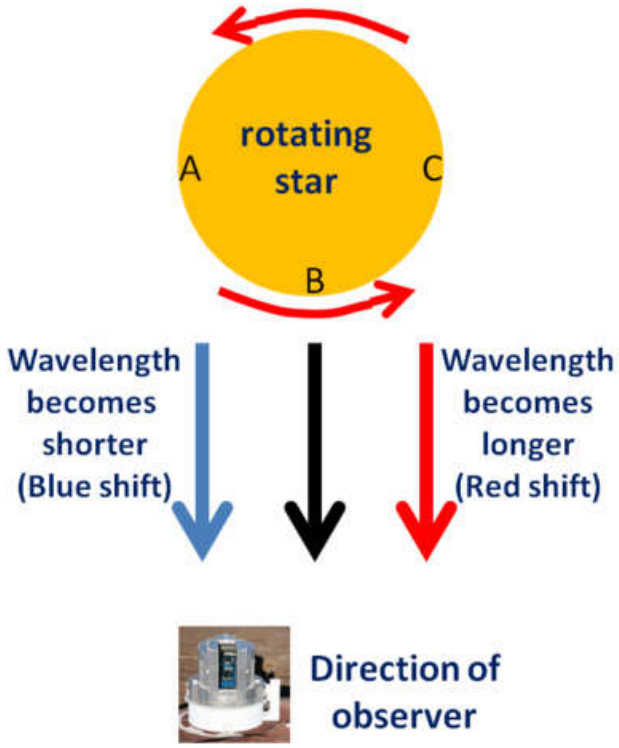

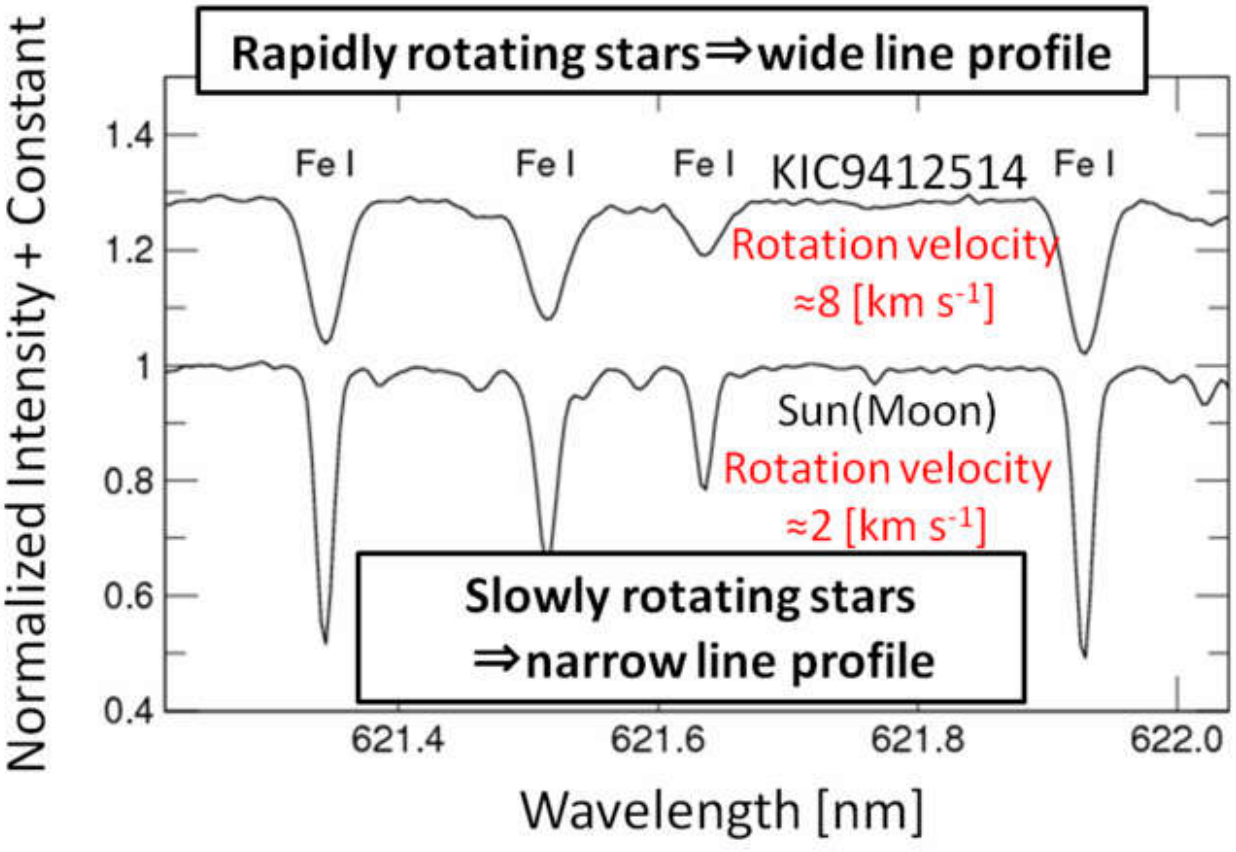

L'effetto P Cygni

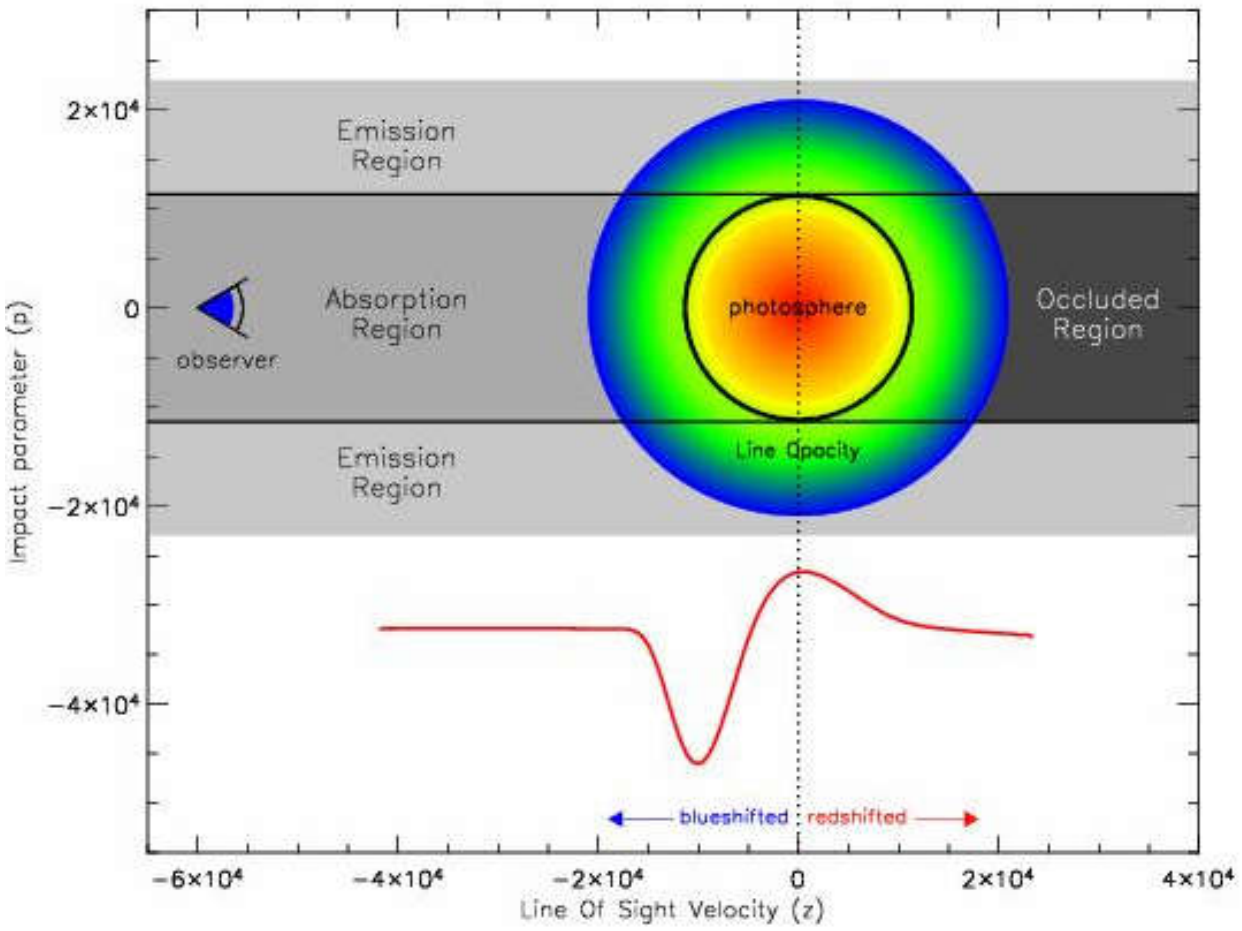

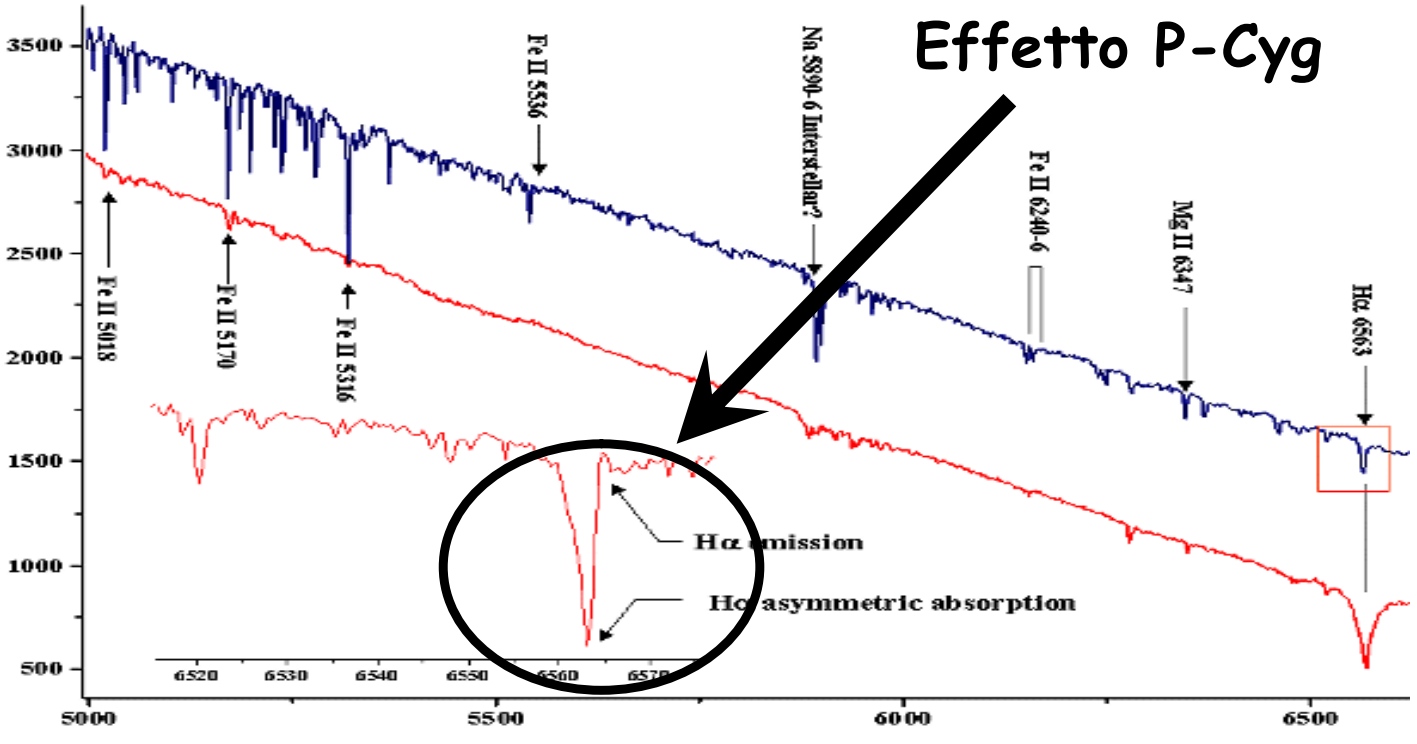

L'effetto P Cygni
(Arp 220)

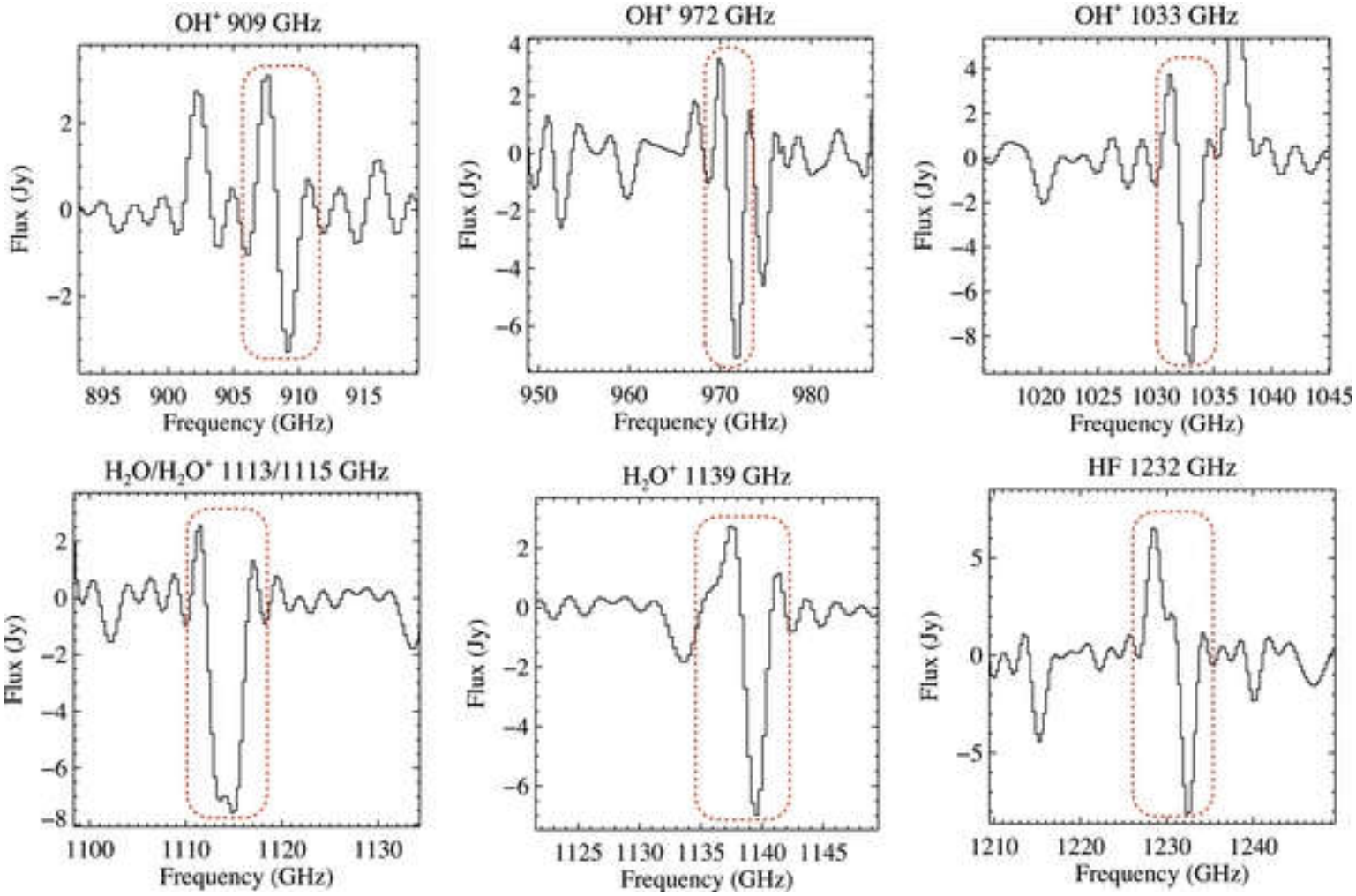

Arp 220 is the nearest Ultra Luminous Infrared galaxy (ULIRG) at a distance of about 77 Mpc and z ~ 0.0181. It has LFIR ~ 10^{12} *Lsun*, and is one of the most popular templates for studies of high-z dusty galaxies. (Rangwala et al., 2011)

Le righe dell'Idrogeno

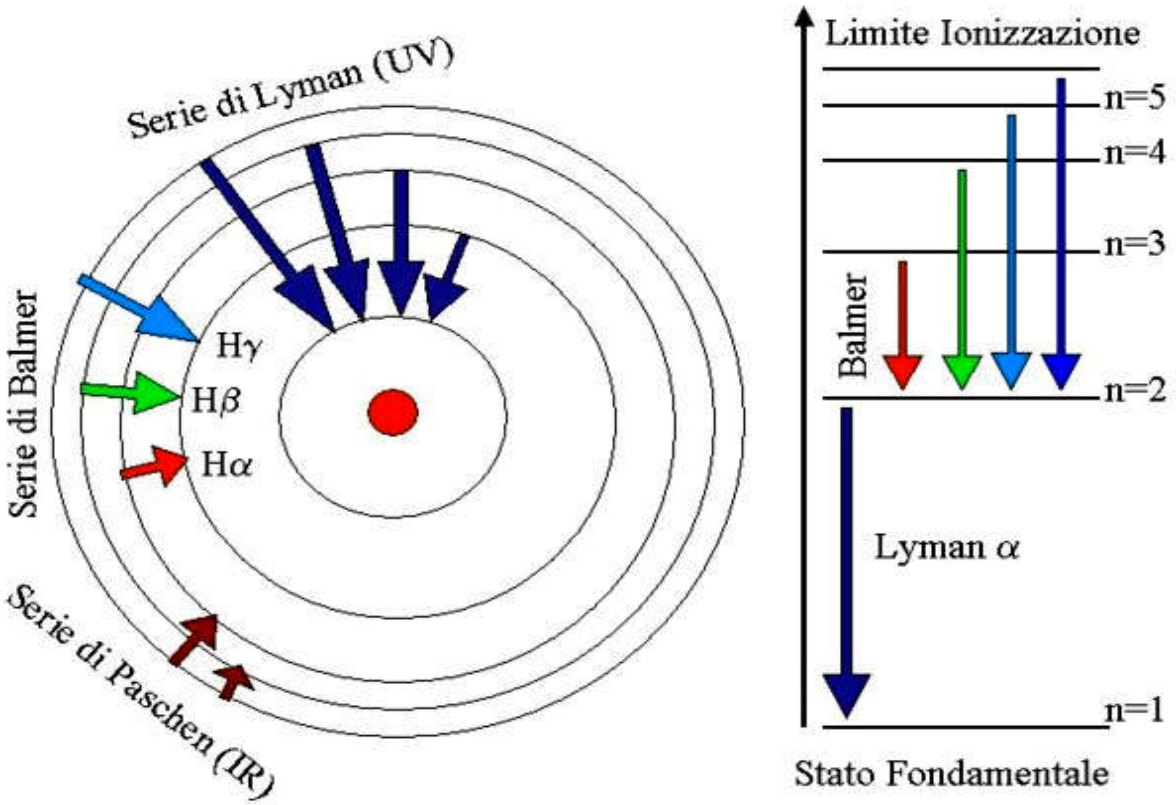

Righe emesse non solo nel visibile

$$\frac{1}{\lambda} = R\left(\frac{1}{m^2} - \frac{1}{n^2}\right) \quad m = 1,2,3,\ldots \quad n = m+1,\ldots.$$

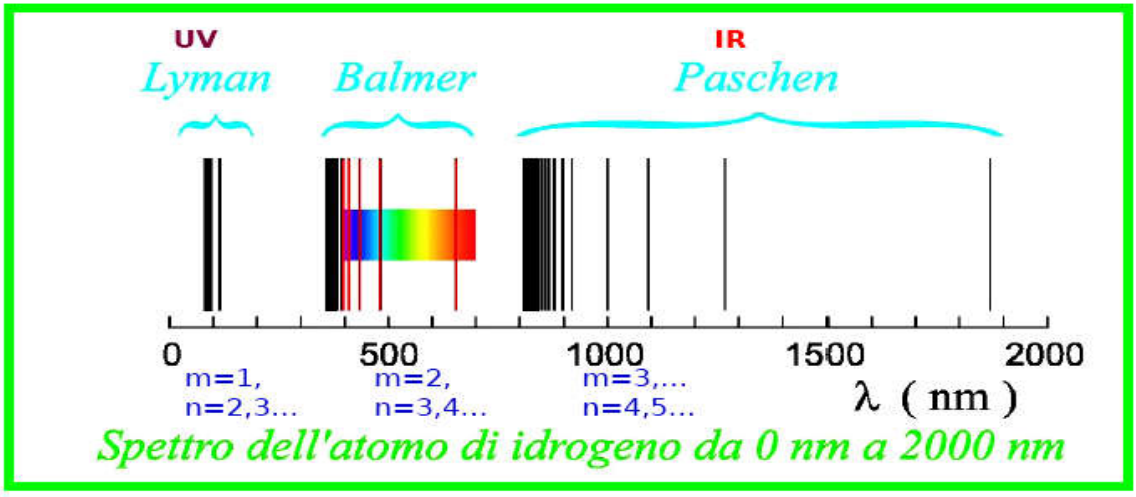

Le serie di righe

Nome della serie	Anno della scoperta	m nella formula di Rydberg	Limite della serie (nm)	λ_{max} ($n=m+1$) (nm)	Regione spettrale
Lyman	1906-1914	1	**91.126**	**121.5**	UV lontano
Balmer	(1885)	2	**364.506**	**656.1**	Visibile-UV
Paschen	1908	3	**820.14**	**1874.6**	Infrarosso
Brackett	1922	4	**1458.03**	**4050.1**	Infrarosso
Pfund	1924	5	**2278.17**	**7455.8**	Infrarosso
Humphreys	1953	6	**3280.56**	**12365.1**	Infrarosso
Hansen-Strong	1973	7	**4465.21**	**19051.5**	Infrarosso

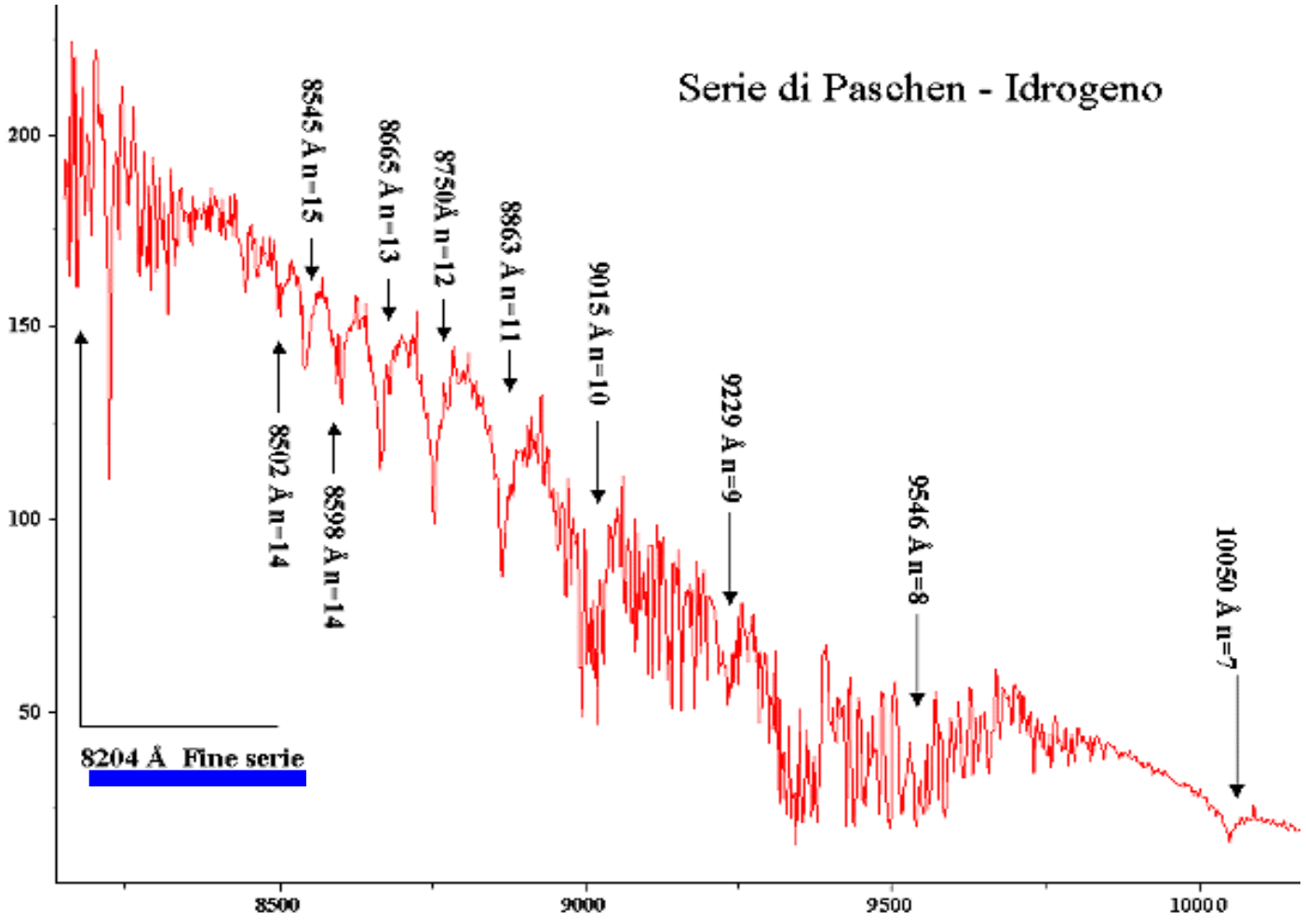

Spettri & masse delle galassie

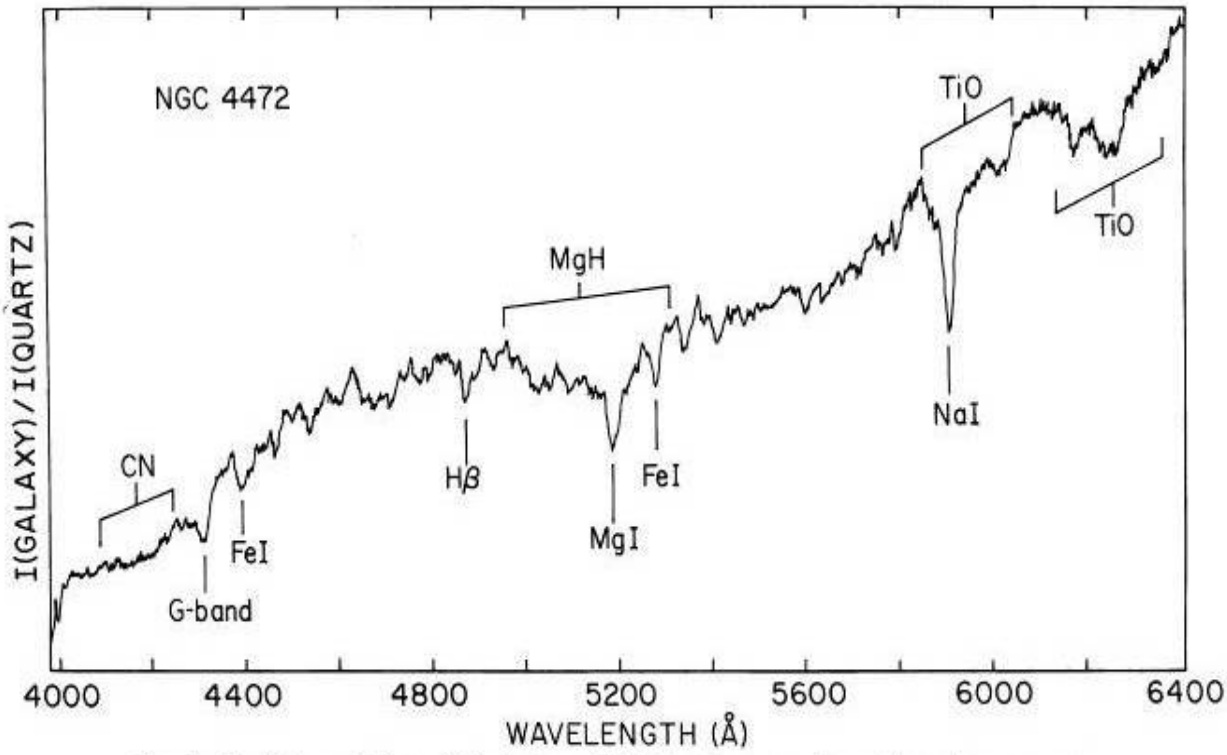

FIG. 1.—Typical scan of giant elliptical galaxy, divided by the tungsten lamp (denoted by "quartz")

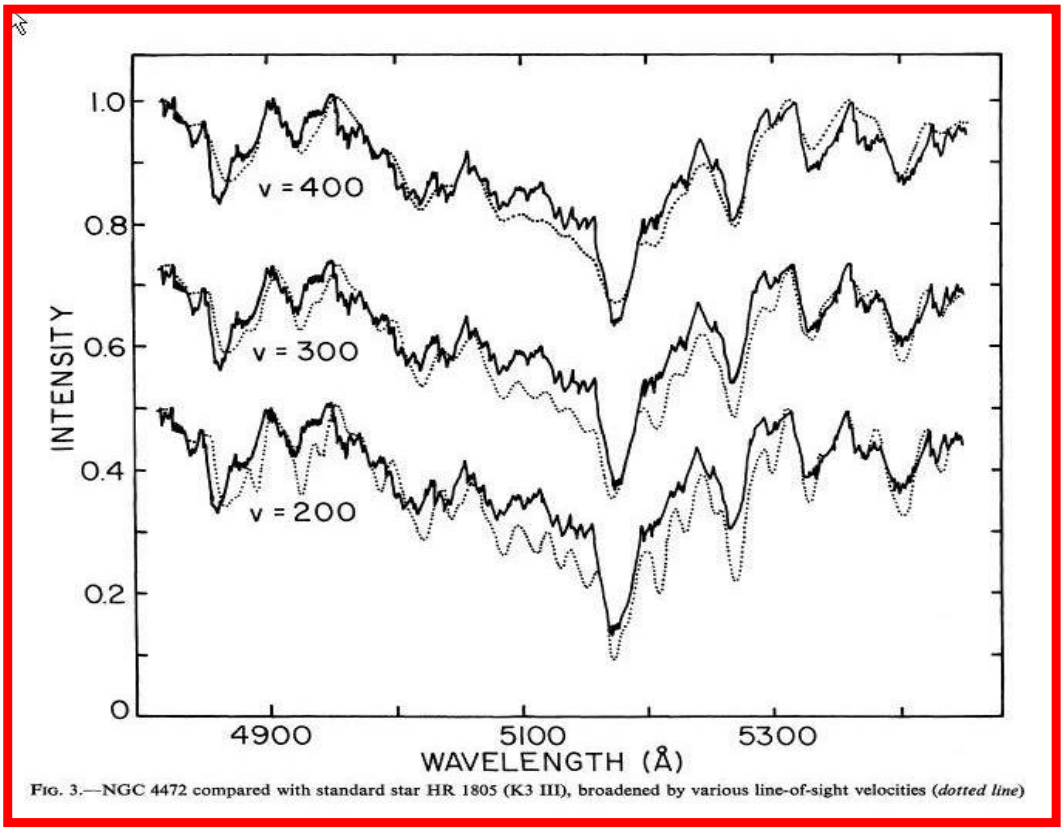

FIG. 3.—NGC 4472 compared with standard star HR 1805 (K3 III), broadened by various line-of-sight velocities (*dotted line*)

La legge di Faber-Jackson (1976)

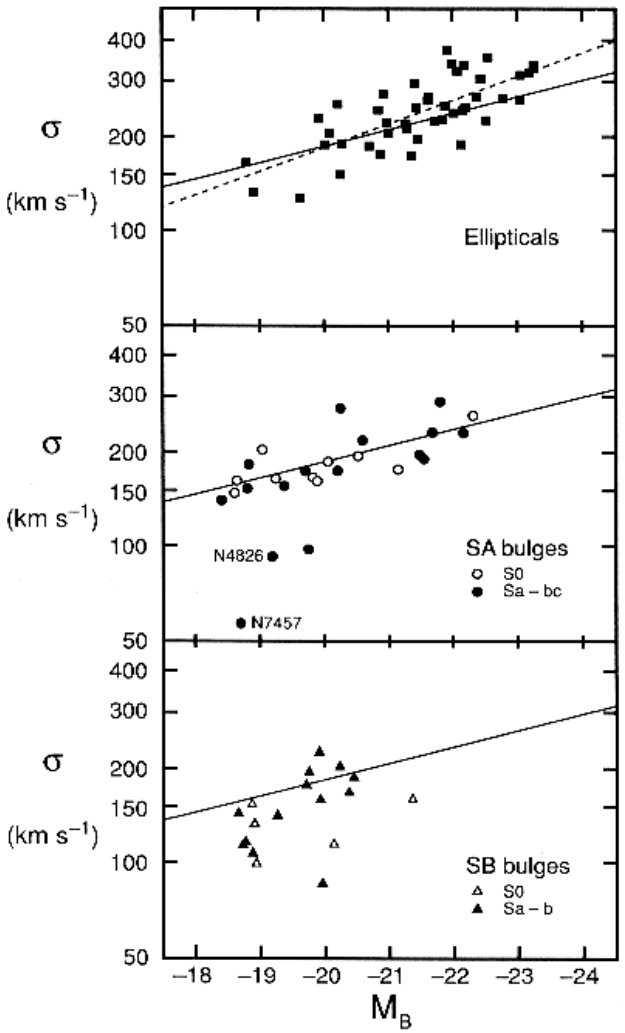

Fig. 6. Correlation between central velocity dispersion σ and absolute magnitude M_B for elliptical galaxies and for bulges of unbarred (SA) and barred (SB) disk galaxies. The solid line is a fit to the galaxies in the middle panel; the dashed line is a fit to the ellipticals. Except for the NGC 4826 point, this figure is from Kormendy and Illingworth (1983).

$$v^2 \approx \frac{GM}{R}$$

$$\mu = \frac{L}{\pi R^2} \approx \text{const}$$

$$\left(\frac{M}{L}\right) = \text{const}$$

Se il moto e' caotico, allora $v^2 \equiv \sigma^2$

$$\sigma^4 \propto \mu L$$

Spettri & Massa delle Spirali

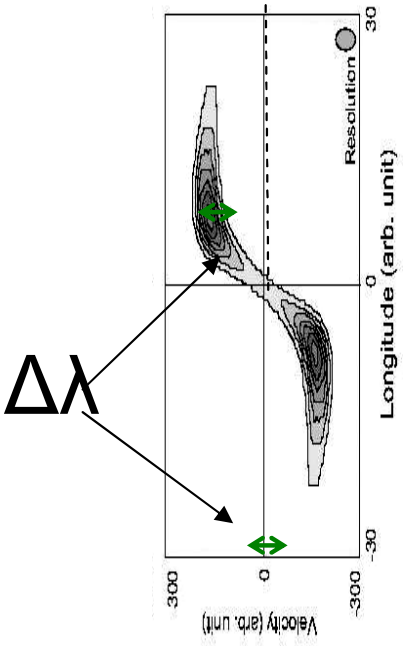

$$\frac{\Delta\lambda}{\lambda} = \frac{v}{c}$$

$$\frac{v^2}{R} = \frac{GM}{R^2}$$

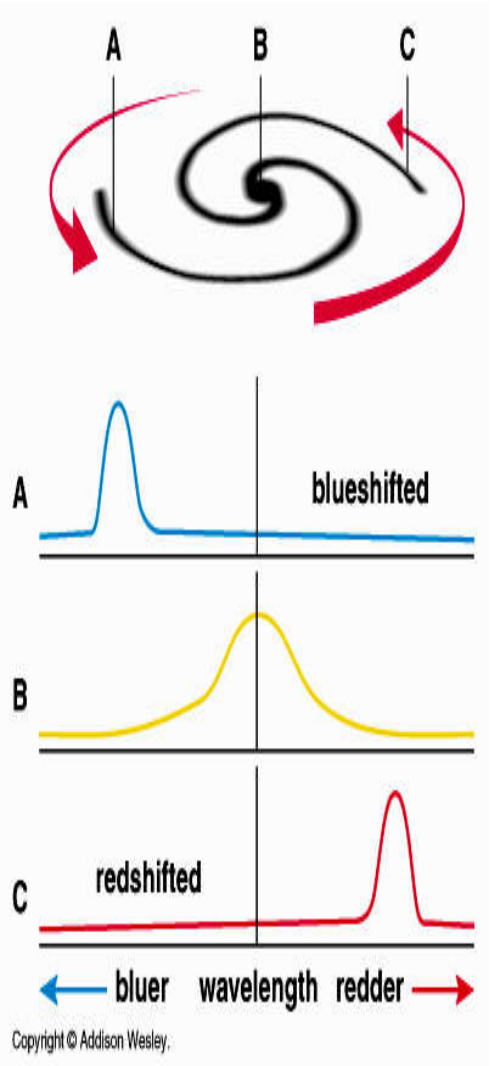

Acc. centrifuga

Acc. gravitazionale

La materia oscura

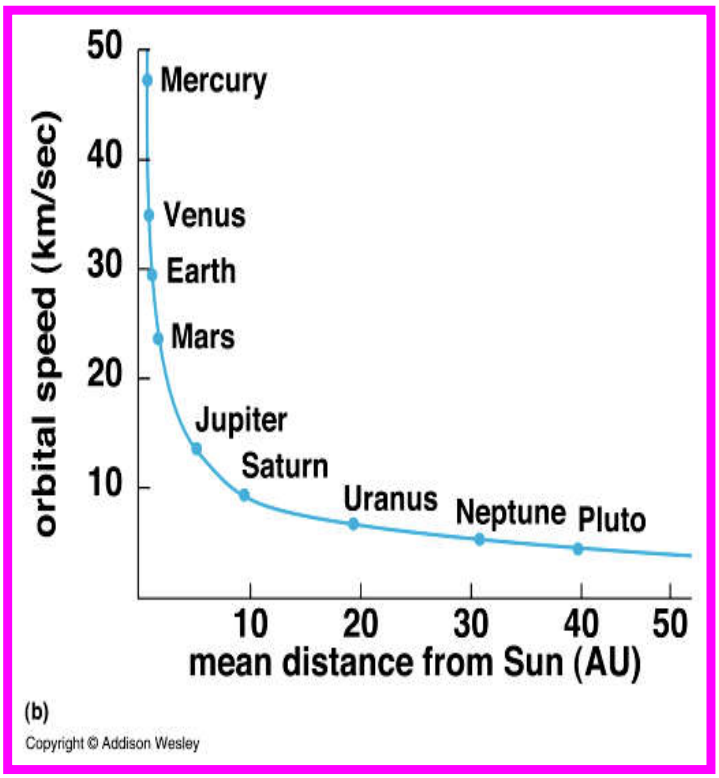

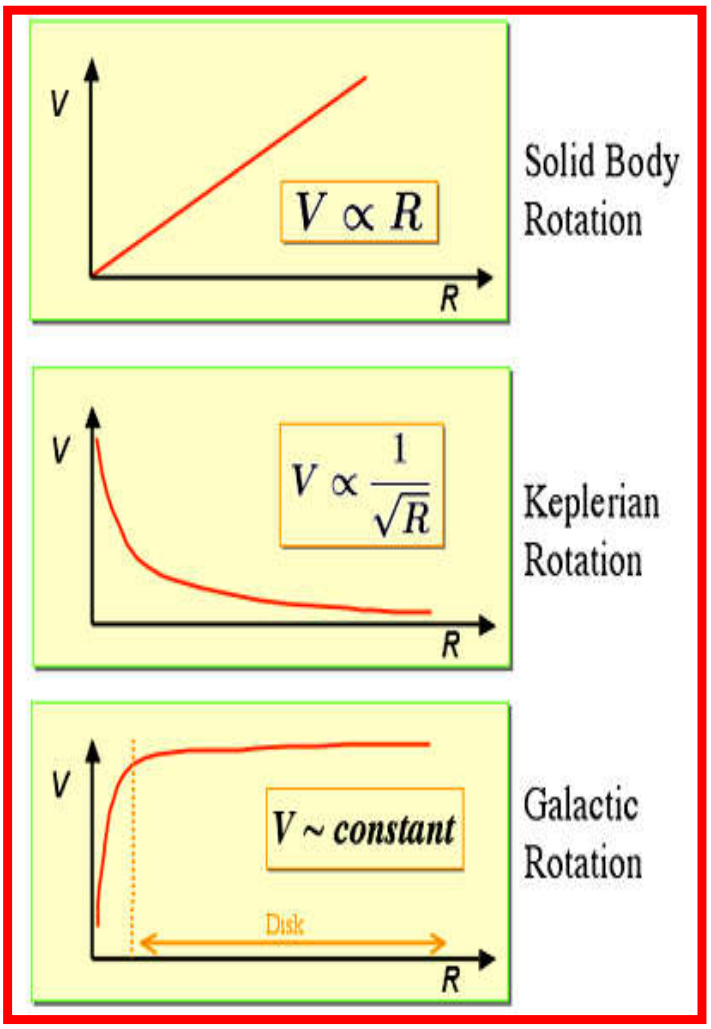

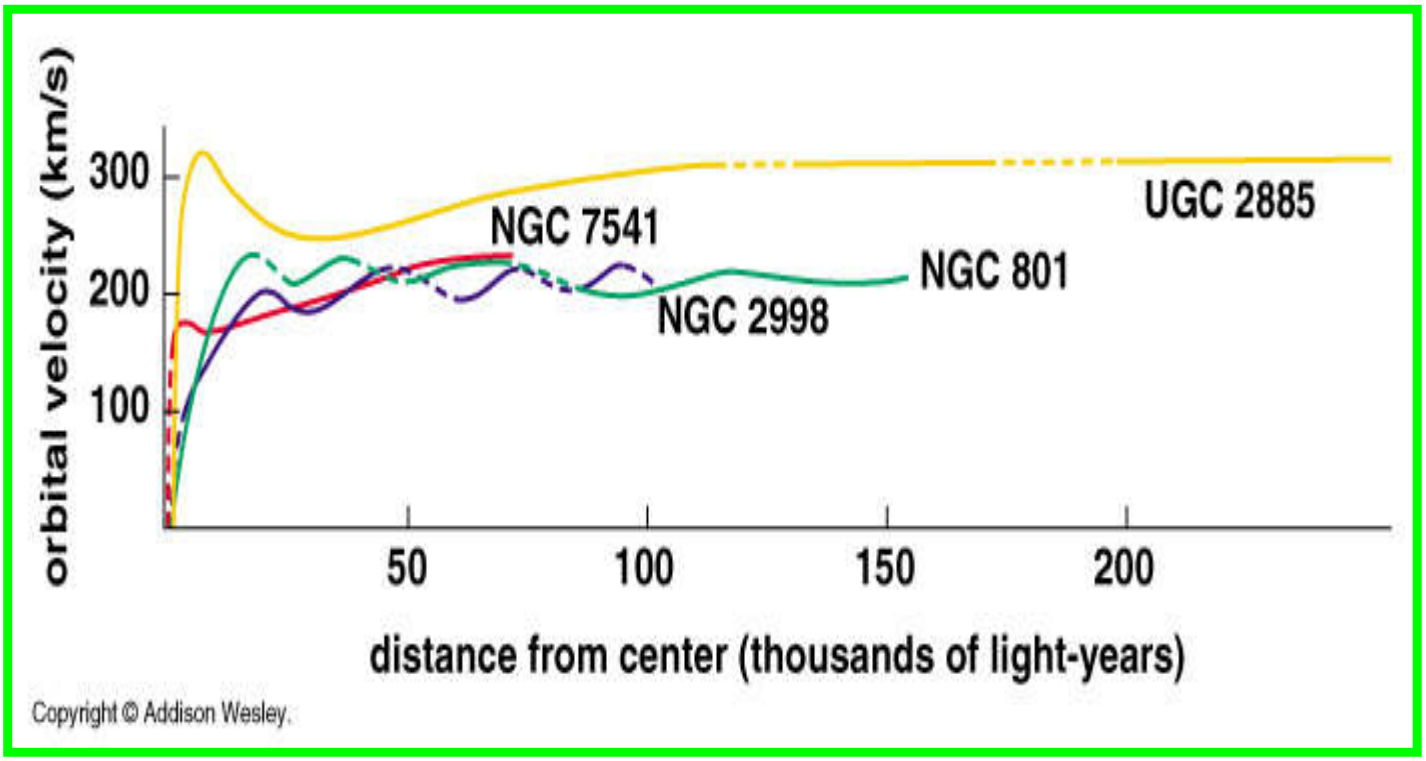

Forza di indice e Ampiezza equivalente

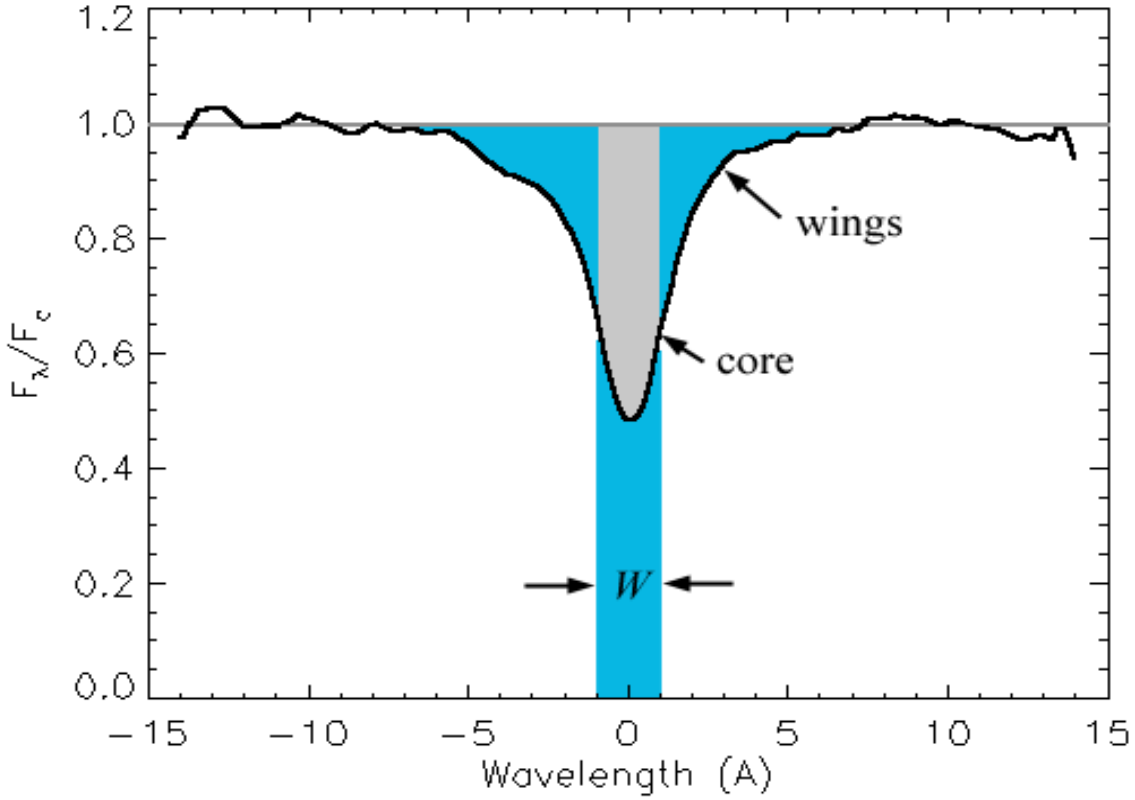

$$EW = \int \frac{f_c - f_f}{f_c} d\lambda$$

a T_{eff} fissato!!

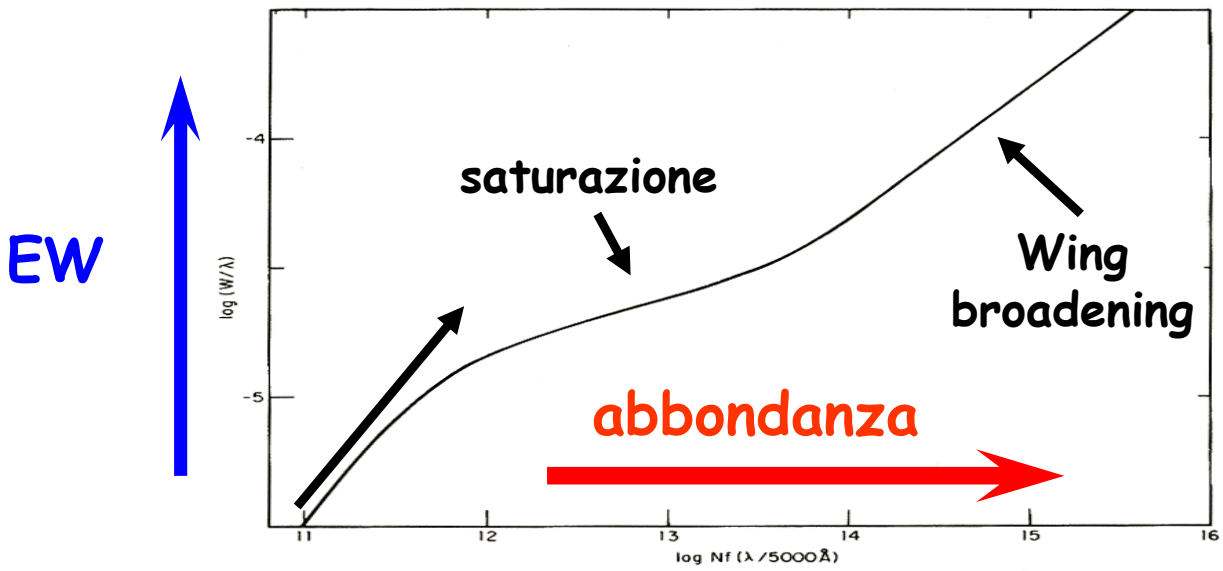

Indici in EW e in magnitudini

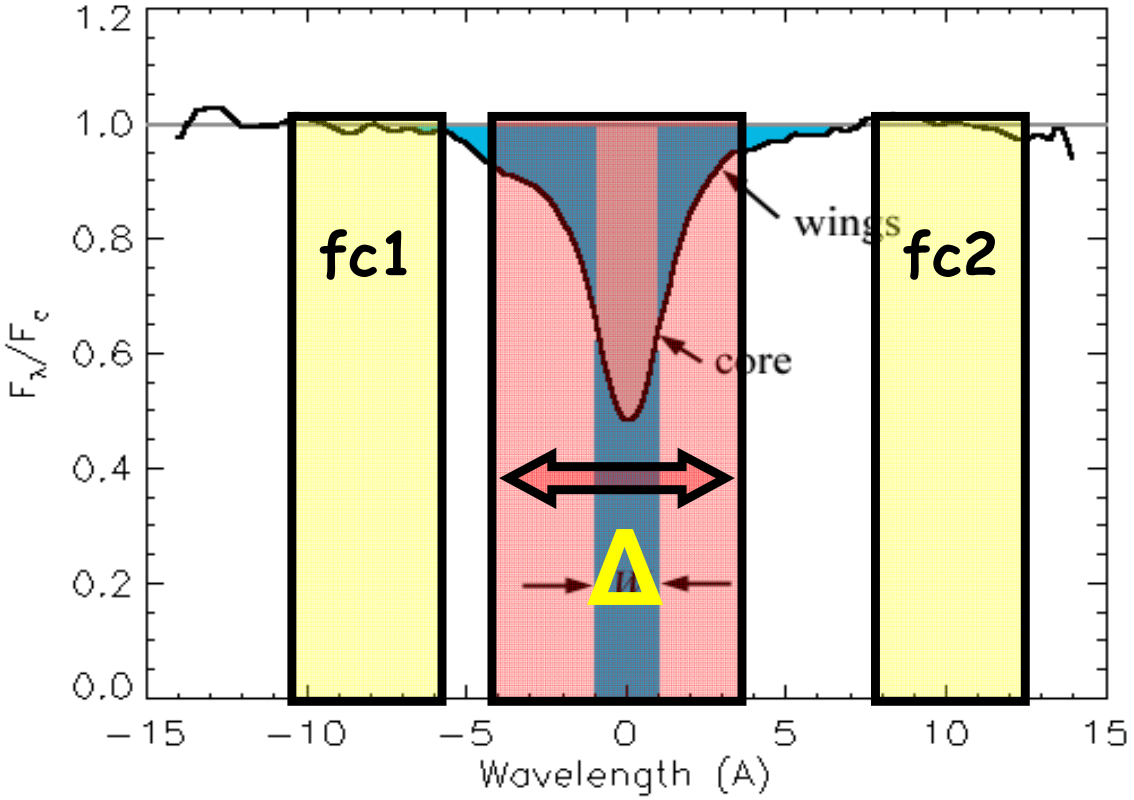

Tipicamente,

- se la riga e' atomica, l'indice si misura in EW
- se la banda e' molecolare si misura in mag

$$I_A = \Delta \frac{(f_c - f_f)}{f_c}$$

$$I_{mag} = -2.5 \log \left[1 - \left(\frac{I_A}{\Delta} \right) \right]$$

$$I_{mag} = -2.5 \log \left(\frac{f_f}{f_c} \right)$$

$$I_A = \Delta \left[1 - 10^{-0.4 I_{mag}} \right]$$

Il sistema di Lick

TABLE 1
INDEX DEFINITIONS

	Name	Index Bandpass	Pseudocontinua	Units	Measures	Error[1]	Notes
01	CN_1	4143.375-4178.375	4081.375-4118.875 4245.375-4285.375	mag	CN, Fe I	0.021	
02	CN_2	4143.375-4178.375	4085.125-4097.625 4245.375-4285.375	mag	CN, Fe I	0.023	2
03	Ca4227	4223.500-4236.000	4212.250-4221.000 4242.250-4252.250	Å	Ca I, Fe I, Fe II	0.27	2
04	G4300	4282.625-4317.625	4267.625-4283.875 4320.125-4336.375	Å	CH, Fe I	0.39	
05	Fe4383	4370.375-4421.625	4360.375-4371.625 4444.125-4456.625	Å	Fe I, Ti II	0.53	2
06	Ca4455	4453.375-4475.875	4447.125-4455.875 4478.375-4493.375	Å	Ca I, Fe I, Ni I, Ti II, Mn I, V I	0.25	2
07	Fe4531	4515.500-4560.500	4505.500-4515.500 4561.750-4580.500	Å	Fe I, Ti I, Fe II, Ti II	0.42	2
08	Fe4668	4635.250-4721.500	4612.750-4631.500 4744.000-4757.750	Å	Fe I, Ti I, Cr I, Mg I, Ni I, C_2	0.64	2
09	Hβ	4847.875-4876.625	4827.875-4847.875 4876.625-4891.625	Å	Hβ, Fe I	0.22	3
10	Fe5015	4977.750-5054.000	4946.500-4977.750 5054.000-5065.250	Å	Fe I, Ni I, Ti I	0.46	2,3
11	Mg_1	5069.125-5134.125	4895.125-4957.625 5301.125-5366.125	mag	MgH, Fe I, Ni I	0.007	3
12	Mg_2	5154.125-5196.625	4895.125-4957.625 5301.125-5366.125	mag	MgH, Mg *b*, Fe I	0.008	3
13	Mg *b*	5160.125-5192.625	5142.625-5161.375 5191.375-5206.375	Å	Mg *b*	0.23	3
14	Fe5270	5245.650-5285.650	5233.150-5248.150 5285.650-5318.150	Å	Fe I, Ca I	0.28	3
15	Fe5335	5312.125-5352.125	5304.625-5315.875 5353.375-5363.375	Å	Fe I	0.26	3
16	Fe5406	5387.500-5415.000	5376.250-5387.500 5415.000-5425.000	Å	Fe I, Cr I	0.20	2,3
17	Fe5709	5698.375-5722.125	5674.625-5698.375 5724.625-5738.375	Å	Fe I, Ni I, Mg I Cr I, V I	0.18	2
18	Fe5782	5778.375-5798.375	5767.125-5777.125 5799.625-5813.375	Å	Fe I, Cr I Cu I, Mg I	0.20	2
19	Na D	5878.625-5911.125	5862.375-5877.375 5923.875-5949.875	Å	Na I	0.24	
20	TiO_1	5938.375-5995.875	5818.375-5850.875 6040.375-6105.375	mag	TiO	0.007	
21	TiO_2	6191.375-6273.875	6068.375-6143.375 6374.375-6416.875	mag	TiO	0.006	

FWHM = 8.5Å

Worthey et al. (1994)

+ Trager et al. (1998)

Indici Blu-Vis

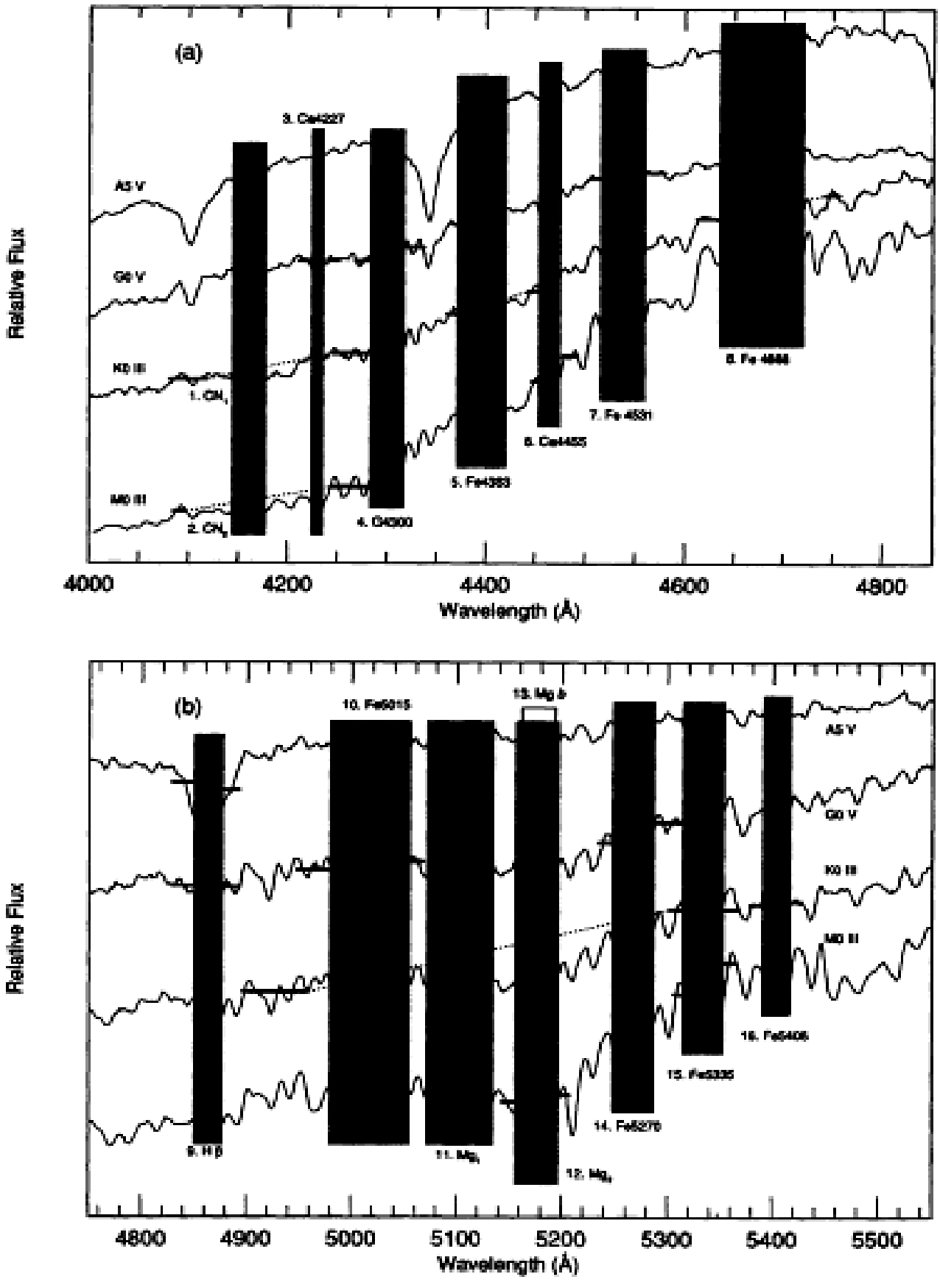

Indici Rossi

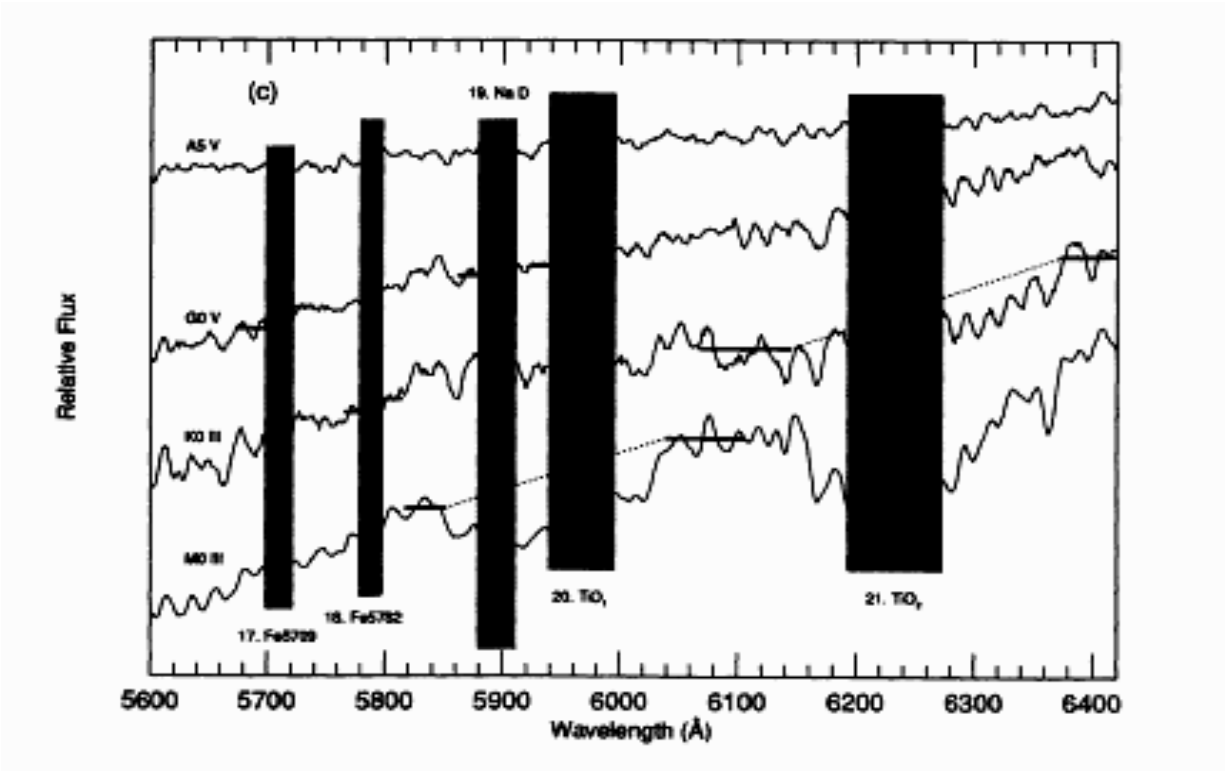

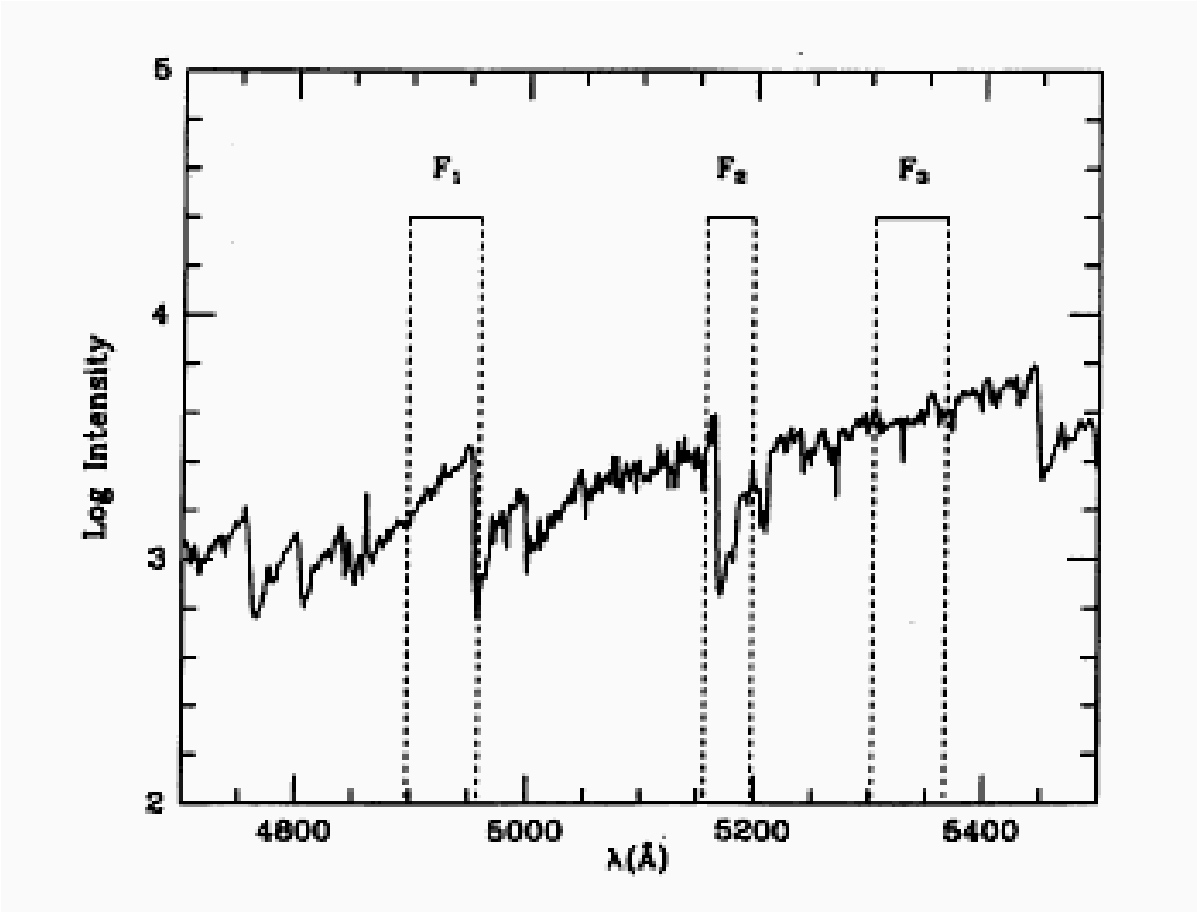

Narrow-band indices & SSP tomography

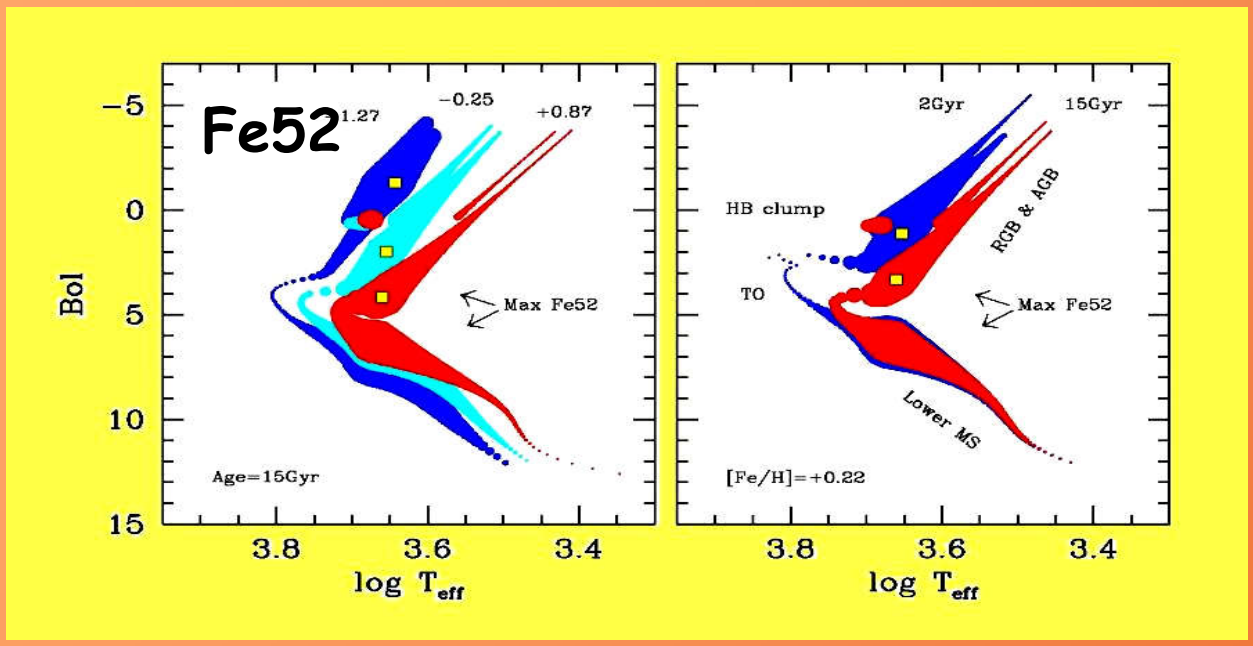

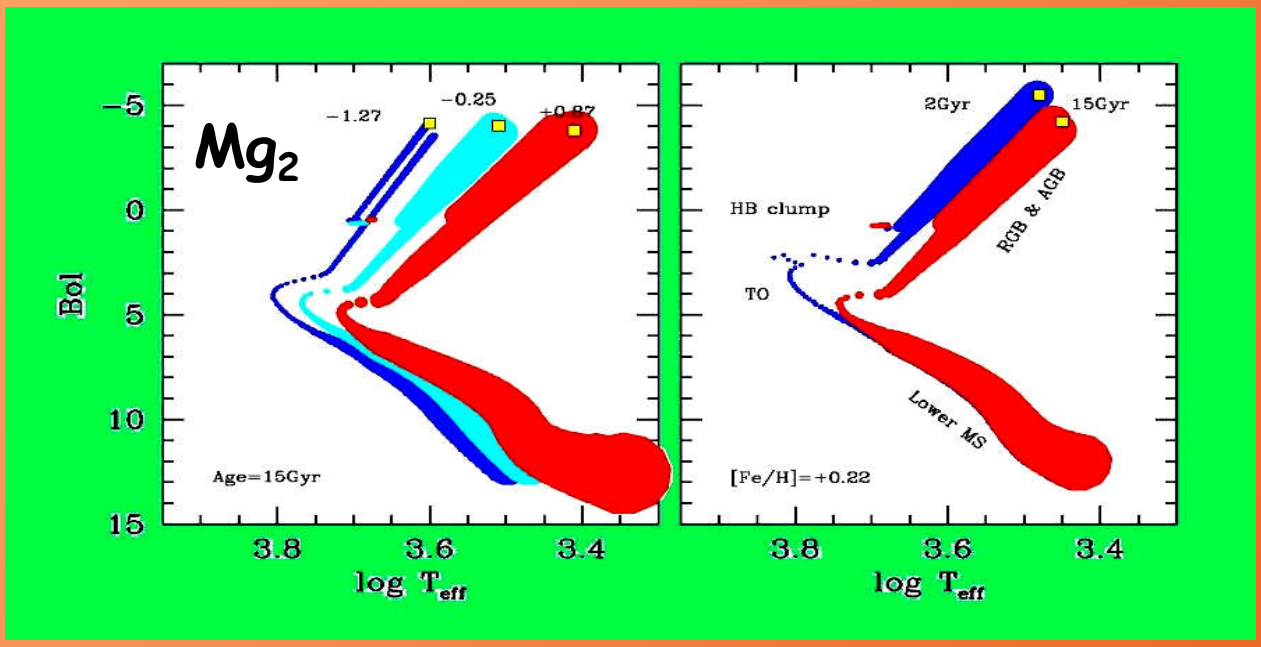

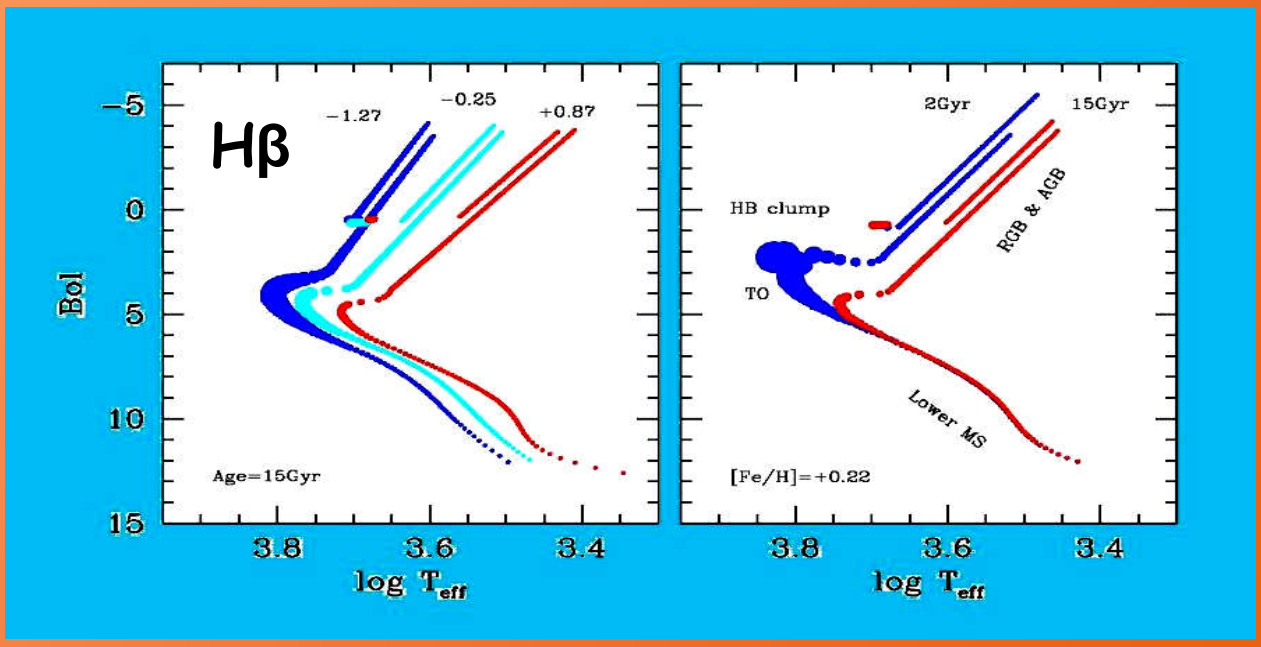

Articoli consigliati (vedi Webpage):
http://www.bo.astro.it/~eps/lezioni/lezioni.html

- **Spectral Properties of Galaxies (Kennicutt 1992)**
- **Galaxy Spectral Atlas (Kennicutt 1992)**
- **Faber & Jackson (1976)**
- **M/L clusters (Girardi et al. 2002)**
- **Balmer break (Hamilton 1985)**
- **Lick indices (Worthey et al. 1994)**

Il bias di Malmquist

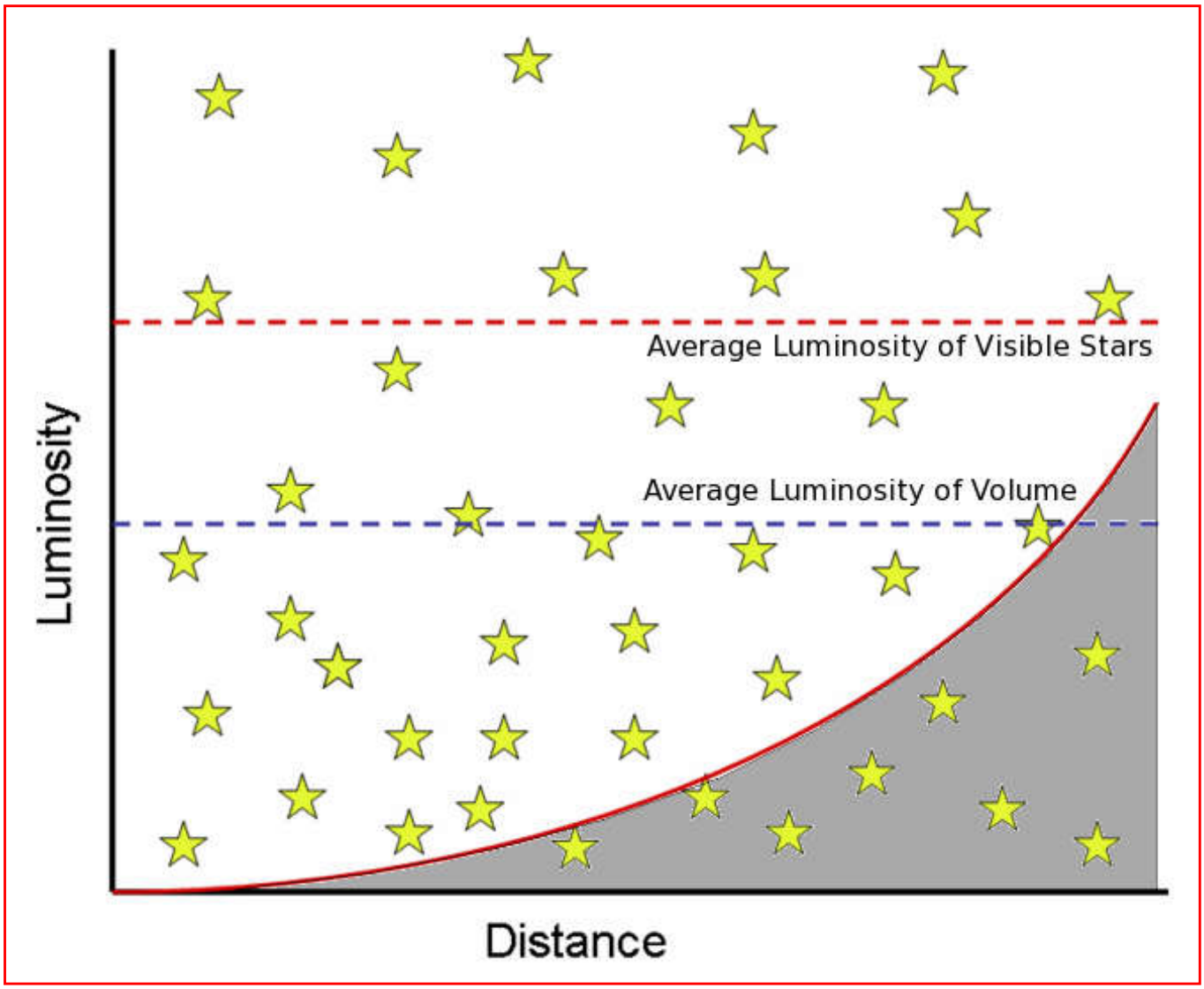

http://en.wikipedia.org/wiki/Malmquist_bias

Il bias di Malmquist

Tammann & Sandage (1983)

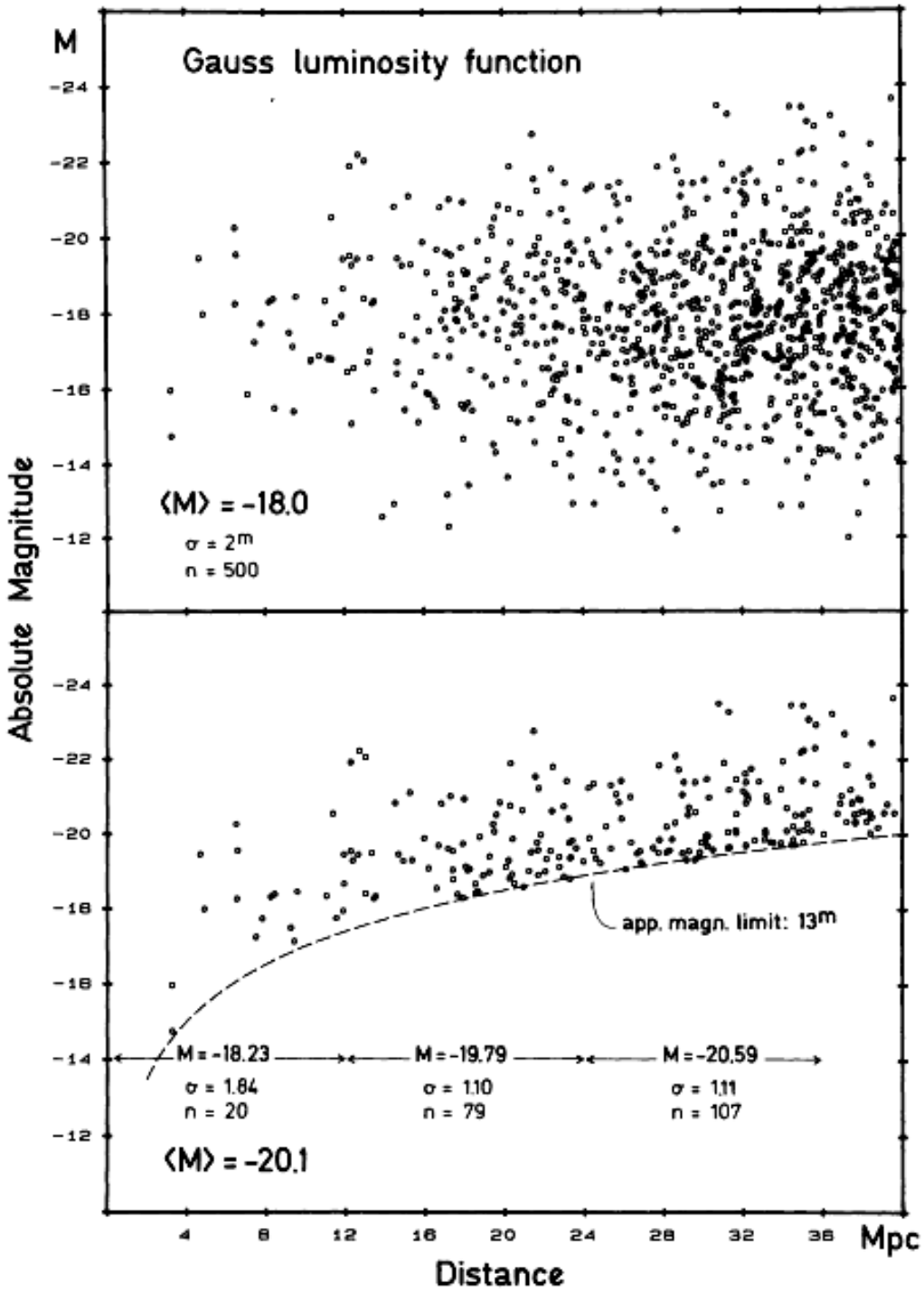

Fig. 1. Upper panel: Monte Carlo distribution in distance and absolute magnitude of 500 galaxies within 38 Mpc. Constant space density and a mean absolute magnitude of $< M > = -18^m$ with a Gauss standard deviation of $\sigma_M = 2^m$ are assumed. Lower pannel: The same sample cut by an apparent-magnitude limit of $m = 13^m.0$. Note the increase of the galaxian luminosities with increasing distance and the small effective (observable) scatter σ_M within individual distance intervals.

Bias morfologico & Bias fotometrico

Disk-dominated Bulge-dominated

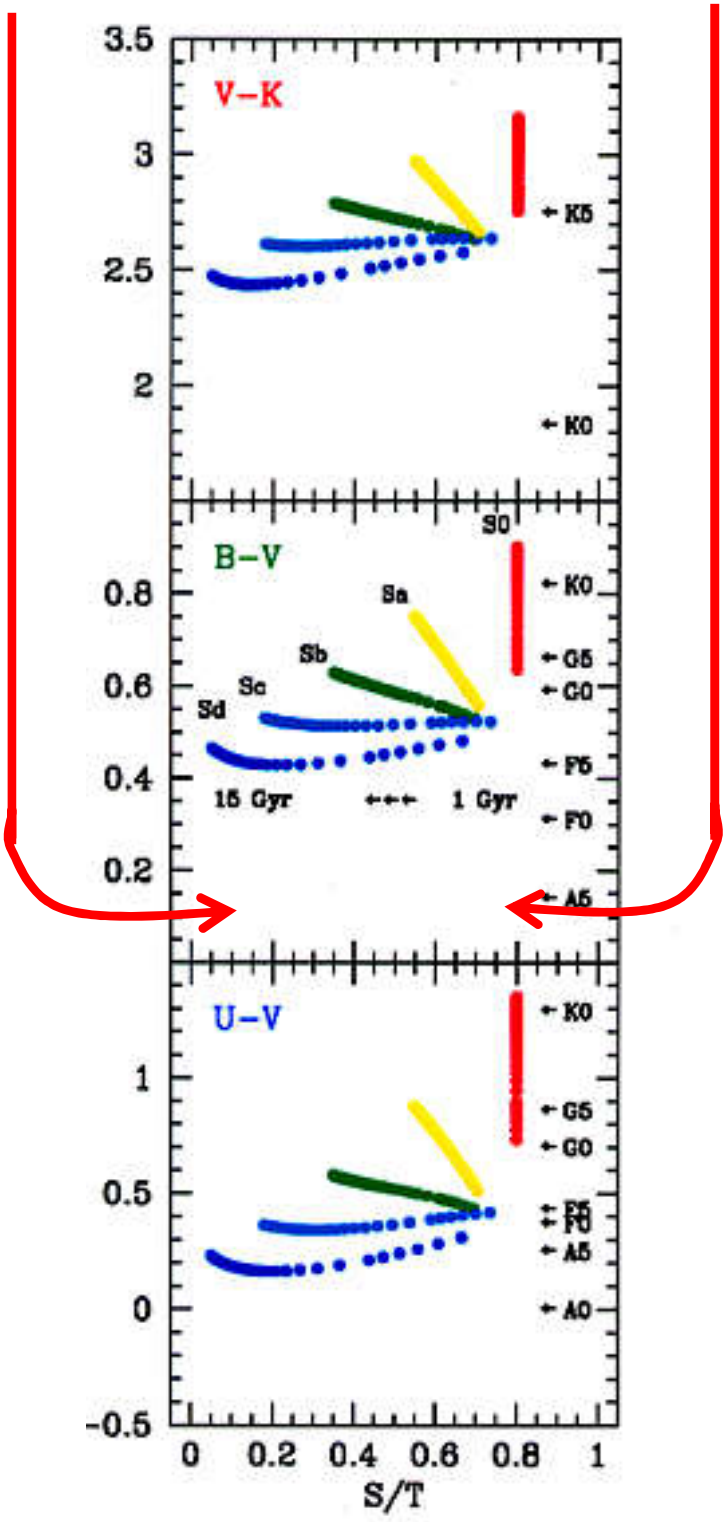

L(Spheroid)/L(Tot)

Bias Morfologico

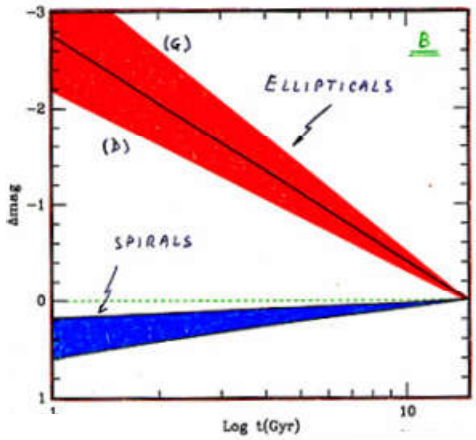

All'aumentare del redshift

1) Andiamo indietro nel tempo (bulge +luminoso e disco –luminoso)

2) La morfologia tende ad essere quella nell'Ultravioletto

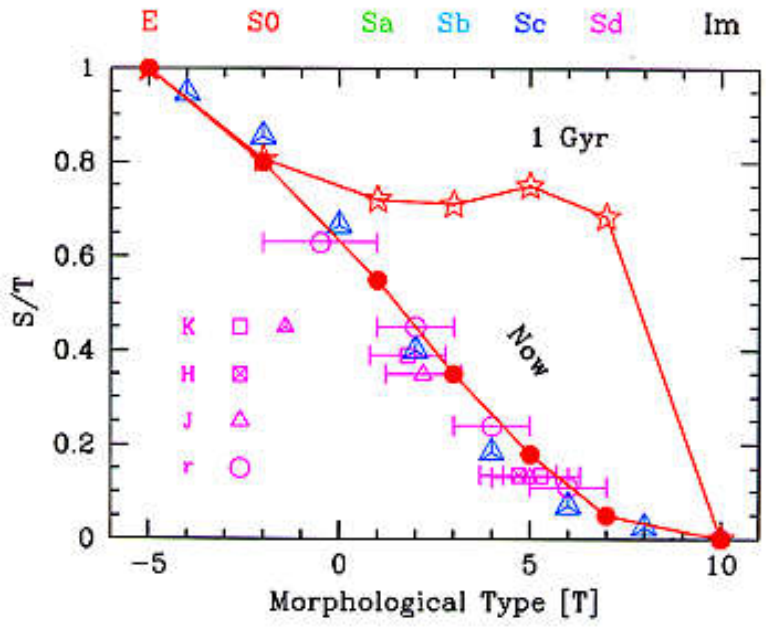

Buzzoni (2005)

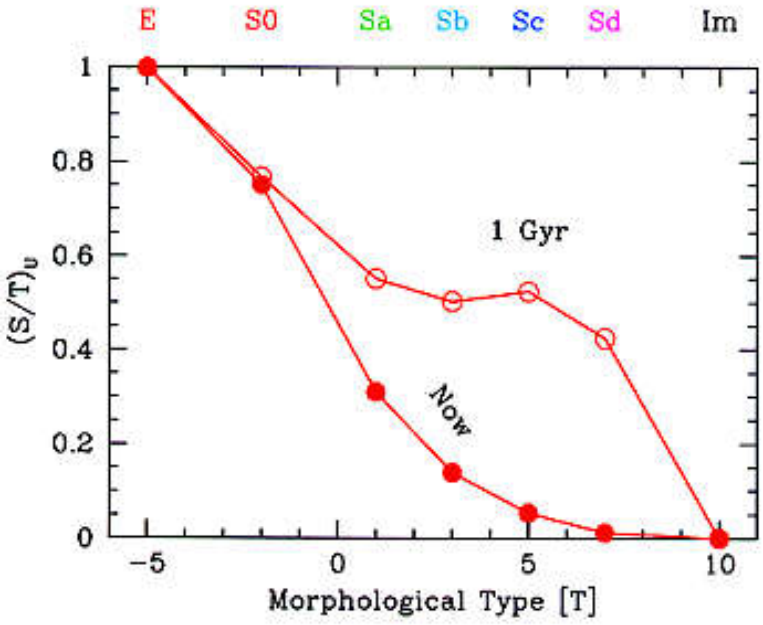

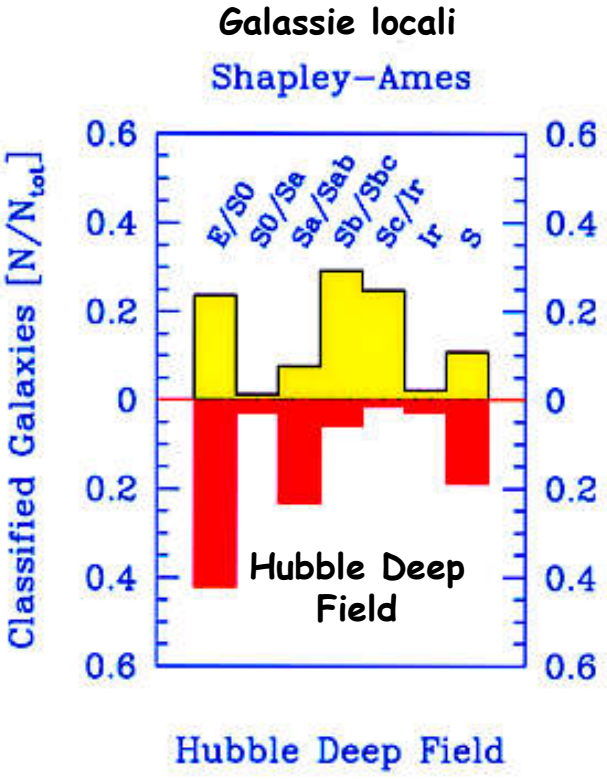

Van den Bergh et al. (1996)

Il Redshift

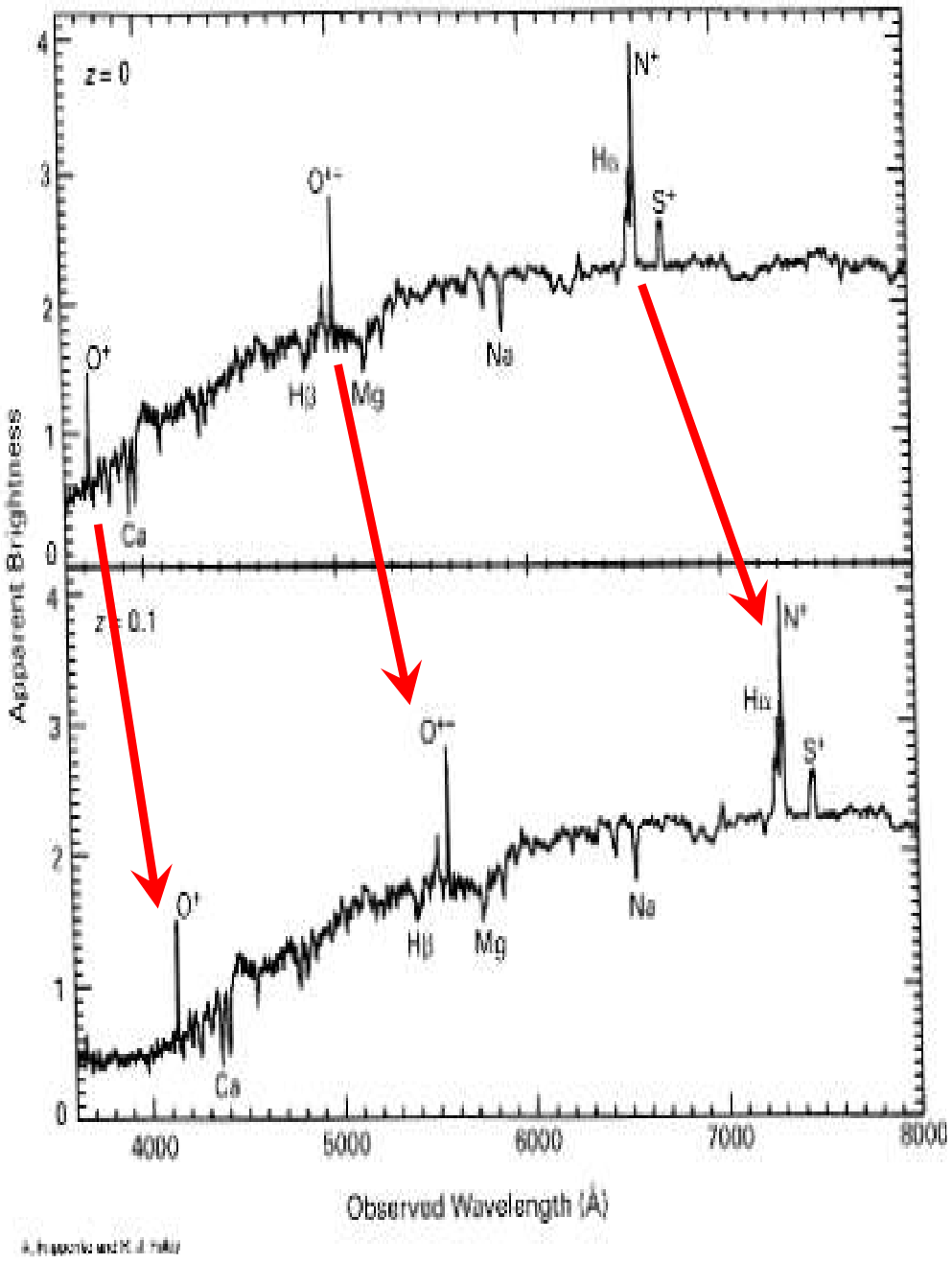

$$\frac{\lambda_{oss} - \lambda_{lab}}{\lambda_{lab}} = z$$

$$\frac{\Delta\lambda}{\lambda} = \frac{v}{c} = z$$

$$\frac{\lambda_{oss}}{\lambda_{lab}} = (1+z)$$

L'effetto di "streching"

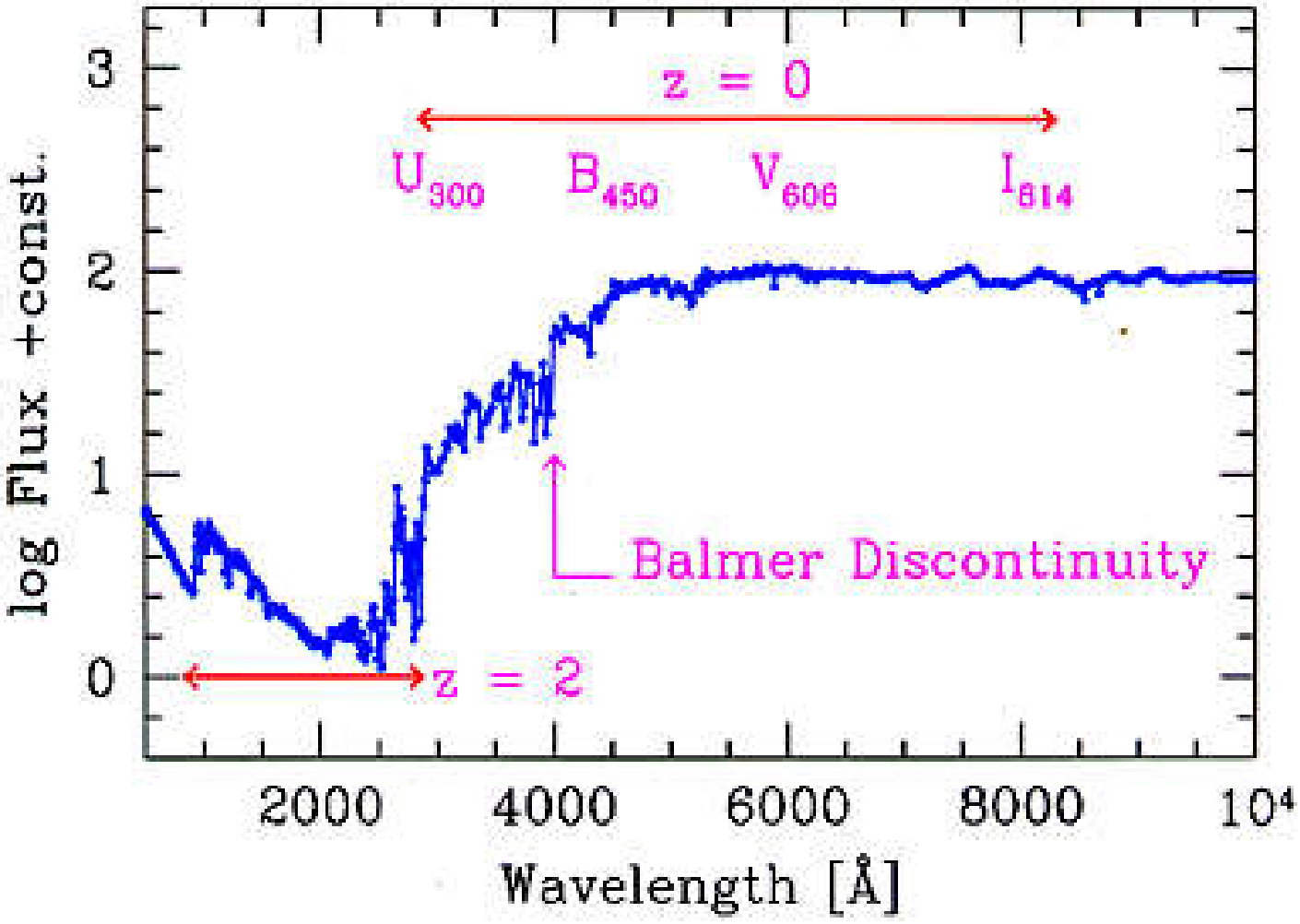

Massarotti et al. (2001)

Correzione k

$$M - M_0 = 5 \log \frac{l}{l_0} + K(z) + \varepsilon(z)$$

$$K(z) = 2.5 \log(1+z) - 2.5 \log \int F_{(\lambda/1+z)} R_\lambda \, d\lambda \Big/ \int F_\lambda R_\lambda \, d\lambda$$

$$\varepsilon(z) = -2.5 \log \int F_{(\lambda/1+z;\, t_z)} R_\lambda \, d\lambda \Big/ \int F_{(\lambda/1+z;\, 0)} R_\lambda \, d\lambda$$

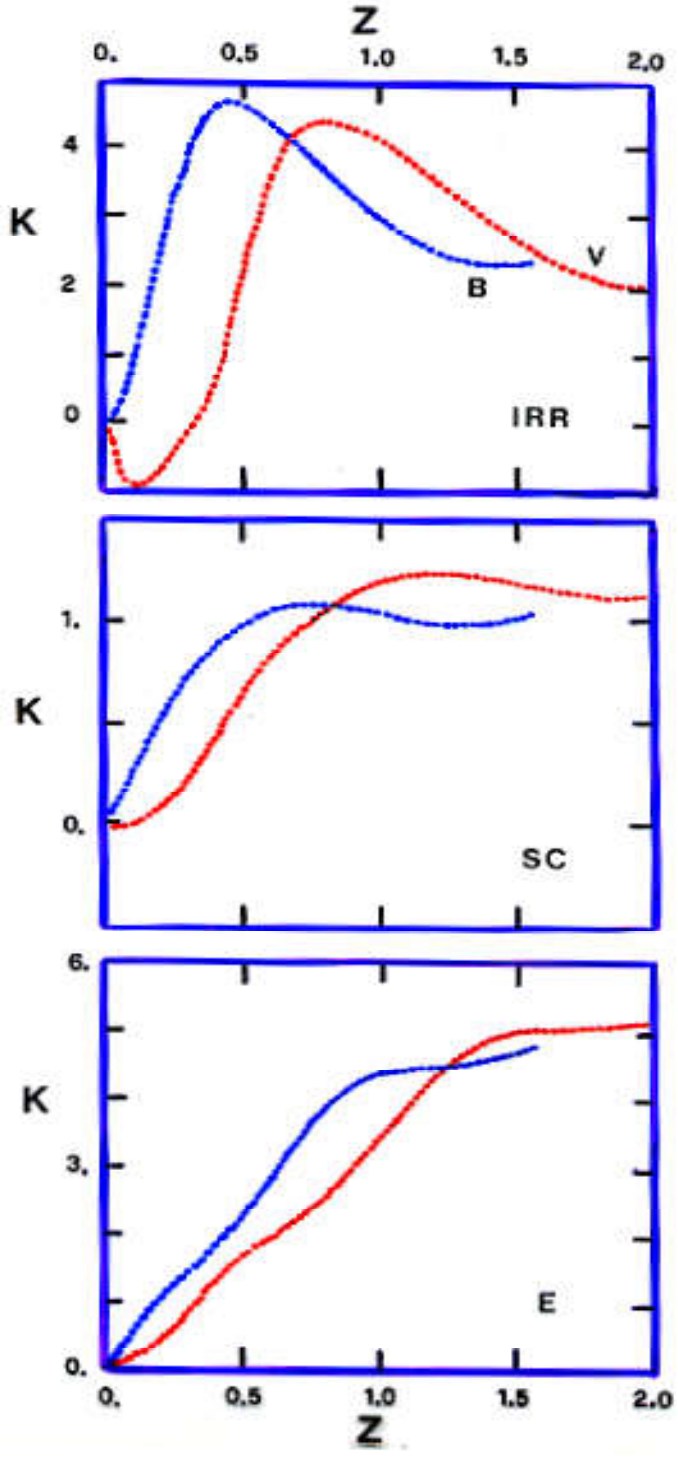

Notare che $\forall$ morfologia

$$\lim_{z \to 0} k = +2.5 Log(1+z)$$

Dato che $F(\lambda/(1+z) \rightarrow F(\lambda)$

http://arxiv.org/abs/astro-ph/0210394

Esempi di correzione k passiva (k) ed evolutiva (k+e)

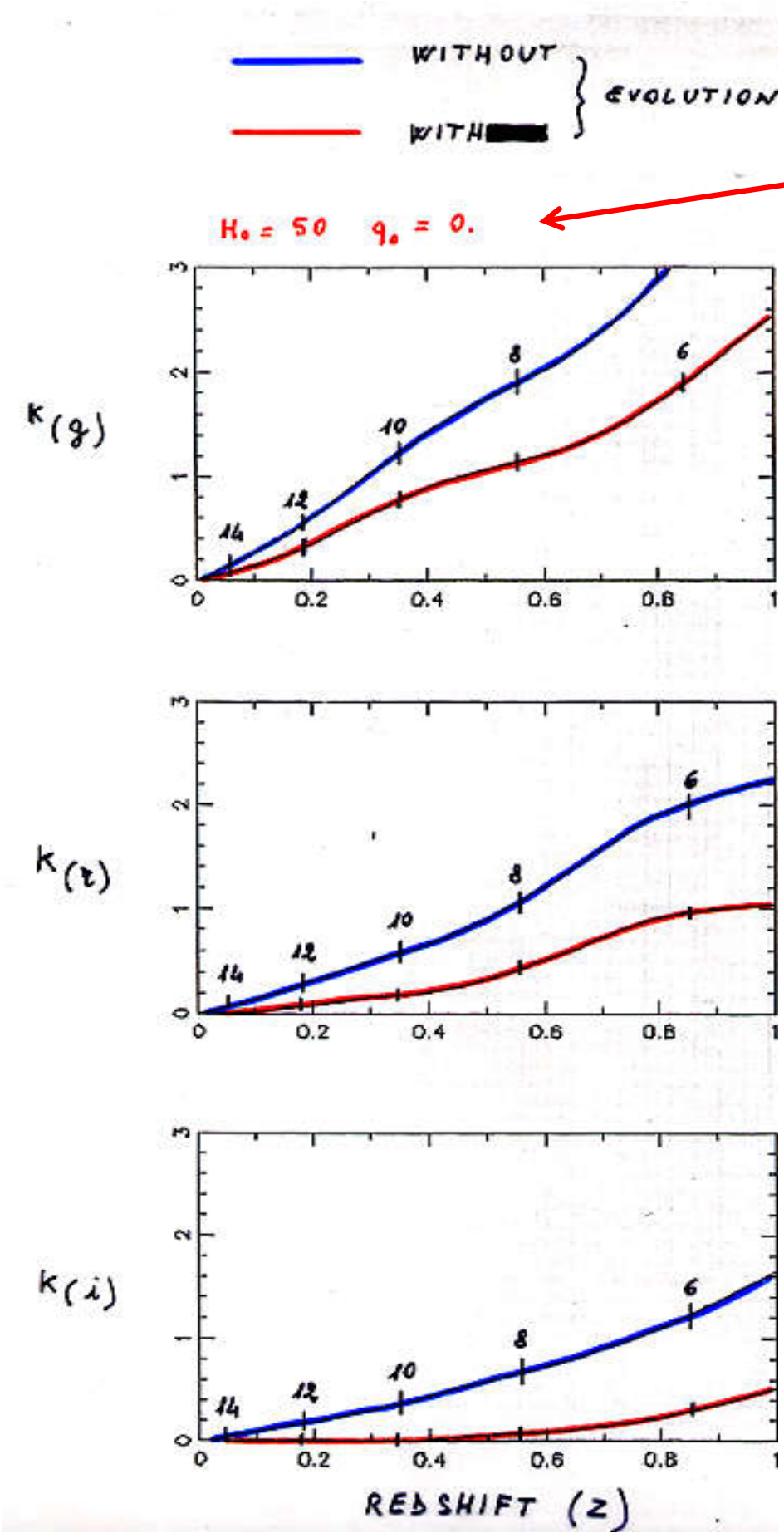

Importante!:

La correzione evolutiva e(z) dipende dal modello cosmologico assunto

k(z)

k(z)+e(z)

Apparent Color vs. Redshift

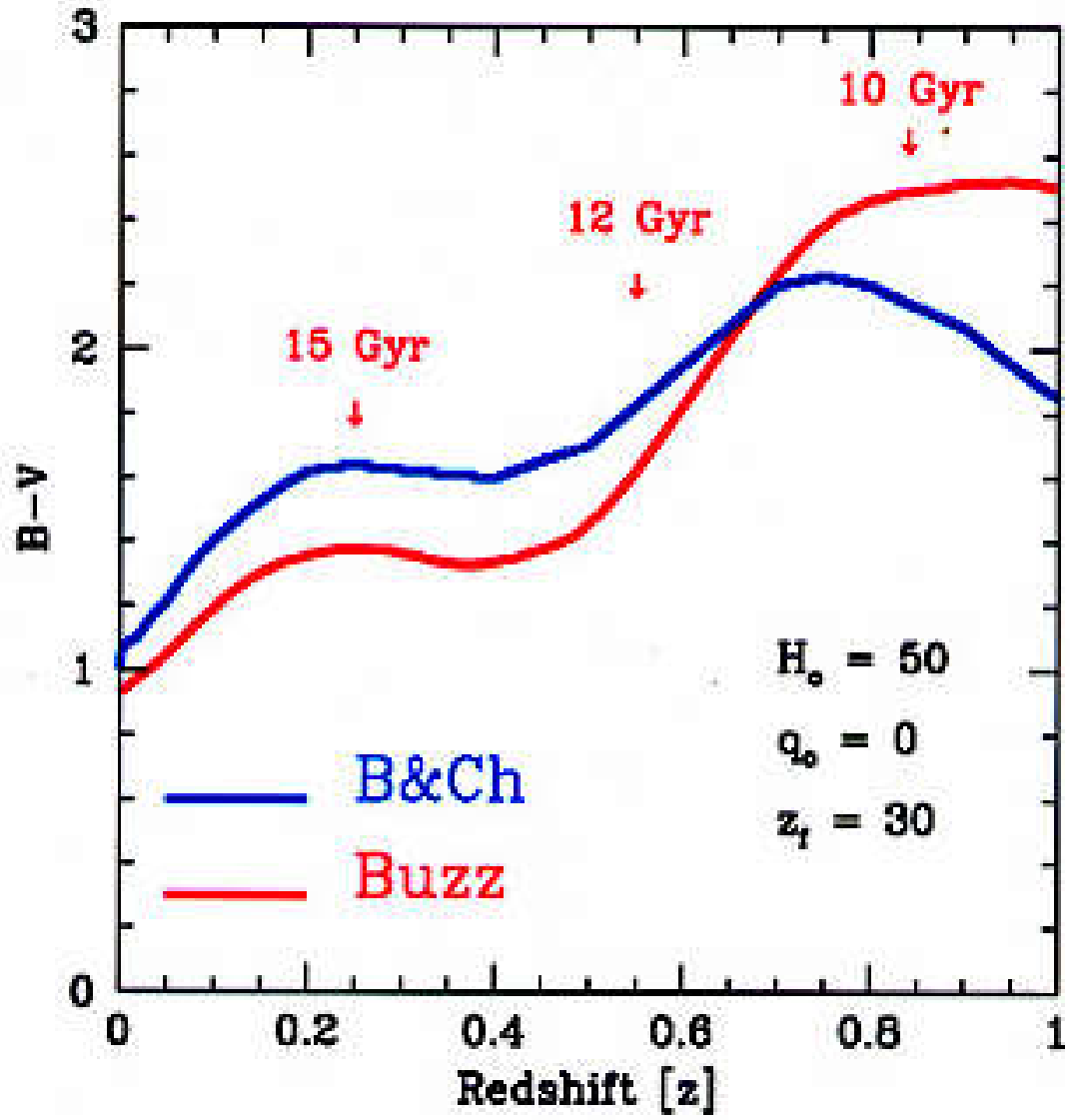

$$(B-V)_z = (B-V)_o + (k_B - k_V) + (e_B - e_V)$$

Colore apparente

Colore restframe

Opzionale, nel caso si voglia/possa tenere in conto della evoluzione con z

Selezione fotometrica delle galassie ad alto redshift: un esempio

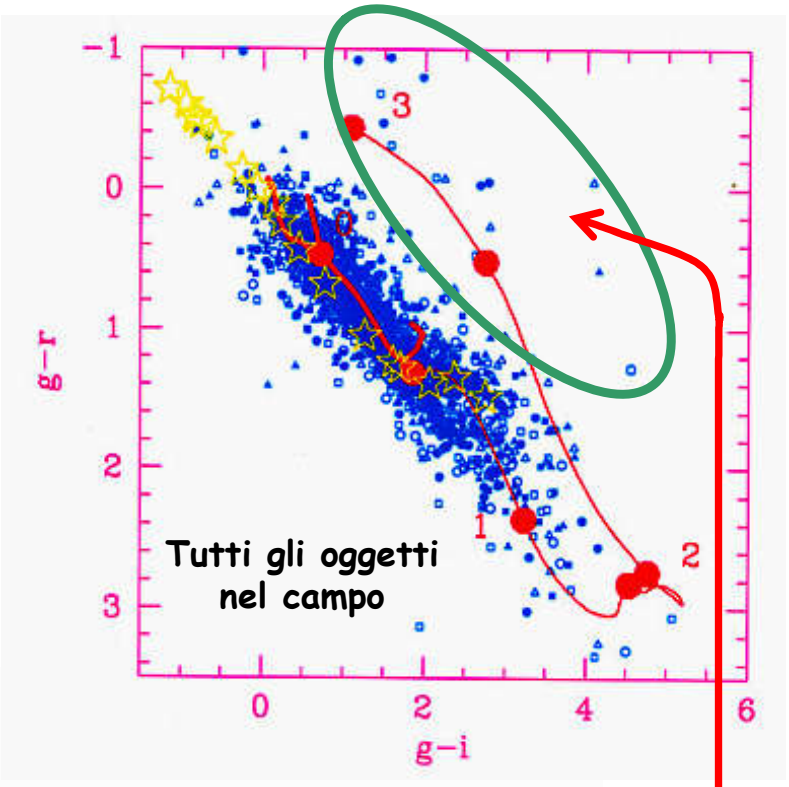

Galassie ellittiche a z>2

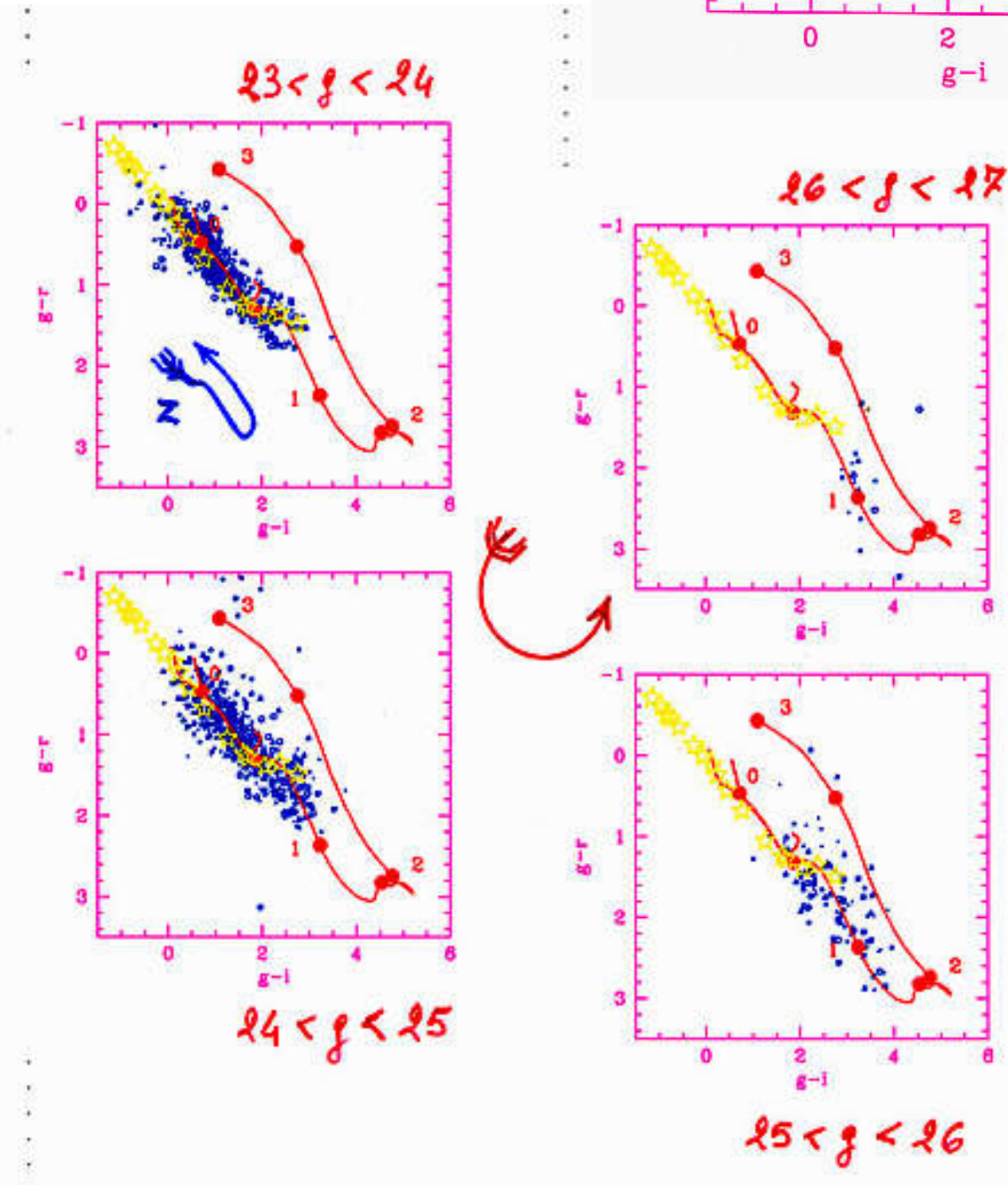

Selezione fotometrica delle galassie ad alto redshift: "Dropout galaxies"

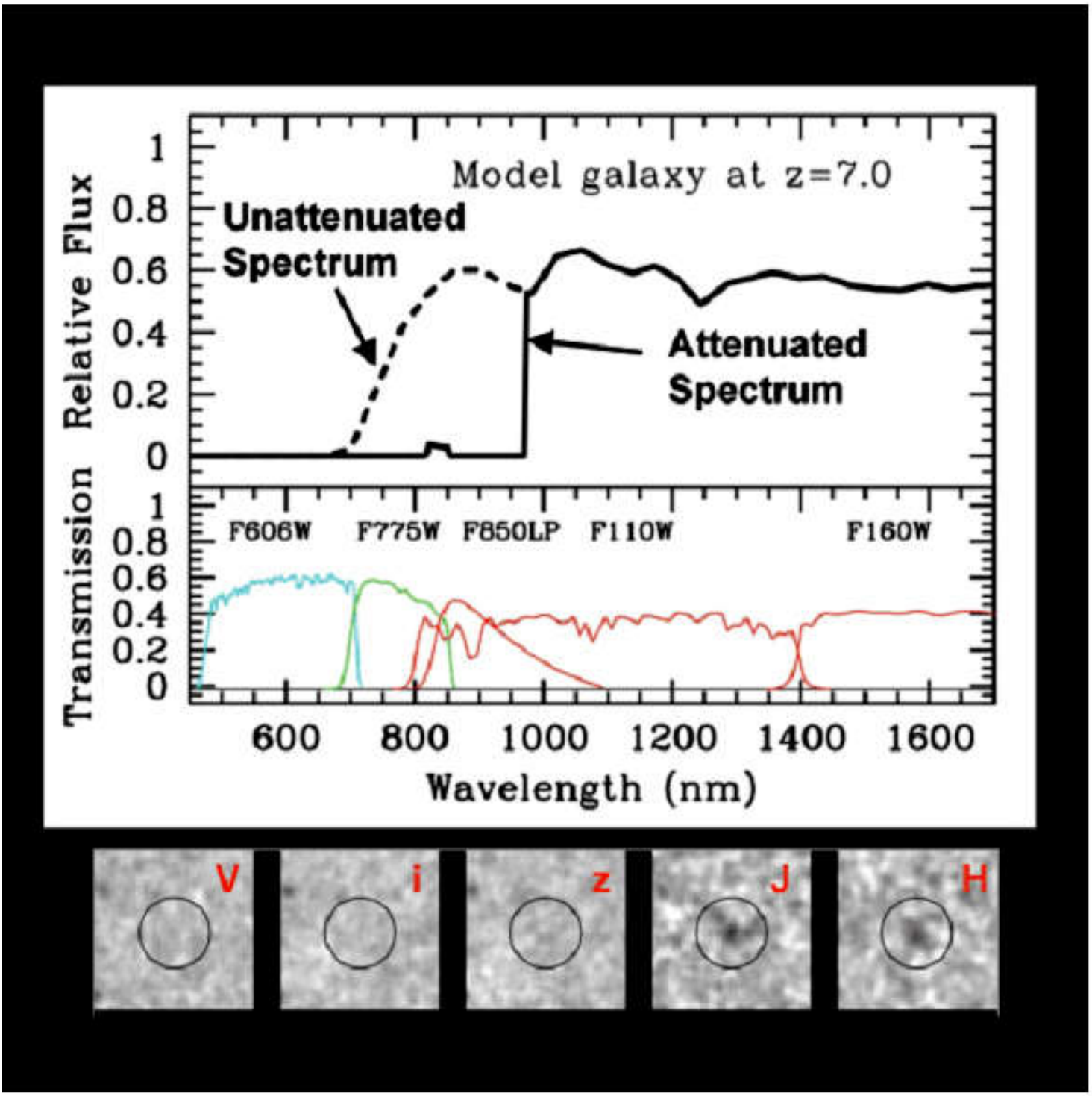

Steidel et al. (1996)

Articoli consigliati (vedi Webpage):
http://www.bo.astro.it/~eps/lezioni/lezioni.html

- **Galaxy Colors (Buzzoni 2005)**
- **Spectral Properties of Galaxies (Kennicutt 1992)**
- **Galaxy Spectral Atlas (Kennicutt 1992)**
- **Balmer break (Hamilton 1985)**
- **SFR & Hubble Sequence (Kennicutt 1988)**
- **Cosmic SFR (Madau & Dickinson (2014)**
- **Galaxy mass assembly (Pan 2015)**
- **K-correction (Hogg et al. 2002)**